

UNIVERSITÀ DEGLI STUDI DI VERONA

DEPARTMENT OF
NEUROSCIENCE BIOMEDICINE AND MOVEMENT SCIENCES

GRADUATE SCHOOL OF
APPLIED HEALTH AND LIFE SCIENCES
DOCTORAL PROGRAMM IN
APPLIED HEALTH AND LIFE SCIENCES

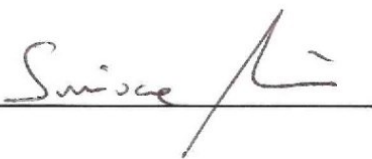
Establishment and characterization of two human miR-34a knockout cell lines, HeLa and HEK293T, applying the CRISPR/Cas9 system.

WITH THE FINANCIAL CONTRIBUTION OF
ATENEIO-UNIVERSITY OF VERONA

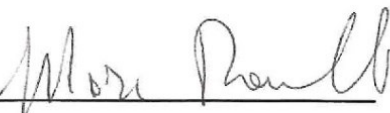
Cycle XXXV, year 2019-2022

S.S.D. BIO13


Coordinator: Prof. Simone Accordini

Signature 

Tutor: Prof.ssa Maria Grazia Romanelli

Signature 

Doctoral Student: Dott.ssa Tonia De Simone

Signature 

ABSTRACT

The Clustered Regularly Interspaced Short Palindromic Repeats (CRISPR)/Cas (CRISPR associated) system was discovered in 1987 and it is used by bacteria as defense mechanism. Thanks to its ability to target a specific DNA sequence, this system showed up as a promising genome editing tool. In this PhD thesis is presented the application of the CRISPR/Cas9 system to produce two miR-34a knock-out cell lines in order to study the role of this microRNA in the expression of genes that may be involved in tumorigenesis.

Micro-RNAs (miRNAs) are small non-coding and regulatory RNAs of about 21 nucleotides that act as regulators of gene expression; generally, they have an inhibitory effect by either blocking protein translation or promoting mRNA degradation. These small RNAs have an important role both in physiological events like cell proliferation, differentiation, and development as well as in pathological conditions such as cancer and neurodegenerative diseases. One of the most studied miRNAs in cancer is the miR-34a that, inhibiting the expression of different pro-tumorigenic genes, like CDK4/6, BCL2, SNAIL and CD44, behaves as a tumor suppressor. Indeed, this miRNA is frequently dysregulated in different types of tumors like gliomas, neuroblastomas, breast, prostate cancer, and hematological malignancies.

In this study, we characterized HeLa and HEK293T miR-34a Knock-Out (KO) cell clones that were produced by using the CRISPR/Cas9 technology, in terms of proliferation rate, expression of already known and predicted targets, through quantitative PCR (qPCR), and Western blot analyzes.

The characterization of the two cell lines started, first of all, with the evaluation of their proliferation rate. Following the evaluation of the proliferation rate, the expression of different validated (BCL2, IK β α , AXL, TWIST1, RAD51 and SIRT1) and predicted miR-34 targets (REL, MAP1B, COL6A2, NR3C1, ZBTB20, PCLO, ONECUT2 and KMT2D) was analyzed through qPCR and Western blot experiments. Looking at the proliferation assay results, miR-34a KO HeLa and HEK293T clones (the 2G10 and 3.1D3 clones respectively) showed a similar proliferation rate as HeLa and HEK293T WT cells.

As regards the evaluation of the expression of validated and predicted targets in the two miR-34a KO clones; qPCR experiments, performed in the HeLa line, showed a significant increase in the expression of BCL2 (p-value = 0.01196), REL (p-value = 0.02762) MAP1B (p-value = 0.013) and NR3C1 (valore p= 0,03) in HeLa KO clone (2G10) versus WT cells. Instead, a statistically significant downregulation of the predicted COL6A2 target was found in the KO clone (p-value = 0.00161).

qPCR analyzes performed in HEK293T KO clone (3.1D3) showed significant overexpression of IK β α (p value = 0.02367), AXL (p value = 0.00848), TWIST1 (p value = 0.028), ONECUT2 (p-value = 0.01143), and KMT2D (p-value = 0.03464) versus WT cells. In contrast to HeLa, MAP1B was downregulated in the HEK293T KO clone compared to WT cells.

Experimental duplicate Western blot experiments confirmed the upregulation of ONECUT2 in HeLa and HEK293T miR-34a-KO clones compared to WT cells. In conclusion, the results of the analysis of cell lines silenced with miR-34a indicate that: a) miR-34a is not indispensable for the control of cell proliferation; b) miR-34a may be involved in different signaling pathways and act differently according to cell type, suggesting a tissue-specific role of miR-34a; c) ONECUT2, a transcription factor that stimulates the expression of genes involved in the differentiation of melanocytes and hepatocytes, could be a novel target of miR-34a. Future functional studies on the pathways regulated by this transcription factor in miR-34a KO clones will help to clarify the role of miR-34a in cell differentiation and transformation.

RIASSUNTO

Il sistema Clustered Regularly Interspaced Short Palindromic Repeats (CRISPR)/Cas (associato a CRISPR) è stato scoperto nel 1987 ed è utilizzato dai batteri come meccanismo di difesa. Grazie alla sua capacità di mirare a una specifica sequenza di DNA, questo sistema si è rivelato un promettente strumento di modifica del genoma. In questo lavoro il sistema CRISPR/Cas9 è stato utilizzato per produrre due linee cellulari knock-out per miR-34a al fine di studiare il ruolo di questo microRNA nell'espressione di geni che potrebbero essere coinvolti nella tumorigenesi.

I micro-RNA (miRNA) sono piccoli RNA non codificanti e regolatori di circa 21 nucleotidi. Il primo miRNA identificato nel 1993, in *Caenorhabditis Elegans*, era lin-4. I miRNA agiscono come regolatori dell'espressione genica; generalmente, hanno un effetto inibitorio bloccando la traduzione proteica o promuovendo la degradazione dell'mRNA. Questi piccoli RNA hanno un ruolo importante sia in eventi fisiologici come la proliferazione cellulare, la differenziazione e lo sviluppo, sia in condizioni patologiche come il cancro e le malattie neurodegenerative. Uno dei miRNA più studiati nel cancro è il miR-34a che, inibendo l'espressione di diversi geni oncogeni, come CDK4/6, BCL2, SNAIL e CD44, si comporta come un oncosoppressore. In effetti, questo miRNA è spesso deregolato in diversi tipi di tumori come gliomi, neuroblastomi, cancro al seno, alla prostata e neoplasie ematologiche. In questo studio, abbiamo caratterizzato i cloni HeLa e HEK293T miR-34a Knock-Out (KO) prodotti utilizzando la tecnologia CRISPR/Cas9, in termini di tasso di proliferazione, espressione di bersagli già noti e previsti, mediante PCR quantitativa (qPCR) e analisi di Western Blot. La caratterizzazione delle due linee cellulari è iniziata, con la valutazione della loro velocità di proliferazione. Successivamente attraverso PCR quantitativa e Western Blot è stata analizzata, l'espressione di diversi bersagli di miR-34a precedentemente validati (BCL2, IK β α , AXL, TWIST1, RAD51 e SIRT1) e bersagli predetti del miR-34a (REL, MAP1B, COL6A2, NR3C1, ZBTB20, PCLO, ONECUT2 e KMT2D). I risultati del test di proliferazione, mostrano che i cloni HeLa e HEK293T miR-34a-KO (rispettivamente i cloni 2G10 e 3.1D3) hanno un tasso di proliferazione simile alle cellule WT.

La valutazione dell'espressione dei trascritti di bersagli validati e predetti di miR-34a nei due cloni miR-34a KO. I risultati di qPCR eseguita nella linea HeLa hanno mostrato un aumento significativo dell'espressione di BCL2 (valore p = 0,01196), REL (valore p = 0,02762), MAP1B (valore p = 0,013) e NR3C1 (valore p = 0,03) nel clone HeLa KO (2G10) rispetto alle cellule WT. Diversamente, nei cloni KO l'espressione del gene COL6A2, target putativo di miR-34a, è significativamente ridotta (valore p = 0,00161). Le analisi di PCR quantitativa eseguite sul clone HEK293T KO (3.1D3) hanno

mostrato un significativo aumento dell'espressione di $IK\beta\alpha$ ($p= 0,02367$), AXL ($p = 0,00848$), TWIST1 ($p = 0,028$), ONECUT2 ($p = 0,01143$) e KMT2D ($p = 0,03464$) rispetto a WT. Al contrario delle HeLa, MAP1B risulta sotto regolato nel clone HEK293T KO rispetto alle cellule WT. Gli esperimenti di Western Blot in duplicato sperimentale hanno confermato la sovra-regolazione di ONECUT2 in entrambi i cloni, HeLa e HEK293T miR-34a-KO, rispetto alle cellule WT.

In conclusione, i risultati dell'analisi delle linee cellulari silenziate per il miR-34a indicano che: a) il miR-34a non è indispensabile per il controllo della proliferazione cellulare; b) miR-34a può essere coinvolto in diverse vie di segnalazione e agire in modo diverso a seconda del tipo di cellula, suggerendo un ruolo tessuto-specifico di miR-34a; c) ONECUT2, un fattore di trascrizione che stimola l'espressione di geni coinvolti nella differenziazione di melanociti ed epatociti, potrebbe essere un nuovo bersaglio del miR-34a. Futuri studi funzionali sulle vie regolate da questo fattore di trascrizione nei cloni miR-34a KO aiuteranno a chiarire il ruolo del miR-34a nella differenziazione e trasformazione cellulare.

INDEX

ABSTRACT.....	1
RIASSUNTO	3
LIST OF FIGURES	8
LIST OF TABLES	10
ABBREVIATIONS	11
1. INTRODUCTION	17
1.1 MiRNA.....	17
1.1.1 The canonical biogenesis pathway	18
1.1.2 Non canonical miRNA Biogenesis Pathways.....	19
1.1.3 Mechanisms of miRNA-mediated gene regulation	20
1.1.4 MicroRNA-Mediated Translational Activation.....	20
1.1.5 Dynamics of miRNA actions.....	21
1.1.6 Circulation of miRNAs.....	21
1.2 miRNA in cancer	21
1.2.1 miRNA Deregulation in Cancer	22
1.2.2 Dysregulation of miRNA transcription in cancer	22
1.2.3 Dysregulation of Pri-miRNA Processing in Cancer	25
1.2.4 Dysregulation of Pre-miRNA Processing in Cancer	26
1.3 MiR-34a	28
1.3.1 miR-34a in cancer.....	29
1.3.2 Functions of miR-34a in cancer.....	30
1.3.3 Upstream regulators of miR-34a in cancer.....	33
1.3.4 miPEP133 as a novel tumor-suppressor microprotein encoded by miR-34a pri-miRNA.	35
1.4 CRISPR/CAS	36
1.4.1 General	36
1.4.2 CRISPR/Cas9 Application	39
1.4.3 miR-34a KO cell lines	41
2. AIM OF THE RESEARCH	42
3. MATERIALS AND METHODS	43
3.1 Cell cultures	43
3.2 miR-34a knock-out cell lines.	43
3.3 Genomic DNA extraction and PCR analysis on gDNA clones	44
3.4 miR-34a knock-out validation	45
3.5 miR-34a KO validation in HeLa and HEK293T cell clones	47
3.6 Cell proliferation assay	48
3.7 Plasmids Transfection.....	49
3.8 RNA extraction	49
3.9 Proteins extraction.....	50
3.10 Reverse transcription.....	50
3.11 miR-34 predicted targets selection.....	51
3.12 Reverse Transcription Real-Time/quantitative PCR (RT-qPCR).....	52

3.13 Western Blot	54
3.13.1 Running and Stacking gel preparation.....	55
3.13.2 Running buffer preparation.	55
3.13.3 Transfer buffer preparation.....	56
3.13.4 Western Blotting.....	56
3.14 Cloning of the 3'-UTR of KMT2D into the pGL3-promoter vector	57
3.15 Colony PCR	58
3.16 Purification of plasmid DNA	58
3.17 Plasmid digestion with restriction enzyme	58
3.18 Statistical analysis	58
4. RESULTS	59
4.1 Generation of HeLa and HEK293T miR-34a-5p KO cell lines.....	59
4.2 miR-34a KO cell lines validation.....	62
4.2.2 Evaluation of the expression of miR-34a target genes in HeLa and HEK293T edited cells.	62
4.3 miR-34a KO HeLa cell line characterization.....	65
4.3.1 Proliferation assay.....	65
4.3.2 Scratch test.....	66
4.3.3 HeLa cell line transcriptome analysis	66
4.3.4 Expression of validated and predicted miR-34 targets	67
4.4 miR-34a KO HEK293T cell line characterization.....	70
4.4.1 Proliferation assay	70
4.4.2 Expression of validated and predicted miR-34a targets.....	70
4.5 ONECUT2 is upregulated at protein level in both HeLa and HEK293T miR-34a-KO cells compared to WT cell lines.	74
4.6 Cloning KMT2D 3'-UTR in the pGL3 Luciferase promoter vector.	76
5. DISCUSSION.....	77
6. CONCLUSIONS AND FUTURE PERSPECTIVES	81
7. REFERENCES.....	83

LIST OF FIGURES

Figure 1 Canonical and non- canonical microRNAs biogenesis and mechanism of action (Jacob O'Brien et al. 2018).	18
Figure 2 Genomic structure and regulation of miR-34a. (A) Sequence alignment of the mature human and mouse miR-34a. The seed sequences are highlighted in red. (B) Structure of miR-34a genomic loci. Green boxes represent exons. Horizontal arrow marks transcription start site. (C) Regulation of miR-34a. At the transcriptional level, p53, p63, and p73 induces whereas DNA methylation, TME-TFs such as SNAIL and ZEB1, STAT3, and Myc repress miR-34a expression. At the posttranscriptional level, EZH2, lncRNAs, and competing endogenous RNAs (ceRNAs) may negatively regulate miR-34a expression (Wen (Jess) Li et al. 2021).	28
Figure 3 MicroRNA-34a regulation of CSCs. Presented are direct targets of miR-34a and biological consequences on CSCs in the indicated cancer types (Wen (Jess) Li et al. 2021).	29
Figure 4 Crucial tumor-suppressive effects of miR-34a mediated by downstream targets. As a well-defined tumor suppressor, miR-34a has been convincingly validated to directly repress various downstream targets and affect critical signaling pathways, hence exerting multifaceted antitumor roles to block tumor progression (Sijing Li et al.2021).	32
Figure 5 Predicted upstream transcription factors (TFs) of miR-34s. a Putative upstream TFs of miR-34s predicted by Animal TFDB 3.0 (http://bioinfo.life.hust.edu.cn/AnimalTFDB/#/), JASPAR (http://jaspar.genereg.net/), GeneCards (https://www.genecards.org/), and PROMO (http://algggen.lsi.upc.es/cgi-bin/promo_v3/promo/promoinit.cgi?dirDB=TF_8.3). The detailed information is shown in Additional File 4. b Common potential TFs upstream of miR-34a.....	34
Figure 6 The mechanism of CRISPR–Cas9–mediated genome engineering.....	38
Figure 7 Schematic representations of the proposed mechanisms of CRISPR–Cas9-mediated target DNA recognition and cleavage.	40
Figure 8 RT-qPCR on RNA from HeLa and HEK293T WT cells and miR-34a-KO clones (respectively only 2G10 and 3.1D3 clones). Values were normalized to RNU6-1 and results were expressed as relative fold change of expression levels.	48
Figure 9 Survey of validation strategies for CRISPR/Cas9 editing. (A) PCR of genomic DNA extracted from selected clones. HeLa cells are the control (Ctrl). The bp length of the bands of HeLa KO clone was approximatively identified using GeneRuler 100 bp DNA Ladder (Thermo Fisher): Ctrl = 325 bp, 2G10 = 272 bp, 1D3 = 325 bp, 2E2 = 416 bp + 258 bp, 1G9 = 258 bp. (B) Multiple sequence alignment via Multiple sequence alignment tool (Clustal omega): gRNA1(green), gRNA2 (purple), gRNA3 (light blue), sequences non homologous to the Ctrl sequence (yellow) and PAM sequences (purple).....	60
Figure 10 Survey of validation strategies for CRISPR/Cas9 editing in HEK293T cells. PCR of genomic DNA extracted from selected clones. HEK293T cells are the control (Ctrl). The bp length of the bands of HEK293T KO clone was approximatively identified using GeneRuler 100 bp DNA Ladder (Thermo Fisher). (B) Multiple sequence alignment via Multiple sequence alignment tool (Clustal omega).	62
Figure 11 Evaluation of the expression of miR-34a target genes (BCL2 and IK β α) in edited cells. (A) RT-qPCR analysis on HeLa and HEK293T WT cells (blue bar) and miR-34a-KO clones (red bar); BCL2 gene was chosen for the analysis (*p=0,012). Normalization was performed relative to RPLP0 gene expression and standard deviation analysis was calculated between triplicates. The statistical significance was set at *p \leq 0.05 that was measured by using the T-student test for	

independent data with GraphPad. (B) Differential expression of endogenous IKβα in HeLa KO clone (2G10). (C) Differential expression of endogenous IKβα in HEK293T KO clone (3.1D3). miR-34a-KO clones protein levels detected were normalized on β-tubulin.	64
Figure 12 Proliferation rate of HeLa WT cells vs HeLa KO clone.....	65
Figure 13 Scratch Assay: HeLa WT cells and miR-34a KO clone were cultured for 1 day until confluence before scratch. Results of the analysis were obtained in triplicates.	66
Figure 14 Heat map on the enriched RNAs representing the top 50 most variable genes. The green bar identifies the HeLa KO clone while, the purple bar identifies the HeLa WT cells. The difference in the expression is signalled by the colour and its intensity: the less expressed genes are in blue, those more expressed in one line than the other are in red, while the genes in which there is no significant variation in the expression are represented in yellow.	67
Figure 15 Sequence alignment achieved by TargetScan tool between the consensus sequence of miR-34a and the 3'-UTR of the known and putative target genes.	68
Figure 16 RT-qPCR analysis on RNA extracted from HeLa cells (WT) vs KO clone. BCL2 (*p=0,012), MAP1B (*p=0,013), COL6A2 (**p=0,0016), NR3C1(*p=0,03), REL (*p=0,03), IKβα, ONECUT2 and KMT2D mRNA level of expression in HeLa WT cells (blue bar) vs HeLa KO clone (red bar). BCL2 and IKβα, known gene targets of miR-34a, were chosen as controls. Normalization was performed relative to RPLP0 gene expression. All data reported are representative of at least 3 independent experiments and error bars represent standard deviation (SD). The statistical significance was set at *p ≤ 0.05 or **p ≤ 0.01 that was measured by using the T-student test for independent data with GraphPad.....	69
Figure 17 Proliferation rate of HEK293T WT cells vs HEK293T KO clone.	70
Figure 18 RT-qPCR analysis on RNA extracted from HEK293T cells (WT) vs KO clones. IKβα (*p=0,024), AXL (**p=0,0085), TWIST1 (*p=0,028), MAP1B(*p=0,024), ONECUT2 (*p=0,011) and KMT2D (*p=0,035) mRNA level of expression in HeLa WT cells (blue bar) vs HEK293T KO clone (red bar). IKβα, AXL, TWIST1, BCL2, SIRT1, RAD51 known gene targets of miR-34a, were chosen as controls. Normalization was performed relative to RPLP0 gene expression. All data reported are representative of at least 3 independent experiments and error bars represent standard deviation (SD). The statistical significance was set at *p ≤ 0.05 or **p ≤ 0.01 that was measured by using the T-student test for independent data with GraphPad.	71
Figure 19 SIRT1 protein expression in HEK293T WT vs miR-34a KO cell lines; Western blot (A). All data reported are representative of at least 3 independent experiments and error bars represent standard deviation (SD). Densitometric analysis with ImageJ (*p = 0,035) (B).	72
Figure 20 IKβα protein expression in HEK293T cells (WT) vs HEK293T KO clone; Western blot (A). All data reported are representative of at least 3 independent experiments and error bars represent standard deviation (SD). Densitometric analysis with ImageI (B).	73
Figure 21 Western Blot analyses of ONECUT2 in HeLa (A) and HEK293T (B) miR-34a-KO clones compared to WT cell lines. Data reported are representative of at least 2 independent experiments and error bars represent standard deviation (SD). (C) Densitometric analysis with ImageJ.	75
Figure 22 Sanger Sequencing: the plasmid extracted from colony 3 contains the 512 bp fragment cloned and well oriented within the pGL3 vector.....	76

LIST OF TABLES

Table 1	Dysregulation of miRNA transcription in cancer (Zainab Ali Syeda et al. 2020).	24
Table 2	Dysregulation of miRNA biogenesis (Zainab Ali Syeda et al. 2020).	27
Table 3	Target site and gRNA sequences; gRNA1 targets the coding sequence of mature miR-34a; gRNA2 and 3 target the two DROSHA processing site (In red are highlighted the cloning sites.).	43
Table 4	Salting out reagents	44
Table 5	Salting out solutions.	44
Table 6	Reagents and primers for the PCR analysis on clones.	45
Table 7	Cycles for the PCR analysis on clones.	45
Table 8	RT master mix protocol.	46
Table 9	RT reaction protocol.	46
Table 10	qPCR master mix protocol.	46
Table 11	qPCR reaction protocol	47
Table 12	Genomic DNA elimination reaction.	51
Table 13	Reverse-transcription reaction.	51
Table 14	miR-34 predicted targets primer sequence.	52
Table 15	Primers for miR-34 validated target genes.	53
Table 16	Normalizer primer sequence.	53
Table 17	Mix PCR reaction.	53
Table 18	PCR condition.	54
Table 19	Western blot antibodies and molecular weight (MW) of the target proteins.	54
Table 20	Running gel reagents.	55
Table 21	Stacking gel reagents.	55
Table 22	Running buffer 10X reagents.	56
Table 23	Transfer buffer overnight 1X reagents.	56
Table 24	Forward (green) and Reverse (red) primers used for 3'-UTR-KMT2D 428 bp fragment amplification. The portions highlighted in green are 8-nucleotide tails added to improve cloning efficiency; XbaI restriction sites are highlighted in yellow.	57
Table 25	Colony PCR applied conditions.	58

ABBREVIATIONS

2G10 = HeLa miR-34a-KO

3.1D3 = HEK293T miR-34a-KO

3'-UTR = 3' untranslated region

5'-UTR = 5' untranslated region

A = adenosine

ADAR = RNA-acting adenosine deaminase

AGO = Argonaute

AKT = Serine/Threonine Kinase

AR = Androgen Receptor

ARE = AU-rich elements

ARGE = Tyrosine-Protein Kinase ARG

ARHGAP1 = Rho GTPase Activating Protein 1

ATP = Adenosine triphosphate

AXL = Receptor Tyrosine Kinase

BCL2 = B-cell lymphoma 2

BCL6 = B-Cell Lymphoma 6 Protein

Bp = base pair

C/EBP β = CCAAT/beta enhancer binding protein

CCNE1 = cyclin E1

CCR4-NOT = poly(A)-deadenylase complexes

CD44 = CD44 Molecule (Indian Blood Group)

CDK4/6 = Cyclin Dependent Kinase 4/6

cKit = KIT Proto-Oncogene, Receptor Tyrosine Kinase

c-Myc = MYC Proto-Oncogene, BHLH Transcription Factor

COL6A2 = Collagen Type VI Alpha 2 Chain

CRC = Colorectal cancer

CRISPR = Clustered Regularly Interspaced Short Palindromic Repeats

crRNA = mature CRISPR RNA

CSCs = cancer stem cells

c-SRC = SRC Proto-Oncogene, Non-Receptor Tyrosine Kinase

CTGF = connective tissue growth factor

DCP2 = Decapping protein 2

DDX17 = DEAD-box helicases p72

DDX5 = DEAD-box helicases p68

DGCR8 = RNA-binding protein DiGeorge Syndrome Critical Region 8

DICER = Ribonuclease III

DLBCL = diffuse large B-cell lymphoma

DLL1 = Delta-like 1

DMEM = Dulbecco's Modified Eagle Medium

DSB = double-strand break

dsRNA = double-stranded RNA

E2F1/5 = E2F Transcription Factor 1/5

Eag1 = Potassium Voltage-Gated Channel Subfamily H Member 1

EBNA2 = Staphylococcal Nuclease Domain-Containing Protein, Coactivator P100

eEF2K = Eukaryotic Elongation Factor 2 Kinase

EGFR = Epidermal Growth Factor Receptor

EHCC = cholangiocarcinoma extrahepatic

ELK1 = ETS Transcription Factor ELK1

EMT = epithelial-to-mesenchymal transition

ERBB2 = Erb-B2 Receptor Tyrosine Kinase 2

ERK = MAPK (Mitogen-Activated Protein Kinase)

ESCC = squamous cell carcinoma of the esophagus

FBS = Fetal bovine serum

FLOT2 = Flotillin 2

FMNL2 = Formin Like 2

FNDC3B = Fibronectin Type III Domain Containing 3B

FOXO = fork head transcription factors

FUT8 = Fucosyltransferase 8

FXR1 = Fragile-x-mental retardation related protein 1

GALNT7 = Polypeptide N-Acetylgalactosaminyltransferase 7

gRNA = guide RNA

HCC = hepatocellular carcinoma

HDL = high-density lipoprotein

HDR = error-free homology directed repair

HK1 = Hexokinase 1

HNF4G = Hepatocyte Nuclear Factor 4 Gamma

HNSC = head and neck squamous cell carcinoma

I = inosine

IK β α = NF-kB Inhibitor Alpha

IL-6R = Interleukin 6 Receptor

KMT2D = histone-lysine N-methyltransferase 2D

KO = Knock-Out

L1CAM = L1 Cell Adhesion Molecule

LDHA = Lactate Dehydrogenase A

LEF1 = Lymphoid Enhancer Binding Factor 1

LMTK3 = Lemur Tyrosine Kinase 3

m7G cap = 7-methylguanine capped

MAP1B = microtubule associated protein 1B

MAPK = Mitogen-Activated Protein Kinase

MAZ = MYC Associated Zinc Finger Protein

MET = Proto-Oncogene, Receptor Tyrosine Kinase

MicroRNPs = miRNA-protein complex

miPEP133 = peptide 133 encoded by pri-microRNA

miR-34a = microRNA 34a

MIR34AHG = precursor of miR-34a

miRISC = miRNA-induced silencing complex

miRNA = microRNA

MMP2/9 = Matrix Metalloproteinase 2/9

MREs = miRNA response elements

MYC = oncogenic transcription factor c-Myc

NF- κ B = NF-Kappa-B Transcription Factor P65 inhibitor

NHEJ = error-prone nonhomologous end joining

Notch = Receptor family

NPC = nasopharyngeal carcinoma

NPM1 = nucleophosmin 1

NSCLC = EGFR Epidermal Growth Factor Receptor

nt = nucleotides

ONECUT2 = One Cut Homeobox 2

p19ARF = CDKN, Cyclin Dependent Kinase Inhibitor

p53 = TP53 Tumor Protein P53

PAI-1 = SERPINE1, Serpin Family E Member 1

PAM = Proto-spacer Adjacent Motif

PAN2-PAN3 = poly(A)-deadenylase complexes

PCLO = Piccolo Presynaptic Cytomatrix Protein

PCR = polymerase chain reaction

PDGFR = Platelet Derived Growth Factor Receptor

PD-L1 = CD274 Programmed Cell Death 1 Ligand 1

pGL3-3'-UTR-KMT2D = pGL3 Promoter Vector with 3'-UTR of KMT2D

pGL3 \emptyset = pGL3 empty Promoter Vector

PI3K = Phosphatidylinositol-4,5-Bisphosphate 3-Kinase

PPP1R11 = Protein Phosphatase 1 Regulatory Inhibitor Subunit 11

pre-crRNA = precursor CRISPR RNA

pre-miRNA = precursor miRNA

pri-miRNA = primary transcript miRNA

PTEN = homologues of phosphatase and tensin

qPCR = quantitative PCR

RAD51 = RAD51 Recombinase

RNP = Ribonucleoprotein complex

Ser = Serine

sgRNA = single guide RNA

shRNA = small hairpin RNAs

SIRT1 = Sirtuin 1

SMAD4 = Mothers Against Decapentaplegic Homolog 4

SNAIL = Snail Family Transcriptional Repressor 1

STAT3 = Signal Transducer and Activator of Transcription 3

STMN1 = Stathmin 1

TALENs = Transcription Activator-Like Effector Nuclease

TARBP2 = Trans-Activation-Responsive RNA-Binding Protein

TCF4/7 = beta-catenin/T cell factor 4/7

TF = Transcription Factor

THBS1 = thrombospondin 1

Thr = Threonine

TWIST1 = Twist Family BHLH Transcription Factor 1

U = uracil

WB = Western blot

Wnt = Wingless-Type MMTV Integration Site Family

WT = wild type

XPO5 = exportin 5

XRN1 = exoribonuclease 1

YY1 = Yin Yang 1

ZBTB20 = Zinc Finger and BTB Domain Containing 20

ZEB1/2 = E-box-binding homeobox (ZEB) zinc-finger transcription factors

ZNF281 = Zinc Finger Protein 281

1. INTRODUCTION

1.1 MiRNA

The discovery of the first microRNA (miRNA), *lin-4*, in 1993 by the Ambros and Ruvkun groups in *Caenorhabditis elegans*^{7,8} has revolutionized the field of molecular biology. Since then, miRNAs have been detected in all animal model systems and some were shown to be highly conserved across species^{9,10}. miRNAs are small non-coding RNAs, with an average 22 nucleotides in length mainly active in the regulation of gene expression by binding to complementary sequences located often in the 3' untranslated region (3'-UTR) of target mRNA. miRNAs are transcribed from DNA sequences into primary miRNAs (pri-miRNAs) and processed into precursor miRNAs (pre-miRNAs) and mature miRNAs. In most cases, miRNAs interact with the 3' UTR of target mRNAs to suppress expression¹¹. However, interaction of miRNAs with other regions, including the 5' UTR, coding sequence, and gene promoters, have also been reported¹². miRNAs are critical for normal animal development and are involved in a variety of biological processes¹³. Aberrant expression of miRNAs is associated with many human diseases^{14,15}. In addition, miRNAs are secreted into extracellular fluids. Extracellular miRNAs have been widely reported as potential biomarkers for a variety of diseases and they also serve as signaling molecules to mediate cell-cell communications^{16–18}. miRNA biogenesis starts with the processing of RNA polymerase II/III transcripts post- or co-transcriptionally¹¹. About half of all currently identified miRNAs are intragenic and processed mostly from introns and relatively few exons of protein coding genes, while the remaining are intergenic, transcribed independently of a host gene and regulated by their own promoters^{19,20}. Sometimes miRNAs are transcribed as one long transcript called clusters, which may have similar seed regions, and in which case they are considered a family²¹. MiRNA biogenesis can occur through canonical and non-canonical pathways (**Figure 1**)²².

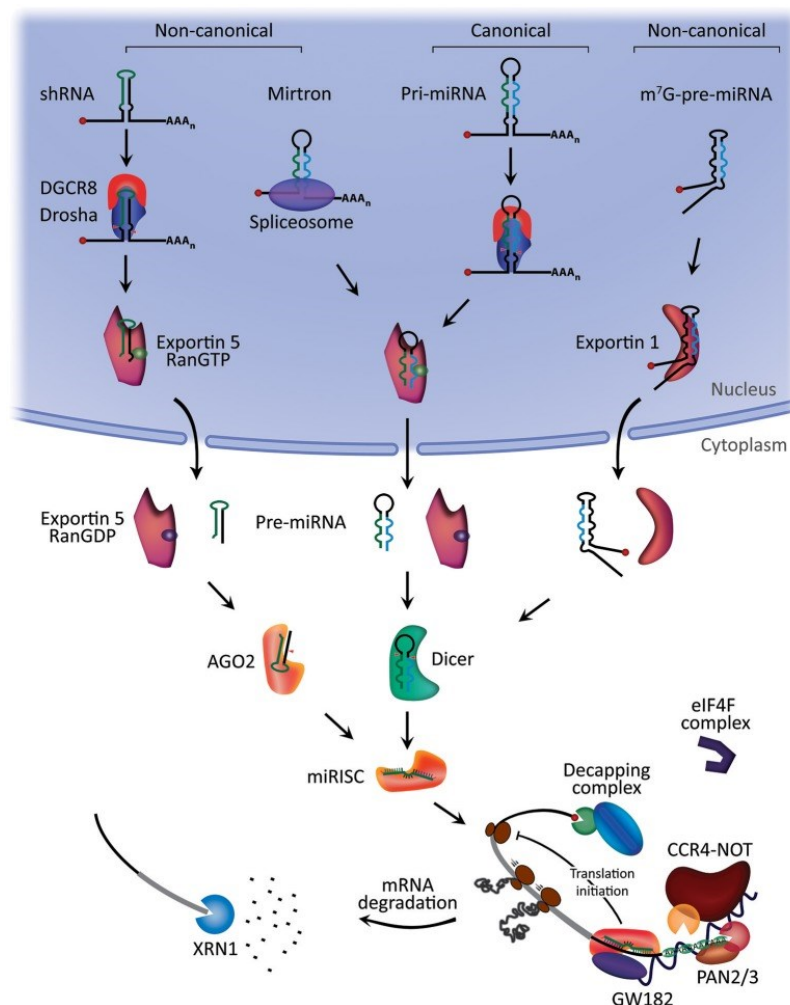


Figure 1 | Canonical and non-canonical microRNAs biogenesis and mechanism of action (Jacob O'Brien et al. 2018).

1.1.1 The canonical biogenesis pathway

The canonical pathway of biogenesis is the dominant pathway by which miRNAs are processed. In this pathway, pri-miRNAs are transcribed from their genes and then transformed into pre-miRNAs by the microprocessor complex, consisting of an RNA-binding protein DiGeorge Syndrome Critical Region 8 (DGCR8) and a ribonuclease III enzyme, Drosha²³. DGCR8 recognizes an N6-methyladenylated GGAC and other motifs within pri-miRNA²⁴, whereas Drosha cleaves the pri-miRNA duplex at the base of its characteristic hairpin structure. This results in the formation of a 2 nt overhang on the 3' of the pre-miRNA²⁵. Once generated, pre-miRNAs are exported to the cytoplasm by an exportin 5 (XPO5)/RanGTP complex and then processed by RNase III endonuclease Dicer^{23,26} which removes the terminal loop, forming a

mature duplex miRNA²⁷. The directionality of the miRNA strand determines the name of the mature form of miRNA: the 5p strand arises from the 5' end of the pre-miRNA hairpin while the 3p strand originates from the 3' end. Both strands derived from the mature miRNA duplex can be loaded by the Argonaute (AGO) protein family (AGO1-4 in humans) in an ATP-dependent manner²⁸. Selection of the 5p or 3p strand is based in part on thermodynamic stability at the 5' ends of the miRNA duplex or on a 5' uracil (U) at nucleotide position 1²⁹. Generally, the strand with lower 5' stability or 5' uracil is preferentially loaded into the AGO and is considered the lead strand. The unloaded strand is called the passenger strand, which will be unwound from the guide strand through various mechanisms according to the degree of complementarity. Passenger strands of miRNAs that do not contain mismatches are cleaved by AGO2 and degraded by cellular machinery that can induce strong strand polarization. Otherwise, miRNA duplexes with central mismatches or miRNAs not loaded with AGO2 are uncoiled and passively degraded¹¹.

1.1.2 Non canonical miRNA Biogenesis Pathways

To date, multiple non-canonical miRNA biogenesis pathways have been elucidated (**Figure 1**) that make use of different combinations of the proteins involved in the canonical pathway, mainly: Drosha, Dicer, exportin 5 and AGO2. In the non-canonical pathways, small hairpin RNAs (shRNA) are initially cleaved by the microprocessor complex and exported to the cytoplasm via Exportin5/RanGTP. They are further processed via AGO2-dependent, but Dicer-independent, cleavage. An example of such pre-miRNAs are mirtrons, produced from mRNA introns during splicing^{30,31} and 7-methylguanine capped (m7G)-pre-miRNA that are dependent on Dicer to complete their cytoplasmic maturation, but they differ in their nucleocytoplasmic shuttling. Mirtrons are exported via Exportin5/RanGTP while m7G-pre-miRNA are exported via Exportin1. There is strong polarization of the 3p filament most likely due to the m7G cap preventing loading of the 5p filament into Argonaute³². On the other hand, Dicer-independent miRNAs are processed by Drosha starting from endogenous short hairpin RNA (shRNA) transcripts³³. These pre-miRNAs require AGO2 to complete their maturation within the cytoplasm because they are of insufficient length to be Dicer substrates³³. This in turn promotes the loading of the entire pre-miRNA into AGO2 and the AGO2-dependent slicing of the 3p strand. The 3'-5' cleavage of the 5p strand completes their maturation³⁴.

1.1.3 Mechanisms of miRNA-mediated gene regulation

Most studies to date have shown that miRNAs bind to a specific sequence at the 3' UTR of their target mRNAs to induce translational repression and mRNA deadenylation and decapping^{35,36}. MiRNA binding sites have also been detected in other mRNA regions including the 5' UTR and coding sequence, as well as within promoter regions³⁷. Binding of miRNAs to the 5' UTR and coding regions has silencing effects on gene expression^{38,39} whereas miRNA interaction with the promoter region has been reported to induce transcription⁴⁰. The minimal miRNA-induced silencing complex (miRISC) consists of the guide strand and AGO⁴¹. The target specificity of miRISC is due to its interaction with complementary sequences on the target mRNA, called miRNA response elements (MREs). The degree of MRE complementarity determines whether there is AGO2-dependent affectation of target mRNA or miRISC-mediated translational inhibition and decay of target mRNA⁴². A fully complementary miRNA:MRE interaction induces AGO2 endonuclease activity and targets mRNA cleavage⁴². However, this interaction destabilizes the association between AGO and the 3' end of the miRNA favoring its degradation^{43,44}. In animal cells, most miRNA:MRE interactions are not completely complementary⁴⁵ but, contain central discrepancies with their guide miRNA, preventing AGO2 endonuclease activity. Consequently, AGO2 serves as a mediator of RNA interference, similar to non-endonucleolytic AGO family members (AGO1, 3 and 4 in humans). In many cases, a functional miRNA:MRE interaction occurs through the 5' seed region (nucleotides 2-8)^{37,46}. However, the additional paring at the 3' end aids the stability and specificity of the miRNA-target interaction¹². The formation of a silencing miRISC complex begins with the recruitment of the GW182 protein family by miRISC that provides the necessary scaffolding to recruit other effector proteins⁴⁷, such as the poly(A)-deadenylase complexes PAN2-PAN3 and CCR4-NOT, following the miRNA:target mRNA interaction^{45,48}. Decapping occurs facilitated by protein 2 (DCP2) and associated proteins⁴⁷, followed by 5'–3' degradation by exoribonuclease 1 (XRN1)⁴⁹ (**Figure 1**).

1.1.4 MicroRNA-Mediated Translational Activation

Although miRNAs are primarily attributed a function of gene expression repression, some studies have also reported miRNA-mediated upregulation of gene expression. In serum starved cells, AGO2 and another protein related to the miRNA-protein complex (microRNPs), Fragile-x-mental retardation related protein 1 (FXR1), were associated with AU-rich elements (AREs) at 3' UTR to activate translation⁵⁰. Several miRNAs, including let7, were found to be associated with AGO2 and FXR1 to activate translation during cell cycle arrest, but they inhibit translation in proliferating cells. Upregulation of gene expression by miRNAs was also observed in quiescent

cells, such as oocytes^{51,52}. The miRNA-mediated activation of translation involves AGO2 and FXR1 instead of GW182⁵¹. Other examples of gene activation by miRNAs include binding to the 5' UTR of mRNAs encoding ribosomal proteins during amino acid starvation⁵³. These results suggest that miRNA-mediated upregulation of gene expression occurs under specific conditions.

1.1.5 Dynamics of miRNA actions

Factors contributing to determine which genes are regulated by miRNAs include functionalized compartmentalization, shuttling of miRISC within cells, availability and abundance of miRNAs and their target mRNAs. MiRNA suppression of mRNA targets is not ubiquitous across cell types. Alternative splicing and alternative polyadenylation affecting 3' UTRs and RNA-binding proteins are cell type specific and affect the secondary structures of the target mRNA, changing the available pool of MREs⁵⁴⁻⁵⁶. This renders mRNA subsets sensitive or insensitive to miRNA-mediated gene regulation in a manner specific to each cell type/state.

1.1.6 Circulation of miRNAs

Numerous studies have demonstrated that miRNAs can be released into extracellular fluids. Extracellular miRNAs can be used as biomarkers for a variety of diseases⁵⁷⁻⁵⁹. They can be delivered to target cells and may act as autocrine, paracrine and/or endocrine regulators to modulate cellular activities⁶⁰ acting similarly to hormones. Many studies have detected extracellular/circulating miRNAs in biological fluids, such as plasma and serum^{61,62}, cerebrospinal fluid⁶³, saliva⁶⁴, breast milk⁶⁵, urine, tears, colostrum, peritoneal fluid, bronchial lavage, seminal fluid⁶⁶, and ovarian follicular fluid⁶⁷. Contrary to cellular RNA species, extracellular miRNAs are highly stable; they resist degradation at room temperature for up to 4 days and under deleterious conditions such as boiling, multiple freeze-thaw cycles, and high or low pH^{61,68}. There are two populations of extracellular miRNAs in biological fluids: one can be found in vesicles such as exosomes, micro vesicles and apoptotic bodies^{60,64} while the other is associated with proteins, particularly AGO2^{64,69}. The existence of predominantly exosomal or vesicle-free miRNAs could depend on the miRNA itself, the cell type they originate from, and/or other factors that influence miRNA secretion in individuals. Other proteins that bind extracellular miRNAs include high-density lipoprotein (HDL)^{70,71} and nucleophosmin 1 (NPM1)^{62,72,73}. The presence of miRNAs in vesicles or with companion proteins is generally believed to protect extracellular miRNAs and increase their stability in the extracellular environment⁶⁴.

1.2 miRNA in cancer

The miRNA-mediated control of gene expression is critical for the cellular response to the environmental stresses, such as starvation, hypoxia, oxidative stress and DNA damage, thus being implicated in human diseases such as cancer. Indeed, numerous miRNAs can function as

oncogenes (referred to as "oncomiRs") or tumor suppressors ("tumor suppressor miRs"), and dysregulation of miRNA expression is closely associated with cancer initiation, progression, and metastasis^{74,75}. MiRNA expression is deregulated in cancer with special attention paid to cancer-associated transcriptional and post-transcriptional programs, including transcriptional control, epigenetic methylation of miRNA loci, and dysregulation of the mature miRNA biogenesis pathway.

1.2.1 miRNA Deregulation in Cancer

miRNAs have been shown to be extensively deregulated in human cancers, highlighting their important role in tumor initiation, growth, and metastasis. Lu et al. demonstrated that the expression of 217 miRNAs in mammalian samples is globally suppressed in tumor cells compared to normal cells⁷⁶. In addition to the global downregulation of miRNA expression, Volinia et al. presented the differentially expressed miRNAs in 540 solid tumor samples. In this study it was demonstrated that during tumor progression, the miRNA regulatory pattern undergoes profound changes indicating that specific and individual alterations of expression exist in different tumors⁷⁷. For example, the expression level of miR-21 is higher in the early stage of diffuse large B-cell lymphoma (DLBCL) than in the later stages⁷⁸. Also, some miRNAs enclosed in exosomes for secretion have been shown to be functionally implicated and clinically relevant in cancer⁷⁹. Indeed, they can circulate throughout the body and act differentially in a tissue-dependent manner. These include miR-21, the miR-200 family, and the miR-17~92 cluster. Cimino et al. further confirmed that miR-15 and miR-16 enclosed in exosomal vesicles induce apoptosis by acting on the B-cell lymphoma 2 (BCL2) gene in leukemia⁸⁰, while let-7 is downregulated in breast, colon and lung⁸¹ and has been shown to be a tumor suppressor miR because it represses the expression of RAS and MYC preventing tumor development^{82,83}.

1.2.2 Dysregulation of miRNA transcription in cancer

The deregulation of miRNA transcription in cancer resides in the aberrant expression of transcription factors (a) or DNA methylation that controls their production at the epigenetic level (b)⁸⁴ (**Table 1**).

(a) Modulation of miRNA expression by transcription factors in cancer

Several studies have provided compelling evidence that alterations in transcriptional activators or repressors cause abnormal pri-miRNA transcription in cancer. For example, the expression of miR-34 family genes (miR-34a, miR-34b and miR-34c) is controlled by the transcription factor p53⁸⁵. In case of DNA damage and oncogenic stress, p53 is activated and regulates the transcription of miR-34, which in turn affects cell cycle arrest, apoptosis and senescence⁸⁶. miR-

145 is also transcriptionally activated by p53 upregulated to induce apoptosis⁸⁷⁻⁸⁹ and by other transcription factors, including CCAAT/beta enhancer binding protein (C/EBP β), beta-catenin/T cell factor 4 (TCF4) and fork head transcription factors FOXO1 and FOXO3 in human cancers^{90,91}. The oncogenic transcription factor c-Myc (MYC) transactivates the expression of the miR-17~92 cluster (also known as oncomiR-1) promoting cancer progression and controlling the expression of E2F1, connective tissue growth factor (CTGF), thrombospondin 1 (THBS1) and homologues of phosphatase and tensin (PTEN) in various tumors⁹²⁻⁹⁷. E-box-binding homeobox (ZEB) zinc-finger transcription factors, ZEB1 and ZEB2, known as key activators to promote epithelial-mesenchymal transition (EMT), repress miR-200 family gene transcription⁹⁸. Furthermore, miR-200c has been identified as a transcriptional target of MYC in nasopharyngeal carcinoma⁹⁹.

(b) Aberrant miRNA expression by DNA methylation modification in cancer

The transcription of pri-miRNA is also influenced by epigenetic control, in particular by methylation of the promoter-associated CpG islands. In human bladder cancer, miR-127 is silenced through hypermethylation of its promoter, resulting in increased expression of its known target gene, BCL6¹⁰⁰. Hypermethylation of the miR-124-1 promoter region has been noted in leukemia, lymphoma, breast, colon, and liver cancers. Epigenetic repression of miR-124-1 leads to the activation of its known target, CDK6^{101,102}, whereas that of miR-220 is frequently found in bladder¹⁰³, breast¹⁰⁴ and non-small lung¹⁰⁵. The miR-34, miR-34a and miR-34b/c family members are located separately on different chromosomes and are hypermethylated in solid tumors and hematologic malignancies^{106,107}. Besides DNA methylation, histone modification also influences the control of miRNA expression by chromatin remodeling¹⁰⁸.

Table 1 | *Dysregulation of miRNA transcription in cancer (Zainab Ali Syeda et al. 2020).*

Regulation of miRNA Expression by DNA Binding Factor				
Factor	miRNA	Mechanism/Function/ Clinical Correlation	Cancer Type	References
Transcriptional activation by p53	miR-34a, miR-34b, miR-34c	Cell cycle arrest, apoptosis & senescence	Various types of cancers	[85]
	miR-145	Apoptosis	Various cancers like prostate cancer	[87,88]
Transcriptional repression by RREB1	miR-143/145 cluster	Transcriptional repression of miR-143/145 cluster	Various cancers like Pancreatic, Colorectal Adenocarcinoma	[109]
Regulation by C/EBPβ, beta-catenin/TCF4, FOXO1 & FOXO3	miR-145		Various cancers like Renal cancer	[90,91]
Regulation by MN1	miR-20a, miR-181b	Inverse correlation between MN1 and miRNAs	acute myeloid leukemia (AML) patients	[110]
Transcriptional activation by Myc	miR-17~92 cluster	Controls the expression of E2F1, THBS1, CTGF, & PTEN	Various types of cancer, including B- Cell lymphoma & Breast cancer	[92–96]
	miR-200c, miR-26, miR-29, miR-30, let-7	Suppresses the expression of their genes	Nasopharyngeal carcinoma & Lymphoma	[99,111–113]
HIF1α	miR-210	Repression of initiation of tumor growth	Various cancers like Head & neck tumor	[114]
	miR-155		[115]	
ZEB1 & ZEB2	miR-200 family		Various cancers	[98]
Repression by ER	miR-221/222	Suppression of miR-221/222 expression by NcoR/SMRT complex	Breast cancer	[116]
	miR-515	Increased levels of oncogenic SK1	Breast cancer	[117]
Androgen/AR	miR-125b, miR-21, miR-221/222, miR-27a, miR-32	Oncogenic role	Prostate cancer & Hematological malignancies	[118] [119,120]
	miR-135a, miR-141	Tumor suppressive role	Prostate cancer	[121,122]

Progesterone receptor /PR	miR-141, miR-23, miR-320, let-7		Breast & ovarian cancer	[123–126]
Glucocorticoids/GR	miR-15, miR-16, miR-223	Increasead expression of miRNA	Leukemia cell lines	[127]
Regulation of miRNA Expression by Epigenetic Alteration				
Factor	miRNA	Mechanism/Function/ Clinical Correlation	Cancer Type	References
Promoter hypermethylation	miR-127	Increased expression of BCL6	Bladder Cancer	[100]
Promoter hypermethylation	miR-124-1	Activation of, CDK6	Breast, Colon, Liver, Leukemias & Lymphomas	[101,102]
Promoter hypermethylation	miR-129-2	Upregulation of SOX4	Endometrial Gastric cancer	[128]

1.2.3 Dysregulation of Pri-miRNA Processing in Cancer

Dysregulation of pri-miRNA processing in cancer can be caused by defects associated with microprocessor proteins (a) or by dysregulation of its editing (b)⁸⁴ (**Table 2**).

(a) Dysregulation of the Microprocessor-Associated Proteins in Cancer such as DROSHA- or DGCR8-associated proteins, pri-miRNA-associated RNA-binding proteins, and cellular signaling components, may affect pri-miRNA processing. Analysis of a DROSHA-containing large complex has revealed that several microprocessor-associated RNA-binding proteins, including DEAD-box helicases p68 (also known as DDX5)¹²⁹ and p72 (also known as DDX17)¹³⁰ facilitate pri-miRNA processing. p68/p72 may serve as scaffold proteins to recruit multiple different protein factors to the DROSHA microprocessor. Interestingly, the p53 tumor suppressor protein interacts with the microprocessor complex via p68/p72 and thereby enhances the biogenesis of oncosuppressor miRs, such as miR-16-1, miR-143, and miR-145⁸⁷.

(b) Dysregulation of pri-miRNA Editing in Cancer

RNA editing is the major post-transcriptional mechanism that modifies specific nucleotides at the RNA level. RNA-acting adenosine deaminases (ADARs) are the RNA modification enzymes that convert adenosine (A) to inosine (I) in double-stranded RNAs (dsRNA). ADAR can modify dsRNA in the pri-miRNA stem region and modify their secondary structure, inhibiting their processing by the DROSHA/DGCR8 microprocessor complex and leading to their degradation

by endonuclease V¹³¹. Recent studies have shown that miRNA editing is dysregulated in human cancers, and miRNA-related editing promotes or inhibits tumor development and progression¹³².

1.2.4 Dysregulation of Pre-miRNA Processing in Cancer

Dysregulation of pre-miRNA processing in cancer includes defects related to pre-miRNA export components (such as XPO5) and proteins directly involved in their processing (such as DICER1 and TARBP2). The pre-miRNA generated by the microprocessor in the nucleus is transported to the cytoplasm by a complex of XPO5 and RAN-GTP, a cofactor of XPO5. DICER1 recognizes 2 nt 30 overhang of the pre-miRNA, 22 nt away from which the cleavage site is defined¹³³. DICER1 is associated with the dsRNA-binding protein TARBP2 to increase the stability of the DICER1-RNA complex and improve the fidelity of miRNA processing. In cancer, defects in the export components of pre-miRNAs may affect their abundance in some districts to the detriment of others. Inactivated mutations of XPO5 cause the pre-miRNA export defect, leading to the accumulation of pre-miRNA in the nucleus. Genetic alterations of XPO5 are also associated with breast cancer risk¹³⁴. Furthermore, the MAPK/ERK pathway can suppress pre-miRNA export through phosphorylation of XPO5 at Thr345, Ser416 and Ser497¹³⁵. XPO5 phosphorylation correlates with global miRNA downregulation and poor prognosis in patients with hepatocellular carcinoma, providing functional and clinical evidence for cancer-associated dysregulation of XPO5 for aberrant miRNA processing and tumorigenesis. Instead, global inhibition of miRNA biogenesis by DICER1 depletion promotes cell growth and tumorigenesis in human cancer cell lines and mouse models of cancer¹³⁶, suggesting the oncogenic role of DICER1 in tumorigenesis. Recurrent somatic and germline mutations of DICER1 that change its protein levels and/or impair its function, leading to defective pre-miRNA processing, are frequently found in many types of cancers, including pleuropulmonary blastoma, rhabdomyosarcoma, non-epithelial and liver cancer¹³⁷⁻¹⁴². TARBP2 frameshift mutations are found in sporadic and heritable carcinomas with microsatellite instability and correlate with reduced levels of DICER1 and mature miRNAs¹⁴³. TARBP2 is overexpressed in cutaneous melanoma, adrenocortical carcinoma, and metastatic breast and prostate cancers¹⁴⁴. Finally, AGO2, a key regulator of miRNA function and maturation, was found to be overexpressed in various types of human cancers, including breast, gastric, and head and neck cancers¹⁴⁵⁻¹⁴⁸

Table 2 | *Dysregulation of miRNA biogenesis (Zainab Ali Syeda et al. 2020).*

The Microprocessor in Cancer				
Factor	miRNA	Mechanism/Function/ Clinical Correlation	Cancer Type	References
Up/downregulation of DROSHA	Global miRNA expression	Cancer progression & poor patient survival	Cervical carcinoma, Wilms tumor	[149,150]
Drosha E147K mutation	Global miRNA expression	Reduced function	Wilms tumors	[151–154]
Upregulation of DGCR8 expression	Global miRNA expression	Dysregulation is associated with poor patient survival	Esophageal, Bladder, Prostate & ovarian cancer	[155]
E518K mutation in the dsRBD1 domain of DGCR8	Decrease of crucial miRNAs		Wilms tumors	[152,154]
Regulation of Microprocessor in Cancer				
Factor	miRNA	Mechanism/Function/ Clinical Correlation	Cancer Type	References
NF90/NF45	pri-let-7, pri-miR-7-1	Inhibits the processing	Hepatocellular carcinoma	[156,157]
Pre-miRNA Export in Cancer				
Factor	miRNA	Mechanism/Function/ Clinical Correlation	Cancer Type	References
Mutations of XPO5	Global miRNA expression	Accumulation of pre-miRNA in the nucleus	Sporadic colon cancer, Gastric & Endometrial cancer	[158]
	Global miRNA expression	Correlates with global miRNA downregulation and with poor survival in patients	Hepatocellular carcinoma	[135]
DICER1 and TARBP2 in Cancer				
Factor	miRNA	Mechanism/Function/ Clinical Correlation	Cancer Type	References
Mutations of DICER1	Global miRNA expression	Somatic and germline DICER1 mutations lead to defective pre-miRNA processing	Pleuropulmonary blastoma, Rhabdomyosarcoma, non-epithelial ovarian cancers, liver tumor	[137–142]
Mutations within the RNase IIIb domain of DICER1	5p miRNAs	Deregulation of pre miRNA expression	Various cancer like ovarian cancer	[155,159]
TARBP2 Deletion	Global miRNA expression		Adenoid cystic carcinoma	[160]
Upregulation of TARBP2 expression			Melanoma, breast & prostate cancer	[144]
Frameshift mutations of TARBP2	Global miRNA expression	Reduced levels of DICER1 and mature miRNAs	Sporadic & hereditary carcinomas	[143]
AGO2 in Cancer				
Factor	miRNA	Mechanism/Function/ Clinical Correlation	Cancer Type	References
AGO2 expression dysregulation	oncomiRs	Repression of the targets of oncomiRs	Breast, gastric, head & neck cancers	[145–148]

1.3 MiR-34a

The miR-34 family, along with the let-7 and miR-200 families, are three major tumor-suppressive miRNA families. The miR-34 family consists of three members: miR-34a (**Figure 2**), miR-34b, and miR-34c. miR-34a is encoded in the second exon of a gene located on chromosome 1p36.22 (**Figure 2B**), whereas miR-34b and miR-34c are expressed from a polycistronic transcript encoded on chromosome 11q23.1. The mature miR34a sequence consists of 22 nucleotides and

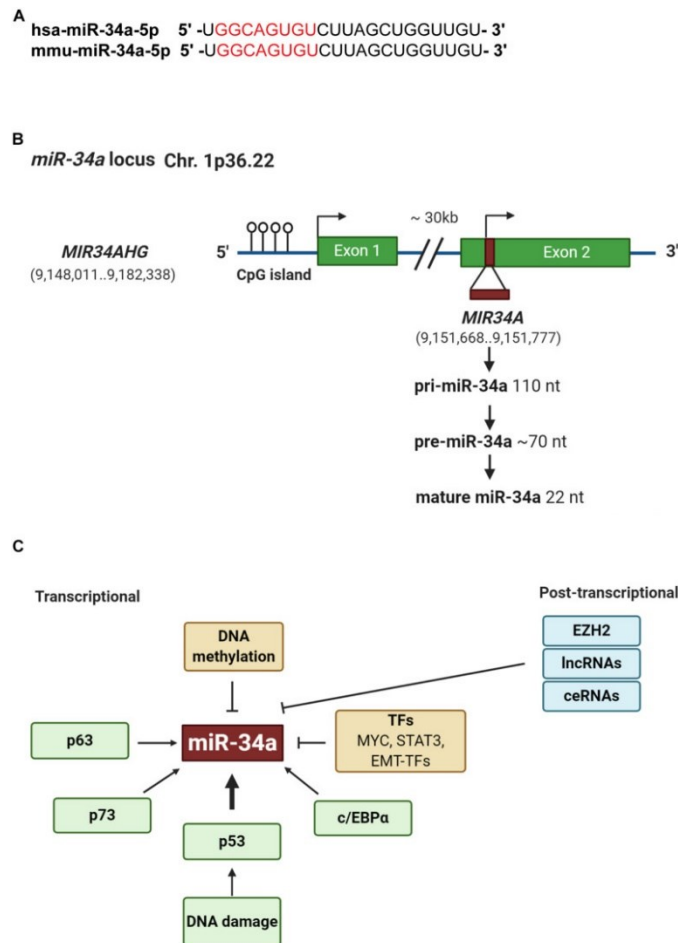


Figure 2 | Genomic structure and regulation of miR-34a. (A) Sequence alignment of the mature human and mouse miR-34a. The seed sequences are highlighted in red. (B) Structure of miR-34a genomic loci. Green boxes represent exons. Horizontal arrow marks transcription start site. (C) Regulation of miR-34a. At the transcriptional level, p53, p63, and p73 induces whereas DNA methylation, TME-TFs such as SNAIL and ZEB1, STAT3, and Myc repress miR-34a expression. At the posttranscriptional level, EZH2, lncRNAs, and competing endogenous RNAs (ceRNAs) may negatively regulate miR-34a expression (Wen (Jess) Li et al. 2021).

shares 86% (19/22 nt) and 82% (18/22 nt) homology with miR-34b and miR-34c, respectively¹⁶¹, suggesting that the miR-34 family members could share a similar set of targets and thus be functionally redundant. miR-34a is the prevailing family member in normal human tissues, whereas miR-34b/c are expressed at lower levels in most tissues except the lung, ovary, testes, and trachea¹⁶². miR-34a in both human and mouse have identical seed sequences, i.e., 5' - GGCAGUGU - 3' (**Figure 2A**).

1.3.1 miR-34a in cancer

Loss of miR-34a expression occurs in a wide range of solid tumors and hematological malignancies¹⁶¹. Since miR-34 was identified as a p53 target in 2007 (**Figure 1C**), extensive research has demonstrated miR-34a as an essential mediator of p53 functions and a potent tumor suppressor. Indeed, miR-34a suppresses tumor growth and cancer progression by inhibiting multiple tumor-promoting processes including the cell cycle, epithelial-to-mesenchymal transition (EMT), metastasis, stemness, and tumor immunity and by inducing tumor-inhibitory events such as apoptosis and senescence. MiR-34a regulates these cellular processes by downregulating target mRNAs. Notably, miR-34a is a potent suppressor of cancer stem cells (CSCs) in various cancers (**Figure 3**)¹⁶³.

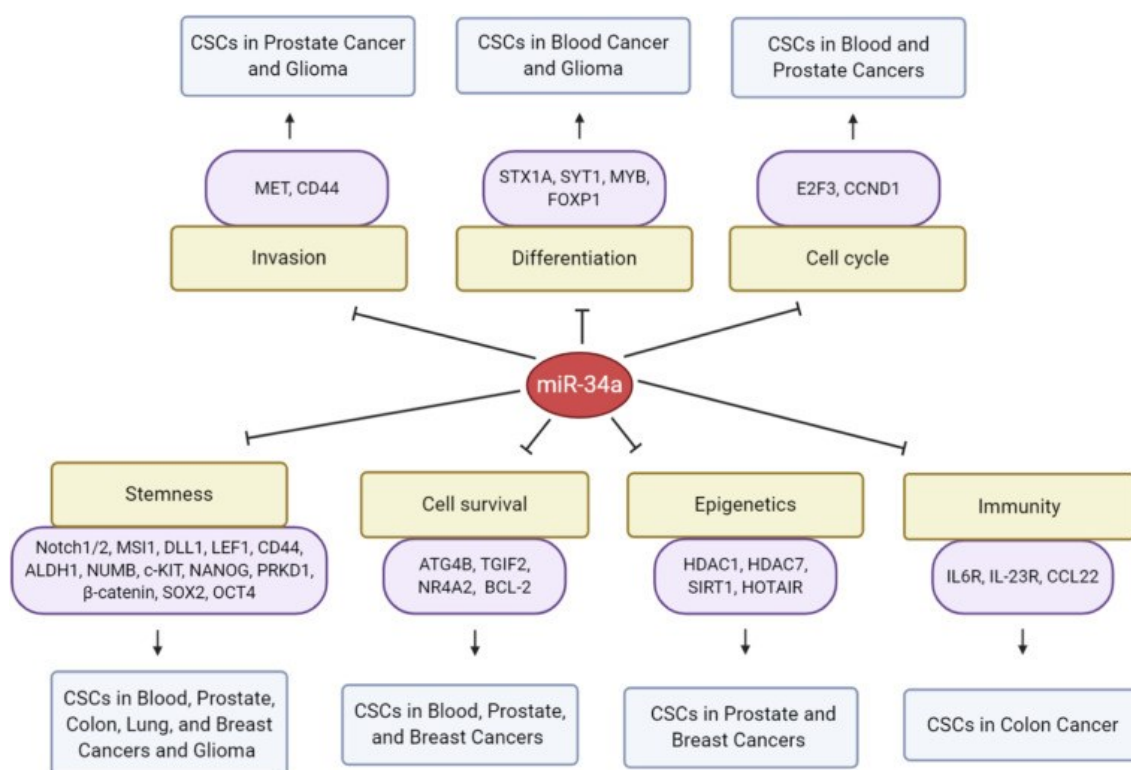


Figure 3 | MicroRNA-34a regulation of CSCs. Presented are direct targets of miR-34a and biological consequences on CSCs in the indicated cancer types (Wen Jess Li et al. 2021).

1.3.2 Functions of miR-34a in cancer

Several common targets of miR-34a, miR-34b and miR-34c, such as MET, FOXP1 and CDK6 are involved in the regulation of signal transduction, macromolecule metabolism and protein modification. Some of them are associated with several key signaling pathways, including MAPK, Notch, Wnt, PI3K/AKT, p53 and Ras, as well as apoptosis, cell cycle and EMT related pathways (**Figure 4**). Furthermore, some highly significant signaling pathways were also identified, such as Rap1, autophagy, and cell differentiation-related pathways (**Figure 4**)¹⁶⁴. Together, the antitumor effects of miR-34 are mediated by numerous downstream targets, which are involved in critical signaling pathways; the main signaling pathways involving miR-34a are reposted below (a) cell proliferation and tumor growth; (b) tumor invasion and metastasis; (c) apoptosis.

(a) Cell proliferation and tumor growth

MiR-34a has been extensively confirmed to attenuate cell proliferation and tumor growth in several cancer types. In breast cancer and in triple negative breast cancer (TNBC), miR-34a accomplishes this function by silencing or downregulating the expression of multiple downstream targets, such as LDHA, LMTK3, ERBB2, tRNAi Met, eEF2K, FOXM1, c-SRC, BCL2, SIRT1 and WNT1¹⁻⁶. MiR-34a performs the function of reducing cell proliferation also by downregulating downstream targets such as PDGFR, MET and YY1 (Yin Yang 1) in gastric cancer and PDGFR- α/β , CCNE1 (cyclin E1) and EGFR in lung cancer, PD-L1 and Notch1 in glioma, delaying thus the growth of different tumors¹⁶⁵⁻¹⁷⁰. miR-34a negatively regulates the expression of LDHA (lactate dehydrogenase A), FUT8 and HK1 in hepatocellular carcinoma (HCC); c-Myc and STMN1 in prostate cancer; Eag1 and STMN1 in osteosarcoma, as well as MYCN and DLL1 in medulloblastoma, thereby attenuating tumor cell proliferation^{171,172,173-179}. Recently, miR-34a has been confirmed to suppress tumor growth in several other cancers, through downregulation of HNF4G in bladder cancer, FLOT2 in melanoma, c-MET and AXL in peritoneal mesothelioma, HDAC1 in ovarian cancer, LDHA in cervical cancer, PDGFR- α in colon cancer, Notch1 in endometrial cancer and DLL1 (Delta-like1) in choriocarcinoma, respectively¹⁸⁰⁻¹⁸⁷. The anti-proliferative effect of miR-34a was also validated in non-solid tumor cells, by downregulating c-SRC in K-562 cells and by targeting FOXP1 in DLBCL cells^{188,189}.

(b) Tumor invasion and metastasis

Ectopic miR-34a expression is fully validated to inhibit colorectal cancer cell migration, invasion and metastasis through downregulation of FMNL2, E2F5, IL6R, PAI-1, PPP1R11, ZNF281 expression, cKit and GALNT7 both in vitro and in vivo and most of the targets are involved in

the EMT process^{168,190–195}. In breast cancer, miR-34a has been shown to target CXCL10, ErbB2, cSRC, Notch1 and FOXM1/Eef2K signaling pathways, thereby limiting tumor invasion and metastasis^{196–199}.

In lung cancer, miR-34a has also been reported to reduce or silence the expression of PAI-1, EGFR, ARHGAP1, and PDGF- α / β , thereby inhibiting tumor cell invasion by affecting the EMT process or cell remodeling cytoskeleton^{169,196,200,201}. With respect to prostate cancer, several pivotal or metastasis-related targets of EMT, including AR, Notch1, TCF7, LEF1, and STMN1, have been shown to be directly modulated by miR-34a, thereby reducing the aggressiveness of prostate cancer^{176,202–204}. miR-34a has also been implicated in HNF4G and CD44 in bladder cancer; and MMP2, MMP9, FNDC3B and YY1 in squamous cell carcinoma of the esophagus (ESCC)^{205–209}. Furthermore, tumor metastasis has been confirmed in various other cancers by targeting vital drivers of tumor invasion, such as c-Met in osteosarcoma, Snail in ovarian cancer, DLL1 in choriocarcinoma, L1CAM in endometrial cancer, SMAD4 in cholangiocarcinoma extrahepatic (EHCC) and nasopharyngeal carcinoma (NPC), FLOT2 in melanoma, IL-6R in oral carcinoma, CD44 in clear renal cell carcinoma, ARGE in head and neck squamous cell carcinoma (HNSC)^{182,187,210–217}.

(c) Apoptosis

miR-34a-mediated tumor cell apoptosis has been confirmed in various cancers such as: lung cancer (EGFR, PDGFR- α / β , AXL and MDM4)^{169,196,218,219}, gastric cancer (MET and SIRT1)^{220,221}, glioma (BCL2 and SIRT1)²²² and colon cancer (SIRT1)²²³. In addition, several other targets, including HDAC1 (hepatocellular carcinoma)²²⁴, E2F3 (neuroblastoma)²²⁵, BIRC5 (laryngeal squamous cell carcinoma)²²⁶, MET (gastric cancer)²²⁰, NOTCH1 (pancreatic cancer)²²⁷ and tRNAi Met (breast cancer)²²⁸, have been found to be involved in miR-34a-dependent tumor cell apoptosis.

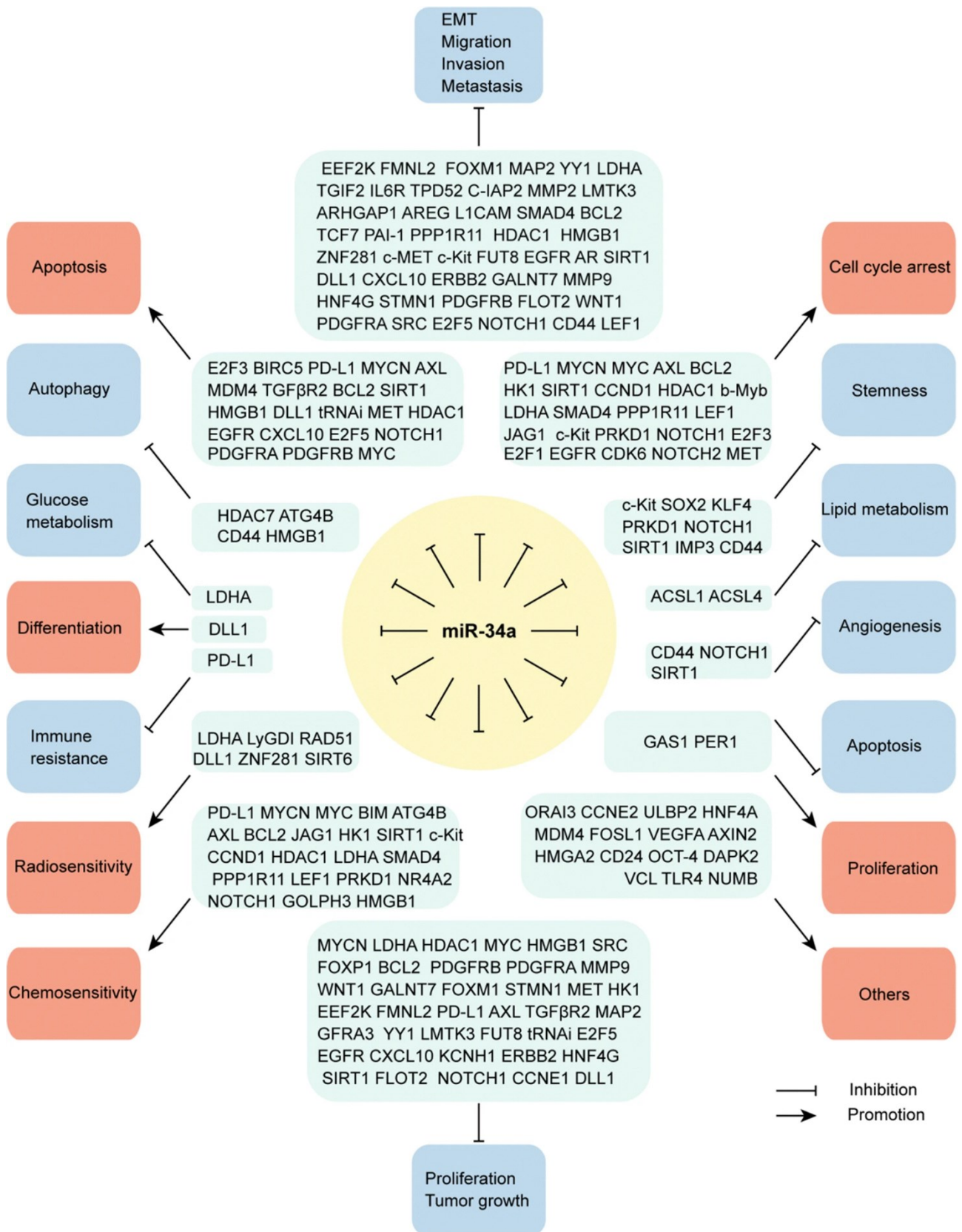


Figure 4 | Crucial tumor-suppressive effects of miR-34a mediated by downstream targets. As a well-defined tumor suppressor, miR-34a has been convincingly validated to directly repress various downstream targets and affect critical signaling pathways, hence exerting multifaceted antitumor roles to block tumor progression (Sijing Li et al.2021).

1.3.3 Upstream regulators of miR-34a in cancer

The upstream deregulation of miR-34a transcription may depend on the upstream transcription factors (a) that regulate its production or on an incorrect methylation status at the level of its regulatory CpG islands (b).

- (a) There are various upstream transcription factors (TFs) of miR-34a, which mediate miR-34a activation or suppression (**Figure 5**). TAp73 and TAp63 (isoforms of p73 and p63, the homologues of p53) have been reported to directly activate miR-34a transcription. TAp63 can also enhance the maturation process of miR-34a via Dicer activation, to attenuate tumorigenesis and tumor metastasis^{201,229–231}. Furthermore, miR-34a plays a crucial role in gastric cancer and acute lymphoblastic leukemia development by upregulating Bmi1, p65 (NF- κ B3) and C/EBP α ^{232–234}. Other TFs, such as ELK1, MAZ and p19ARF, are also reported as positive modulators of miR-34a^{234–236}. MYC and STAT3 negatively regulate miR-34a transcription in tumors (MYC in breast cancer, gastric cancer, and DLBCL; STAT3 in CRC and NSCLC), further promoting tumor cell proliferation and invasion^{112,189,200,237,238}. MiR-34a is involved also in the EMT process of CRC by inhibiting important TFs such as SNAIL and ZEB1^{193,239}. Furthermore, it was recently found that MYCN-mediated miR-34a inhibition is associated with neuronal differentiation in neuroblastoma while EBNA2-mediated miR-34a inhibition is associated with immune resistance (B-cell lymphomas)^{229,240}.

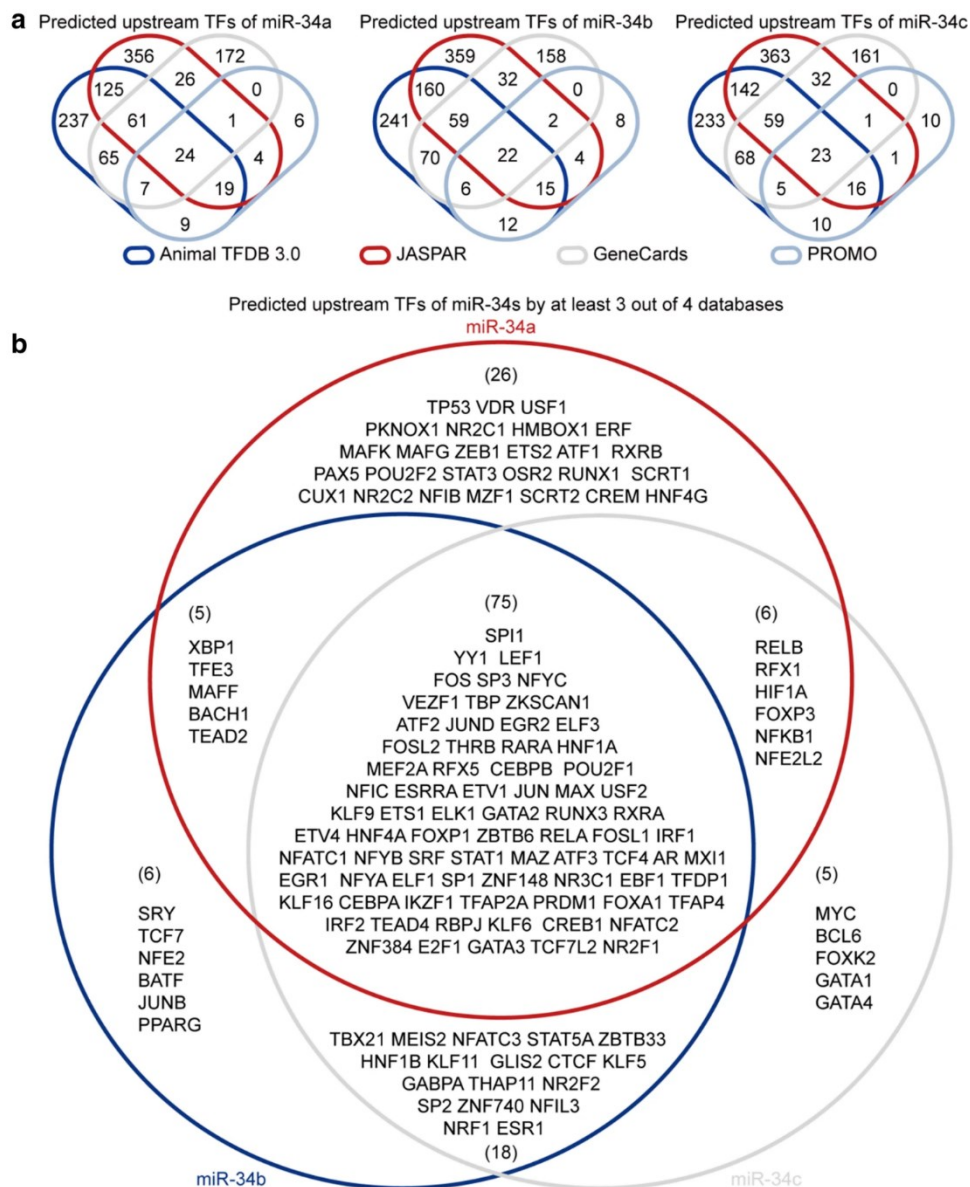


Figure 5 | Predicted upstream transcription factors (TFs) of miR-34s. **a** Putative upstream TFs of miR-34s predicted by Animal TFDB 3.0 (<http://bioinfo.life.hust.edu.cn/AnimalTFDB/#/>), JASPAR (<http://jaspar.genereg.net/>), GeneCards (<https://www.genecards.org/>), and PROMO (http://algggen.lsi.upc.es/cgi-bin/promo_v3/promo/promoinit.cgi?dirDB=TF_8.3).

(b) Aberrant methylation of CpG islands at the promoter level is another cause leading to repression of miR-34a transcription in most solid tumors and malignancies. MiR-34a methylation has been detected in numerous solid tumors: colon, pancreas, kidney, breast, lung, bladder, melanoma and prostate, esophageal carcinoma, and Ph-negative myeloproliferative neoplasms^{241–243}. MiR-34a methylation was shown to range from 4 to 18.8% in chronic lymphocytic leukemia, multiple myeloma, and Hodgkin's lymphoma, whereas this event was more frequent at the cellular level

in lymphoma (75%) and in myeloma (37%) compared to normal cells²⁴⁴. In esophageal cancer, miR-34a methylation was shown to be positively correlated with tumor stages and lymph node metastases²⁴⁵. Furthermore, miR-34a inactivation by methylation can enhance the expression of c-Met and β -catenin which are crucial factors of ETM and which in combination with miR-34a methylation status represent a higher prognostic value for the formation of distant metastases of colon cancer²⁴⁶.

1.3.4 miPEP133 as a novel tumor-suppressor microprotein encoded by miR-34a pri-miRNA.

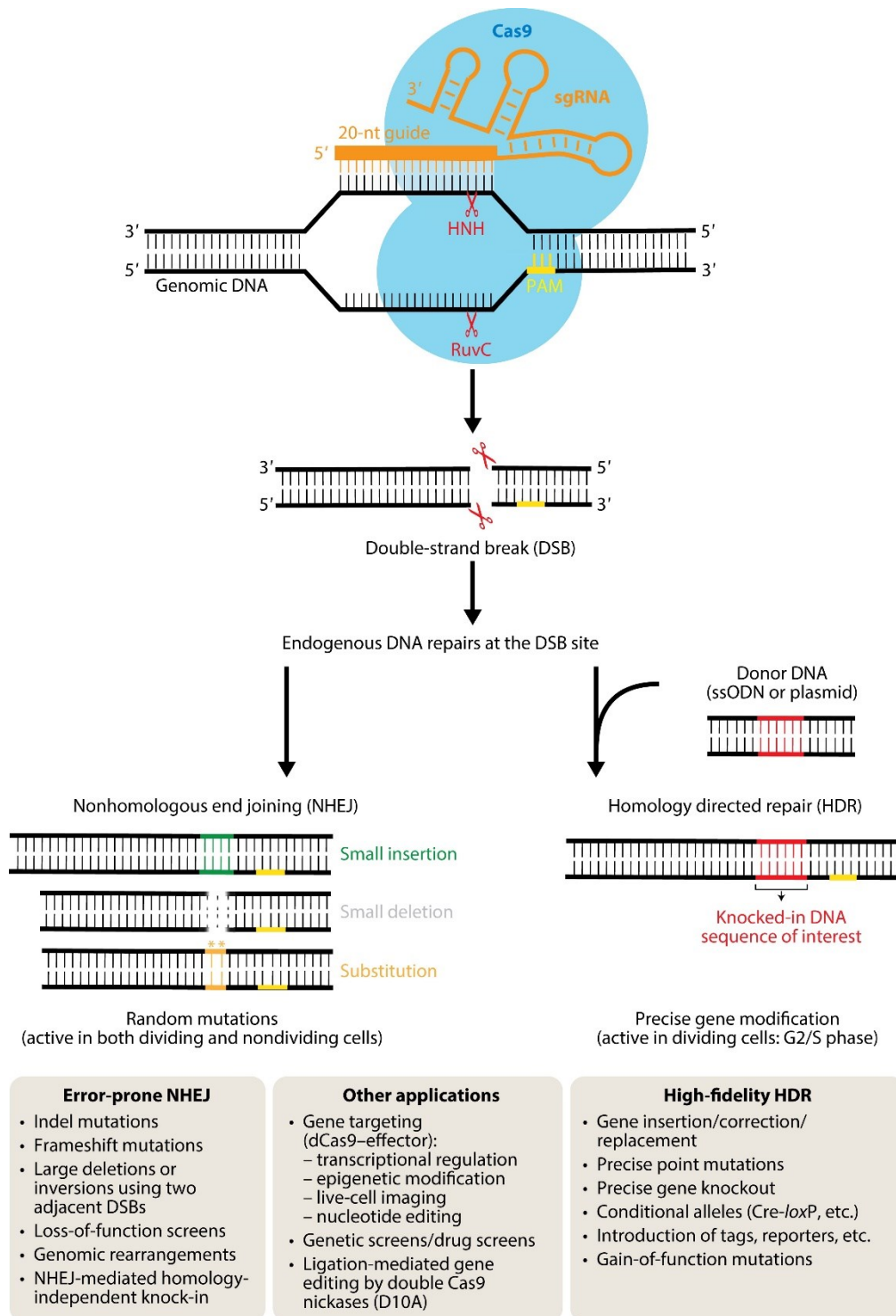
Very few proteins encoded by putative noncoding RNA transcripts have been identified, and their cellular functions remain largely unknown. In a recent study, Min Kang et al. 2020 evaluated the tumor suppressor function of a microprotein located in the mitochondria and encoded by the miR-34a precursor, signaling it as a potential prognostic marker and therapeutic target for multiple types of cancer. The microprotein in question is made up of 133 amino acid residues, from which it takes its name as miPEP133 (peptide 133 encoded by pri-microRNA). Min Kang et al. overexpressed miPEP133 in nasopharyngeal carcinoma (NPC) cell lines, ovarian carcinoma, and cervical carcinoma cells to determine its impact on tumor growth in a xenograft model of NPC. miPEP133 is expressed in normal human colon, stomach, ovaries, uterus, and pharynx, but was downregulated in cancer cell lines and tumors. In this study, miPEP133 overexpression was shown to induce apoptosis in tumor cells and inhibit their migration and invasion, while miPEP133 low expression represents a poor prognostic marker associated with advanced metastatic NPC. Furthermore, wild-type, but not p53-mutant P53 cells were shown to induce miPEP133 expression which in turn enhanced p53 transcriptional activation and miR-34a expression. miPEP133 is located in the mitochondria and interacts with mitochondrial heat shock protein 70kD (HSPA9) to prevent the interaction of HSPA9 with its binding partners, leading to decreased mitochondrial membrane potential and mitochondrial bulk²⁴⁷.

1.4 CRISPR/CAS

1.4.1 General

The Clustered Regularly Interspaced Short Palindromic Repeats (CRISPR)/Cas (CRISPR associated) system is a mechanism used by bacterial cells to defend themselves against phages infection and plasmids transfer and it is used today as genome editing tool. CRISPRs were identified, for the first time by Japanese researchers, studying the genome of *E. coli*, in 1987 and they were defined as a “series of short direct repeats interspaced with short sequences”. The protective function of this system is provided by CRISPR loci and CRISPR associated (Cas) genes. There are three different types of CRISPR/Cas systems that differ in crRNA production and in the Cas proteins used. The type II is the most used in genome editing field since it uses only one Cas protein, the Cas9, and two RNA components. In the CRISPR/Cas9 system, following the exposure to exogenous genetic material, a small fragment of this foreign genomic sequence, is integrated into the CRISPR repeat-spacer array inside the host genome, providing to bacteria or archaea an immunological memory to protect themselves from repeated infections by the same exogenous agent. Then, CRISPR array is transcribed into a precursor CRISPR RNA (pre-crRNA) that is cleaved, by endonucleolytic cleavage, into a short mature CRISPR RNA (crRNA). The crRNA has at the 5' end a short RNA sequence, called spacer, which is complementary to the so-called protospacer at the level of the foreign genetic element, while at the 3' end there is a portion of the CRISPR repeat sequence. Following the crRNA generation, starting from a genomic locus that is upstream the CRISPR locus, the transcription of a second RNA, called transactivating RNA (tracrRNA), occurs. The tracrRNA binds the crRNA forming a crRNA:tracrRNA complex containing only one spacer sequence. This complex associates with the Cas9 protein resulting in an active Ribonucleoprotein complex (RNP). After the binding to the crRNA:tracrRNA 10 complex, Cas9 protein is active and able to cleave the invading DNA. In particular, Cas9 is guided to the target DNA, thanks to the base pairing between the spacer, at the level of the crRNA, and the protospacer in the invading genetic material. In addition, the presence of Proto-spacer Adjacent Motifs (PAMs), within the foreign DNA, is needed to allow the Cas9 cleavage. Indeed, the interaction between Cas9 and PAMs favors the DNA strand unwinding and its degradation if it is complementary to the crRNA spacer. The Cas9 uses two different nuclease domains to cleave the foreign DNA: the HNH domain that cleaves the crRNA complementary strand and the RuvC-like domain that, instead, cuts the strand that is not complementary to the crRNA. The synthetic sgRNA or crRNA–tracrRNA structure directs a Cas9 endonuclease to almost arbitrary DNA sequence in the genome through a user-defined 20-

nt guide RNA sequence and further guides Cas9 to introduce a double-strand break (DSB) in targeted genomic DNA. The DSB generated by two distinct Cas9 nuclease domains is repaired by host-mediated DNA repair mechanisms (**Figure 6**)²⁴⁸. In the absence of a repair template, the prevalent error-prone nonhomologous end joining (NHEJ) pathway is activated and causes random insertions and deletions (indels) or even substitutions at the DSB site, frequently resulting in the disruption of gene function. In the presence of a donor template containing a sequence of interest flanked by homology arms, the error-free homology directed repair (HDR) pathway can be initiated to create desired mutations through homologous recombination, which provides the basis for performing precise gene modification, such as gene knock-in, deletion, correction, or mutagenesis²⁴⁹.

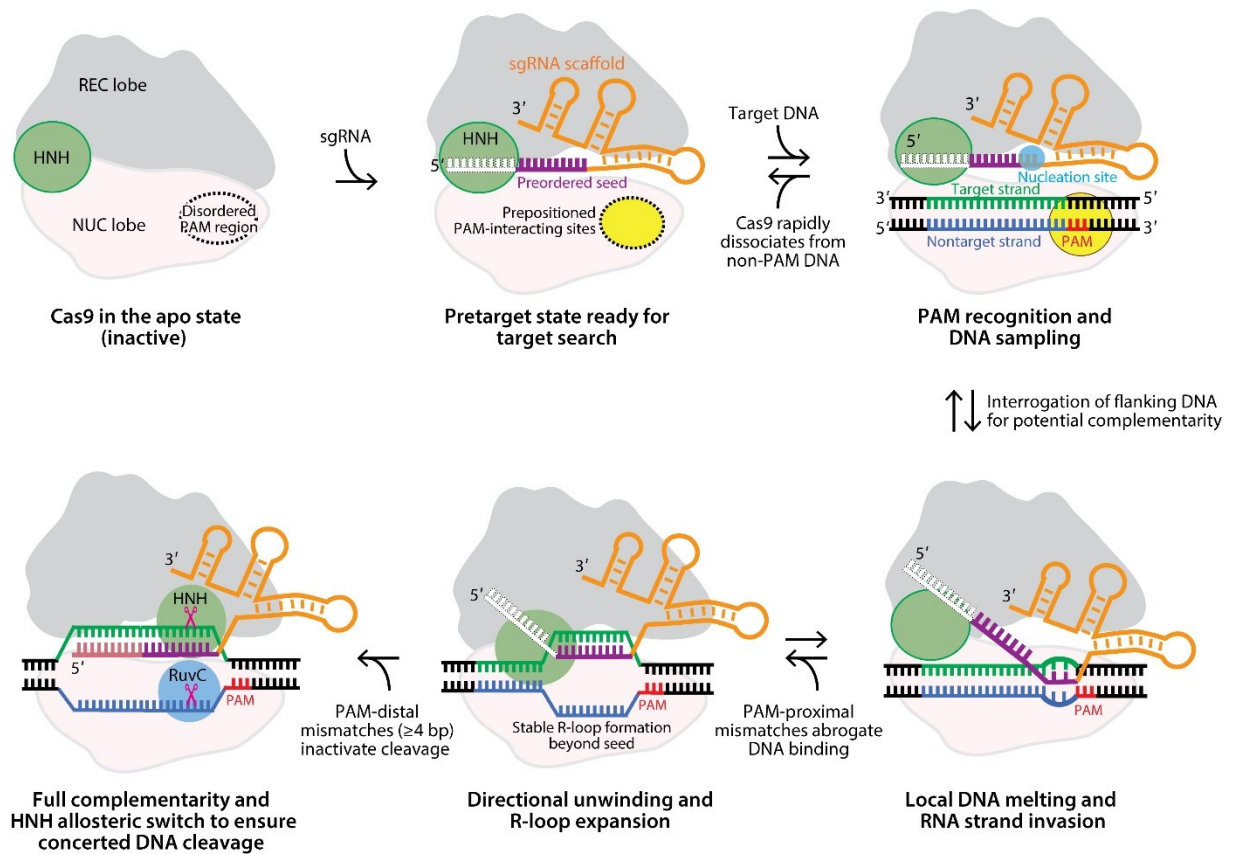


AR Jiang F, Doudna JA. 2017. Annu. Rev. Biophys. 46:505–29

Figure 6 | The mechanism of CRISPR–Cas9–mediated genome engineering.

1.4.2 CRISPR/Cas9 Application

The first step to produce a desired genome modification, by using the CRISPR/Cas9 system, is the design of the guide RNA (gRNA) that, through complementarity, is able to guide the Cas9 enzyme to the desired site in the host genome. Target recognition strictly requires the presence of a short protospacer adjacent motif (PAM) flanking the target site, and subsequent R-loop formation and strand scission are driven by complementary base pairing between the guide RNA and target DNA, Cas9–DNA interactions, and associated conformational changes (**Figure 7**). The use of CRISPR–Cas9 as an RNA-programmable DNA targeting and editing platform is simplified by a synthetic single-guide RNA (sgRNA) mimicking the natural dual trans-activating CRISPR RNA (tracrRNA)–CRISPR RNA (crRNA) structure²⁵⁰. The sgRNA, together with the Cas9 protein, is introduced into the host by means of microinjection, electroporation or transfection. It is, also, possible to provide the host with single or double strand DNA that can be used as template for HDR. The best selection method is the use for the double-strand breaks repair, a template containing a gene that makes only the mutated hosts, resistant to a certain drug²⁴⁹.



AR Jiang F, Doudna JA. 2017.
Annu. Rev. Biophys. 46:505–29

Figure 7 | Schematic representations of the proposed mechanisms of CRISPR–Cas9-mediated target DNA recognition and cleavage.

1.4.3 miR-34a KO cell lines

To investigate the role of miR-34a in physiological and pathological processes, miR-34a Knock-Out (KO) has been performed both in vitro and in vivo. HCT116 cells (colon cancer cell line) has been KO for miR-34a by using TALENs (Transcription Activator-Like Effector Nuclease). These miR-34a KO cells displayed a faster proliferation consistent with the ability of the microRNA to block cell cycle progression and cell growth, inhibiting tumor development²⁵¹. miR-34a KO has been, also, obtained in vivo, in mice, by using the CreLoxP method, to study the role of this microRNA in medulloblastoma development. These KO mice were viable, fertile and they did not display particular phenotypic alterations, however, the tumor suppressor function of miR-34a was further confirmed by the observation of accelerated medulloblastoma formation²⁵².

Finding new therapeutic strategies for cancer treatment by targeting or reverting miRNA expression profiles requires understanding the molecular and cellular regulatory mechanisms that control miRNA expression in cancer. Therefore, it becomes necessary to comprehensively study the regulatory networks of miRNA gene expression and their effects on target mRNAs with advanced technologies such as the CRISPR-Cas9 gene editing system and high-throughput sequencing.

2. AIM OF THE RESEARCH

The aim of this study was to a) investigate the role of miR-34a in cell proliferation and regulation of the expression of specific target genes at mRNA and protein levels developing novel cell models knocked out for miR-34a. Two cell lines, HeLa and HEK293T miR-34a Knock-Out (KO) were produced by using the CRISPR/Cas9 technology, and characterized in terms of proliferation rate, expression of already known and predicted targets, through RT-qPCR and Western blot.

3. MATERIALS AND METHODS

3.1 Cell cultures

HeLa (WT and miR-34a KO), HEK293T (WT and miR-34a KO) cell lines were cultured in Dulbecco's Modified Eagle Medium (DMEM), containing 10% of Fetal Bovine Serum (FBS) and 1% of sodium pyruvate, L – Glutamine, penicillin, and streptomycin, and maintained in incubator at 37 ° C with 5% of CO₂.

3.2 miR-34a knock-out cell lines.

To produce HeLa and HEK293T miR-34 knock-out cell lines (miR-34a KO) three guide RNAs were designed using online tools described elsewhere²⁵³. The three gRNAs were selected for their high target specificity (low off-target sites recognition) and their location on the target sequence. Targeting Dicer and/or DROSHA sites using CRISPR/Cas9 system could interrupt the production of mature miRNA²⁵⁴. Following these parameters, we selected the following gRNAs (listed in **Table 3**); the first gRNA targets the coding sequence of mature miR-34a, while the other gRNAs target two DROSHA processing sites. The plasmid expressing pSpCas9 and each gRNA was prepared cloning each gRNA independently into BbsI restriction sites of the pSpCas9(BB)-2A-Puro (PX459) V2.0 vector (#62988, Addgene) using the T4 DNA ligase (Promega). HeLa and HEK293T cells were transfected using the TransIT®-LT1 transfection reagent (MIR2300, Mirus Bio), following the manufacturer's protocol. For three days after transfection cells were selected in 0,5 µg/ml puromycin. In order to isolate individual clones, cells were diluted and seeded at the density of one cell/well using discrete Poisson distribution probability formula. The absence of miR-34a was verified by qPCR.

Table 3 | Target site and gRNA sequences; gRNA1 targets the coding sequence of mature miR-34a; gRNA2 and 3 target the two DROSHA processing site (In red are highlighted the cloning sites.).

gRNA	Target Sequence	gDNA sequence (5' ... 3')
gRNA1	TTCTTTGGCAGTGTCTTAGCTGG	Fw CACCGTTCTTTGGCAGTGTCTTAGC Rv AAACGCTAAGACACTGCCAAAGAAC
gRNA2	GCCAGCTGTGAGTGTCTTTGG	Fw CACCGCCAGCTGTGAGTGTCTTTCTT Rv AAACAAGAAACACTCACAGCTGGC
gRNA3	TAGAAGTGCTGCACGTTGTGGGG	Fw CACCGCACAACGTGCAGCACTTCTA Rv AAAC TAGAAGTGCTGCACGTTGTGC

3.3 Genomic DNA extraction and PCR analysis on gDNA clones

The genomic DNA (gDNA) of the clones was extracted via salting out procedure from a pellet of cells. The reagents and solutions are listed in the following **table 4** and **5**, while the reagents, primers, and cycles for the PCR analysis on clones are listed in **tables 6** and **7**.

Table 4 | *Salting out reagents*

Reagents
Nonidet-P40 (NP-40) 0.1%;
Lysis Buffer;
SDS 10%;
Proteinase K, 20 mg/ml;
NaCl saturated

Table 5 | *Salting out solutions.*

Lysis buffer (1 litre)	
Reagent	Volume
NaCl 400 mM	100 ml from 4M stock
Tris HCl 10 mM	10 ml from 1M stock
EDTA 2mM	4ml from 0.5M stock
Total volume	1 l
Tris HCl 1M	
Reagent	Volume/amount
Tris	30.25 g
	Adjust pH to 7.5 with HCl
Total volume	250 ml
NaCl 4M	
Reagent	Volume/amount
NaCl	146.1 g
Total volume	250 ml
Na ₂ EDTA 0.5M	
Reagent	Volume/amount
Na₂EDTA	46.5 g
	Adjust pH to 7.5 with NaOH
Total volume	250 ml

Saturated NaCl	
Reagent	Amount
NaCl	90 g
Total volume	250 ml

Table 6 | Reagents and primers for the PCR analysis on clones.

Reagent	Volume/reaction
H ₂ O _{Nf}	7.5 µl
My Taq Red Mix (2X)	12.5 µl
DNA (100 ng)	4.0 µl
Primers mix MIR-34A (10 µM for each forward or reverse primer)	1 µl
Total volume	25 µl
Primers MIR-34A sequences	
GATGGAGTCTTGCTAGTTGCCTGG	Fw MiR-34A (ncRNA)
GCAGAAGAGCTTCCGAAGTCCTGG	Rev MiR-34A (ncRNA)

Table 7 | Cycles for the PCR analysis on clones.

Cycle step	Temp.	Time	Cycles
Initial Denaturation	95°C	1'	
Denaturation	94°C	30''	X 30
Annealing	58°C	30''	
Elongation	72°C	30''	
Final Elongation	72°C	5'	

3.4 miR-34a knock-out validation.

The effective miR-34a knock-out performed through the CRISPR/Cas9 system, was assessed both in HeLa and HEK293T cell lines, through Reverse Transcription (RT) – qPCR experiments by using the TaqMan MicroRNA Assay kit (Applied Biosystems). The RT reaction mix was prepared combining dNTPs, MultiScribe Reverse Transcriptase, Reverse Transcription Buffer, RNase inhibitor, RNA sample, probes, and nuclease-free water (**Table 8**).

Table 8 | RT master mix protocol.

Reagent	Volume/reaction
100 mM dNTPs	0.15 μ l
MultiScribe Reverse transcriptase 50 U/ml	1 μ l
10X Reverse Transcription Buffer	1.50 μ l
RNase inhibitor 20 U/ ml	0.1 μ l
Nuclease-free water	4.16 μ l
RNA sample	5 μ l
Probes	3 μ l
Total volume	15 μ l

The RT reaction was performed as in the following table (**Table 9**).

Table 9 | RT reaction protocol

Temperature	Time
16 °C	30 min
42 °C	30 min
85 °C	5 min

The qPCR master mix was prepared following the protocol described in **table 10**.

Table 10 | qPCR master mix protocol.

Reagent	Volume/reaction
TaqMan MicroRNA assay 20X	1 μ l
Volume from previous RT reaction	1.33 μ l
TaqMan Universal PCR master mic 2X	10 μ l
Nuclease-free water	7.67 μ l
Total volume	20 μ l

The qPCR reaction was run as in the following table (**Table 11**).

Table 11 | *qPCR reaction protocol*

Temperature	Time	Cycles
95 °C	1 min	1
94 °C	30 sec	30
58 °C	30 sec	
72 °C	30 sec	
72 °C	5 min	

To evaluate the level of expression of miR-34a, the results were analyzed by using the $\Delta\Delta C_t$ method²⁵⁵ and normalized considering the expression of U6 that was used as internal reference gene.

In addition, in HeLa cells further assessment of miR-34a knock-out was performed measuring the expression of two already identified miR-34 targets; BCL2 and IK β α . The BCL2 expression was evaluated through qPCR by using the SensiFAST SYBR No-ROX kit (Meridian Life Sciences). The detailed experiment and the primers used were indicated in **tables 9, 10, 11** and **12**. The level of IK β α protein was assessed through Western blot experiments, the primary and secondary antibodies used were listed in **table 14**.

In the case of HEK293T cells miR-34a KO was confirmed, also, through Sanger sequencing that was performed by BMR-Genomics sequencing service.

3.5 miR-34a KO validation in HeLa and HEK293T cell clones

We proceeded evaluating the knockout of miR-34a gene in only 2G10 (HeLa KO) and 3.1D3 (HEK293T KO) isolated clones performing a Reverse Transcription quantitative PCR (RT-qPCR). RT-qPCR analysis was conducted on cDNA derived by miR-34a-KO clones compared to WT HeLa and HEK293T cells. The results represent the relative fold change of expression levels of the mature miR-34a transcript relative to the reference gene, small nuclear RNA U6 (RNU6-1 Homo sapiens). As show in **Figure 8** the relative expression of miR-34a was close to 0 in the knockout clones compared to HeLa and HEK293T WT cells confirming the knockout of MIR-34A gene in 2G10 and 3.1D3, HeLa and HEK293T miR-34a-KO clones respectively.

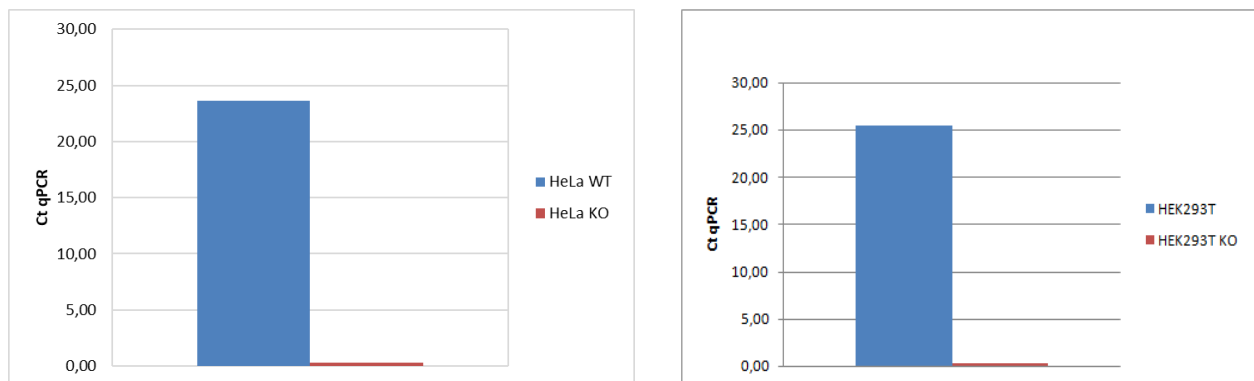


Figure 8 | RT-qPCR on RNA from HeLa and HEK293T WT cells and miR-34a-KO clones (respectively only 2G10 and 3.1D3 clones). Values were normalized to RNU6-1 and results were expressed as relative fold change of expression levels.

3.6 Cell proliferation assay

WT and miR-34a KO HeLa and HEK293T cell lines were seeded at concentration of 0.25×10^5 cells/well in a 96-wells plate. Following two hours, 10 μ l of water-soluble tetrazolium salt reagent (Cell Counting Kit-8 - Dojindo Molecular Technologies) were added in each well. After two hours, cells proliferation at $t=0$ was measured as absorbance at 450 nm by using a spectrophotometer (Absorbance 96 plates reader – Enzo Life Sciences). The same procedure was performed following 24, 48 and 72 hours. The proliferation rate was measured on the basis of a calibration curve in which cells were seeded at concentration of 0.25, 0.5, 1, 2, 4 $\times 10^5$ cells/well.

3.7 Plasmids Transfection

To produce the miR-34a-KO cell lines, HeLa and HEK293T were seeded at a concentration of 2.5×10^5 cells/well and 4×10^5 cells/well, respectively, in 6-well plates with a final volume of 2 mL of DMEM. After about 20 hours (70-80% confluence), the culture medium was removed and replaced with a new one without antibiotics to prepare the cells for subsequent transfection with the plasmids pSpCas9(BB)-2A (PX459) V2.0 vector (Addgene – Plasmid #62988) containing the CRISPR/Cas9 system and the RNA guides (gRNAs) using 2 μ l of TransIT-LT1 transfection reagent (Mirus Bio) for each μ g of DNA. After the addition of TransIT-LT1 transfection agent, the cells were maintained in an incubator at 37°C with 5% CO₂ and selected by the Ampicillin resistance conferred by the plasmids.

3.8 RNA extraction

Following 24 hours after the transfection, RNA was extracted both from transfected and not transfected miR-34a KO, WT HeLa and HEK293T cells. For RNA extraction, cells were lysed by using TRIzol reagent (Ambion) and then, to the cell lysates were added 200 μ l of chloroform. The samples were incubated for 3 minutes at room temperature and then centrifuged at 12.000 g for 15 minutes at 4°C, allowing the formation of three different phases. The aqueous phase, containing the RNA, was collected and then incubated for 15 minutes, at room temperature, adding 500 μ l of isopropanol. The samples were centrifuged at 12.000 g for 15 minutes at 4°C to have the RNA precipitation. Once removed the supernatant, 1 ml of 75% ethanol was added to each sample and then, the samples were centrifuged at 7.500 g for 5 minutes at 4°C. Eventually, the precipitated RNA was resuspended in 30 μ l of nuclease-free water and then quantified by using the spectrophotometer at 260 nm (NanoDrop – Thermo Fisher).

3.9 Proteins extraction

Proteins extraction was performed by using RIPA buffer that was prepared with 150 mM sodium chloride, 1.0% Triton X-100, 0.5% sodium deoxycholate, 0.1% sodium dodecyl sulfate and 50 mM Tris-HCl at pH 7.5. Transfected and not-transfected WT and miR-34a KO HeLa and HEK293T cells were collected and washed in fresh PBS 1X, through two centrifugation steps at 3.000 rpm for 10 minutes at 4°C. Then, the supernatant was removed and 80 µl of RIPA buffer, added with protease inhibitor cocktail to a final concentration 1X, were used to lyse the collected cells and extract their proteins. The samples were incubated in ice for 30 minutes and then stored at -80 °C overnight. The following day, the samples were thawed and centrifuged at 14.000 rpm for 30 minutes at 4°C, the supernatant, containing the extracted proteins, was collected to proceed with the proteins quantification that was performed by Bradford method.

The protein samples to quantify were diluted in water at 1:5 and then, at each one, 750 µl of Bradford reagent (Coomassie Brilliant Blue G -250 - Bio-Rad) were added. The absorbance was measured, by using the spectrophotometer (BioPhotometer D30 – Eppendorf) at 595 nm and then, correlated to protein concentration considering a calibration curve made up of known BSA/water dilutions. Following quantification, protein lysates were stored at – 80°C.

3.10 Reverse transcription

The RNA extracted from WT and miR-34a KO HeLa and HEK293T cell lines was retrotranscribed into cDNA by using the QuantiTect Reverse Transcription kit (Qiagen). The reverse-transcription reaction was preceded with a phase of genomic DNA (gDNA) removal. The detailed Reverse-transcription reaction was described in **table 12** and **table 13**.

Table 12 | *Genomic DNA elimination reaction.*

Reagent	Volume/reaction	Temperature	Time
gDNA wipeout buffer (7x)	2 μ l	42 °C	2 min
Template DNA	1 μ g		
RNase-free water	Variable		
Total volume	14 μ l		

Table 13 | *Reverse-transcription reaction.*

Reagent	Volume/reaction	Temperature	Time
QuantiScript reverse transcriptase	1 μ l	42 °C	15 min
Quantiscript RT buffer (5x)	4 μ l		
RT Primer mix	1 μ l		
Template RNA (obtained from the gDNA removal reaction)	14 μ l		
Total volume	20 μ l		

Following RNA reverse-transcription, the obtained cDNA was quantified through spectrophotometric analysis, measuring the absorbance at 260 nm. The cDNAs samples were stored at -20°C .

3.11 miR-34a predicted targets selection.

miR-34a predicted targets analyzed in qPCR, were selected considering the data coming from the RNA sequencing, previously performed on miR-34a KO HeLa cells, and referring to the Target Scan database. Among the all predicted miR-34a targets identified, ten genes having an important role in tumor development or other pathological processes were selected and analyzed.

3.12 Reverse Transcription Real-Time/quantitative PCR (RT-qPCR)

The cDNAs obtained from the reverse transcription reactions were used to evaluate the expression of different predicted miR-34a target genes, in WT and miR-34a KO HeLa and HEK293T cells. The predicted target genes whose expression was analyzed in qPCR were: PCLO, NR3C1, REL, MAP1B, ZBTB20, COL6A2, ONECUT2, KMT2D (**Table 14**). BCL2²⁵⁶, RAD51, IK β ²⁵⁷, AXL²⁵⁸, TWIST1²⁵⁹ and SIRT1²⁶⁰, since already demonstrated miR-34a targets, were used as controls (**Table 15**) while the Ribosomal Protein Lateral stalk subunit P0 (RPLP0) gene was used as normalizer and internal reference gene (**Table 16**). The qPCR was performed by using the SensiFAST SYBR No-ROX kit (Meridian Life Sciences) and the CFX96 thermocycler (Bio-Rad). The qPCR reaction mix was prepared combining the SensiFAST SYBR No-ROX mix, 10 μ M forward and reverse primers, template cDNA and Nuclease-free water (**Table 17**).

Table 14 | miR-34 predicted targets primer sequence.

Target	Forward primer (5' to 3')	Reverse primer (5' to 3')
PCLO	AAGCTGTGGATAAGGCGAAAT (Song et al 2021)	CTGGGAACGGAAGTGGATC
NR3C1	CGACCAATGTAAACACATGCT	CCGTCCTTAGGAACTGAAGAG
REL	ATTTGACGCTGCTCTTCCTC	TCCTCTGACACTTCCACAATTC
MAP1B	CTCCTTCCAGAACTTCATAGAGATT	TTCAGGACAGAACAGGGTTAAG
ZBTB20	GCTTGGCTACAGCGACATC (Zhang et al 2021)	GAACACATCGCCCACGTTC
COL6A2	AGCTCTACCGCAACGACTA	CCGTAGGCTTCGTGTTTCAT
ONECUT2	GGAATCCAAAACCGTGGAGTAA (Jie Chen et al 2020)	CTCTTTGCGTTTGACGCTG
KMT2D	ACTCTGGTAGTTGCTGACATTG (Jie Chen et al 2020)	TGTCTGTGTTGGAGAAGAGAAC

Table 15| Primers for miR-34 validated target genes.

Control	Forward primer (5' to 3')	Reverse primer (5' to 3')
IKβa	TGCACTTGGCCATCATCCAT (Hart et al 2019)	TCTCGGAGCTCAGGATCACA
AXL	AGCACACGCGTAAACAACAC	GTTATGGGCTTCGCAGGAGA
BCL2	CGGAGGCTGGCTTTGT	CAAGCTCCCAGCCAAA
TWIST1	GGCTCAGCTACGCCTTCTC (Pan et al 2020)	TCCATTTTCTCCTTCTCTGGAA
SIRT1	CCCAGAACATAGACACGCTGGA	ATCAGCTGGGCACCTAGGACA
RAD51	CAACCCATTTACGGTTAGAGC (Pian Liu et al 2022)	TTCTTTGGCGCATAGGCAACA

Table 16| Normalizer primer sequence.

Normalizer	Forward primer (5' to 3')	Reverse primer (5' to 3')
RPLP0	ACATGTTGCTGGCCAATAAGGT	CCTAAAGCCTGGAAAAAGGAGG

Table 17| Mix PCR reaction.

Reagent	Volume/reaction
2x SensiFast SYBR No-ROX mix	10 µl
10 mM Fw primer	0.8 µl
10 mM Rw primer	0.8 µl
Template cDNA	up to 8.4 µl
Nuclease-free water	as required
Total volume	20 µl

10 µl of qPCR reaction mix was added to each well of a 96-well plate. Following centrifugation, the plate was put in the thermocycler and the amplification reaction occurred as described in the following table (Table 18).

Table 18 | PCR condition.

Reaction phase	Temperature	Time	Cycles
Polymerase activation	95°C	2 min	1
Denaturation	95°C	5 sec	40
Primer annealing Extension	60°C	20 sec	

The qPCR results were analyzed by using the $\Delta\Delta C_t$ method²⁵⁵ and normalized on the basis of the expression of RPLP₀ that was used as internal reference gene.

3.13 Western Blot

Proteins extracted from WT and miR-34a KO HeLa and HEK293T cell lines were analyzed through western blot in order to evaluate the concentration of different predicted miR-34 target proteins. The predicted miR-34 target proteins analyzed were: ONECUT2, KMT2D and MAP1B. IK β α and SIRT1 were used as controls while β -tubulin as internal reference protein. The primary and secondary antibodies used, and the Molecular Weights (MW) of the respective target proteins were indicated in the following table (**Table 19**).

Table 19 | Western blot antibodies and molecular weight (MW) of the target proteins.

Predicted target protein	Primary antibody	MW
ONECUT2	Rabbit anti-ONECUT2 (Thermo Fisher – PA5 114396)	50-60 kDa
KMT2D	Rabbit anti-KMT2D (Proteintech – 27266-1-AP)	600 kDa
MAP1B	Rabbit anti-MAP1B (Proteintech – 21633-1-AP)	300 kDa
Controls and normalizer		
IK β α	Rabbit anti- IK β α (Cell Signaling - No. #9242)	36 kDa
SIRT1	Rabbit anti-SIRT1 (Invitrogen – PA5-23063)	97 kDa
β -tubulin	Mouse anti-b-tubulin (BIOSS Antibodies – No. bsm – 33034M)	50 kDa
Secondary antibodies		
Goat Anti-mouse IgG (H+L) peroxidase conjugated (Thermo Scientific – No.31430)		
Goat Anti-rabbit IgG (H+L) peroxidase conjugated (Thermo Scientific – No. 31460)		

3.13.1 Running and Stacking gel preparation.

Three different running gels were prepared at different acrylamide concentrations; the first one at 10% allowing the run of high MW proteins (SIRT1), the second one at 12% to run small MW proteins (IK β and ONECUT2), eventually, the last one was prepared at 4-12% gradient to permit the run of proteins of high MW (MAP1B and KMT2D) (**Table 20**). The stacking gel was prepared at 5% according to the protocol described in the following table (**Table 21**).

Table 20 | Running gel reagents.

Reagent	10% running gel	12% running gel
30% Acrylamide	3.3 ml	3.96 ml
1.5 M Tris (pH 8.8)	2.5 ml	2.5 ml
10% SDS	100 μ l	100 μ l
10% APS	100 μ l	100 μ l
TEMED	12 μ l	12 μ l
H₂O	3.99 ml	3.3 ml

Table 21 | Stacking gel reagents.

Reagent	5% stacking gel
30% Acrylamide	1 ml
1 M Tris (pH 6.8)	750 μ l
10% SDS	60 μ l
100% APS	60 μ l
TEMED	7 μ l
H ₂ O	4.12 μ l

3.13.2 Running buffer preparation.

The running buffer was prepared adding tris base, glycine, 10% SDS and water (**Table 22**).

Table 22 | *Running buffer 10X reagents.*

Reagent	Volume
Tris base	30.3 g
Glycine	144.1 g
10% SDS	100 ml (10 g)
H₂O	900 ml

3.13.3 Transfer buffer preparation

The transfer solution was produced combining tris base, glycine, 10% SDS and 20% methanol and stored at 4°C (**Table 23**).

Table 23 | *Transfer buffer overnight 1X reagents.*

Reagent	Volume
Tris base	4.5 g
Glycine	21.6 g
10% SDS	150 µl
20% methanol	225 ml
H₂O	1260 ml

3.13.4 Western Blotting

50 µg of proteins were loaded in the gel. The electrophoresis was performed at 80 mA at the beginning and then, when the MW marker started to divide, at 130 mA. In the case of 4-12% running gel, the samples were run at 80 mA over-day at 4°C. Further the proteins were transferred to PVDF membrane. The PVDF membrane was incubated with the primary antibody, previously diluted in 5% milk, for overnight incubation. The PVDF membrane was hybridized with the secondary antibody, always diluted in 5% milk, for 1 hour. The hybridization of the antibody on the membrane was evaluated by using the ECL Advance Western Blotting Detection kit (GE Healthcare) and the released chemiluminescence was detected by the imaging system (Azure 300 – Azure Biosystems). Western blot results were analyzed through densitometric analysis by using the ImageJ program. Densitometry data, obtained from the analysis of the internal reference gene β-tubulin, were used to measure the specific concentration of each target protein.

3.14 Cloning of the 3'-UTR of KMT2D into the pGL3-promoter vector

428 bp of the 3'-UTR of KMT2D transcript (NCBI Reference Sequence: >NM_003482.4:17834-20635 Homo sapiens lysine methyltransferase 2D (KMT2D), mRNA) were amplified from genomic DNA with designed primers (**Table 24**) with the restriction sites for XbaI. In addition, a High-Fidelity DNA polymerase (Thermo Fisher Scientific Cat. #F530S and #F530L) was used. The amplified sequence has a length of 428 bp.

Table 24 Forward (green) and Reverse (red) primers used for 3'-UTR-KMT2D 428 bp fragment amplification. The portions highlighted in green are 8-nucleotide tails added to improve cloning efficiency; XbaI restriction sites are highlighted in yellow.

Primer Sequences for 3'-UTR-KMT2D fragment amplification	
Fw:	5'...GGTCTAGAGTCTCTCTATGGGTTGTGTTCC...3'
Rev:	5'...AGGTCTAGAGGAGATATCCTGGTCCTAGGTTA...3'

The amplified fragment and pGL3 Promoter Vector (Promega) were digested, and the plasmid then linearized, by single digestion with XbaI and CutSmart Buffer (NEB). Subsequently, 500 ng of linearized pGL3 was dephosphorylated using FastAP Thermosensitive Dephosphatase (Thermo Fisher Scientific #EF0654) and gel purified before proceeding with the ligation of the protruding ends, generated by the restriction, using a DNA ligase. *E. c. JM109* Competent Cells (Promega #L2005) were transformed following the manufacturer's protocol, then plated and selected by Ampicillin resistance. A control PCR colony was performed and subsequently the extraction of the plasmids was obtained using the "MINI kit" (Qiagen). The extracted plasmids were digested with one or both Hind III and Pvu II restriction enzymes. The plasmid of colony 3 was selected for Sanger sequencing because it showed the expected bands of 3678bp and 1766bp from double digestion. The results of the Sanger sequencing and the alignments with the Clustal Omega online tool allowed to confirm the successful directed cloning.

3.15 Colony PCR

In order to determine the presence or absence of the DNA insert in the plasmid constructs, a colony PCR was performed, using My Taq Red Mix (Bioline #BIO-25043) and primers of the insert. The conditions applied for the colony PCR are reported in **table 25**.

Table 25| Colony PCR applied conditions.

Cycle step	Temp.	Time	Cycles
Initial Denaturation	94°C	5'	
Denaturation	94°C	30''	
Annealing	60.2°C	30''	X 36
Elongation	72°C	30''	
Final Elongation	72°C	5'	

3.16 Purification of plasmid DNA

The resulting colonies containing the DNA insert by colony PCR, were then subjected to plasmid extraction and purification by “MINI kit” (Qiagen), following the manufacturer’s protocol. The DNA concentration was quantified by NanoDrop 2000 Spectrophotometer (Thermo Fisher Scientific), and the absorbance ratio at 260/280 and 260/230 was measured to determine the DNA purity.

3.17 Plasmid digestion with restriction enzyme

pGL3_∞ (pGL3-Promoter Vector - Promega #E1761) and the amplified fragment of 3'-UTR of KMT2D transcript were digested with the restriction enzyme XbaI and CutSmart Buffer (NEB) while, plasmid pGL3-3'-UTR-KMT2D cloned and extracted was submitted to restriction analysis by HindIII or PvuII or both with B buffer (Promega).

3.18 Statistical analysis

All results collected in this work were analyzed fixing the statistical significance at $p \leq 0.05$ or $p \leq 0.01$ that was measured by using the T-student test for independent data with GraphPad.

4. RESULTS

4.1 Generation of HeLa and HEK293T miR-34a-5p KO cell lines

The aim of this thesis is to investigate the role of miR-34a in the cell proliferation and identify new gene targets involved in tumorigenesis, generating new cell models in which miR-34a is silenced. By gene expression analysis of miR-34a KO clones and WT cells, some known target genes were validated, and additional genes predicted for miR-34a were found. Both cell lines, HeLa and HEK293T, do not represent a good cellular model to study the involvement of miR-34a in tumorigenesis, but their comparison allowed to identify new potential miR-34a targets (such as ONECUT2 and KMT2D) which are up-adjusted results in both KO clones versus WT cells. However, to study the mechanisms through which miR-34a is involved in tumorigenesis it is necessary to verify the up-regulation of these potential targets in a more suitable cell line, such as the A375 melanoma cell line. For this purpose, it could be useful to silence miR-34a by siRNA or to generate a third miR-34a knock-out A375 clone by applying the CRISPR/Cas9 system. In order to produce knock out cell lines for the expression of miR-34a, CRISPR /Cas9 genome editing was applied. After the transfection of HeLa and HEK293T cells with each PX459 plasmid expressing gRNAs and Cas9 endonuclease for the induction of gene editing, the isolation and expansion of single-cell clones were exerted and the miR-34a gene knockout was verified. In order to verified the miR-34a knockout , the genomic DNA of HeLa cells and miR-34a-KO clones was isolated and analysed by PCR targeting the region where MIR-34A gene is located. **Figure 9, panel A** reports the electrophoretic analysis of the PCR fragments of genomic DNA extracted. The fragment of amplification in the WT cells was represented by a band at 325 bp. Clones that were genome edited by ins/del showed fragments of different sizes (2G10, 1G9, 2E2).

In order to identify differences in the sequences of miR-34a-KO clones compared to HeLa cells, a multiple sequence alignment analysis was performed on the genomic sequences resulted from Sanger sequencing. As show in **Figure 9, panel A**, 1D3 clone shared the same sequence with HeLa cells, for this reason it was discarded from further analyses. Compared to HeLa cells, 2G10 clone presented a deletion of 112 bp and 1G9 clone a deletion of 98 bp.

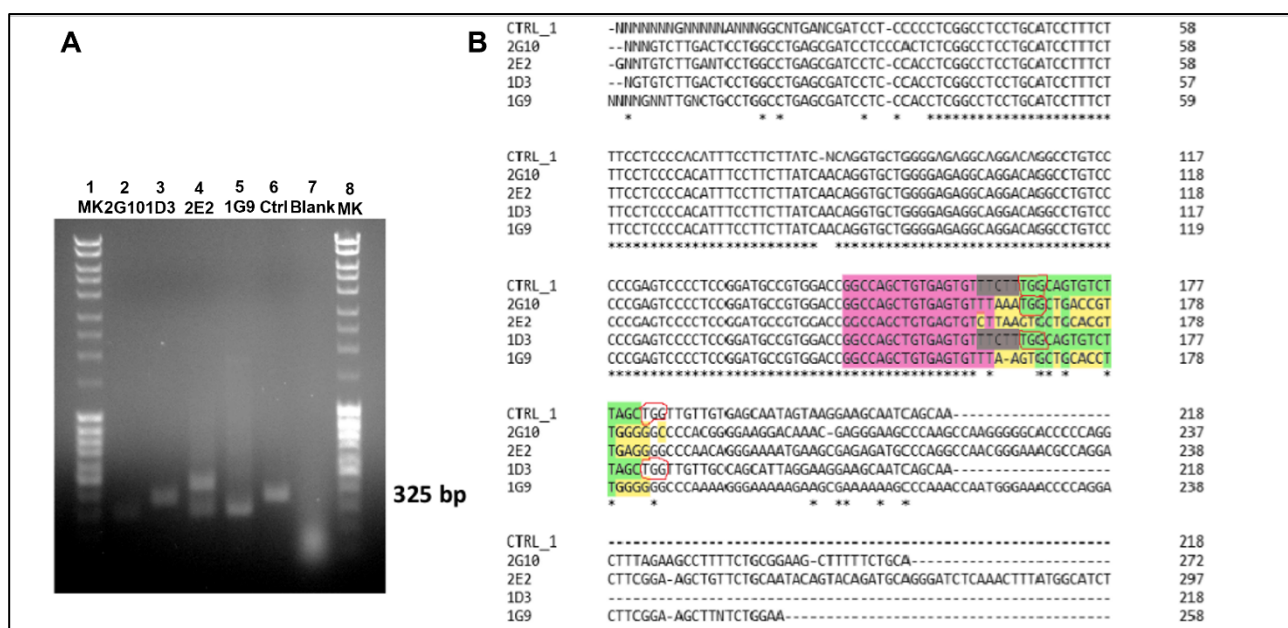
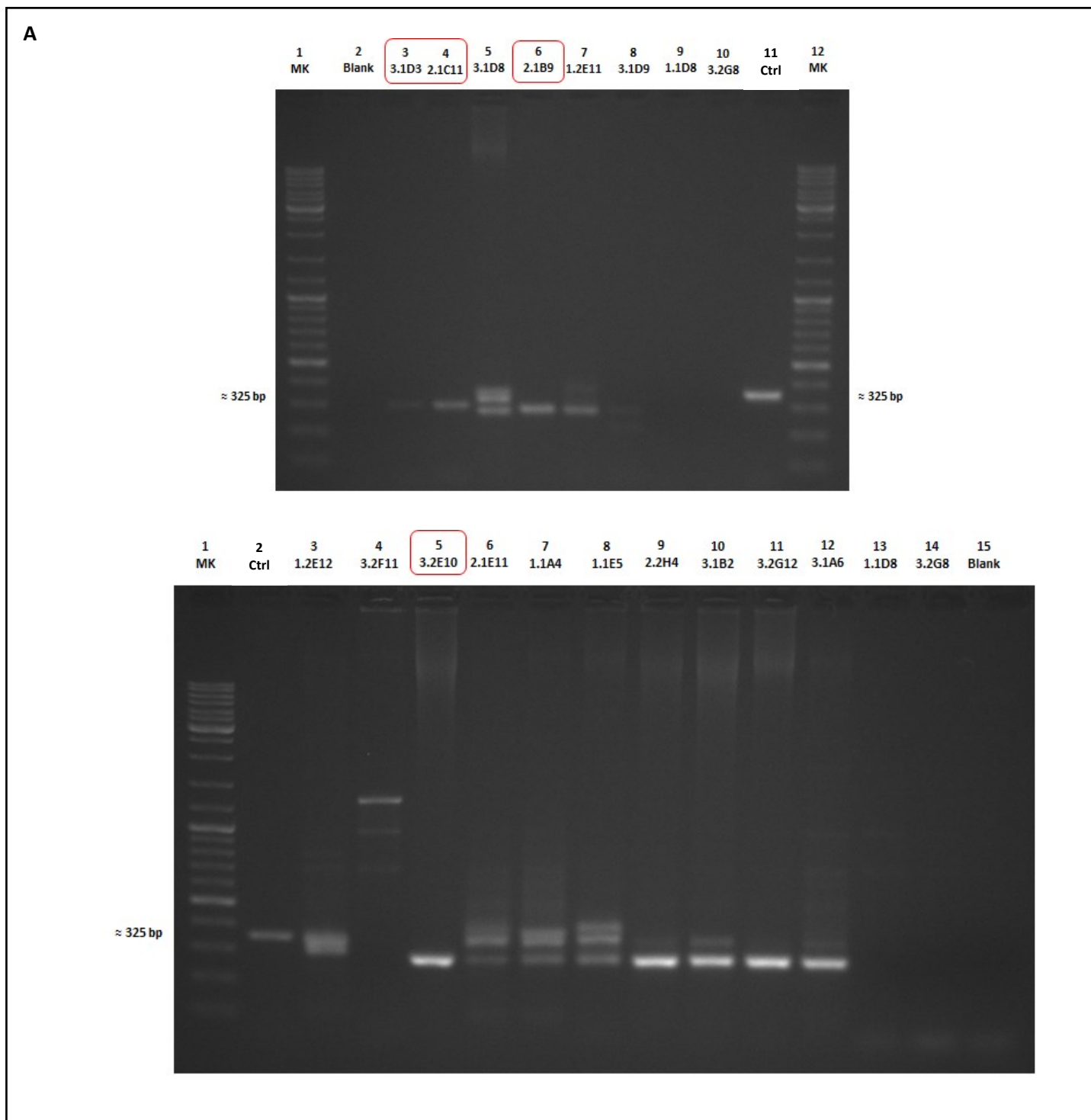


Figure 9 | Survey of validation strategies for CRISPR/Cas9 editing. (A) PCR of genomic DNA extracted from selected clones. HeLa cells are the control (Ctrl). The bp length of the bands of HeLa KO clone was approximately identified using GeneRuler 100 bp DNA Ladder (Thermo Fisher): Ctrl = 325 bp, 2G10 = 272 bp, 1D3 = 325 bp, 2E2 = 416 bp + 258 bp, 1G9 = 258 bp. (B) Multiple sequence alignment via Multiple sequence alignment tool (Clustal omega): gRNA1 (green), gRNA2 (purple), gRNA3 (light blue), sequences non homologous to the Ctrl sequence (yellow) and PAM sequences (purple).

We performed the same analysis in HEK293T KO clones suggest the occurrence of a deletion in 3.1D3, 2.1C11, 2.1B9 and 3.2E10 (**Figure 10, panel A**) that was confirmed by Sanger sequencing. The results show a deletion of ~ 50 bp and the lack of miR-34a transcript in the 3.1D3 and 2.1C11 miR-34a-KO clones and a deletion of ~ 62 bp in 2.1B9 and 3.2E10 clones. Only the KEK293T miR-34a-KO clone was selected for subsequent analyses.



B

CLUSTAL O(1.2.4) multiple sequence alignment

WT	--CNTTTTGGNNTNGTCTTNTGGCNTGAGCGATCCTCCCCCTCGGCCTCCTGCATCCTTT	58
2.1C11	-----TTNCCCCACNCTCGGCCTCCTGCATCCTTT	31
3.1D3	NNNNNGGGCTTCTCTTNTGCACCTGAANCATCCTCCCCCTCGGCCTCCTGCATCCTTT	60
2.1E10	-----NNNNNCNNGAAGCCGATCCTCCACCCTCGGCCTCCTGCATCCTTT	46
	* * *****	
WT	CTTTCCTCCCCACATTTCTTCTTATCAACAGGTGCTGGGGAGAGGCAGGACAGGCCTGT	118
2.1C11	CTTTCCTCCCCACATTTCTTCTTATCAACAGGTGCTGGGGAGAGGCAGGACAGGCCTGT	91
3.1D3	CTTTCCTCCCCACATTTCTTCTTATCAACAGGTGCTGGGGAGAGGCAGGACAGGCCTGT	120
2.1E10	CTTTCCTCCCCACATTTCTTCTTATCAACAGGTGCTGGGGAGAGGCAGGACAGGCCTGT	106

WT	CCCCCGAGTCCCCTCCGGATGCCGTGGACCGGCCAGCTGTGAGTGTTTCTTTGGCAGTGT	178
2.1C11	CCCCCGAGTCCCCTCCGGATGCCGTGGACCGGCCAGCTGTGAGTGTTTCTTTGGCAGTGT	151
3.1D3	CCCCCGAGTCCCCTCCGGATGCCGTGGACCGGCCAGCTGTGAGTGTTTCTTTGGCAGTGT	180
2.1E10	CCCCCGAGTCCCCTCCGGATGCCGTGGACCGGCCAGCTGTGAGTGTTTAAAGTGCTGC---	163
	***** **	
WT	CTTAGCTGGTTGTTGTGAGCAATAGTAAGGAAGCAATCAGCAAGTATACTGCCCTAGAAG	238
2.1C11	CTTAAGTGTGCAC-----	165
3.1D3	CTTAAGTGTGCAC-----	194
2.1E10	-----	163

WT	TGCTGCACGTTGTGGGGCCCAAGAGGGAAGATGAAGCGAGAGATGCCCAGACCAGTGGGA	298
2.1C11	-----GTTGTGGGGCCCAAGAGGGAAGATGAAGCGAGAGATGCCCAGACCAGTGGGA	217
3.1D3	-----GTTGTGGGGCCCAAGAGGGAAGATGAAGCGAGAGATGCCCAGACCAGTGGGA	246
2.1E10	-----ACGTTGTGGGGCCCAAGAGGGAAGATGAAGCGAGAGATGCCCAGACCAGTGGGA	217

WT	GACGCCAGGACTTCGGAAGCTCTTCTGCA	328
2.1C11	GACGCCAGGACTTCGGAAGCTCTTCTGCA-	246
3.1D3	GACGCCAGGACTTCGGAAGCTCTTCTGCA-	275
2.1E10	GACGCCAGGACTTCGGAAGCTCTTCTGCA-	246

Figure 10 | Survey of validation strategies for CRISPR/Cas9 editing in HEK293T cells. PCR of genomic DNA extracted from selected clones. HEK293T cells are the control (Ctrl). The bp length of the bands of HEK293T KO clone was approximately identified using GeneRuler 100 bp DNA Ladder (Thermo Fisher). (B) Multiple sequence alignment via Multiple sequence alignment tool (Clustal omega).

4.2 miR-34a KO cell lines validation

Preliminary analyses to assess the effective knock-out, performed by using the CRISPR/Cas9 technology, of the miR-34a were done, before proceeding with the characterization of the miR-34a KO HeLa and HEK293T cell clones.

4.2.2 Evaluation of the expression of miR-34a target genes in HeLa and HEK293T edited cells.

Identification of gene targets of miRNAs is an important step for functional characterization of miRNAs and provides new insight into biological processes connected to miRNAs. Identification and validation of miRNA targets in laboratory can be expensive and time-consuming, while sophisticated computational approaches for miRNA target prediction allow narrowing down potential targets for experimental validation²⁶¹.

Prediction of natural targets of miR-34a was performed using miRwalk2.0 online tool (<http://mirwalk.umm.uni-heidelberg.de/>), IK β and BCL2 were chosen for further functional

analysis. Previous studies had already verified that the apoptosis regulator BCL2 and the NF- κ B inhibitor IK β α are targets of miR-34a^{256,257}. RT-qPCR analysis was performed in order to quantify BCL2 expression in 2G10 and 3.1D3 miR-34a-KO clones compared to HeLa and HEK293T WT cells. As reported in **Figure 11, panel A**, BCL2 mRNA expression showed a significant increase in 2G10 clone compared to HeLa WT, while 3.1D3 clone showed a non-significant increase compared to HEK293T WT, so after we tested other control genes. Since miRNAs can inhibit gene expression at the mRNA or protein level²⁶², to assess the expression levels of IK β α in miR-34a-KO clones compared with HeLa and HEK293T cells, detection of protein expression levels was performed by western blot analysis. To functionally validate our KO clone models, we evaluated whether the expression levels of IK β α , a previously validated target of miR-34a, underwent an increase in miR-34a-KO clones compared to HeLa and HEK293T cells. As shown in **Figure 11, panel B and C**, western blot analysis and densitometric analysis reported an increase of IK β α expression levels in 2G10 and 3.1D3 miR-34a-KO clones. Taken together the results confirmed that BCL2 and IK β α are target genes of miR-34a, reporting increased levels of expression for both targets in the absence of miR-34a.

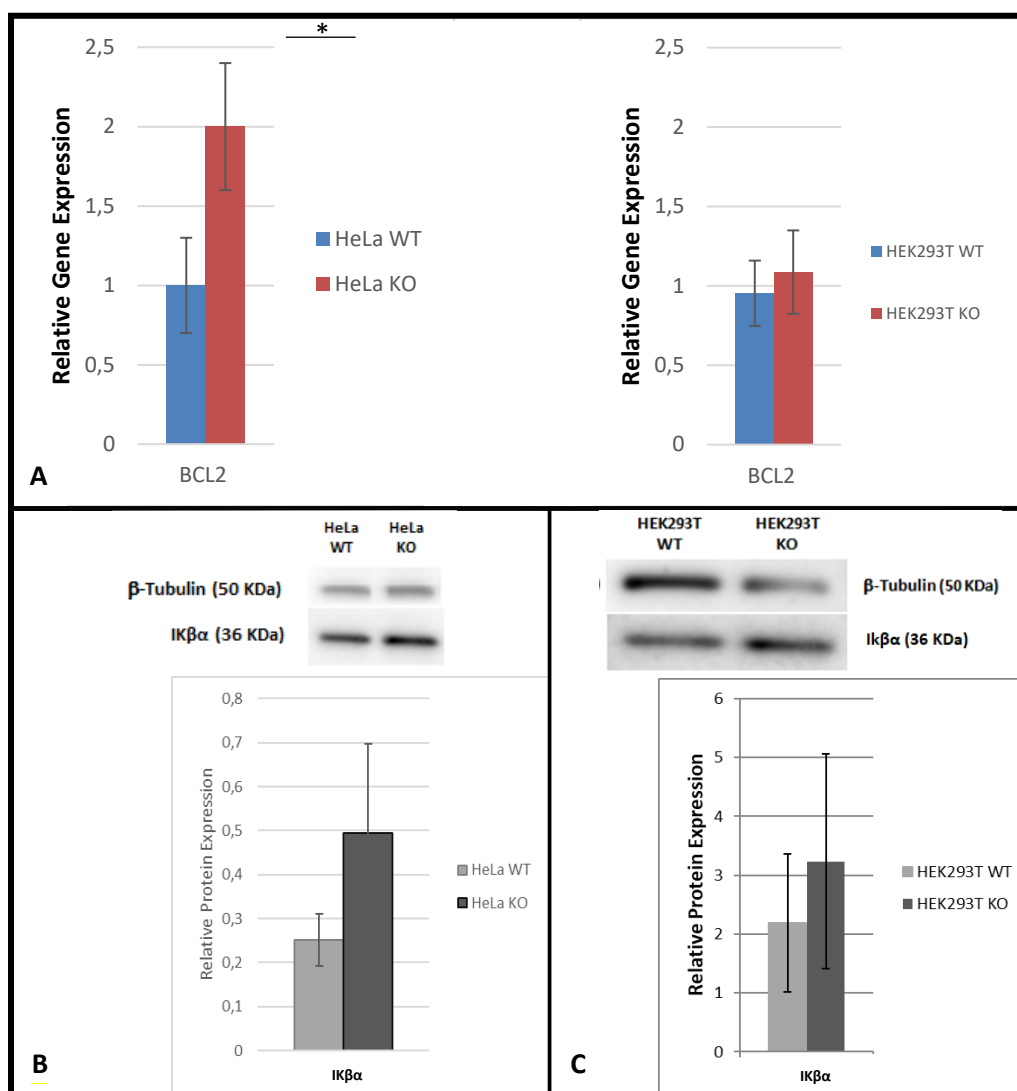


Figure 11 | Evaluation of the expression of miR-34a target genes (*BCL2* and *IKβa*) in edited cells. (A) RT-qPCR analysis on HeLa and HEK293T WT cells (blue bar) and miR-34a-KO clones (red bar); *BCL2* gene was chosen for the analysis (* $p=0,012$). Normalization was performed relative to *RPLP0* gene expression and standard deviation analysis was calculated between triplicates. The statistical significance was set at $*p \leq 0.05$ that was measured by using the T-student test for independent data with GraphPad. (B) Differential expression of endogenous *IKβa* in HeLa KO clone (2G10). (C) Differential expression of endogenous *IKβa* in HEK293T KO clone (3.1D3). miR-34a-KO clones protein levels detected were normalized on β -tubulin.

4.3 miR-34a KO HeLa cell line characterization

4.3.1 Proliferation assay

Altered expression of miR-34a has been associated to different proliferation rates in tumor tissues. In order to verify if miR-34a is necessary to maintain the proliferation rate of HeLa cells, the proliferation of HeLa KO clone was compared to HeLa cells. The results showed that WT cells and KO clone had a similar proliferation rate (**Figure 12**).

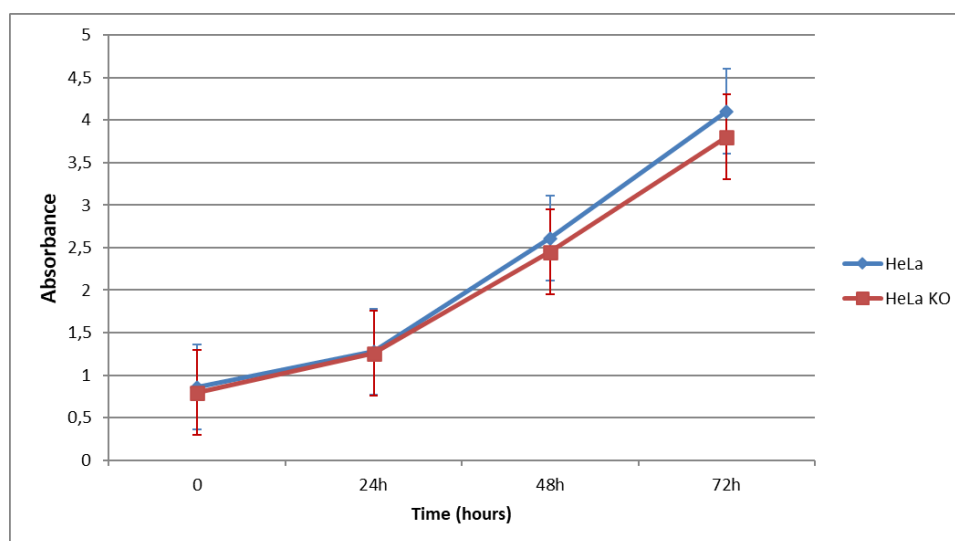


Figure 12 | Proliferation rate of HeLa WT cells vs HeLa KO clone.

4.3.2 Scratch test

To evaluate HeLa KO clone motility, a Scratch Assay was performed. Cell motility was calculated as the average speed of coverage of the scratch area/time using 1 hour interval for images capture by CytoSmart Omni system. Results show no significant differences in the migration compared to WT (**Figure 13**).

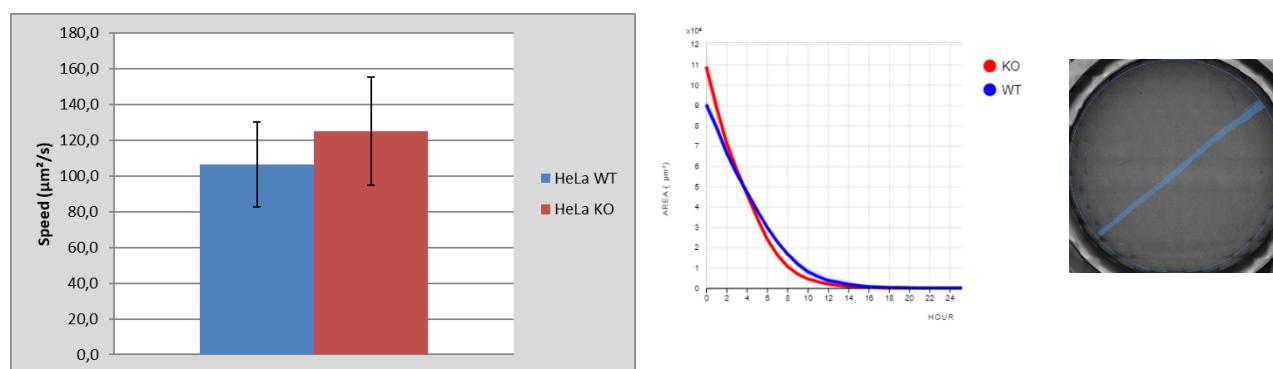


Figure 13 | Scratch Assay: HeLa WT cells and miR-34a KO clone were cultured for 1 day until confluence before scratch. Results of the analysis were obtained in triplicates.

4.3.3 HeLa cell line transcriptome analysis

To identify a set of genes deregulated in absence of miR-34a, we performed an RNA sequencing (**Figure 14**) on the RNA extracted from HeLa WT and HeLa miR-34a KO (2G10 clone). The first 50 genes differentially expressed between HeLa cells and the HeLa KO clone are listed in the following Heat Map. The first 23 genes are downregulated in the KO clone compared to HeLa cells while, the remaining 27 genes of the list are upregulated in the KO clone compared to WT cells. To verify the results obtained from the transcriptome analysis, we evaluated the expression of some genes by RT-qPCR, such as COL6A2 (improbable direct target gene of miR-34a because it is downregulated in the HeLa KO clone), ZBTB20, PCL0, REL, MAP1B, NR3C1, ONECUT2 and KMT2D (probable target genes of miR-34a). It is interesting to note that in the KO clone there is an increase, corresponding to an accumulation, of precursor of miR-34a (MIR34AHG). The qPCR data demonstrate the total absence of mature miR-34a within our KO clones (**Figure 8**) so, in all likelihood, the miR-34a marker is retained, but not processed in a mature and functional miR-34a transcript.

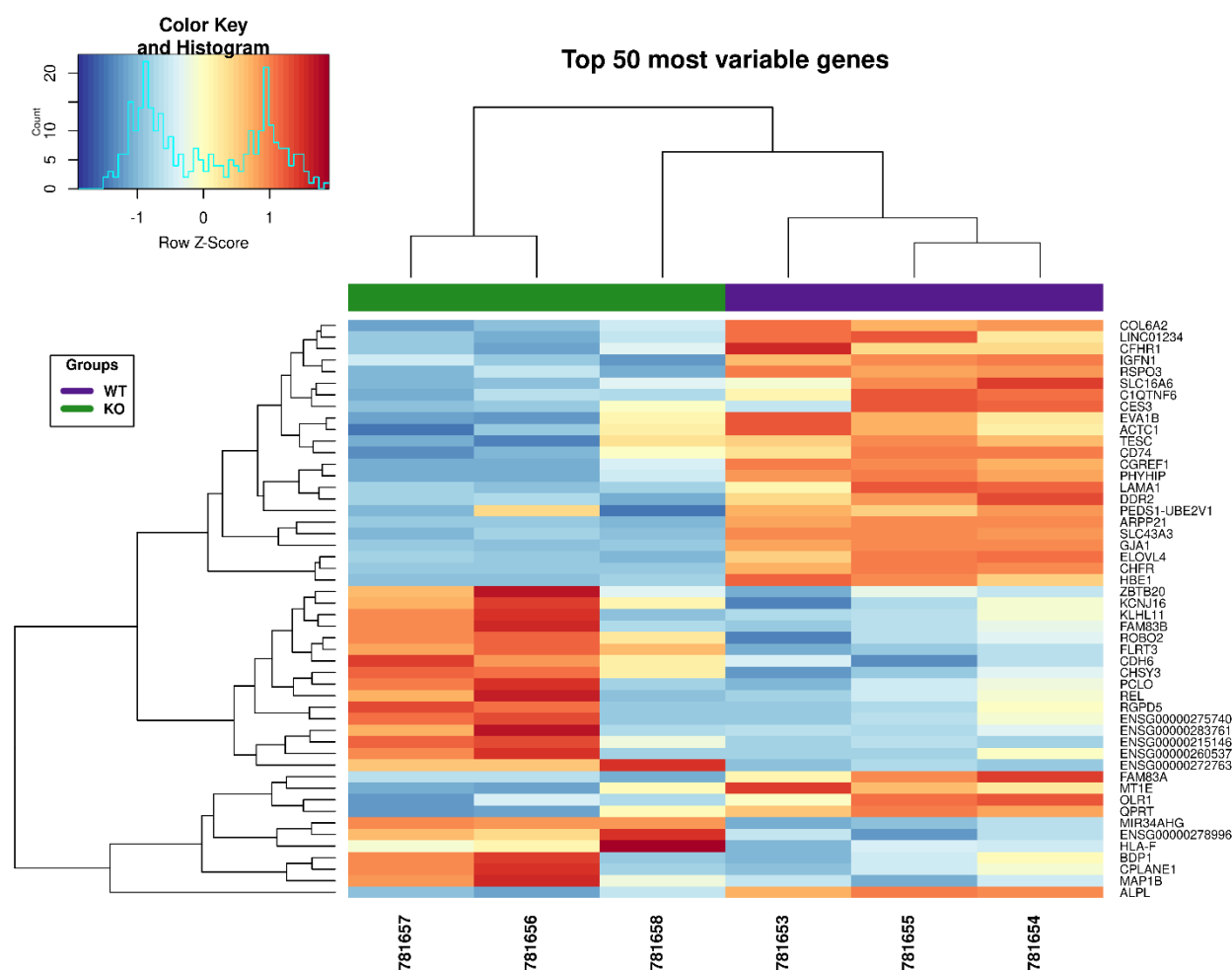


Figure 14 | Heat map on the enriched RNAs representing the top 50 most variable genes. The green bar identifies the HeLa KO clone while, the purple bar identifies the HeLa WT cells. The difference in the expression is signalled by the colour and its intensity: the less expressed genes are in blue, those more expressed in one line than the other are in red, while the genes in which there is no significant variation in the expression are represented in yellow.

4.3.4 Expression of validated and predicted miR-34 targets

Based on transcriptome data and the alignment analyses between the consensus sequence of miR-34a and the 3'-UTR of predicted target genes with Target Scan tool (**Figure 15**), we chose seven genes that were found to be deregulated in the absence of miR-34a from the transcriptome analysis (ZBTB20, PCLO, REL, MAP1B, NR3C1, ONECUT2 and KMT2D). We analyzed their expression in the KO clone, using $IK\beta\alpha$ and BCL2 as validated target genes. ZBTB20 and PCLO are not represented because they were poorly expressed in the HeLa cell model.

Position 762-768 of KMT2D 3' UTR	5' ...CCCUCUCCCCACCUCACUGCCC...
hsa-miR-34a-5p	3' UGUUGGUCGAUUCUGUGACGGU
Position 10175-10181 of ONECUT2 3' UTR	5' ...GUAUUAUGAUUAGCAACUGCCAA...
hsa-miR-34a-5p	3' UGUUGGUCGAUUCUGUGACGGU
Position 118-124 of IK β 3' UTR	5' ...UAUAUCCACACUGCACACUGCCU...
hsa-miR-34a-5p	3' UGUUGGUCGAUUCUGUGACGGU
203-209 of BCL2 3'-UTR	5' - TCGAATCAGCTATTTACTGCCA -3'
hsa-miR-34a	3' - TGTGGTTCGATTCTGTGACGGT -5'
	.

Figure 15 | Sequence alignment achieved by TargetScan tool between the consensus sequence of miR-34a and the 3'-UTR of the known and putative target genes.

The expression of the known miR-34a targets, BCL2 and IK β , and of the predicted targets, ZBTB20, PCLO, REL, MAP1B, NR3C1, ONECUT2 and KMT2D was measured through reverse transcription and quantitative PCR (RT-qPCR) experiments. Furthermore, COL6A2 expression was verified to be consistent with the results obtained from transcriptome analysis. The results showed a significant overexpression of BCL2, REL, MAP1B and NR3C1 and a significant decreased expression of COL6A2 in HeLa KO clone compared to WT cells (**Figure 16, panel A**) according to RNA sequencing results. Other two predicted targets also identified through bioinformatic analyses, ONECUT2 and KMT2D, resulted to be slightly upregulated in HeLa KO clone, at mRNA level (**Figure 16, panel B**), although not significantly.

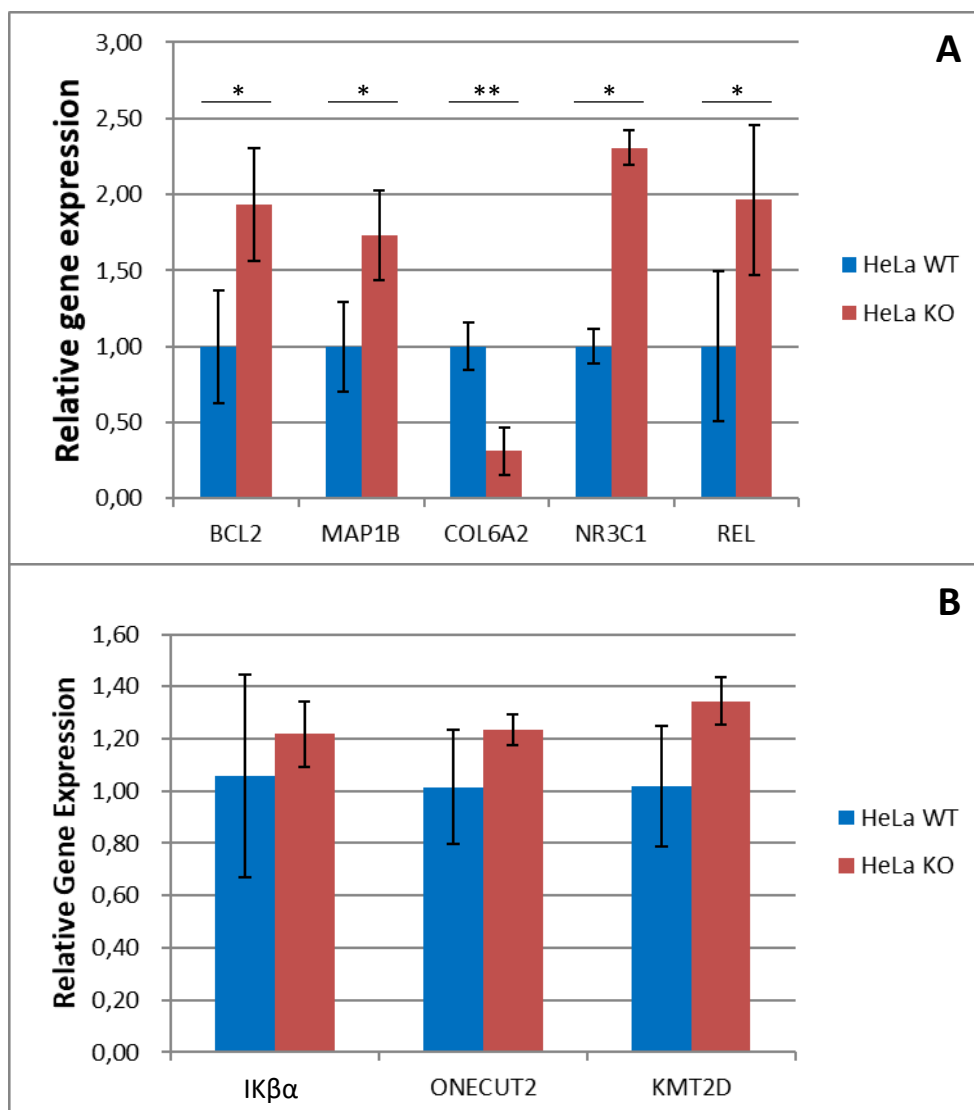


Figure 16 | RT-qPCR analysis on RNA extracted from HeLa cells (WT) vs KO clone. *BCL2* (* $p=0,012$), *MAP1B* (* $p=0,013$), *COL6A2* (** $p=0,0016$), *NR3C1*(* $p=0,03$), *REL* (* $p=0,03$), *IKβα*, *ONECUT2* and *KMT2D* mRNA level of expression in HeLa WT cells (blue bar) vs HeLa KO clone (red bar). *BCL2* and *IKβα*, known gene targets of *miR-34a*, were chosen as controls. Normalization was performed relative to *RPLP0* gene expression. All data reported are representative of at least 3 independent experiments and error bars represent standard deviation (SD). The statistical significance was set at * $p \leq 0.05$ or ** $p \leq 0.01$ that was measured by using the T-student test for independent data with GraphPad.

4.4 miR-34a KO HEK293T cell line characterization

4.4.1 Proliferation assay

As well as for HeLa miR-34a KO, the results of the proliferation assay performed on HEK293T cell line showed a similar proliferation rate between HEK293T KO and WT cells. (**Figure 17**) confirming that miR-34a is not essential to drive the proliferation rate of HeLa and HEK293T cell lines.

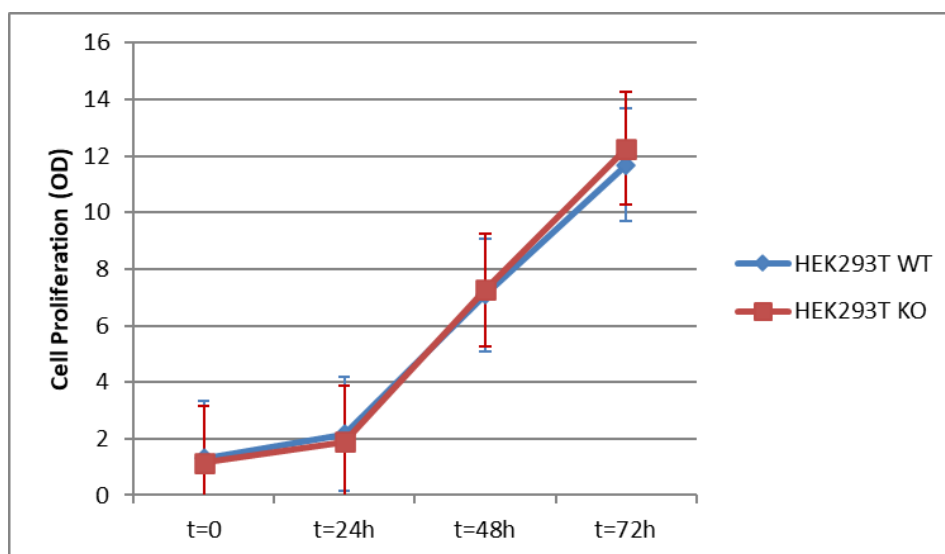


Figure 17 | Proliferation rate of HEK293T WT cells vs HEK293T KO clone.

4.4.2 Expression of validated and predicted miR-34a targets

qPCR and Western blot experiments were done to evaluate the expression of 13 selected, validated and predicted miR-34a targets. Through quantitative PCR, IK β α , AXL, TWIST1, BCL2, RAD51 and SIRT1 (known miR-34a targets) mRNA expression was evaluated. Statistically significant upregulation of IK β α , AXL, TWIST1 was detected in miR-34a KO cells (**Figure 18A**), but not of BCL2, RAD51 and SIRT1 (**Figure 18A**). Moreover, qPCR analyses were also used to measure the expression of predicted and selected miR-34 targets: REL, NR3C1, MAP1B, ZBTB20, PCLO (**Figure 18A**), ONECUT2 and KMT2D (**Figure 18B**). In comparison to HEK293T WT cells, MAP1B, the microtubule associated protein 1B, showed a statistically significant decreased expression in miR-34a KO clones (**Figure 18A**). Other two predicted targets, ONECUT2 and KMT2D, are a transcription factor and a lysine methyltransferase respectively showed to be significantly overexpressed in KO clones, with p values $\leq 0,05^*$ or $\leq 0,01^{**}$ (**Figure 18B**).

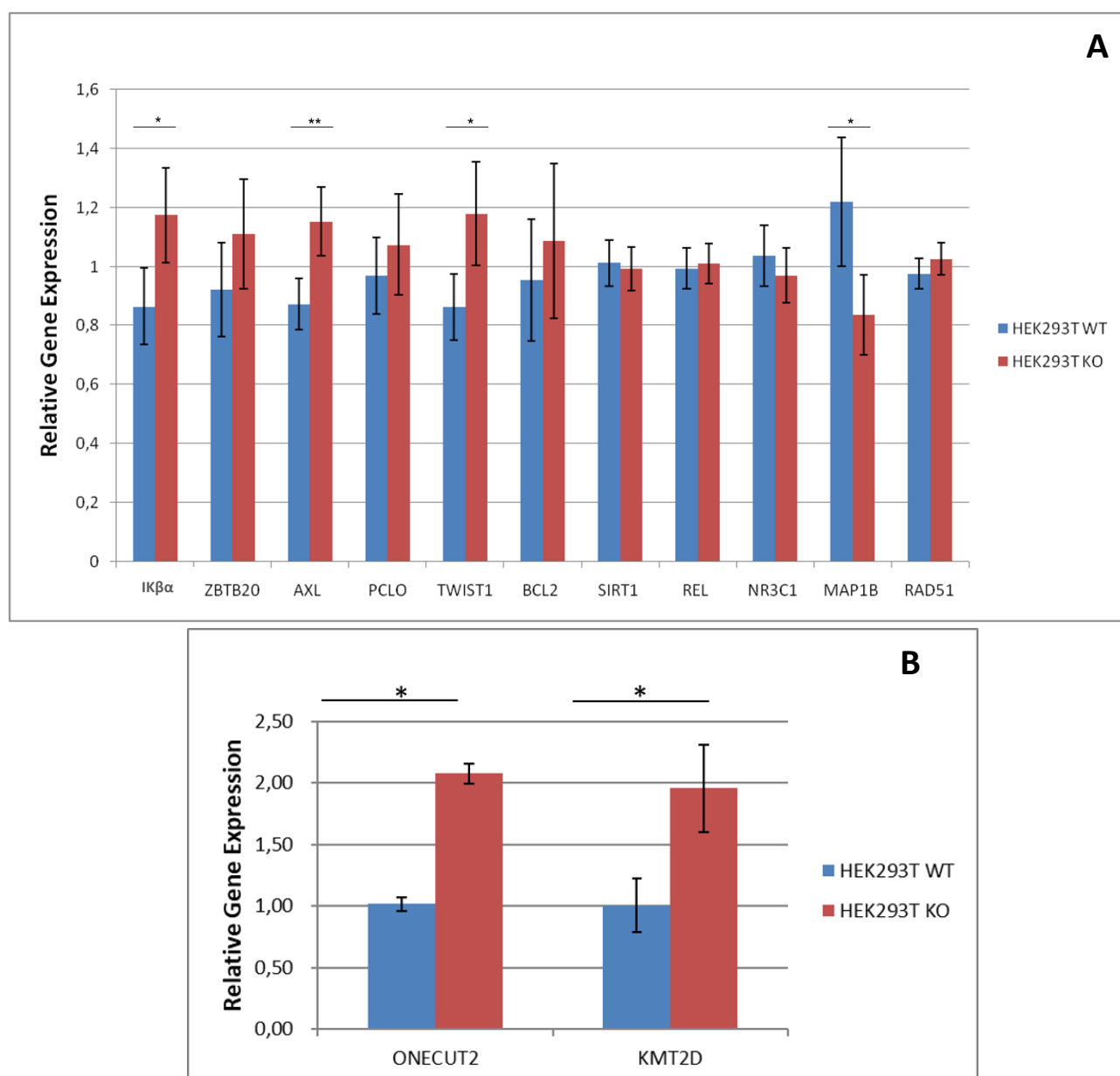


Figure 18 | RT-qPCR analysis on RNA extracted from HEK293T cells (WT) vs KO clones. *IKβ* (* $p=0,024$), *AXL* (** $p=0,0085$), *TWIST1* (* $p=0,028$), *MAP1B* (* $p=0,024$), *ONECUT2* (* $p=0,011$) and *KMT2D* (* $p=0,035$) mRNA level of expression in HeLa WT cells (blue bar) vs HEK293T KO clone (red bar). *IKβ*, *AXL*, *AXL*, *TWIST1*, *BCL2*, *SIRT1*, *RAD51* known gene targets of miR-34a, were chosen as controls. Normalization was performed relative to *RPLP0* gene expression. All data reported are representative of at least 3 independent experiments and error bars represent standard deviation (SD). The statistical significance was set at * $p \leq 0.05$ or ** $p \leq 0.01$ that was measured by using the T-student test for independent data with GraphPad.

The expression of some of the above-mentioned known and predicted targets was, also, tested at protein level, through Western blot analysis. The protein expression of SIRT1 and $\text{IK}\beta\alpha$, two miR-34a regulated genes, was analyzed. SIRT1 showed a significant (p value = 0,03548) reduced expression, in miR-34 KO HEK293T cells, compared to WT cells (**Figure 19**) while, it was observed an upregulation of $\text{IK}\beta\alpha$, although not significant, in KO cells respect to WT cells (**Figure 20**). In the replicates, the expression showed a high variability.

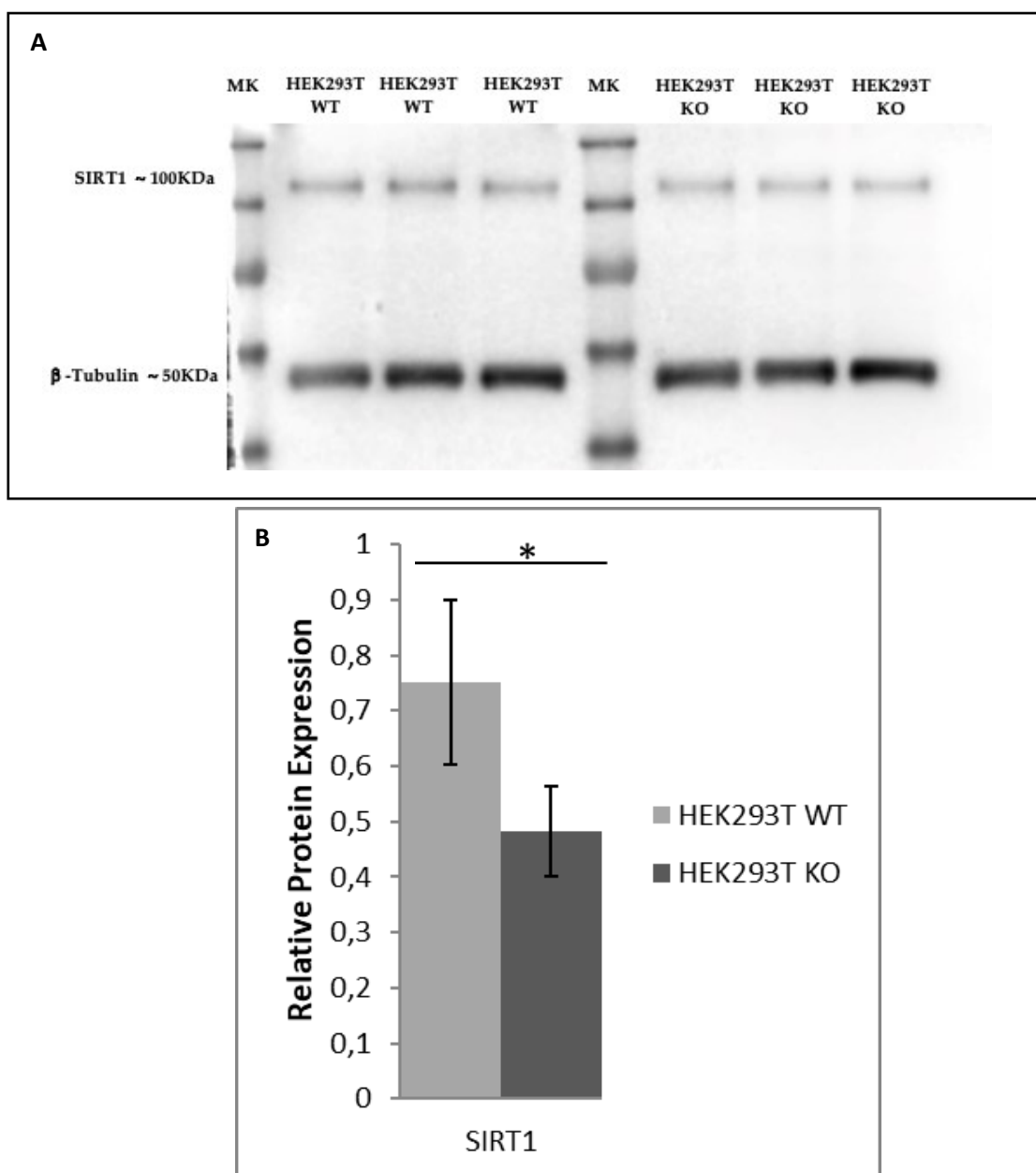


Figure 19 | *SIRT1* protein expression in HEK293T WT vs miR-34a KO cell lines; Western blot (A). All data reported are representative of at least 3 independent experiments and error bars represent standard deviation (SD). Densitometric analysis with ImageJ ($*p = 0,035$) (B).

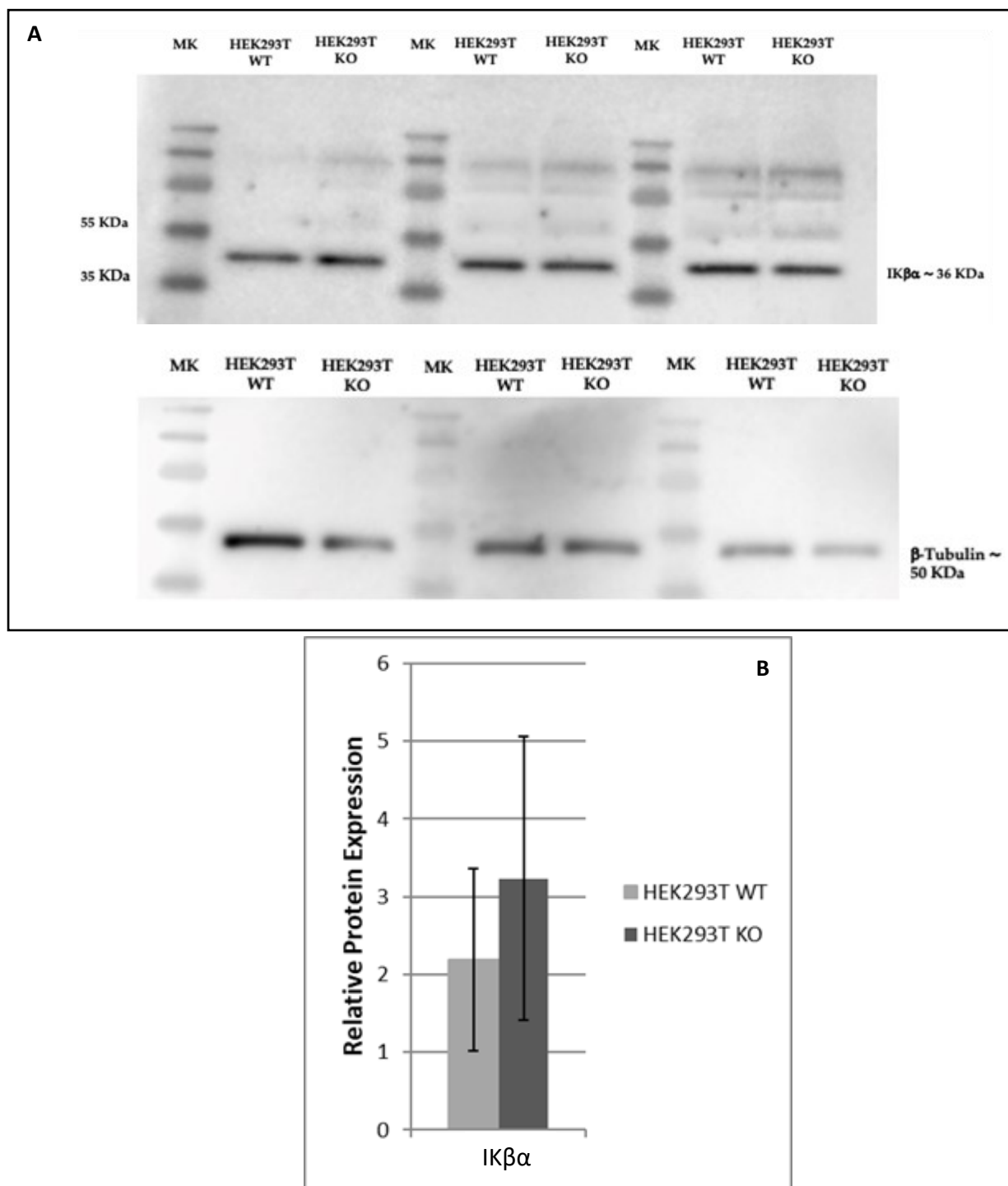
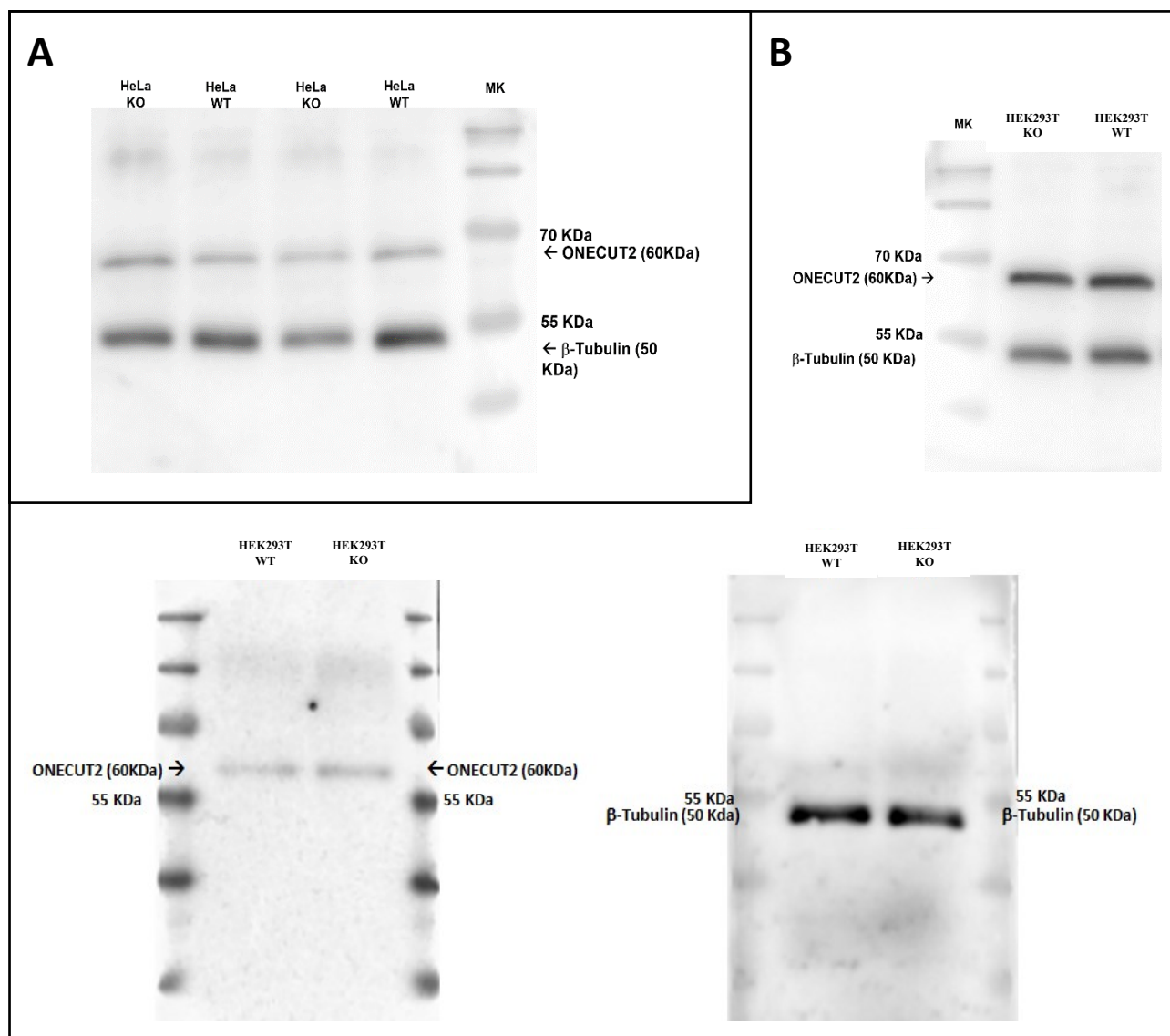


Figure 20 | *IKβα* protein expression in HEK293T cells (WT) vs HEK293T KO clone; Western blot (A). All data reported are representative of at least 3 independent experiments and error bars represent standard deviation (SD). Densitometric analysis with ImageJ (B).

Concerning the evaluation of the expression, at protein level, of the two putative targets MAP1B and KMT2D, only preliminary Western blot experiments were performed. Due to lower specificity of the antibodies commercially available, it was not possible to complete the analyses.

4.5 ONECUT2 is upregulated at protein level in both HeLa and HEK293T miR-34a-KO cells compared to WT cell lines.

Western blot analyses of the transcription factor, ONECUT2, showed an increase in the protein level detected in HeLa (**Figure 21, panel A and C**) and HEK293T (**Figure 21, panel B and C**) miR-34a-KO clones compared to the WT cell lines.



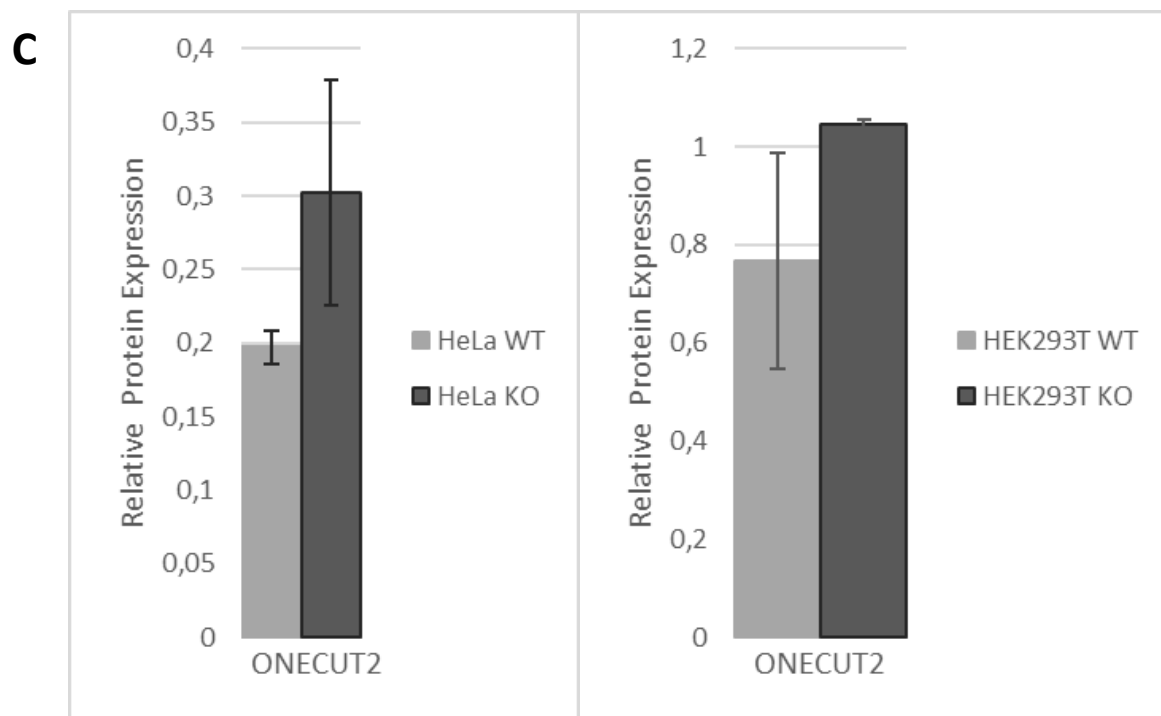


Figure 21 | Western Blot analyses of ONECUT2 in HeLa (A) and HEK293T (B) miR-34a-KO clones compared to WT cell lines. Data reported are representative of at least 2 independent experiments and error bars represent standard deviation (SD). (C) Densitometric analysis with ImageJ.

4.6 Cloning KMT2D 3'-UTR in the pGL3 Luciferase promoter vector.

Bioinformatics analyses identified a putative miR-34a target sequence in the 3'-UTR region of the histone-lysine N-methyltransferase 2D (KMT2D) transcripts (Figure 15). In order to functionally analyze the contribution of the 3' –UTR *cis*-sequence, the consensus (called “seed”) sequence of miR-34a was amplified with specific primers containing the restriction sites for XbaI starting from the genomic DNA and subsequently cloned into the pGL3 promoter vector upstream to the gene coding for the Luciferase. The bacteria clones containing the KMT2D 3'-UTR inserted in the pGL3 Luciferase promoter vector were selected by colony PCR. Recombinant colonies showed the expected band of about 500 bp. Sanger sequencing was performed to verify that the KMT2D 3'-UTR 428 bp fragment was present and correctly oriented within the pGL3 vector (Figure 22).

This plasmid will be applied in Luciferase assays to evaluate the role of miR-34a in regulating the KMT2D transcript.

[Tools \(/Tools/\)](#) > [Multiple Sequence Alignment \(/Tools/msa\)](#) > Clustal Omega

Results for job clustalo-l20221031-120302-0519-78427247-p1m

```

CLUSTAL O(1.2.4) multiple sequence alignment

Reference      GTCTCTCTATGGGTTGTGTTTCCCTTGTTTTCCACTCTGACAAATGCAACATGAACGGGAA   60
pGL3_COL3     GTCTCTCTATGGGTTGTGTTTCCCTTGTTTTCCACTCTGACAAATGCAACATGAACGGGAA   60
*****

Reference      AGAGGCGCCAGCTGCCAGGAGGGCAAGCTGGGCAAGCCGGGCAAGGAGACCCCGCAC   120
pGL3_COL3     AGAGGCGCCAGCTGCCAGGAGGGCAAGCTGGGCAAGCCGGGCAAGGAGACCCCGCAC   120
*****

Reference      CACACCTACCTCATTAAAGTGTGGATTTTTTGCTGTTTTGAAATGTGAGACCCCTCCA   180
pGL3_COL3     CACACCTACCTCATTAAAGTGTGGATTTTTTGCTGTTTTGAAATGTGAGACCCCTCCA   180
*****

Reference      AGCCCCCTACTGCCCAACCTCTCCCCACCTCACTGCCCTCTTCTGAGTGGTGGAAAG   240
pGL3_COL3     AGCCCCCTACTGCCCAACCTCTCCCCACCTCACTGCCCTCTTCTGAGTGGTGGAAAG   240
*****

Reference      GGGGTAGGAGGGAAGAAAAACAACAACAAAAATCCATCTTTGTTTTAATTATGGG   300
pGL3_COL3     GGGGTAGGAGGGAAGAAAAACAACAACAAAAATCCATCTTTGTTTTAATTATGGG   300
*****

Reference      CATGGGATGGTGGTTGAGGCAATGATGATGAAGATTGGGGATGACTGGCCCTAGTTGC   360
pGL3_COL3     CATGGGATGGTGGTTGAGGCAATGATGATGAAGATTGGGGATGACTGGCCCTAGTTGC   360
*****

Reference      TCTAGGACTTCTTCTCATCTGGACATGGGGCAGGAGGGAGCTAAACCTAGGACCAGG   420
pGL3_COL3     TCTAGGACTTCTTCTCATCTGGACATGGGGCAGGAGGGAGCTAAACCTAGGACCAGG   420
*****

Reference      ATATCTCTTAGAGTCGGGGCGGCCGGCCGCTTCGAGCAGACATGATAAGATACATTGA   480
pGL3_COL3     ATATCTCT----- 429
*****

Reference      TGAGTTTGGACAAACCACAACCTAGAATGCAGT   512
pGL3_COL3     ----- 429

```

Figure 22 | Sanger Sequencing: the plasmid extracted from colony 3 contains the 512 bp fragment cloned and well oriented within the pGL3 vector.

5. DISCUSSION

Micro-RNAs are small non-coding RNAs that are approximately 21 nucleotides in length²⁶³. They are important post-transcriptional regulators involved both in physiological events, such as proliferation, differentiation and development, and in pathological processes such as tumors and neurodegenerative diseases²⁶⁴. miRNAs perform an inhibitory effect on gene expression and exert this function either through inhibition of translation or, also, by promoting mRNA degradation²⁶⁵.

One of the most studied miRNAs is miR-34; dysregulations involving this micro-RNA are frequently observed in neuroblastomas, gliomas, breast, non-small cell lung, prostate, and hematological malignancies²⁶⁵. The miR-34 family has a crucial role in tumor formation, thanks to its antitumor function which is exerted by inhibiting the expression of several proto-oncogenes and, furthermore, promoting the activity of the most important tumor suppressor gene: p53²⁶⁶.

Over the years, to further investigate the role of the miR-34 family in pathological conditions, several researchers have attempted to knock out miR-34a both in vitro and in vivo, using TALENS (Transcription Activator-like Effector Nuclease)²⁵¹ or the Cre-LoxP method²⁵².

The aim of this work was to characterize HeLa and HEK293T miR-34a KO cell lines produced using CRISPR/Cas9 technology. These KO cell lines were characterized in terms of proliferation rate and expression of known and putative miR-34 targets, by quantitative PCR and Western blot analysis.

In both cell lines, by means of quantitative PCR experiments, the absence of miR-34a expression was demonstrated. Quantitative PCR demonstrated increased expression of BCL2, a known target, in HeLa cells and HeLa KO clones, 2G10. While an overexpression of another validated target, IK β α was detected in both clones by Western blot analysis. Later Sanger sequencing confirmed a deletion in the miR-34a genomic sequence.

The first step in the characterization of the miR-34a KO clones was to analyze their growth with respect to the HeLa and HEK293T WT cell lines through a proliferation assay. The results showed that both miR-34a KO HeLa and HEK293T clones had similar proliferation rates compared to HeLa and HEK293T WT cell lines, indicating that miR-34a is not essential in

controlling proliferation rate in cell culture models. Then, to further characterize these cell lines, the expression of selected known and putative miR-34a targets was evaluated by qPCR and Western blot. In particular, the expression of previously validated targets, BCL2, IK β α , AXL, TWIST1, RAD51 and SIRT1, was analyzed at the mRNA level. All these genes have important roles in tumor development and can be inhibited by miR-34a in different cell models. BCL2 is an anti-apoptotic protein and its inhibition by miR-34a has been shown to promote apoptosis, reducing cell survival²⁵⁶. IK β α is involved in the inhibition of the NF- κ B pathway which, in turn, has an important role in the activation of the immune system²⁵⁷. AXL is a tyrosine kinase receptor that promotes invasion and metastasis²⁵⁸. TWIST1 stimulates epithelial-mesenchymal transition (EMT)²⁵⁹. RAD51 is a recombinase involved in tumor formation, as it promotes cell proliferation and aerobic glycolysis²⁶⁷, while SIRT1, an NAD-dependent deacetylase, may be involved in deacetylation and thus inhibition of the tumor suppressor gene p53²⁶⁸.

Among the genes differentially expressed by transcriptome analysis and those selected for the presence of a binding sequence with miR-34a by Target Scan database, we selected 9 genes (REL, NR3C1, MAP1B, COL6A2, ZBTB20, PCLO, ONECUT2 and KMT2D) based on their role in tumor development. REL is a transcription factor and, by promoting B cell survival and proliferation, has been implicated in oncogenic processes²⁶⁹. NR3C1 encodes a glucocorticoid receptor that has a role in promoting tumor formation, in fact it is often overexpressed in adrenal malignancies²⁷⁰. MAP1B, which controls microtubule dynamics, has been shown to promote aggressiveness of tumors²⁷¹. COL6A2 encodes the α -chain of collagen VI, and its increased expression has been detected in renal tumors. It is involved in tumorigenesis due to its role in several tumor-related pathways such as glioma²⁷². ZBTB20 is a transcriptional repressor that, through different mechanisms, is implicated in the development of liver tumors²⁷³. PCLO encodes a protein that belongs to the presynaptic cytoskeletal matrix and is involved in the release of neurotransmitters. It is frequently upregulated in diffuse large B-cell lymphomas; however, its specific pro-tumorigenic role is still not well understood²⁷⁴.

The last two alleged targets tested, ONECUT2 and KMT2D are a transcription factor and a lysine methyltransferase, respectively. ONECUT2 promotes cell proliferation, adhesion, migration and metabolism and its expression appears to be upregulated in prostate, colorectal, hepatocellular and lung cancers²⁷⁵. KMT2D, on the other hand, is involved in the modifications of histones and favors the survival of cancer cells as it is able to increase the expression of antioxidant genes²⁷⁶.

Therefore, the expressions of BCL2, MAP1B, COL6A2, REL, ONECUT2 and KMT2D genes were measured in the HeLa cell line. Real-time PCR experiments showed that the known target BCL2 was significantly overexpressed in the HeLa miR-34a KO cell line, reproducing results previously reported in the literature. Furthermore, the predicted targets REL and MAP1B showed a significant increase in expression in KO cells, suggesting their regulation by miR-34a. COL6A2, was shown to be significantly downregulated in KO cells, indicating that miR-34a may not directly regulate its mRNA level. Concerning the HEK293T cell line, the known targets, IK β , TWIST1 and AXL, were significantly overexpressed, in quantitative PCR, in miR-34a KO cells, as described by previous studies. Instead, SIRT1, another validated miR-34a target, showed decreased expression, both by qPCR and Western blot, in KO cells. These results may demonstrate that the inhibitory effect of miR-34a can be compensated by other mechanisms in miR-34a KO cells. A similar interpretation can be applied to MAP1B whose expression was found to be differentially regulated in miR-34a KO HeLa and HEK293T cells.

Among the genes previously selected for analysis, COL6A2 was excluded from the list of putative direct miR-34a targets because it was found to be downregulated in the HeLa miR-34a-KO cell line compared to WT in quantitative PCR analyses, also confirming the data obtained from transcriptome analysis; REL, NR3C1 and MAP1B were then excluded because they were shown to be differentially regulated between the two miR-34a-KO cell lines; while ZBTB20 and PCLO were poorly expressed in our two model cell lines, for which the choice fell on ONECUT2 and KMT2D.

In HEK293T cells, two predicted targets, ONECUT2 and KMT2D, behaved as true miR-34a targets. Indeed, both genes showed a significant overexpression, at the mRNA level, in KO cells. Preliminary Western blot analyzes were performed to further study the regulation of ONECUT2 and KMT2D by miR-34a, also at the protein level. ONECUT2 was overexpressed in miR-34a-KO clones compared to HeLa and HEK293T WT cells. As far as the KMT2D protein is concerned however, due to the high molecular weight (600KDa) and the non-specificity of the antibody, it was not possible to obtain significant results. Thus, in order to have more conclusive information regarding the regulation of these two predicted targets by miR-34a, we proceeded with the analysis of the 3'-UTR of ONECUT2 and KMT2D transcripts by Target Scan online tool. From bioinformatic analyses, the 3'-UTR of ONECUT2 was shown to have as many as 4 potential binding sequences to the miR-34a seed region, three of which were poorly conserved. Instead, the 3'-UTR of KMT2D showed only one predicted site for the hypothetical binding of

miR-34a. For simplicity and speed of analysis, we preferred to clone 428 bp of the KMT2D 3'-UTR fragment containing the seed sequence for miR-34a into the pGL3 Promoter.

Furthermore, observing the results on the expression of known and putative targets in the two KO cell lines, it is possible to deduce that miR-34a has a different behavior depending on the cells and tissues in which it acts. Indeed, from Western blot analyzes on our HeLa and HEK293T miR-34a-KO model cell lines, IK β α , a known miR-34a target, showed only a non-statistically significant upregulation trend compared to WT cell lines; moreover, SIRT1, also a known target of miR-34a, showed a significant and unexpected downregulation in HEK293T miR-34a-KO compared to WT cell line.

Numerous factors contribute to determining which genes are regulated by miRNAs such as: functionalized compartmentalization, movement of miRISCs within cells, availability and abundance of miRNAs and their target mRNAs. Furthermore, miRNA suppression of mRNA targets is not ubiquitous across cell types. Alternative splicing and alternative polyadenylation affecting the 3' UTRs and RNA binding proteins are cell type specific and affect the secondary structures of the target mRNA, modifying the available pool of MREs⁵⁴⁻⁵⁶. This renders the mRNA subsets sensitive or insensitive to miRNA-mediated gene regulation in a manner specific to each cell type/state.

6. CONCLUSIONS AND FUTURE PERSPECTIVES

In conclusion, all these results indicate that miR-34a gene expression may participate in different gene expression regulation mechanisms according to cell type. Furthermore, they suggest that the inhibitory effect of miR-34a could be counterbalanced by feedback loop processes which could explain the absence of effect of the expression of selected miR-34a target genes in KO cells. They suggest that ONECUT2, a transcription factor that stimulates the expression of genes involved in the differentiation of melanocytes and hepatocytes, and KMT2D, a histone lysine methyl transferase, may be novel targets of miR-34a. To confirm KMT2D and ONECUT2 as targets of miR-34a, it would be necessary to conclude Western blot analyzes and luciferase assays also by mutating the binding sequences of miR-34a to their 3'-UTRs. A preliminary analysis with the Agilent online tool (<https://www.agilent.com/store/primerDesignProgram.jsp>) made it possible to generate and verify the hypothetical mutation to be induced in the 3'-UTR-KMT2D fragment cloned in the pGL3 promoter vector at the level of the predicted miR-34a-binding sequence (CACTGCC). A mutation in which the CAC triplet is mutated to the GAG triplet, in addition to destroying the miR-34a binding site, generates a single restriction site recognized by the *Ale* I enzyme which would allow the mutated fragment to be discriminated from the non-mutated one. Regarding ONECUT2, the study is more complex because its 3'-UTR has as many as 4 potential miR-34a binding sites, one of which is conserved and the other three poorly conserved. Furthermore, HeLa and HEK293T KO clones are a valuable tool to study the general role of miR-34a in cell proliferation and gene expression regulation. However, they do not represent a good cellular model to study its involvement in tumorigenesis. To study the mechanisms by which miR-34a is involved in tumorigenesis, the melanoma A375 cell line represents a more suitable cell line, and it will be chosen to confirm the preliminary data obtained in the KO clones.

These further analyzes will confirm these preliminary results and help identify a new target protein for cancer therapy.

7. REFERENCES

1. Li, L. *et al.* MiR-34a inhibits proliferation and migration of breast cancer through down-regulation of Bcl-2 and SIRT1. *Clin. Exp. Med.* **13**, 109–117 (2013).
2. Bayraktar, R. *et al.* Dual Suppressive Effect of miR-34a on the FOXM1/eEF2-Kinase Axis Regulates Triple-Negative Breast Cancer Growth and Invasion. *Clin. Cancer Res. Off. J. Am. Assoc. Cancer Res.* **24**, 4225–4241 (2018).
3. Liu, K. *et al.* MIR34A regulates autophagy and apoptosis by targeting HMGB1 in the retinoblastoma cell. *Autophagy* **10**, 442–452 (2014).
4. Xiao, X. *et al.* The miR-34a-LDHA axis regulates glucose metabolism and tumor growth in breast cancer. *Sci. Rep.* **6**, 21735 (2016).
5. Zhao, G. *et al.* MicroRNA-34a suppresses cell proliferation by targeting LMTK3 in human breast cancer mcf-7 cell line. *DNA Cell Biol.* **32**, 699–707 (2013).
6. Wang, Y. *et al.* MiR-34a modulates ErbB2 in breast cancer. *Cell Biol. Int.* **41**, 93–101 (2017).
7. Lee, R. C., Feinbaum, R. L. & Ambros, V. The *C. elegans* heterochronic gene *lin-4* encodes small RNAs with antisense complementarity to *lin-14*. *Cell* **75**, 843–854 (1993).
8. Wightman, B., Ha, I. & Ruvkun, G. Posttranscriptional regulation of the heterochronic gene *lin-14* by *lin-4* mediates temporal pattern formation in *C. elegans*. *Cell* **75**, 855–862 (1993).
9. Pasquinelli, A. E. *et al.* Conservation of the sequence and temporal expression of *let-7* heterochronic regulatory RNA. *Nature* **408**, 86–89 (2000).
10. Friedländer, M. R. *et al.* Evidence for the biogenesis of more than 1,000 novel human microRNAs. *Genome Biol.* **15**, R57 (2014).
11. Ha, M. & Kim, V. N. Regulation of microRNA biogenesis. *Nat. Rev. Mol. Cell Biol.* **15**, 509–524 (2014).
12. Broughton, J. P., Lovci, M. T., Huang, J. L., Yeo, G. W. & Pasquinelli, A. E. Pairing beyond the Seed Supports MicroRNA Targeting Specificity. *Mol. Cell* **64**, 320–333 (2016).
13. Fu, G., Brkić, J., Hayder, H. & Peng, C. MicroRNAs in Human Placental Development and Pregnancy Complications. *Int. J. Mol. Sci.* **14**, 5519–5544 (2013).
14. Tüfekci, K. U., Oner, M. G., Meuwissen, R. L. J. & Genç, S. The role of microRNAs in human diseases. *Methods Mol. Biol. Clifton NJ* **1107**, 33–50 (2014).
15. Paul, P. *et al.* Interplay between miRNAs and human diseases. *J. Cell. Physiol.* **233**, 2007–2018 (2018).
16. Hayes, J., Peruzzi, P. P. & Lawler, S. MicroRNAs in cancer: biomarkers, functions and therapy. *Trends Mol. Med.* **20**, 460–469 (2014).
17. Wang, J., Chen, J. & Sen, S. MicroRNA as Biomarkers and Diagnostics. *J. Cell. Physiol.* **231**, 25–30 (2016).

18. Huang, W. MicroRNAs: Biomarkers, Diagnostics, and Therapeutics. *Methods Mol. Biol. Clifton NJ* **1617**, 57–67 (2017).
19. de Rie, D. *et al.* An integrated expression atlas of miRNAs and their promoters in human and mouse. *Nat. Biotechnol.* **35**, 872–878 (2017).
20. Kim, Y.-K. & Kim, V. N. Processing of intronic microRNAs. *EMBO J.* **26**, 775–783 (2007).
21. Tanzer, A. & Stadler, P. F. Molecular evolution of a microRNA cluster. *J. Mol. Biol.* **339**, 327–335 (2004).
22. O'Brien, J., Hayder, H., Zayed, Y. & Peng, C. Overview of MicroRNA Biogenesis, Mechanisms of Actions, and Circulation. *Front. Endocrinol.* **9**, 402 (2018).
23. Denli, A. M., Tops, B. B. J., Plasterk, R. H. A., Ketting, R. F. & Hannon, G. J. Processing of primary microRNAs by the Microprocessor complex. *Nature* **432**, 231–235 (2004).
24. Alarcón, C. R., Lee, H., Goodarzi, H., Halberg, N. & Tavazoie, S. F. N6-methyladenosine marks primary microRNAs for processing. *Nature* **519**, 482–485 (2015).
25. Han, J. *et al.* The Drosha-DGCR8 complex in primary microRNA processing. *Genes Dev.* **18**, 3016–3027 (2004).
26. Okada, C. *et al.* A high-resolution structure of the pre-microRNA nuclear export machinery. *Science* **326**, 1275–1279 (2009).
27. Zhang, H., Kolb, F. A., Jaskiewicz, L., Westhof, E. & Filipowicz, W. Single processing center models for human Dicer and bacterial RNase III. *Cell* **118**, 57–68 (2004).
28. Yoda, M. *et al.* ATP-dependent human RISC assembly pathways. *Nat. Struct. Mol. Biol.* **17**, 17–23 (2010).
29. Khvorova, A., Reynolds, A. & Jayasena, S. D. Functional siRNAs and miRNAs exhibit strand bias. *Cell* **115**, 209–216 (2003).
30. Ruby, J. G., Jan, C. H. & Bartel, D. P. Intronic microRNA precursors that bypass Drosha processing. *Nature* **448**, 83–86 (2007).
31. Babiarz, J. E., Ruby, J. G., Wang, Y., Bartel, D. P. & Blelloch, R. Mouse ES cells express endogenous shRNAs, siRNAs, and other Microprocessor-independent, Dicer-dependent small RNAs. *Genes Dev.* **22**, 2773–2785 (2008).
32. Xie, M. *et al.* Mammalian 5'-capped microRNA precursors that generate a single microRNA. *Cell* **155**, 1568–1580 (2013).
33. Yang, J.-S. *et al.* Conserved vertebrate mir-451 provides a platform for Dicer-independent, Ago2-mediated microRNA biogenesis. *Proc. Natl. Acad. Sci. U. S. A.* **107**, 15163–15168 (2010).
34. Cheloufi, S., Dos Santos, C. O., Chong, M. M. W. & Hannon, G. J. A dicer-independent miRNA biogenesis pathway that requires Ago catalysis. *Nature* **465**, 584–589 (2010).
35. Huntzinger, E. & Izaurralde, E. Gene silencing by microRNAs: contributions of translational repression and mRNA decay. *Nat. Rev. Genet.* **12**, 99–110 (2011).

36. Ipsaro, J. J. & Joshua-Tor, L. From guide to target: molecular insights into eukaryotic RNA-interference machinery. *Nat. Struct. Mol. Biol.* **22**, 20–28 (2015).
37. Xu, W., San Lucas, A., Wang, Z. & Liu, Y. Identifying microRNA targets in different gene regions. *BMC Bioinformatics* **15 Suppl 7**, S4 (2014).
38. Forman, J. J., Legesse-Miller, A. & Collier, H. A. A search for conserved sequences in coding regions reveals that the let-7 microRNA targets Dicer within its coding sequence. *Proc. Natl. Acad. Sci. U. S. A.* **105**, 14879–14884 (2008).
39. Zhang, J. *et al.* Oncogenic role of microRNA-532-5p in human colorectal cancer via targeting of the 5'UTR of RUNX3. *Oncol. Lett.* **15**, 7215–7220 (2018).
40. Dharap, A., Pokrzywa, C., Murali, S., Pandi, G. & Vemuganti, R. MicroRNA miR-324-3p induces promoter-mediated expression of RelA gene. *PLoS One* **8**, e79467 (2013).
41. Kawamata, T. & Tomari, Y. Making RISC. *Trends Biochem. Sci.* **35**, 368–376 (2010).
42. Jo, M. H. *et al.* Human Argonaute 2 Has Diverse Reaction Pathways on Target RNAs. *Mol. Cell* **59**, 117–124 (2015).
43. Krützfeldt, J. *et al.* Silencing of microRNAs in vivo with 'antagomirs'. *Nature* **438**, 685–689 (2005).
44. Ameres, S. L. *et al.* Target RNA-directed trimming and tailing of small silencing RNAs. *Science* **328**, 1534–1539 (2010).
45. Jonas, S. & Izaurralde, E. Towards a molecular understanding of microRNA-mediated gene silencing. *Nat. Rev. Genet.* **16**, 421–433 (2015).
46. Ellwanger, D. C., Büttner, F. A., Mewes, H.-W. & Stümpflen, V. The sufficient minimal set of miRNA seed types. *Bioinforma. Oxf. Engl.* **27**, 1346–1350 (2011).
47. Behm-Ansmant, I. *et al.* mRNA degradation by miRNAs and GW182 requires both CCR4:NOT deadenylase and DCP1:DCP2 decapping complexes. *Genes Dev.* **20**, 1885–1898 (2006).
48. Christie, M., Boland, A., Huntzinger, E., Weichenrieder, O. & Izaurralde, E. Structure of the PAN3 pseudokinase reveals the basis for interactions with the PAN2 deadenylase and the GW182 proteins. *Mol. Cell* **51**, 360–373 (2013).
49. Braun, J. E. *et al.* A direct interaction between DCP1 and XRN1 couples mRNA decapping to 5' exonucleolytic degradation. *Nat. Struct. Mol. Biol.* **19**, 1324–1331 (2012).
50. Vasudevan, S. & Steitz, J. A. AU-rich-element-mediated upregulation of translation by FXR1 and Argonaute 2. *Cell* **128**, 1105–1118 (2007).
51. Truesdell, S. S. *et al.* MicroRNA-mediated mRNA translation activation in quiescent cells and oocytes involves recruitment of a nuclear microRNP. *Sci. Rep.* **2**, 842 (2012).
52. Bukhari, S. I. A. *et al.* A Specialized Mechanism of Translation Mediated by FXR1a-Associated MicroRNP in Cellular Quiescence. *Mol. Cell* **61**, 760–773 (2016).
53. Ørom, U. A., Nielsen, F. C. & Lund, A. H. MicroRNA-10a binds the 5'UTR of ribosomal protein mRNAs and enhances their translation. *Mol. Cell* **30**, 460–471 (2008).

-
54. Bottini, S. *et al.* Post-transcriptional gene silencing mediated by microRNAs is controlled by nucleoplasmic Sfpq. *Nat. Commun.* **8**, 1189 (2017).
55. Nam, J.-W. *et al.* Global analyses of the effect of different cellular contexts on microRNA targeting. *Mol. Cell* **53**, 1031–1043 (2014).
56. Blazie, S. M. *et al.* Alternative Polyadenylation Directs Tissue-Specific miRNA Targeting in *Caenorhabditis elegans* Somatic Tissues. *Genetics* **206**, 757–774 (2017).
57. Roderburg, C. & Luedde, T. Circulating microRNAs as markers of liver inflammation, fibrosis and cancer. *J. Hepatol.* **61**, 1434–1437 (2014).
58. Sohn, W. *et al.* Serum exosomal microRNAs as novel biomarkers for hepatocellular carcinoma. *Exp. Mol. Med.* **47**, e184 (2015).
59. Pereira-da-Silva, T. *et al.* Circulating microRNA profiles in different arterial territories of stable atherosclerotic disease: a systematic review. *Am. J. Cardiovasc. Dis.* **8**, 1–13 (2018).
60. Iftikhar, H. & Carney, G. E. Evidence and potential in vivo functions for biofluid miRNAs: From expression profiling to functional testing: Potential roles of extracellular miRNAs as indicators of physiological change and as agents of intercellular information exchange. *BioEssays News Rev. Mol. Cell. Dev. Biol.* **38**, 367–378 (2016).
61. Chen, X. *et al.* Characterization of microRNAs in serum: a novel class of biomarkers for diagnosis of cancer and other diseases. *Cell Res.* **18**, 997–1006 (2008).
62. Arroyo, J. D. *et al.* Argonaute2 complexes carry a population of circulating microRNAs independent of vesicles in human plasma. *Proc. Natl. Acad. Sci. U. S. A.* **108**, 5003–5008 (2011).
63. Cogswell, J. P. *et al.* Identification of miRNA changes in Alzheimer’s disease brain and CSF yields putative biomarkers and insights into disease pathways. *J. Alzheimers Dis. JAD* **14**, 27–41 (2008).
64. Gallo, A., Tandon, M., Alevizos, I. & Illei, G. G. The majority of microRNAs detectable in serum and saliva is concentrated in exosomes. *PLoS One* **7**, e30679 (2012).
65. Zhou, Q. *et al.* Immune-related microRNAs are abundant in breast milk exosomes. *Int. J. Biol. Sci.* **8**, 118–123 (2012).
66. Weber, J. A. *et al.* The microRNA spectrum in 12 body fluids. *Clin. Chem.* **56**, 1733–1741 (2010).
67. da Silveira, J. C., Veeramachaneni, D. N. R., Winger, Q. A., Carnevale, E. M. & Bouma, G. J. Cell-secreted vesicles in equine ovarian follicular fluid contain miRNAs and proteins: a possible new form of cell communication within the ovarian follicle. *Biol. Reprod.* **86**, 71 (2012).
68. Mitchell, P. S. *et al.* Circulating microRNAs as stable blood-based markers for cancer detection. *Proc. Natl. Acad. Sci. U. S. A.* **105**, 10513–10518 (2008).
69. Turchinovich, A., Weiz, L., Langheinz, A. & Burwinkel, B. Characterization of extracellular circulating microRNA. *Nucleic Acids Res.* **39**, 7223–7233 (2011).
70. Vickers, K. C., Palmisano, B. T., Shoucri, B. M., Shamburek, R. D. & Remaley, A. T. MicroRNAs are transported in plasma and delivered to recipient cells by high-density lipoproteins. *Nat. Cell Biol.* **13**, 423–433 (2011).

71. Tabet, F. *et al.* HDL-transferred microRNA-223 regulates ICAM-1 expression in endothelial cells. *Nat. Commun.* **5**, 3292 (2014).
72. Wang, K., Zhang, S., Weber, J., Baxter, D. & Galas, D. J. Export of microRNAs and microRNA-protective protein by mammalian cells. *Nucleic Acids Res.* **38**, 7248–7259 (2010).
73. Turchinovich, A., Weiz, L. & Burwinkel, B. Extracellular miRNAs: the mystery of their origin and function. *Trends Biochem. Sci.* **37**, 460–465 (2012).
74. Di Leva, G., Garofalo, M. & Croce, C. M. MicroRNAs in cancer. *Annu. Rev. Pathol.* **9**, 287–314 (2014).
75. Ventura, A. & Jacks, T. MicroRNAs and cancer: short RNAs go a long way. *Cell* **136**, 586–591 (2009).
76. Lu, J. *et al.* MicroRNA expression profiles classify human cancers. *Nature* **435**, 834–838 (2005).
77. Volinia, S. *et al.* A microRNA expression signature of human solid tumors defines cancer gene targets. *Proc. Natl. Acad. Sci. U. S. A.* **103**, 2257–2261 (2006).
78. Chen, W. *et al.* Clinical significance and detection of microRNA-21 in serum of patients with diffuse large B-cell lymphoma in Chinese population. *Eur. J. Haematol.* **92**, 407–412 (2014).
79. Cui, M. *et al.* Circulating MicroRNAs in Cancer: Potential and Challenge. *Front. Genet.* **10**, 626 (2019).
80. Cimmino, A. *et al.* miR-15 and miR-16 induce apoptosis by targeting BCL2. *Proc. Natl. Acad. Sci. U. S. A.* **102**, 13944–13949 (2005).
81. Thammaiah, C. K. & Jayaram, S. Role of let-7 family microRNA in breast cancer. *Non-Coding RNA Res.* **1**, 77–82 (2016).
82. Johnson, S. M. *et al.* RAS is regulated by the let-7 microRNA family. *Cell* **120**, 635–647 (2005).
83. Manier, S. *et al.* The LIN28B/let-7 axis is a novel therapeutic pathway in multiple myeloma. *Leukemia* **31**, 853–860 (2017).
84. Ali Syeda, Z., Langden, S. S. S., Munkhzul, C., Lee, M. & Song, S. J. Regulatory Mechanism of MicroRNA Expression in Cancer. *Int. J. Mol. Sci.* **21**, 1723 (2020).
85. He, L. *et al.* A microRNA component of the p53 tumour suppressor network. *Nature* **447**, 1130–1134 (2007).
86. Navarro, F. & Lieberman, J. miR-34 and p53: New Insights into a Complex Functional Relationship. *PLoS One* **10**, e0132767 (2015).
87. Suzuki, H. I. *et al.* Modulation of microRNA processing by p53. *Nature* **460**, 529–533 (2009).
88. Zhang, J. *et al.* Loss of microRNA-143/145 disturbs cellular growth and apoptosis of human epithelial cancers by impairing the MDM2-p53 feedback loop. *Oncogene* **32**, 61–69 (2013).
89. Suh, S. O. *et al.* MicroRNA-145 is regulated by DNA methylation and p53 gene mutation in prostate cancer. *Carcinogenesis* **32**, 772–778 (2011).
90. Gan, B. *et al.* FoxOs enforce a progression checkpoint to constrain mTORC1-activated renal tumorigenesis. *Cancer Cell* **18**, 472–484 (2010).

-
91. Zeinali, T., Mansoori, B., Mohammadi, A. & Baradaran, B. Regulatory mechanisms of miR-145 expression and the importance of its function in cancer metastasis. *Biomed. Pharmacother. Biomedicine Pharmacother.* **109**, 195–207 (2019).
92. Dews, M. *et al.* Augmentation of tumor angiogenesis by a Myc-activated microRNA cluster. *Nat. Genet.* **38**, 1060–1065 (2006).
93. Mogilyansky, E. & Rigoutsos, I. The miR-17/92 cluster: a comprehensive update on its genomics, genetics, functions and increasingly important and numerous roles in health and disease. *Cell Death Differ.* **20**, 1603–1614 (2013).
94. O'Donnell, K. A., Wentzel, E. A., Zeller, K. I., Dang, C. V. & Mendell, J. T. c-Myc-regulated microRNAs modulate E2F1 expression. *Nature* **435**, 839–843 (2005).
95. Ventura, A. *et al.* Targeted deletion reveals essential and overlapping functions of the miR-17 through 92 family of miRNA clusters. *Cell* **132**, 875–886 (2008).
96. Li, Y., Choi, P. S., Casey, S. C., Dill, D. L. & Felsher, D. W. MYC through miR-17-92 suppresses specific target genes to maintain survival, autonomous proliferation, and a neoplastic state. *Cancer Cell* **26**, 262–272 (2014).
97. Mihailovich, M. *et al.* miR-17-92 fine-tunes MYC expression and function to ensure optimal B cell lymphoma growth. *Nat. Commun.* **6**, 8725 (2015).
98. Guan, T. *et al.* ZEB1, ZEB2, and the miR-200 family form a counterregulatory network to regulate CD8(+) T cell fates. *J. Exp. Med.* **215**, 1153–1168 (2018).
99. Chen, P. *et al.* MiR-200c is a cMyc-activated miRNA that promotes nasopharyngeal carcinoma by downregulating PTEN. *Oncotarget* **8**, 5206–5218 (2017).
100. Saito, Y. *et al.* Specific activation of microRNA-127 with downregulation of the proto-oncogene BCL6 by chromatin-modifying drugs in human cancer cells. *Cancer Cell* **9**, 435–443 (2006).
101. Liang, Y.-J. *et al.* MiR-124 targets Slug to regulate epithelial-mesenchymal transition and metastasis of breast cancer. *Carcinogenesis* **34**, 713–722 (2013).
102. Lujambio, A. *et al.* Genetic unmasking of an epigenetically silenced microRNA in human cancer cells. *Cancer Res.* **67**, 1424–1429 (2007).
103. Shindo, T. *et al.* Epigenetic silencing of miR-200b is associated with cisplatin resistance in bladder cancer. *Oncotarget* **9**, 24457–24469 (2018).
104. Davalos, V. *et al.* Dynamic epigenetic regulation of the microRNA-200 family mediates epithelial and mesenchymal transitions in human tumorigenesis. *Oncogene* **31**, 2062–2074 (2012).
105. Ceppi, P. *et al.* Loss of miR-200c expression induces an aggressive, invasive, and chemoresistant phenotype in non-small cell lung cancer. *Mol. Cancer Res. MCR* **8**, 1207–1216 (2010).
106. Schmid, G. *et al.* Expression and promotor hypermethylation of miR-34a in the various histological subtypes of ovarian cancer. *BMC Cancer* **16**, 102 (2016).
107. Wong, M. Y. W., Yu, Y., Walsh, W. R. & Yang, J.-L. microRNA-34 family and treatment of cancers with mutant or wild-type p53 (Review). *Int. J. Oncol.* **38**, 1189–1195 (2011).

-
108. Yeoh, G., Barton, S. & Kaestner, K. The International Journal of Biochemistry & Cell Biology. Preface. *Int. J. Biochem. Cell Biol.* **43**, 172 (2011).
109. Kent, O. A., Fox-Talbot, K. & Halushka, M. K. RREB1 repressed miR-143/145 modulates KRAS signaling through downregulation of multiple targets. *Oncogene* **32**, 2576–2585 (2013).
110. Seipel, K., Messerli, C., Wiedemann, G., Bacher, U. & Pabst, T. MN1, FOXP1 and hsa-miR-181a-5p as prognostic markers in acute myeloid leukemia patients treated with intensive induction chemotherapy and autologous stem cell transplantation. *Leuk. Res.* **89**, 106296 (2020).
111. Chang, T.-C. *et al.* Widespread microRNA repression by Myc contributes to tumorigenesis. *Nat. Genet.* **40**, 43–50 (2008).
112. Molenaar, J. J. *et al.* LIN28B induces neuroblastoma and enhances MYCN levels via let-7 suppression. *Nat. Genet.* **44**, 1199–1206 (2012).
113. Zhang, X. *et al.* Coordinated silencing of MYC-mediated miR-29 by HDAC3 and EZH2 as a therapeutic target of histone modification in aggressive B-Cell lymphomas. *Cancer Cell* **22**, 506–523 (2012).
114. Huang, X. *et al.* Hypoxia-inducible mir-210 regulates normoxic gene expression involved in tumor initiation. *Mol. Cell* **35**, 856–867 (2009).
115. Nallamshetty, S., Chan, S. Y. & Loscalzo, J. Hypoxia: a master regulator of microRNA biogenesis and activity. *Free Radic. Biol. Med.* **64**, 20–30 (2013).
116. Di Leva, G. *et al.* MicroRNA cluster 221-222 and estrogen receptor alpha interactions in breast cancer. *J. Natl. Cancer Inst.* **102**, 706–721 (2010).
117. Pinho, F. G. *et al.* Downregulation of microRNA-515-5p by the estrogen receptor modulates sphingosine kinase 1 and breast cancer cell proliferation. *Cancer Res.* **73**, 5936–5948 (2013).
118. Takayama, K.-I., Misawa, A. & Inoue, S. Significance of microRNAs in Androgen Signaling and Prostate Cancer Progression. *Cancers* **9**, (2017).
119. Löffler, D. *et al.* Interleukin-6 dependent survival of multiple myeloma cells involves the Stat3-mediated induction of microRNA-21 through a highly conserved enhancer. *Blood* **110**, 1330–1333 (2007).
120. Pan, X., Wang, Z.-X. & Wang, R. MicroRNA-21: a novel therapeutic target in human cancer. *Cancer Biol. Ther.* **10**, 1224–1232 (2010).
121. Coarfa, C. *et al.* Comprehensive proteomic profiling identifies the androgen receptor axis and other signaling pathways as targets of microRNAs suppressed in metastatic prostate cancer. *Oncogene* **35**, 2345–2356 (2016).
122. Liu, C. *et al.* MicroRNA-141 suppresses prostate cancer stem cells and metastasis by targeting a cohort of pro-metastasis genes. *Nat. Commun.* **8**, 14270 (2017).
123. Finlay-Schultz, J. *et al.* Progesterone downregulation of miR-141 contributes to expansion of stem-like breast cancer cells through maintenance of progesterone receptor and Stat5a. *Oncogene* **34**, 3676–3687 (2015).
124. Cittelly, D. M. *et al.* Progestin suppression of miR-29 potentiates dedifferentiation of breast cancer cells via KLF4. *Oncogene* **32**, 2555–2564 (2013).

-
125. Xia, H.-F. *et al.* Temporal and spatial regulation of miR-320 in the uterus during embryo implantation in the rat. *Int. J. Mol. Sci.* **11**, 719–730 (2010).
126. Wendler, A., Keller, D., Albrecht, C., Peluso, J. J. & Wehling, M. Involvement of let-7/miR-98 microRNAs in the regulation of progesterone receptor membrane component 1 expression in ovarian cancer cells. *Oncol. Rep.* **25**, 273–279 (2011).
127. Rainer, J. *et al.* Glucocorticoid-regulated microRNAs and mirtrons in acute lymphoblastic leukemia. *Leukemia* **23**, 746–752 (2009).
128. Tsai, K.-W. *et al.* Epigenetic regulation of miR-34b and miR-129 expression in gastric cancer. *Int. J. Cancer* **129**, 2600–2610 (2011).
129. Wang, D., Huang, J. & Hu, Z. RNA helicase DDX5 regulates microRNA expression and contributes to cytoskeletal reorganization in basal breast cancer cells. *Mol. Cell. Proteomics MCP* **11**, M111.011932 (2012).
130. Lambert, M.-P. *et al.* The RNA helicase DDX17 controls the transcriptional activity of REST and the expression of proneural microRNAs in neuronal differentiation. *Nucleic Acids Res.* **46**, 7686–7700 (2018).
131. Nishikura, K. A-to-I editing of coding and non-coding RNAs by ADARs. *Nat. Rev. Mol. Cell Biol.* **17**, 83–96 (2016).
132. Wang, Y. & Liang, H. When MicroRNAs Meet RNA Editing in Cancer: A Nucleotide Change Can Make a Difference. *BioEssays News Rev. Mol. Cell. Dev. Biol.* **40**, (2018).
133. Park, J.-E. *et al.* Dicer recognizes the 5' end of RNA for efficient and accurate processing. *Nature* **475**, 201–205 (2011).
134. Wu, K., He, J., Pu, W. & Peng, Y. The Role of Exportin-5 in MicroRNA Biogenesis and Cancer. *Genomics Proteomics Bioinformatics* **16**, 120–126 (2018).
135. Sun, H.-L. *et al.* ERK Activation Globally Downregulates miRNAs through Phosphorylating Exportin-5. *Cancer Cell* **30**, 723–736 (2016).
136. Ramírez-Moya, J., Wert-Lamas, L., Riesco-Eizaguirre, G. & Santisteban, P. Impaired microRNA processing by DICER1 downregulation endows thyroid cancer with increased aggressiveness. *Oncogene* **38**, 5486–5499 (2019).
137. Caruso, S. *et al.* Germline and somatic DICER1 mutations in familial and sporadic liver tumors. *J. Hepatol.* **66**, 734–742 (2017).
138. Fernández-Martínez, L. *et al.* Identification of somatic and germ-line DICER1 mutations in pleuropulmonary blastoma, cystic nephroma and rhabdomyosarcoma tumors within a DICER1 syndrome pedigree. *BMC Cancer* **17**, 146 (2017).
139. Foulkes, W. D., Priest, J. R. & Duchaine, T. F. DICER1: mutations, microRNAs and mechanisms. *Nat. Rev. Cancer* **14**, 662–672 (2014).
140. Heravi-Moussavi, A. *et al.* Recurrent somatic DICER1 mutations in nonepithelial ovarian cancers. *N. Engl. J. Med.* **366**, 234–242 (2012).
141. Hill, D. A. *et al.* DICER1 mutations in familial pleuropulmonary blastoma. *Science* **325**, 965 (2009).

-
142. Stewart, C. J. R., Charles, A. & Foulkes, W. D. Gynecologic Manifestations of the DICER1 Syndrome. *Surg. Pathol. Clin.* **9**, 227–241 (2016).
143. Garre, P., Pérez-Segura, P., Díaz-Rubio, E., Caldés, T. & de la Hoya, M. Reassessing the TARBP2 mutation rate in hereditary nonpolyposis colorectal cancer. *Nat. Genet.* **42**, 817–818; author reply 818 (2010).
144. Fish, L. *et al.* Nuclear TARBP2 Drives Oncogenic Dysregulation of RNA Splicing and Decay. *Mol. Cell* **75**, 967–981.e9 (2019).
145. Casey, M. C. *et al.* Quantifying Argonaute 2 (Ago2) expression to stratify breast cancer. *BMC Cancer* **19**, 712 (2019).
146. Yang, F.-Q. *et al.* Argonaute 2 is up-regulated in tissues of urothelial carcinoma of bladder. *Int. J. Clin. Exp. Pathol.* **7**, 340–347 (2014).
147. Zhang, J. *et al.* Up-regulation of Ago2 expression in gastric carcinoma. *Med. Oncol. Northwood Lond. Engl.* **30**, 628 (2013).
148. Zhang, Y., Wang, B., Chen, X., Li, W. & Dong, P. AGO2 involves the malignant phenotypes and FAK/PI3K/AKT signaling pathway in hypopharyngeal-derived FaDu cells. *Oncotarget* **8**, 54735–54746 (2017).
149. Muralidhar, B. *et al.* Functional evidence that Drosha overexpression in cervical squamous cell carcinoma affects cell phenotype and microRNA profiles. *J. Pathol.* **224**, 496–507 (2011).
150. Gurtner, A., Falcone, E., Garibaldi, F. & Piaggio, G. Dysregulation of microRNA biogenesis in cancer: the impact of mutant p53 on Drosha complex activity. *J. Exp. Clin. Cancer Res. CR* **35**, 45 (2016).
151. Rakheja, D. *et al.* Somatic mutations in DROSHA and DICER1 impair microRNA biogenesis through distinct mechanisms in Wilms tumours. *Nat. Commun.* **2**, 4802 (2014).
152. Torrezan, G. T. *et al.* Recurrent somatic mutation in DROSHA induces microRNA profile changes in Wilms tumour. *Nat. Commun.* **5**, 4039 (2014).
153. Walz, A. L. *et al.* Recurrent DGCR8, DROSHA, and SIX homeodomain mutations in favorable histology Wilms tumors. *Cancer Cell* **27**, 286–297 (2015).
154. Wegert, J. *et al.* Mutations in the SIX1/2 pathway and the DROSHA/DGCR8 miRNA microprocessor complex underlie high-risk blastemal type Wilms tumors. *Cancer Cell* **27**, 298–311 (2015).
155. Hata, A. & Kashima, R. Dysregulation of microRNA biogenesis machinery in cancer. *Crit. Rev. Biochem. Mol. Biol.* **51**, 121–134 (2016).
156. Higuchi, T. *et al.* Suppression of MicroRNA-7 (miR-7) Biogenesis by Nuclear Factor 90-Nuclear Factor 45 Complex (NF90-NF45) Controls Cell Proliferation in Hepatocellular Carcinoma. *J. Biol. Chem.* **291**, 21074–21084 (2016).
157. Grasso, G. *et al.* NF90 modulates processing of a subset of human pri-miRNAs. *Nucleic Acids Res.* **48**, 6874–6888 (2020).
158. Melo, S. A. *et al.* A genetic defect in exportin-5 traps precursor microRNAs in the nucleus of cancer cells. *Cancer Cell* **18**, 303–315 (2010).

-
159. Anglesio, M. S. *et al.* Cancer-associated somatic DICER1 hotspot mutations cause defective miRNA processing and reverse-strand expression bias to predominantly mature 3p strands through loss of 5p strand cleavage. *J. Pathol.* **229**, 400–409 (2013).
160. Ho, A. S. *et al.* The mutational landscape of adenoid cystic carcinoma. *Nat. Genet.* **45**, 791–798 (2013).
161. Bader, A. G. miR-34 - a microRNA replacement therapy is headed to the clinic. *Front. Genet.* **3**, 120 (2012).
162. Rokavec, M., Li, H., Jiang, L. & Hermeking, H. The p53/miR-34 axis in development and disease. *J. Mol. Cell Biol.* **6**, 214–230 (2014).
163. Li, W. (Jess) *et al.* MicroRNA-34a: Potent Tumor Suppressor, Cancer Stem Cell Inhibitor, and Potential Anticancer Therapeutic. *Front. Cell Dev. Biol.* **9**, 640587 (2021).
164. Li, S. *et al.* The comprehensive landscape of miR-34a in cancer research. *Cancer Metastasis Rev.* **40**, 925–948 (2021).
165. Peng, Y., Guo, J.-J., Liu, Y.-M. & Wu, X.-L. MicroRNA-34A inhibits the growth, invasion and metastasis of gastric cancer by targeting PDGFR and MET expression. *Biosci. Rep.* **34**, (2014).
166. Wang, A.-M. *et al.* Yin Yang 1 is a target of microRNA-34 family and contributes to gastric carcinogenesis. *Oncotarget* **5**, 5002–5016 (2014).
167. Park, E. Y. *et al.* Targeting of miR34a-NOTCH1 axis reduced breast cancer stemness and chemoresistance. *Cancer Res.* **74**, 7573–7582 (2014).
168. Si, W. *et al.* MiR-34a Inhibits Breast Cancer Proliferation and Progression by Targeting Wnt1 in Wnt/ β -Catenin Signaling Pathway. *Am. J. Med. Sci.* **352**, 191–199 (2016).
169. Garofalo, M. *et al.* MiR-34a/c-Dependent PDGFR- α/β Downregulation Inhibits Tumorigenesis and Enhances TRAIL-Induced Apoptosis in Lung Cancer. *PLoS One* **8**, e67581 (2013).
170. Han, Z. *et al.* miR-497 and miR-34a retard lung cancer growth by co-inhibiting cyclin E1 (CCNE1). *Oncotarget* **6**, 13149–13163 (2015).
171. Li, Y. *et al.* MicroRNA-34a inhibits glioblastoma growth by targeting multiple oncogenes. *Cancer Res.* **69**, 7569–7576 (2009).
172. Thor, T. *et al.* MiR-34a deficiency accelerates medulloblastoma formation in vivo. *Int. J. Cancer* **136**, 2293–2303 (2015).
173. Zhang, H.-F., Wang, Y.-C. & Han, Y.-D. MicroRNA-34a inhibits liver cancer cell growth by reprogramming glucose metabolism. *Mol. Med. Rep.* **17**, 4483–4489 (2018).
174. Cheng, L. *et al.* Comprehensive N-glycan profiles of hepatocellular carcinoma reveal association of fucosylation with tumor progression and regulation of FUT8 by microRNAs. *Oncotarget* **7**, 61199–61214 (2016).
175. Yamamura, S. *et al.* MicroRNA-34a modulates c-Myc transcriptional complexes to suppress malignancy in human prostate cancer cells. *PLoS One* **7**, e29722 (2012).

176. Chakravarthi, B. V. S. K. *et al.* miR-34a Regulates Expression of the Stathmin-1 Oncoprotein and Prostate Cancer Progression. *Mol. Cancer Res. MCR* **16**, 1125–1137 (2018).
177. Wu, X. *et al.* MicroRNA-34a inhibits human osteosarcoma proliferation by downregulating ether à go-go 1 expression. *Int. J. Med. Sci.* **10**, 676–682 (2013).
178. Vetter, N. S., Kolb, E. A., Mills, C. C. & Sampson, V. B. The Microtubule Network and Cell Death Are Regulated by an miR-34a/Stathmin 1/ β III-Tubulin Axis. *Mol. Cancer Res. MCR* **15**, 953–964 (2017).
179. de Antonellis, P. *et al.* MiR-34a targeting of Notch ligand delta-like 1 impairs CD15+/CD133+ tumor-propagating cells and supports neural differentiation in medulloblastoma. *PLoS One* **6**, e24584 (2011).
180. El Bezawy, R. *et al.* Antitumor activity of miR-34a in peritoneal mesothelioma relies on c-MET and AXL inhibition: persistent activation of ERK and AKT signaling as a possible cytoprotective mechanism. *J. Hematol. Oncol. J Hematol Oncol* **10**, 19 (2017).
181. Sun, H., Tian, J., Xian, W., Xie, T. & Yang, X. miR-34a inhibits proliferation and invasion of bladder cancer cells by targeting orphan nuclear receptor HNF4G. *Dis. Markers* **2015**, 879254 (2015).
182. Liu, R. *et al.* Identification of FLOT2 as a novel target for microRNA-34a in melanoma. *J. Cancer Res. Clin. Oncol.* **141**, 993–1006 (2015).
183. Lv, T. *et al.* miRNA-34a decreases ovarian cancer cell proliferation and chemoresistance by targeting HDAC1. *Biochem. Cell Biol. Biochim. Biol. Cell.* **96**, 663–671 (2018).
184. Zhang, R. *et al.* HPV E6/p53 mediated down-regulation of miR-34a inhibits Warburg effect through targeting LDHA in cervical cancer. *Am. J. Cancer Res.* **6**, 312–320 (2016).
185. Li, C. *et al.* MiR-34a inhibits colon cancer proliferation and metastasis by inhibiting platelet-derived growth factor receptor α . *Mol. Med. Rep.* **12**, 7072–7078 (2015).
186. Wang, Z. *et al.* MicroRNA-34a inhibits cells proliferation and invasion by downregulating Notch1 in endometrial cancer. *Oncotarget* **8**, 111258–111270 (2017).
187. Pang, R. T. *et al.* MicroRNA-34a is a tumor suppressor in choriocarcinoma via regulation of Delta-like1. *BMC Cancer* **13**, 25 (2013).
188. Yang, Y. *et al.* The epigenetically-regulated miR-34a targeting c-SRC suppresses RAF/MEK/ERK signaling pathway in K-562 cells. *Leuk. Res.* **55**, 91–96 (2017).
189. Craig, V. J. *et al.* Myc-mediated repression of microRNA-34a promotes high-grade transformation of B-cell lymphoma by dysregulation of FoxP1. *Blood* **117**, 6227–6236 (2011).
190. Lu, G. *et al.* MicroRNA-34a targets FMNL2 and E2F5 and suppresses the progression of colorectal cancer. *Exp. Mol. Pathol.* **99**, 173–179 (2015).
191. Öner, M. G. *et al.* Combined Inactivation of TP53 and MIR34A Promotes Colorectal Cancer Development and Progression in Mice Via Increasing Levels of IL6R and PAI1. *Gastroenterology* **155**, 1868–1882 (2018).
192. Li, H., Rokavec, M., Jiang, L., Horst, D. & Hermeking, H. Antagonistic Effects of p53 and HIF1A on microRNA-34a Regulation of PPP1R11 and STAT3 and Hypoxia-induced Epithelial to Mesenchymal Transition in Colorectal Cancer Cells. *Gastroenterology* **153**, 505–520 (2017).

193. Hahn, S., Jackstadt, R., Siemens, H., Hüntten, S. & Hermeking, H. SNAIL and miR-34a feed-forward regulation of ZNF281/ZBP99 promotes epithelial-mesenchymal transition. *EMBO J.* **32**, 3079–3095 (2013).
194. Siemens, H., Jackstadt, R., Kaller, M. & Hermeking, H. Repression of c-Kit by p53 is mediated by miR-34 and is associated with reduced chemoresistance, migration and stemness. *Oncotarget* **4**, 1399–1415 (2013).
195. Li, Y. *et al.* Long non-coding RNA-SNHG7 acts as a target of miR-34a to increase GALNT7 level and regulate PI3K/Akt/mTOR pathway in colorectal cancer progression. *J. Hematol. Oncol. J Hematol Oncol* **11**, 89 (2018).
196. Li, Y.-L. *et al.* MicroRNA-34a/EGFR axis plays pivotal roles in lung tumorigenesis. *Oncogenesis* **6**, e372 (2017).
197. Fujita, Y. *et al.* Effects of miR-34a on cell growth and chemoresistance in prostate cancer PC3 cells. *Biochem. Biophys. Res. Commun.* **377**, 114–119 (2008).
198. Wen, D., Peng, Y., Lin, F., Singh, R. K. & Mahato, R. I. Micellar Delivery of miR-34a Modulator Rubone and Paclitaxel in Resistant Prostate Cancer. *Cancer Res.* **77**, 3244–3254 (2017).
199. Li, X. *et al.* MicroRNA-34a modulates chemosensitivity of breast cancer cells to adriamycin by targeting Notch1. *Arch. Med. Res.* **43**, 514–521 (2012).
200. Lin, X. *et al.* PAI-1/PIAS3/Stat3/miR-34a forms a positive feedback loop to promote EMT-mediated metastasis through Stat3 signaling in Non-small cell lung cancer. *Biochem. Biophys. Res. Commun.* **493**, 1464–1470 (2017).
201. Ahn, Y.-H. *et al.* ZEB1 drives prometastatic actin cytoskeletal remodeling by downregulating miR-34a expression. *J. Clin. Invest.* **122**, 3170–3183 (2012).
202. Kashat, M. *et al.* Inactivation of AR and Notch-1 signaling by miR-34a attenuates prostate cancer aggressiveness. *Am. J. Transl. Res.* **4**, 432–442 (2012).
203. Chen, W.-Y. *et al.* MicroRNA-34a regulates WNT/TCF7 signaling and inhibits bone metastasis in Ras-activated prostate cancer. *Oncotarget* **6**, 441–457 (2015).
204. Liang, J. *et al.* LEF1 Targeting EMT in Prostate Cancer Invasion Is Regulated by miR-34a. *Mol. Cancer Res. MCR* **13**, 681–688 (2015).
205. Li, N. *et al.* miR-34a inhibits migration and invasion by down-regulation of c-Met expression in human hepatocellular carcinoma cells. *Cancer Lett.* **275**, 44–53 (2009).
206. Yu, G. *et al.* MicroRNA-34a functions as an anti-metastatic microRNA and suppresses angiogenesis in bladder cancer by directly targeting CD44. *J. Exp. Clin. Cancer Res. CR* **33**, 779 (2014).
207. Yang, L. *et al.* Tumor suppressor microRNA-34a inhibits cell migration and invasion by targeting MMP-2/MMP-9/FNDC3B in esophageal squamous cell carcinoma. *Int. J. Oncol.* **51**, 378–388 (2017).
208. Nie, J. *et al.* miR-34a inhibits the migration and invasion of esophageal squamous cell carcinoma by targeting Yin Yang-1. *Oncol. Rep.* **34**, 311–317 (2015).
209. Bernardi, C., Soffientini, U., Piacente, F. & Tonetti, M. G. Effects of microRNAs on fucosyltransferase 8 (FUT8) expression in hepatocarcinoma cells. *PLoS One* **8**, e76540 (2013).

210. Dong, P. *et al.* MiR-137 and miR-34a directly target Snail and inhibit EMT, invasion and sphere-forming ability of ovarian cancer cells. *J. Exp. Clin. Cancer Res. CR* **35**, 132 (2016).
211. Yu, G. *et al.* miRNA-34a suppresses cell proliferation and metastasis by targeting CD44 in human renal carcinoma cells. *J. Urol.* **192**, 1229–1237 (2014).
212. Yan, K. *et al.* MicroRNA-34a inhibits the proliferation and metastasis of osteosarcoma cells both in vitro and in vivo. *PLoS One* **7**, e33778 (2012).
213. Schirmer, U. *et al.* Role of miR-34a as a suppressor of L1CAM in endometrial carcinoma. *Oncotarget* **5**, 462–472 (2014).
214. Qiao, P. *et al.* microRNA-34a inhibits epithelial mesenchymal transition in human cholangiocarcinoma by targeting Smad4 through transforming growth factor-beta/Smad pathway. *BMC Cancer* **15**, 469 (2015).
215. Huang, G. *et al.* MiRNA-34a reversed TGF- β -induced epithelial-mesenchymal transition via suppression of SMAD4 in NPC cells. *Biomed. Pharmacother. Biomedecine Pharmacother.* **106**, 217–224 (2018).
216. Li, T., Li, L., Li, D., Wang, S. & Sun, J. MiR-34a inhibits oral cancer progression partially by repression of interleukin-6-receptor. *Int. J. Clin. Exp. Pathol.* **8**, 1364–1373 (2015).
217. Zhang, J. *et al.* MiR-34a suppresses amphiregulin and tumor metastatic potential of head and neck squamous cell carcinoma (HNSCC). *Oncotarget* **6**, 7454–7469 (2015).
218. Jiang, Z.-Q. *et al.* Luteolin Inhibits Tumorigenesis and Induces Apoptosis of Non-Small Cell Lung Cancer Cells via Regulation of MicroRNA-34a-5p. *Int. J. Mol. Sci.* **19**, (2018).
219. Cho, C.-Y. *et al.* Negative feedback regulation of AXL by miR-34a modulates apoptosis in lung cancer cells. *RNA N. Y. N* **22**, 303–315 (2016).
220. Zhang, Z. *et al.* Upregulation of microRNA-34a enhances the DDP sensitivity of gastric cancer cells by modulating proliferation and apoptosis via targeting MET. *Oncol. Rep.* **36**, 2391–2397 (2016).
221. Deng, X. *et al.* MicroRNA-34a regulates proliferation and apoptosis of gastric cancer cells by targeting silent information regulator 1. *Exp. Ther. Med.* **15**, 3705–3714 (2018).
222. Duan, J., Zhou, K., Tang, X., Duan, J. & Zhao, L. MicroRNA-34a inhibits cell proliferation and induces cell apoptosis of glioma cells via targeting of Bcl-2. *Mol. Med. Rep.* **14**, 432–438 (2016).
223. Yamakuchi, M., Ferlito, M. & Lowenstein, C. J. miR-34a repression of SIRT1 regulates apoptosis. *Proc. Natl. Acad. Sci. U. S. A.* **105**, 13421–13426 (2008).
224. Sun, T.-Y. *et al.* miR-34a regulates HDAC1 expression to affect the proliferation and apoptosis of hepatocellular carcinoma. *Am. J. Transl. Res.* **9**, 103–114 (2017).
225. Welch, C., Chen, Y. & Stallings, R. L. MicroRNA-34a functions as a potential tumor suppressor by inducing apoptosis in neuroblastoma cells. *Oncogene* **26**, 5017–5022 (2007).
226. Shen, Z. *et al.* MicroRNA-34a affects the occurrence of laryngeal squamous cell carcinoma by targeting the antiapoptotic gene survivin. *Med. Oncol. Northwood Lond. Engl.* **29**, 2473–2480 (2012).

227. Xia, J. *et al.* Genistein inhibits cell growth and induces apoptosis through up-regulation of miR-34a in pancreatic cancer cells. *Curr. Drug Targets* **13**, 1750–1756 (2012).
228. Kang, L. *et al.* MicroRNA-34a suppresses the breast cancer stem cell-like characteristics by downregulating Notch1 pathway. *Cancer Sci.* **106**, 700–708 (2015).
229. Pieraccioli, M. *et al.* ZNF281 inhibits neuronal differentiation and is a prognostic marker for neuroblastoma. *Proc. Natl. Acad. Sci. U. S. A.* **115**, 7356–7361 (2018).
230. Galtsidis, S. *et al.* Unravelling a p73-regulated network: The role of a novel p73-dependent target, MIR3158, in cancer cell migration and invasiveness. *Cancer Lett.* **388**, 96–106 (2017).
231. Su, X. *et al.* TAp63 suppresses metastasis through coordinate regulation of Dicer and miRNAs. *Nature* **467**, 986–990 (2010).
232. Li, J. *et al.* Transcriptional activation of microRNA-34a by NF-kappa B in human esophageal cancer cells. *BMC Mol. Biol.* **13**, 4 (2012).
233. Wang, X. *et al.* Bmi-1 regulates stem cell-like properties of gastric cancer cells via modulating miRNAs. *J. Hematol. Oncol. J Hematol Oncol* **9**, 90 (2016).
234. Pulikkan, J. A. *et al.* C/EBP α regulated microRNA-34a targets E2F3 during granulopoiesis and is down-regulated in AML with CEBPA mutations. *Blood* **116**, 5638–5649 (2010).
235. Peurala, H. *et al.* MiR-34a expression has an effect for lower risk of metastasis and associates with expression patterns predicting clinical outcome in breast cancer. *PLoS One* **6**, e26122 (2011).
236. Iqbal, N., Mei, J., Liu, J. & Skapek, S. X. miR-34a is essential for p19(Arf)-driven cell cycle arrest. *Cell Cycle Georget. Tex* **13**, 792–800 (2014).
237. Xu, T.-P. *et al.* KLF5 and MYC modulated LINC00346 contributes to gastric cancer progression through acting as a competing endogenous RNA and indicates poor outcome. *Cell Death Differ.* **26**, 2179–2193 (2019).
238. Rokavec, M. *et al.* IL-6R/STAT3/miR-34a feedback loop promotes EMT-mediated colorectal cancer invasion and metastasis. *J. Clin. Invest.* **124**, 1853–1867 (2014).
239. Siemens, H. *et al.* miR-34 and SNAIL form a double-negative feedback loop to regulate epithelial-mesenchymal transitions. *Cell Cycle Georget. Tex* **10**, 4256–4271 (2011).
240. Anastasiadou, E. *et al.* Epstein-Barr virus-encoded EBNA2 alters immune checkpoint PD-L1 expression by downregulating miR-34a in B-cell lymphomas. *Leukemia* **33**, 132–147 (2019).
241. Lodygin, D. *et al.* Inactivation of miR-34a by aberrant CpG methylation in multiple types of cancer. *Cell Cycle Georget. Tex* **7**, 2591–2600 (2008).
242. Chen, X. *et al.* CpG island methylation status of miRNAs in esophageal squamous cell carcinoma. *Int. J. Cancer* **130**, 1607–1613 (2012).
243. Chim, C. S. *et al.* Methylation of miR-34a, miR-34b/c, miR-124-1 and miR-203 in Ph-negative myeloproliferative neoplasms. *J. Transl. Med.* **9**, 197 (2011).

-
244. Liu, H., Deng, H., Zhao, Y., Li, C. & Liang, Y. LncRNA XIST/miR-34a axis modulates the cell proliferation and tumor growth of thyroid cancer through MET-PI3K-AKT signaling. *J. Exp. Clin. Cancer Res. CR* **37**, 279 (2018).
245. Cui, X. *et al.* Inactivation of miR-34a by aberrant CpG methylation in Kazakh patients with esophageal carcinoma. *J. Exp. Clin. Cancer Res. CR* **33**, 20 (2014).
246. Siemens, H. *et al.* Detection of miR-34a promoter methylation in combination with elevated expression of c-Met and β -catenin predicts distant metastasis of colon cancer. *Clin. Cancer Res. Off. J. Am. Assoc. Cancer Res.* **19**, 710–720 (2013).
247. Kang, M. *et al.* Identification of miPEP133 as a novel tumor-suppressor microprotein encoded by miR-34a pri-miRNA. *Mol. Cancer* **19**, 143 (2020).
248. Jiang, F. & Doudna, J. A. CRISPR–Cas9 Structures and Mechanisms. *Annu. Rev. Biophys.* **46**, 505–529 (2017).
249. Thurtle-Schmidt, D. M. & Lo, T.-W. Molecular biology at the cutting edge: A review on CRISPR/CAS9 gene editing for undergraduates. *Biochem. Mol. Biol. Educ. Bimon. Publ. Int. Union Biochem. Mol. Biol.* **46**, 195–205 (2018).
250. Jiang, F. & Doudna, J. A. CRISPR-Cas9 Structures and Mechanisms. *Annu. Rev. Biophys.* **46**, 505–529 (2017).
251. Navarro, F. & Lieberman, J. miR-34 and p53: New Insights into a Complex Functional Relationship. *PLoS One* **10**, e0132767 (2015).
252. Thor, T. *et al.* MiR-34a deficiency accelerates medulloblastoma formation in vivo. *Int. J. Cancer* **136**, 2293–2303 (2015).
253. Ran, F. A. *et al.* Genome engineering using the CRISPR-Cas9 system. *Nat. Protoc.* **8**, 2281–2308 (2013).
254. Chang, H. *et al.* CRISPR/cas9, a novel genomic tool to knock down microRNA in vitro and in vivo. *Sci. Rep.* **6**, 22312 (2016).
255. Livak, K. J. & Schmittgen, T. D. Analysis of relative gene expression data using real-time quantitative PCR and the 2^{(-Delta Delta C(T))} Method. *Methods San Diego Calif* **25**, 402–408 (2001).
256. Bommer, G. T. *et al.* p53-mediated activation of miRNA34 candidate tumor-suppressor genes. *Curr. Biol. CB* **17**, 1298–1307 (2007).
257. Hart, M. *et al.* miR-34a: a new player in the regulation of T cell function by modulation of NF- κ B signaling. *Cell Death Dis.* **10**, 46 (2019).
258. Cho, C.-Y. *et al.* Negative feedback regulation of AXL by miR-34a modulates apoptosis in lung cancer cells. *RNA N. Y. N* **22**, 303–315 (2016).
259. Imani, S. *et al.* MicroRNA-34a targets epithelial to mesenchymal transition-inducing transcription factors (EMT-TFs) and inhibits breast cancer cell migration and invasion. *Oncotarget* **8**, 21362–21379 (2017).
260. Yamakuchi, M., Ferlito, M. & Lowenstein, C. J. miR-34a repression of SIRT1 regulates apoptosis. *Proc. Natl. Acad. Sci. U. S. A.* **105**, 13421–13426 (2008).

-
261. Sticht, C., De La Torre, C., Parveen, A. & Gretz, N. miRWalk: An online resource for prediction of microRNA binding sites. *PLoS One* **13**, e0206239 (2018).
262. Martinez-Sanchez, A. & Murphy, C. L. MicroRNA Target Identification-Experimental Approaches. *Biology* **2**, 189–205 (2013).
263. Ha, M. & Kim, V. N. Regulation of microRNA biogenesis. *Nat. Rev. Mol. Cell Biol.* **15**, 509–524 (2014).
264. Fabian, M. R., Sonenberg, N. & Filipowicz, W. Regulation of mRNA translation and stability by microRNAs. *Annu. Rev. Biochem.* **79**, 351–379 (2010).
265. Agostini, M. & Knight, R. A. miR-34: from bench to bedside. *Oncotarget* **5**, 872–881 (2014).
266. Hermeking, H. The miR-34 family in cancer and apoptosis. *Cell Death Differ.* **17**, 193–199 (2010).
267. Zhang, X., Ma, N., Yao, W., Li, S. & Ren, Z. RAD51 is a potential marker for prognosis and regulates cell proliferation in pancreatic cancer. *Cancer Cell Int.* **19**, 356 (2019).
268. Wilking, M. J. & Ahmad, N. The role of SIRT1 in cancer: the saga continues. *Am. J. Pathol.* **185**, 26–28 (2015).
269. Gilmore, T. D., Kalaitzidis, D., Liang, M.-C. & Starczynowski, D. T. The c-Rel transcription factor and B-cell proliferation: a deal with the devil. *Oncogene* **23**, 2275–2286 (2004).
270. Tacon, L. J. *et al.* The glucocorticoid receptor is overexpressed in malignant adrenocortical tumors. *J. Clin. Endocrinol. Metab.* **94**, 4591–4599 (2009).
271. Chien, T.-M. *et al.* Role of Microtubule-Associated Protein 1b in Urothelial Carcinoma: Overexpression Predicts Poor Prognosis. *Cancers* **12**, (2020).
272. Zhu, J., Lin, Q., Zheng, H., Rao, Y. & Ji, T. The pro-invasive factor COL6A2 serves as a novel prognostic marker of glioma. *Front. Oncol.* **12**, 897042 (2022).
273. To, J. C. *et al.* ZBTB20 regulates WNT/CTNNB1 signalling pathway by suppressing PPAR γ during hepatocellular carcinoma tumorigenesis. *JHEP Rep. Innov. Hepatol.* **3**, 100223 (2021).
274. Lohr, J. G. *et al.* Discovery and prioritization of somatic mutations in diffuse large B-cell lymphoma (DLBCL) by whole-exome sequencing. *Proc. Natl. Acad. Sci. U. S. A.* **109**, 3879–3884 (2012).
275. Yu, J., Li, D. & Jiang, H. Emerging role of ONECUT2 in tumors. *Oncol. Lett.* **20**, 328 (2020).
276. Dhar, S. S. & Lee, M. G. Cancer-epigenetic function of the histone methyltransferase KMT2D and therapeutic opportunities for the treatment of KMT2D-deficient tumors. *Oncotarget* **12**, 1296–1308 (2021).

PUBLICATIONS

1. “*Effects of a 4400 km ultra-cycling non-competitive race and related training on body composition and circulating progenitors differentiation*” Maria Teresa Valenti², Michele Braggio¹, Arianna Minoia¹, Gianluigi Dorelli¹, Jessica Bertacco¹, Francesco Bertoldo¹, Mattia Cominacini¹, **Tonia De Simone**², Maria Grazia Romanelli², Lekhana Bhandary³, Monica Mottes² and Luca Dalle Carbonare¹ Journal of Translational Medicine (2022) 20:397 <https://doi.org/10.1186/s12967-022-03591-5>
2. Review: “*Regulation of microRNAs in Satellite Cell Renewal, Muscle Function, Sarcopenia and the Role of Exercise*” Stefania Fochi¹, Gaia Giuriato¹, **Tonia De Simone**¹, Macarena Gomez-Lira¹, Stefano Tamburin¹, Lidia Del Piccolo¹, Federico Schena¹, Massimo Venturelli^{1,2} and Maria Grazia Romanelli¹ Int. J. Mol. Sci. 2020, 21, 6732; doi: 10.3390/ijms21186732 www.mdpi.com/journal/ijms

Articles under review:

“*Weaker sex: fact or prejudice? Neuromuscular and biological 5 determinants of maximal force.*”

Gaia Giuriato¹, Maria Grazia Romanelli¹, Desirée Bartolini², Gianluca Vernillo³, Anna Pedrinolla¹, Tatiana Moro⁴, Martino Franchi⁴, Elena Locatelli¹, Mehran Emadi Andani¹, Fabio Giuseppe Laginestra¹, Chiara Barbi¹, Gloria Fiorini Aloisi¹, Valentia Cavedon¹, Chiara Milanese¹, Elisa Orlandi¹, **Tonia De Simone**¹, Stefania Fochi¹, Cristina Patuzzo¹, Giovanni Malerba¹, Paolo Fabene¹, Massimo Donadelli¹, Anna Maria Stabile⁶, Alessandra Pistilli⁶, Mario Rende⁶, Francesco Galli², Federico Schena¹, Massimo Venturelli^{*1,5}

The data obtained in this thesis work will be published in an article that is currently in progress.

CONGRESSES ATTENDED AND ABSTRACTS

1. *New miR-34a target genes identification by applying the CRISPR / Cas9 system for the generation of human miR-34a knock-out cell lines* (2022) - XVI FISV CONGRESS Reggio di Portici (Naples) 3R: Research, Resilience, Reprise 14-15-16 September 2022 **Tonia De Simone**¹, S. Fochi¹, A. Corsi¹, C. Stefani¹, C. Vignoli¹, C. Patuzzo¹, D. Zipeto¹, M. G. Romanelli¹ ¹Department of Neurosciences, Biomedicine and Movement Sciences, University of Verona, Verona, Italy
2. *Identification of novel targets for miR-34a generating CRISPR/Cas9 miR-34a knock-out human cell lines* (2021) - 33rd AICC ANNUAL CONFERENCE: INTERNATIONAL MEETING ON CANCER METABOLISM **Tonia De Simone**¹, Chiara Stefani¹, Stefania Fochi¹, Cristina Patuzzo¹, Andrea Corsi¹, Donato Zipeto¹, Maria Grazia Romanelli¹ ¹Department of Neurosciences, Biomedicine and Movement Sciences, University of Verona, Verona, Italy
3. *Establishment and characterization of CRISPR/Cas9 miR-34a knockout HeLa cell line* (2021) - SIBBM 2021 • 7-10 June 2021 **De Simone Tonia**¹, Stefani C.¹, Fochi S. ¹, Patuzzo C.¹, Zipeto D. ¹, Romanelli MG¹. ¹Department of Neurosciences, Biomedicine and Movement Sciences, University of Verona, Verona, Italy

POSTERS AND ABSTRACTS IN COLLABORATION

1. *Physical activity modulates SIRTUIN 1 levels in progenitor cells during the adipogenic differentiation* (2021) Arianna Minoia¹, Gianluigi Dorelli¹, Daniele Gabbiani¹, Gessica Bertacco^{1,2}, **Tonia De Simone**², Michele Braggio¹, Cantor Tarperi², Federico Schena², Maria Graia Romanelli², Monica Motte², Luca Dalle Carbonare¹ and Maria Teresa Valenti¹. ¹Department of Neurosciences, Biomedicine and Movement Sciences, University of Verona, Verona, Italy
2. "Identification of trans factors regulating Tau exon 6 alternative splicing" (16 December 2022) Corsi A, Stefani C, **De Simone T**, Lorenzi P, Romanelli MG
Young Minds at Work: Blending Biology and Bioinformatics
3. "Enriched Cell Pathways Associated with Dysregulated miRNAs Expression by HTLV-2 Infection" (8-11 May 2022) Corsi A, Begnami F, **De Simone T**, Minoia A, Valenti MT, Forlani G, Pilotti E, Romanelli MG
International Virtual Conference on Human Retrovirology: HTLV-2, Melbourne (Australia).

Popular scientific conference "COMPORAMENTI E BENESSERE, Un approccio multidisciplinare per favorire la qualità della vita in condizioni di vulnerabilità" 24 October 2022, Verona:

1. Il complesso mitocondriale II è strettamente correlato all'aumento dell'affaticamento periferico durante l'esercizio fisico (2022) G. Giuriato, E. Calabria, M.E. Andani, C. Barbi, F. Laginestra, A. Pedrinolla, C. Martignon, F. Schena, **T. De Simone**, E. Orlandi, M.M. Gomez Lira, M.G. Romanelli, M. Venturelli Dipartimento di Neuroscienze Biomedicina e Movimento; Dipartimento di Eccellenza 2018/2022
2. Effetti dell'invecchiamento di successo sulla forza (2022) G. Giuriato, G. Fiorini, M.E. Andani, C. Barbi, F. Laginestra, A. Pedrinolla, C. Martignon, **T. De Simone**, E. Orlandi, M.M. Gomez Lira, F. Schena, M. Venturelli, M.G. Romanelli Dipartimento di Neuroscienze Biomedicina e Movimento; Dipartimento di Eccellenza 2018/2022



Review

Regulation of microRNAs in Satellite Cell Renewal, Muscle Function, Sarcopenia and the Role of Exercise

Stefania Fochi ¹, Gaia Giuriato ¹, Tonia De Simone ¹, Macarena Gomez-Lira ¹,
Stefano Tamburin ¹ , Lidia Del Piccolo ¹ , Federico Schena ¹, Massimo Venturelli ^{1,2}
and Maria Grazia Romanelli ^{1,*}

¹ Department of Neurosciences, Biomedicine and Movement Sciences, University of Verona, 37134 Verona, Italy; stefania.fochi@univr.it (S.F.); gaia.giuriato@univr.it (G.G.); tonia.desimone@univr.it (T.D.S.); macarena.gomezlira@univr.it (M.G.-L.); stefano.tamburin@univr.it (S.T.); lidia.delpiccolo@univr.it (L.D.P.); federico.schena@univr.it (F.S.); massimo.venturelli@univr.it (M.V.)

² Department of Internal Medicine, University of Utah, Salt Lake City, UT 84132, USA

* Correspondence: mariagrazia.romanelli@univr.it

Received: 4 August 2020; Accepted: 12 September 2020; Published: 14 September 2020



Abstract: Sarcopenia refers to a condition of progressive loss of skeletal muscle mass and function associated with a higher risk of falls and fractures in older adults. Musculoskeletal aging leads to reduced muscle mass and strength, affecting the quality of life in elderly people. In recent years, several studies contributed to improve the knowledge of the pathophysiological alterations that lead to skeletal muscle dysfunction; however, the molecular mechanisms underlying sarcopenia are still not fully understood. Muscle development and homeostasis require a fine gene expression modulation by mechanisms in which microRNAs (miRNAs) play a crucial role. miRNAs modulate key steps of skeletal myogenesis including satellite cells renewal, skeletal muscle plasticity, and regeneration. Here, we provide an overview of the general aspects of muscle regeneration and miRNAs role in skeletal mass homeostasis and plasticity with a special interest in their expression in sarcopenia and skeletal muscle adaptation to exercise in the elderly.

Keywords: microRNA; aging; sarcopenia; myogenesis; exercise; satellite cells

1. Introduction

Sarcopenia is a pathophysiological process characterized by progressive loss of skeletal muscle mass and function that contributes to a higher risk of falls and fractures among older adults [1]. It often leads to frailty that impacts considerably on the quality of life in elderly people. After the age of 50, the rate of muscle loss is estimated to be 1–2% per year, being faster in men than women [2]. The advances in transcriptomics technologies and high throughput analyses allow for detection of a broad repertoire of cellular factors that participate to gene expression regulation during skeletal muscle aging changes and adaptations such as growth factors, transcription factors, cell signaling pathways activators, and non-coding RNA, including microRNAs (miRNAs) [3].

miRNAs are a class of non-coding transcripts specifically involved in negatively modulated gene expression at the post-transcriptional levels by specifically targeting the 3'-untranslated regions (3'-UTR) of their target mRNAs. Several miRNAs have been demonstrated to participate in the molecular mechanisms that control skeletal muscle plasticity during aging. miRNAs that are preferentially expressed in striated muscle are termed as myomiRs, and they act as regulators of muscle development, homeostasis, and functionality [4,5]. Expression of skeletal myomiRs may be altered in old skeletal muscle, in age- and activity-related muscle changes (e.g., hypertrophy, atrophy), as well as in myopathies, such as muscular dystrophy [6–9]. Recent studies have demonstrated that muscle-specific

miRNAs play a pivotal role in the control of sarcopenia, modulating key steps of skeletal myogenesis, including satellite cells senescence, cell proliferation, and differentiation [10,11].

The reduction in force of skeletal muscle in older people is primarily due to the loss and weakening of muscle fibers. For instance, during aging, the locomotor skeletal muscles face a marked switch to slow type I myofibers, a process of atrophy of fast (type IIa and IIx) fibers, with a reduction in the myofiber count [12–14]. Similar changes have been associated with sedentary lifestyles, and reported in some neuromuscular disorders [6,15–18]. Thus, exercise is considered an effective intervention to delay the onset and progression of sarcopenia. Regular exercise training has been associated with an increase in skeletal muscle cross-sectional area, force, and resistance to fatigue [19], as well as improvements in cardiovascular fitness and quality of life [20]. Exercise training promotes positive adaptations in skeletal muscle, acting as an important stimulator of extra/intracellular signals, leading to changes in gene expression. Several studies have revealed that miRNA expression in skeletal muscle is modulated in response to physical exercise, see the exhaustive reviews [21–23], highlighting the relevance of the miRNAs role in the process of adaptation to exercise. More recently, circulating miRNAs have been investigated as possible biomarkers of exercise training [24].

This review will synthesize the most relevant advancements in the knowledge of the miRNAs role in muscle regeneration and their involvement in sarcopenia. We will further review the current knowledge on circulating miRNAs and their potential as non-invasive biomarkers of muscle function and adaptation to exercise in healthy adults and sarcopenic elderly.

2. miRNA Biogenesis and Functional Role

miRNAs are small non-coding RNAs of 20 nucleotides in length, transcribed by about 2000 human genes, that regulate gene expression at the post-transcriptional level [25,26]. miRNAs play crucial roles in various biological processes such as cell proliferation, apoptosis, differentiation as well as epigenetic changes and metabolic homeostasis. miRNA genes are often found in clusters and may derive from intragenic or intergenic regions, both intronic and exonic [27]. miRNAs biogenesis begins with the synthesis of primary miRNAs (pri-miRNAs) by RNA polymerase II that are processed in the nucleus into precursor miRNAs of approximately 70 nt (pre-miRNAs) by a complex consisting of the RNA binding protein, DGCR8 microprocessor subunit, and the endoribonuclease, Drosha [28]. Pre-miRNAs are then exported to the cytoplasm via the nuclear transport protein Exportin 5, where the endoribonuclease Dicer cuts the stem loop region producing miRNAs duplexes. miRNAs duplexes harbor the mature miRNA strand that, once associated with the RNA induced silencing (RISC) complex, works as a gene modulator at the transcriptional level.

miRNAs regulate transcripts expression generally by annealing to the 3' untranslated region (3'UTR), leading to inhibition of mRNA translation and/or degradation of mRNA transcripts. miRNA may target mRNA not only at their 3'-UTR, but also at the 5'UTR, promoters and exon sequences, generally leading to downregulation of the expressed genes [29]. Each miRNA can target several mRNAs involved in different cell functions and in a crosstalk between cell signaling pathways. Deregulation of miRNA expression has been associated with several pathological processes, including cancer, neurodegenerative diseases, cardiovascular diseases, and host response to viral infections [30–33].

3. Skeletal Myogenesis and Sarcopenia

Skeletal myogenesis refers to the process of muscle development, whereby myogenic precursor cells can differentiate and fuse to form myofibers. During development, most of the precursor cells undergo proliferation and differentiation, while a subset remains capable of regeneration, repairing tissue injuries in adulthood. Myogenesis involves an intricate regulatory network of gene expression that coordinates (i) activation and proliferation of stem cells that differentiate into myoblasts, (ii) early differentiation that consists in the fusion of myoblasts to form myocytes and (iii) terminal differentiation into myofibers (Figure 1). The skeletal myogenic process is finely regulated by transcription factors known as myogenic regulatory factors (MRFs), such as MyoD (myogenic differentiation), myogenin,

Myf5 (myogenic factor 5), and MRF4 (myogenic regulatory factor 4) [34]. In adults, muscle stem cells, termed satellite cells, are characterized by the expression of the paired box transcription factor Pax7 and to a small extent of Pax3, whereas MyoD is not expressed. This pattern of expression allows the maintenance of satellite cells in a quiescent status. Activation of satellite cells from the quiescent status is first determined by a co-expression of Pax7, MyoD, and Myf5 [3]. At this step, Pax factors promote the expression of genes accountable for inducing a transient cell proliferation suppressing genes that induce differentiation. During myogenic differentiation, the expression of Pax proteins is suppressed, allowing the expression of MRFs. At this step, myogenin plays a key role in the terminal differentiation of myogenic progenitor cells, whereas MyoD undergoes to downregulation. In the aging muscle, the expression of the myogenic genes, MyoD, and myogenin, have been reported to be upregulated, suggesting a modification of the committed status of the muscle satellite cells [35].

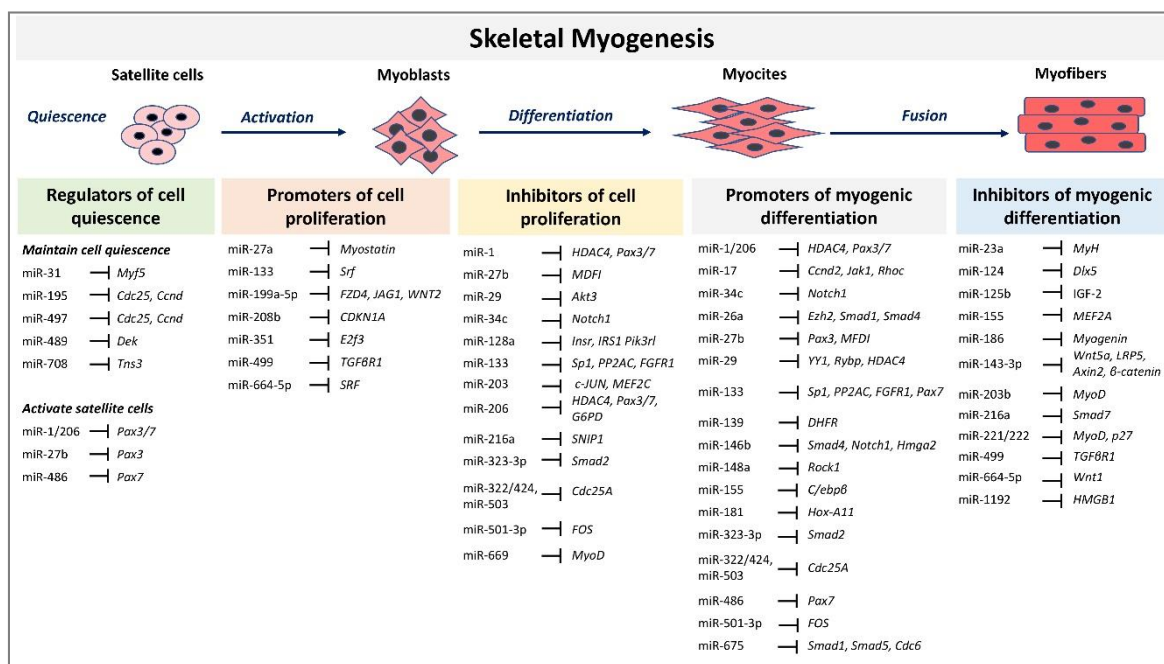


Figure 1. MicroRNAs (miRNAs) and target genes implicated in skeletal muscle myogenesis.

The altered ability of satellite cells to maintain quiescent status and their loss of self-renewal and regenerative capacity are major causes of age-related muscle changes [36]. In skeletal muscle, aging is manifested as sarcopenia, the progressive loss of skeletal muscle mass and strength with accumulation of functional deficits [17,18,37]. This age-related muscle atrophy strictly correlates with physical disability, poor quality of life and increased risk of negative outcomes for elderly people. From a cellular point of view, satellite cell depletion, senescence, inflammation, and mitochondrial dysfunction have been proposed to be associated with sarcopenia development [38–41].

A decrease in the number of stem cells and in their capability to proliferate during aging has been proposed to impact myogenesis [42]. Study in mice have demonstrated that reduction of satellite cells affects muscle regenerative capacity without affecting sarcopenia, and does not contribute to the maintenance of muscle size during aging, however in sedentary adult mice, in the absence of injury, satellite cells may contribute to myofibers at different extent between muscle and with age [43,44]. More recently, it has been also demonstrated that satellite cells depletion in adult mice contributes to preserve physical function and to increase in muscle fiber size when physical activity is lifelong sustained [45]. In humans, the role of satellite cells in contributing to hypertrophy and to regeneration in the elderly is not clearly defined, also due to the difficulty of studying muscle regeneration in human subjects. Satellite cells may be responsible for reduced regenerative muscle potential in older individuals due to the switching of reversible quiescence into senescence [40]. Interestingly, a recent study has contributed

to better understanding the role of satellite cells in elderly individuals compared to young ones, in a regeneration model obtained inducing muscle injury by electrically stimulated eccentric contraction of the vastus lateralis, followed by 13 weeks of resistance training. Surprisingly, the results clearly demonstrate that satellite cells increase in young and elderly to a similar extent, confirming a complete muscle regeneration, whereas the increased number of satellite cells does not enhance hypertrophy in response to resistance training [46].

Recently, attention has been directed to the role of inflammation in the development of sarcopenia. Increased inflammation in the elderly, the so-called inflammaging, is driven by the expression of proinflammatory cytokines activated by transcription factor nuclear factor-kappa B (NF- κ B) and response to oxidative stress and has been considered a crucial mediator of muscle wasting in sarcopenia [47–49]. Increasing evidence shows that mitochondrial dysfunction is a cause of sarcopenia, contributing to inflammation via reactive oxygen species (ROS) production and NF- κ B activation, accelerating the aging process of skeletal muscle [50]. The decline of mitochondrial function is a typical feature of the senescence-associated secretory phenotype of senescent cells, which leads to muscle wasting [51]. It is not clear if during aging muscle cells undergo an increase of cell senescence that may contribute to sarcopenia. However, a recent study had attempted to quantify senescent cells in human skeletal muscle using the phosphorylated form of the histone H2A variant gamma-H2AX (γ H2AX) as a marker of DNA damage. In muscle cell biopsy of young subjects compared to elderly ones, the latter did not show a significant increase of senescent cells [52]. Interestingly, the same study demonstrated a higher cells senescence and senescence-associated secretory phenotype in muscle from obese individuals and in *in vitro* obesogenic environments, suggesting that DNA damage, which may reduce the function of the muscle, is more directly linked to obesity than aging.

4. The Role of miRNAs during Skeletal Myogenesis in Adults

MRFs expression can be regulated by miRNAs highlighting their involvement in modulating myogenesis. A set of miRNAs, referred to as myomiRs, such as miR-1, miR-133a, miR-133b, miR-206, miR-208, miR-208b, miR-486, and miR-499, are highly enriched in muscle fibers [4]. MyomiRs may modulate size and type transition of muscle fibers in structural adaptation to aging and exercise. Specifically, miR-499, miR-208 and miR-208b, encoded by intron sequences of myosin heavy chain genes, have been demonstrated in mice models to participate in a network of miRNAs that regulate not only myosin expression, but also fiber type genes expression and muscle performance [53]. Skeletal muscle-specific Dicer knockout in mice results in low expression of specific miRNAs, reduced skeletal muscle mass, and abnormal myofibers morphology, confirming that a correct maturation of miRNAs is necessary for muscle development and function [54]. In adult mice, depletion of Dicer has been demonstrated to reduce the expression of miR-1, miR-133a and miR-206 expression; however, this reduction had no effect on skeletal muscle mass and phenotype, even after a long-life reduction [55]. In contrast, the reduction of myomiRs after Dicer knockout affects skeletal muscle regeneration [56]. Unexpected results derived by Dicer depletion studies in adult mice skeletal muscle showed that, even if Dicer expression might be reduced of almost 80%, myomiRs expression was not as much significantly reduced. This finding opens interest for further studies that may investigate the effectiveness of Dicer function and myomiRs stability and function in adult muscle. Several reviews have extensively described the role of miRNAs during embryonal skeletal myogenesis [8,9,57]. Here we report and discuss the most recent evidence concerning miRNA regulatory network in adults. A selected list of myomiRs and miRNAs implicated in the different phases of skeletal myogenesis from quiescence to the proliferation of satellite cells and myofibers differentiation are represented in Figure 1.

4.1. miRNAs Role in the Control of Satellite Cells Quiescence Status

During the first steps of myogenesis or muscle regeneration, miRNAs can affect the expression of MRFs, Pax3/7 transcription factors and other transcripts that control the cell cycle, playing a key role in the maintenance of cell quiescence status or in the activation of satellite cells [4,58]. In satellite

cells of adult mice, the ablation of Dicer results in the interruption of quiescence status and impaired ability of injured muscle regeneration [59]. The essential role of miRNAs in maintaining stem cells proliferation is confirmed by the observation that Dicer deletion in adult mice muscle cells causes apoptosis of proliferating satellite cells [59,60].

Several miRNAs have been found to play a crucial role in the maintenance of satellite cells in a quiescence status. One of the miRNAs most intensively studied is miR-31, which has been demonstrated to directly participate in the regulation of myogenic transcription factors. miR-31 has been reported to downregulate the expression of Myf5 in quiescent satellite cells by sequestering Myf5 in messenger ribonucleoprotein particles (mRNPs) [61]. Activation of satellite cells allows mRNPs dissociation and the release of Myf5 transcripts that are rapidly translated, promoting the myogenesis process. Another mechanism by which miRNAs control satellite cells quiescence is by targeting the cell cycle regulators. Sato and co-workers demonstrated a close link between quiescence and inhibition of myogenesis in adult satellite cells. miR-195/497 convert the proliferating juvenile muscle satellite cells into quiescent ones directly targeting cell division cycle 25C (Cdc25) and cyclin D (CcnD) factors [62]. Conversely, inhibition of miR-195/497 results in the activation of Cdc25 and CcnD and reduction of Pax7 expression. Although *in silico* analyses show no evidence for direct targeting of Pax7 or MyoD transcripts by miR-195/497, their action on Cdc25/CcnD transcripts elicit the upregulation of Pax7 and downregulation of MyoD expression, which are characteristics of quiescent adult skeletal muscle cells [62].

Proliferative expansion of myogenic progenitors is regulated by another miRNA, miR-489, which has been demonstrated to inhibit the expression of the oncogene Dek that regulates cell proliferation and mRNA splicing. miR-489 is highly expressed in quiescent satellite cells and is downregulated during their activation. Induced expression of Dek during asymmetric division of satellite cells promotes the transient proliferative expansion and differentiation of myogenic progenitors, whereas Dek is absent in self-renewing cells [60].

A new regulatory axis that controls the satellite quiescent cells transition to their activated state involving Notch, miR-708 and Tns3 (Tns3) has been recently proposed [63]. Notch signaling is known to stimulate the proliferation and to inhibit the differentiation of muscle satellite cells. Notch-mediated induction of miR-708 transcription allows the inhibition of Tns3 transcript, a regulator of cell migration. Low levels of Tns3 mediated by miR-708 allow the anchored quiescent status of satellite cells. Upon activation of satellite cells, Notch and therefore miR-708 are downregulated, resulting in high levels of Tns3 and the migration of activated cells, suggesting that suppression of the migratory ability is essential for maintaining the quiescent status of stem cell within its niche, where miR-708 acts as a gate-keeper of quiescence [63].

4.2. miRNAs Role in Myogenesis

Once satellite cells are activated, they first undergo a rapid and short step of cell proliferation followed by a phase of cell differentiation. In skeletal muscle, the processes of proliferation and differentiation are mutually exclusive. Indeed, various miRNAs here described as promoters of cell differentiation, are also inhibitors of cell proliferation and vice versa. Several miRNAs participate to satellite cells myogenic differentiation mainly targeting transcripts encoding transcription factors, cell cycle regulators and cell signaling pathways factors. miR-1/206 family, miR-27b, miR-486 and miR-133b have been demonstrated to downregulate the expression of the transcription factors Pax3/7 allowing satellite cell activation [64–69]. The reduction of Pax7 protein levels is mediated by miR-1 and miR-206 in activated satellite cells. Overexpression of miR-1 and miR-206 has been demonstrated to restrict the proliferative potential of satellite cells and to accelerate their myogenic differentiation [65]. miR-1 and miR-206 have also been reported to target Pax3, which leads to the timely expression of myogenin expression in committed myoblasts [68]. A model of miR-1/206 function that requires an initial step of Pax3-mediated MRFs activation to induce the expression of miR-1/206, which in turn repress Pax3 in a negative feedback loop, has been proposed [68]. A recent study identified the

glucose-6-phosphate dehydrogenase (G6PD) gene as a new target of miR-206 [70]. Suppression of G6PD by miR-206 results in the inhibition of muscle cell proliferation and cell cycle arrest in G0/G1 phase. In addition to miR-1/206, miR-27b, and miR-486 have been also demonstrated to promote satellite cells differentiation downregulating Pax proteins expression. Overexpression of miR-27b results in a specific downregulation of Pax3, not effecting Pax7 expression. In vivo analyses revealed that injection of miR-27b antagonists at a site of muscle injury alters levels of Pax3 and affects the regeneration of injured muscle [64], suggesting the possibility to modulate the Pax gene expression by miRNA injection as a new challenge in the development of therapeutic strategies against muscle damage.

In an additional study, Dey and colleagues propose an intricate regulatory network between Pax7, miR-486 and miR-206 [67]. Pax7 expression in the satellite cells differentiation step mediates the activation of the inhibitor of DNA Binding 2 (Id2) factor, which suppresses MyoD-mediated transcriptional activation of miR-486 and miR-206. Conversely, in a MyoD-dominated state, the upregulation of miR-486 and miR-206 allows repression of Pax7 and Id2, allowing a shift of the equilibrium toward the MyoD-active myotube state.

Both miR-1 and miR-133 have been associated with skeletal myogenic processes. miR-1 and miR-133 are clustered on the same chromosomal loci (miR-1-1 and miR-133a-2 on chromosome 20, miR-1-2 and miR-133a-1 on chromosome 18) and transcribed together as a single transcript, becoming then two mature miRNAs that suppress different target genes. An early study revealed that increased levels of miR-1 promote myogenesis by suppressing the expression of histone deacetylase 4 (HDAC4) [71]. HDAC4 has been shown to inhibit muscle differentiation, mainly reducing myocyte enhancer factor 2 (MEF2), suggesting that miR-1 mediated suppression of HDAC4 may promote cell differentiation. If the miR-1 activity in promoting cell differentiation is commonly accepted, the effect of miR-133 activity in the skeletal myogenic process is more debated. At first, it has been demonstrated that miR-133a suppresses the expression of serum response factor (SRF), a central regulator of muscle cells proliferation and differentiation, enhancing myoblast proliferation. Further studies suggest that miR-133 may reduce myoblast proliferation, inducing myoblasts cell differentiation directly targeting the transcription factor Sp1 [72]. In addition, miR-133 may suppress extracellular signal-regulated kinases ERK1/2 expression, through targeting FGFR1 and PP2AC, which are part of a pro-proliferation signaling cascade [73]. Recently, it has been demonstrated that Wnt3, a member of the Wnt signaling, well-known to promote myoblast differentiation, increases the expression of miR-133b and miR-206, but does not influence the expression of miR-1 and miR-133a [69]. miR-133b targets Pax7, suppressing its expression more efficiently than miR-206 by targeting a site adjacent to the miR-206 binding site in the Pax7 3'UTR [69].

Other miRNAs have been implicated in the promotion of myogenic differentiation targeting specific cell signaling pathways and cell cycle regulators. Early studies revealed that the upregulation of two specific miRNAs, miR-26a and miR-214 during myogenesis correlates with a decline in the expression of enhancer of zeste homolog 2 (Ezh2), a chromatin-modifying enzyme that negatively regulates myogenesis [74,75]. miR-26a has also been found to be upregulated in both mice and human skeletal muscles and it has been demonstrated to inhibit transforming growth factor-beta (TGF β) signaling by targeting Smad1 and Smad4 [76]. Alteration of TGF β signaling pathway, whose members are potent inhibitors of myoblasts differentiation mainly affecting the expression of MyoD and myogenin, is a strategy adopted by various miRNAs to regulate myogenesis. Furthermore, miR-675 has been shown to target Smad1, Smad5, and cell division cycle 6 (Cdc6) promoting cell differentiation [77].

Specific miRNAs have also been demonstrated to promote myogenesis by suppressing the expression of various targets belonging to the inflammatory NF- κ B signaling pathway. It has been demonstrated that miR-29 targets YY1 (yin yang 1), a transcription factor downstream of the NF- κ B signaling and YY1 binding protein (Rybp), participating to a feedback loop mechanism that ensure myogenic differentiation. YY1 and Rybp act together to impair myogenesis by suppressing the expression of myogenic genes. They form a repressive complex Rybp/YY1/Ezh2/HDAC4 that

epigenetically inhibits miR-29. Upon myogenesis, MyoD/SRF displace this repressive complex promoting miR-29 expression and myogenic differentiation [78,79].

miR-322/424 and -503 have been demonstrated to repress the expression of cell division cycle 25A (Cdc25A) protein phosphatase during myoblast C2C12 differentiation [80].

More recently, miR-17 and miR-19 have been demonstrated to act in concert to promote cell differentiation and muscle regeneration after injury in vivo [81]. miR-17 mediates repression of regulators of cell proliferation, such as the cyclin Ccnd2 and the tyrosine kinase protein Jak1, and regulators of cell fusion and repressors of cell motility, such as the small G protein Rhoc. Furthermore, the miR-17 expression has been shown to correlate to the upregulation of the transcription factors Myh3 and MyoD1 [81].

An additional regulatory feedback loop involving miRNAs in promoting satellite cells differentiation has been demonstrated to reduce MyoD family inhibitor (MDFI) expression. miR-27b has been shown to inhibit the proliferation of pig satellite cells and to promote their differentiation in vitro, through the suppression of MDFI [82]. MDFI hides the nuclear localization signal of MyoD family protein, leading to the accumulation of transcription factors in the cytoplasm. In mouse models, the suppression of MDFI expression promotes muscle regeneration after injury. MDFI has been also demonstrated to take part of a regulatory circuit in which the proto-oncogene FOS inhibits the expression of MDFI, which, in turn, promotes MyoD-induced differentiation. MyoD upregulates the miR-501-3p muscle-specific miRNA, which dampens FOS expression promoting myoblast differentiation in a negative regulatory feedback loop mechanism [83].

As expected, miRNAs not only participate in the promotion of myogenic differentiation, but they also inhibit this process suppressing MRFs expression. The overexpression of miR-124 is associated with low levels of myogenic transcription factors such as Myf5, MyoD, and myogenin [84]. A miR-221/222-MyoD-myomiRs regulatory pathway has been demonstrated to regulate the expression of miR-1, miR-133 miR-206, myomiRs in C2C12 cell models. [85]. In addition to MRFs, miRNAs may also inhibit factors belonging to the Mef2 family, which is composed of transcription factors that regulate the myogenic process in concert with MRFs. In vitro experiments demonstrated that miR-155 directly represses the expression of MEF2A isoform, contrasting cell differentiation [86].

Furthermore, selected miRNAs have been demonstrated to inhibit the myogenic differentiation acting on TGF β and Wnt/ β -catenin signaling. The myomiR miR-499 may inhibit TGF β -receptor 1, promoting the proliferation of C2C12 cells [87], whereas miR-216a targets Smad7, a member of the inhibitory Smads family that can specifically inhibit TGF β pathway and bovine primary muscle cells differentiation [88]. Inhibition of cell self-renewal progression of muscle precursors in the myogenic lineage has been attributed to miR-143-3p and miR-664-5p that downregulate Wnt5a, LRP5, Axin2, β -catenin and Wnt1 expression [89,90].

An additional mechanism by which satellite cells may contribute to muscle fiber adaptation influencing extracellular matrix related gene expression is the release of extracellular vesicles, such as exosomes [91,92]. Exosomes are small cell-secreted endocytic membrane-derived vesicles that contribute to cell-to-cell communication, transporting proteins, DNA, mRNA, miRNAs. During skeletal muscle modeling, miR-206 has been demonstrated to be secreted via exosomes by skeletal muscle myogenic progenitor cells and to target the ribosomal binding protein Rbp1, which regulates the collagen expression in the extracellular matrix [60]. The relevant role of miRNAs delivered by extracellular vesicles in muscle fiber hypertrophy has been further demonstrated in mice in response to mechanical load. Not only miR-206 is enriched in vesicles derived by primary myogenic progenitor cells, but also several additional miRNAs, including mi-24, miR-149, miR-486, let-7e, miR-133 a/b and miR-320. All these miRNAs are known to regulate the process of extracellular matrix remodeling, reducing the expression of extracellular matrix-related genes such as matrix metalloproteinase 9 Mmp9 [93].

5. Role of miRNAs in Skeletal Muscle Aging and Sarcopenia

Several studies have demonstrated that miRNAs are implicated in the alteration of skeletal muscle homeostasis and function during aging. Comparative studies in young and old muscle tissues of rodents, monkeys and humans showed differential expression of several miRNAs involved in the control of the myogenic processes [94–96]. The differentially expressed miRNA during aging, target factors that regulate cell cycle progression, the insulin-like growth factors (IGFs), factors involved in the process of cell senescence such as SIRT1 and telomerase reverse transcriptase (TERT), and factors of the transforming growth factor- β (TGF- β) cell signaling pathways (Figure 2).

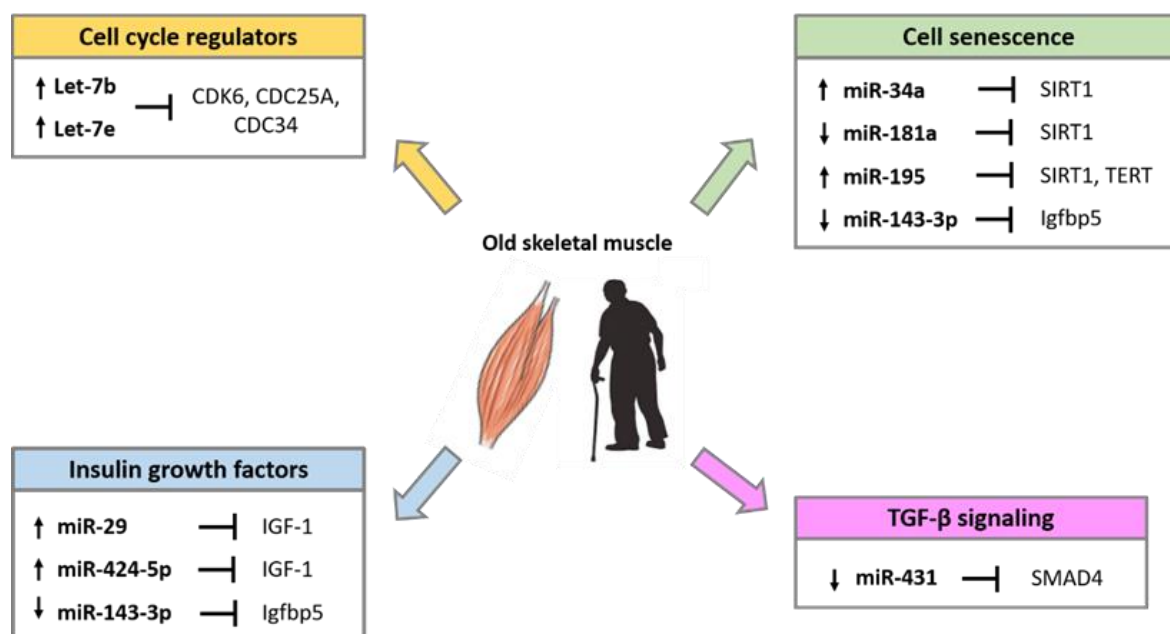


Figure 2. miRNAs involved in the regulation of age-related pathways in skeletal muscle.

miRNA expression profile analyses of skeletal muscle biopsy samples of healthy adults demonstrated that precursor of myomiRs miR-1, miR-133a, and miR-206 are upregulated in older subjects compared with younger ones [94]. This difference is not detected when analyzing the expression of mature miRNAs, suggesting that the maintenance of mature myomiRs might be useful to counteract muscle loss associated with aging. Higher expression of two miRNAs of the let-7 family, Let-7b and Let-7e, has been demonstrated in the elderly compared to young adults [97]. It has been proposed that the Let-7 miRNA family expression can reduce satellite cells proliferation in aged skeletal muscle by targeting regulators of cell cycle progression, such as CDK6, CDC25A and CDC34 [97].

Genome-wide miRNAs profile analyses in aging animal models confirm that miRNAs may be differentially expressed in old compared to young muscle [95,96]. In old muscle, a specific role has been attributed to miR-181a lower expression. During muscle differentiation, the miR-181 higher levels reduce the expression of the homeobox protein Hox-A11, a suppressor of MyoD, resulting in the upregulation of myogenin and other muscle marker proteins [98]. It has been proposed that the downregulation of miR-181a in old muscle tissue may lead to restriction of satellite cells proliferation, allowing a higher expression of activin receptor type IIA (ActRIIA), a member of the TGF β receptor family, which suppresses cell proliferation via Smad2/3 phosphorylation [21]. As miR-181a controls the expression of well-known proinflammatory cytokines such as TNF- α , IL-6, IL-1 β , and IL-8 [99], it is expected that miR-181a downregulation participates to inflammatory processes in the elderly. A more recent study showed that miR-181a and Sirtuin 1 (SIRT1) protein expression are inversely correlated in aged mice muscle [100]. Sirtuins have a crucial role in suppressing cellular senescence and extend longevity by interacting with several age-related signaling pathways such as insulin/insulin-like growth

factor-1 (IGF-1), AMP-activated protein kinase, and forkhead box O [101]. It is reasonable to speculate that the downregulation of miR-181a may overcome SIRT1 repression and delay cellular senescence participating in the autophagic cell mechanisms. SIRT1 is an important regulator of autophagy and autophagy processes participate in maintaining muscle mass, neuromuscular communication, stem cell self-renewal and differentiation [102–105].

An additional miRNA, miR-195, has been recently demonstrated to decrease SIRT1 and TERT expression in old skeletal myoblasts [106]. Inhibition of miR-195 reversed the senescent into the juvenile phenotype, thus miR-195 may be a potential target for senescent cell fate reversion. Besides, miR-29 and miR-143-3p have been shown to be involved in the regulation of cellular senescence. miR-29 targets IGF-1 and the p85 α regulatory subunit of PI3K and miR-29 overexpression is associated with high levels of the marker of cellular senescence, SA- β gal [107]. miR-143-3p expression is absent in the satellite cells and primary myoblasts of older mice and humans, whereas its target gene, insulin growth factor-binding protein 5 (Igfbp5), is present at high levels [108]. Age-related decrease of miR-143 expression may be a compensatory mechanism required to improve the myogenic process impaired by the concomitant increased levels of Igfbp5 that in turn induces cell senescence [109].

In mice, the ectopic expression of miR-431, which binds to a conserved site on SMAD4 3' UTR, has been demonstrated to enhance old myoblasts differentiation and to restore the regeneration of the tissue, suggesting that miR-431 may play a key role in the maintenance of the myogenic capability of myoblasts with age [110].

miR-155, which is known to be involved in inflammatory processes, is upregulated in aged muscle satellite cells [109]. Notch1 normally binds to the promoter region of miR-155, participating in its suppression. In aged muscle, Notch1 expression is reduced, resulting in higher expression of miR-155. Both events, Notch 1 downregulation and miR155 overexpression therefore might contribute to inflammation status and muscle stem cell differentiation process [109].

Increased oxidative stress during aging can lead to muscle loss and function due to the activation of various catabolic pathways, including apoptosis. Recently, it has been observed that miR-434-3p is downregulated in the skeletal muscle of aged mice, and its expression negatively correlated with the levels of eukaryotic translation initiation factor 5A1 (eIF5A1), a factor demonstrated to induce apoptosis via the mitochondrial apoptotic pathway [111]. Low levels of miR-434-3p has also been detected in the serum of aged mice, indicating miR-434-3p as a potential biomarker of muscle atrophy related to age [10].

In sarcopenic people, several studies confirmed an accentuated increase in the expression level of miR-34a-5p, miR-449b-5p and miR-424-5p [11,112,113]. miR-34a targets cell senescence factors such as SIRT1 and the Endothelial Growth Factor A (VEGFA) and it should be considered a muscle aging key factor, whose expression is modulated in the cellular process leading to age-related skeletal muscle decline [114]. Moreover, in vitro and in vivo experiments show that miR-424-5p regulates the expression of transcripts that are involved in the synthesis of rRNA and its overexpression reduces the protein synthesis, a phenomenon that contributes to the loss of muscle mass in sarcopenia and aging, i.e., “anabolic resistance” [114]. Anabolic resistance may derive from a reduced muscle sensitivity to anabolic signaling as demonstrated for insulin, IGF-1 signaling, and inhibition of Akt/mTOR by inflammatory signals. miR-424-5p was proposed to contribute to this component of anabolic resistance based on the evidence that IGF-1 is one of its most enriched targets [112]. Elevated expression of miR-424 detected in patients with muscle wasting correlates with a reduction of protein synthesis and loss of muscle mass [112]. The possibility to modulate miRNAs expression could provide potential therapeutic prospectives to enhance protein synthesis and reduce muscle loss in the elderly.

6. miRNAs Are Regulated by Exercise in Sarcopenia

Skeletal muscle exhibits an extraordinary plasticity dictated by a fine balance between anabolic and catabolic processes [2]. Muscle composition is influenced by internal and external stimuli (e.g., the intrinsic cellular aging process or environmental factors) that can accelerate or temporize the functional

muscle impairment associated with aging and the sedentary behavior [15,16,115]. Indeed, aging is associated with a decrease in muscle protein synthesis [116], mitochondrial dysfunction, as well as a loss of fast glycolytic fibers and reduced blood perfusion [117–119]. Therefore, older people show a characteristic weakening, deterioration, and muscle loss, accompanied by microvascular impaired perfusion and an underlying state of inflammation [47,120]. This turnover is detrimental for healthy aging but is partially reversible with physical activity [121,122]. To date, lifestyle interventions and exercise training represent the primary, most effective, and non-pharmacological approach to prevent and treat sarcopenia-related decline.

Exercise is prescribed with different approaches, including customized type, frequency, intensity, and duration, to endorse positive outcomes. The most common and studied models of exercise can be distinguished in endurance and resistance: the latter is characterized by low intensity, long-duration aerobic activity, the former by higher intensities, short bouts with primary involvement of the anaerobic pathways. Endurance training is mainly known for its positive effects on the cardiovascular fitness (i.e., maximal oxygen consumption), but it also induces mitochondrial biogenesis, increases oxidative enzyme activity with a reduction in ROS generation, promotes muscle vascularization and regulates vascular tone [123,124]. The changes in muscle metabolism enhance the all-body aerobic fitness capacity (peak VO_2 uptake) and attenuate the age-associated decline in the peripheral and central vasculature and cardiac functions [125,126]. Considering that the main feature of aging and sarcopenia is muscle atrophy, resistance exercise training is the most indicated, as it elicits the biosynthesis of contractile and structural proteins, resulting in muscle hypertrophy [127]. Specifically, resistance training significantly increases the number and cross-sectional area of type II fibers [123,124]. This improvement in muscle fibers results in a general improvement in functional capacity, muscular endurance, and quality of life [20].

miRNA expression may be adapted in response to exercise and altered miRNA profile may contribute to affect the plasticity of aged muscle [128,129]. Understanding the signaling pathways regulated by these miRNAs allows to shed light on the molecular mechanisms associated to improved muscle anatomy and function and may help establish specific protocols of training.

6.1. Exercise Modulates Muscle miRNAs Expression

Several studies have investigated the miRNAs changes to exercise. A comprehensive review of studies analyzing the miRNAs expression in human serum, plasma, whole blood, saliva, or muscle biopsy has been recently published [23]. To integrate more information and understand better the role of exercise on miRNAs expression, in this review, the pure long-duration moderate-intensity endurance exercise will be differentiated from the high-intensity endurance training. In these terms, a long-duration moderate-intensity intervention (>30 min @ ~70% $\text{VO}_{2\text{max}}$) elicits mainly the aerobic processes and, if performed for 6 weeks, significantly increases mitochondrial capacity [130]. A wide gene expression analysis study indicates that 6 weeks of endurance training (4 days/week, 45min @ 70% $\text{VO}_{2\text{max}}$) may reduce the expression of miR-1 and miR-133, together with miR-101 and miR-455 in young healthy adults [131]. On the other hand, medium-duration high-intensity endurance training utilizes intensities usually above the lactate threshold (~85% to 90% $\text{VO}_{2\text{max}}$). The energy transformation is a combination of aerobic and anaerobic pathways, and the expression of myomiRs appears different. miR-1, miR-133a, miR-133b and miR-206 were downregulated at rest following 12 weeks of mixed-endurance training (2 days of continuous 60–150 min @ ~60% peak power output (PO_{peak}), 2 days of interval 70–80 min @ 75–90% PO_{peak} and one day of maximal incremental test) and return to a high level of expression 14 days after cessation of regular training [132]. Additionally, increasing even more the exercise intensity, mixed endurance training (45–90 min @ 75% $\text{VO}_{2\text{peak}}$) with high-intensity interval training (HIIT; 6 sets of 5 min @ 90–100% $\text{VO}_{2\text{peak}}$) provided evidence that miR-1, miR-133a, miR-133b and miR-181a levels are increased, whereas miR-9, miR-23a, miR-23b and miR-31 are decreased [133]. Using reporter assays, miR-31 was reported to directly interact with HDAC4, which belongs to the MAPK pathway, and with Nuclear Respiratory Factor 1 (NRF1), which is involved

in mitochondrial biogenesis and metabolism. To investigate if different types of exercise, even if all considered aerobic, have different outcomes on the myomiR expression, different endurance exercise modalities were explored on a group of young adults [134]. A single bout (90 min) of traditional non-weight-bearing endurance exercise on a cycle ergometer was compared to a walking trial with a loaded vest equivalent to the 30% of the individual body mass. MyomiR expression was different between the two modalities, even if the intensity was matched. The load carriage exercise diminished miR-1-3p, miR-206, miR-208a-5p, and miR-499 expression, while traditional endurance exercise on the cycle ergometer increased myomiR expression. In other words, the endurance exercise with a predominant anabolic part, resulted in diminished myomiR expression [134]. All the aforementioned studies investigated young adults, and further studies should explore if similar results occur in elderly people.

As mentioned before, resistance training is the more indicated and effective type of training for the older population. A limited number of studies have investigated the potential correlation between the decline of protein synthesis and anabolism of skeletal muscle during aging and the modulation in miRNA expression [94,135,136]. Representative examples of miRNAs specifically expressed in skeletal muscle modulate after exercise in young and elderly people are listed in Table 1.

In particular, Drummond et al. studied the impact of an acute resistance training session (8 sets of 10 repetitions @ 70% 1 maximal repetition (RM)), and for the first time determined that miR-1 skeletal muscle expression is downregulated in young men but not in older men, after stimulation of muscle protein synthesis [94]. As mentioned above, miR-1 targets many transcripts responsible for muscle growth and satellite cell function, such as the IGF-1 factor. Reduction of miR-1 expression may allow the activation of the mTORC1 pathway through IGF-1 signaling that, in turn, increases mRNA translational efficiency and muscle protein synthesis. The maintenance of miR-1 expression levels in the elderly results in reduced mTORC1-related intracellular events, which may explain the lack of anabolic response to the bout of resistance exercise in the elderly [137]. Evidence has been provided that the levels of thirteen miRNA species, including members of the miR-378, miR-30 and miR-128 families, were increased following 30 min of acute resistance exercise in adult healthy sedentary people [138]. Of particular interest is the role of miR-378a, which is located within intron 1 of the PPARGC1B gene, a coactivator of nuclear receptors and other transcription factors that regulate metabolic processes, including mitochondrial biogenesis and respiration, hepatic gluconeogenesis, and muscle fiber-type switching [139]. miR-378 isoforms have been implicated in the control of mitochondrial function and energy balance in mice, suggesting that miR-378 may participate in the adaptation of mitochondrial function and metabolic balance in the exercise [140]. Mouse models lacking miR-378-3p and -5p, but leaving the PPARGC1B gene intact, are resistant to diet-induced obesity, thus, the changes seen in miR-378 in muscle following exercise could also have effects on mitochondrial function and energy homeostasis [140].

HIIT, but not moderate-intensity continuous training has been shown to modulate the post-exercise expression of miR-133a, miR-378 and miR-486, all involved in skeletal muscle adaptation to resistance exercise. HIIT exercises are particularly effective in inducing anabolic responses increasing mTOR signaling and intermediates phosphorylation [141].

Table 1. Expression of skeletal muscle miRNAs after exercise reviewed in the text.

Subjects	Type of Exercise	Duration ^a	MyomiRs	Other miRNAs	References
Older man(70 yr)	Resistance acute exercise bout	3/6 hrs	↓miR-1		[94]
30–35 yr old healthy, trained men	Endurance acute exercise bout	1 hr	↑miR-1, miR-133a/b, miR-206		[132]
	Endurance training	12 wks	↓miR-1, miR-133a/b, miR-206		
18–30 yr old men (low responders)	Resistance exercise training	12 wks		↑miR-451, ↓miR-26a, miR-29a, miR-378	[143]
24 yr old young sedentary healthy men	Endurance training	6 wks	↓miR-1, miR-133a	↓miR-101, miR-455	[131]
Males 23 yr old	Endurance acute exercise bout	3 hrs	↑miR-1, miR-133a/b, miR-206	↑miR-181a, ↓miR-9, miR-23a/b, miR-31	[133]
Healthy young (18–30 yr old) and older (60–75 yr) men	Resistance acute exercise bout	2 hrs	Young		[136]
			↑miR-486-3p,	↓miR-149-3p, miR-520g-3p, miR-99b-5p, miR-100-5p	
			Old		
			↑miR-499a-5p	↑ miR-99a-5p, ↓miR-186-5p, miR-196b, miR-335-5p, miR-628-5p, miR-489-5p	
Young, healthy (22 yr) and old (74 yr) men	Resistance acute exercise bout	6 hrs	↓miR-133a, miR-133b	Young ↓miR-23b-3p, miR-24-3p, miR-26a-5p, miR-26b-5p, miR-27a-3p, miR-27b-3p, miR-29c-3p, miR-30a-5p, miR-30d-5p, miR-95-3p, miR-126-3p, miR-140-3p, miR-181a-5p	[135]
Older men and women (65–80 yr)	Resistance exercise training	5 mos	↓miR-133b		[142]
Sedentary Healthy men and women (31–35 yr old)	Resistance acute exercise bout	30 min		↑miR-10a-5p, miR-30a-5p, miR-30d-5p, miR-22-3p, miR-128, miR-378a-3p, miR-378f, miR-378a-5p, miR-378g, miR-378i, miR-422a, miR-532-5p	[138]
Healthy males (23–31 yr old)	HIIT or MICT ^b + RE	1/3 hrs	↓miR-486, miR-133a	↓miR-378	[141]
25 adults (18–27 yr old)	Endurance single 90 min exercise bout (Load carriage or cycle ergometry)	Immediately/3 hrs	↓miR-1-3p, miR-206, miR-208a-5, miR-499		[134]

^a hrs, hours; mos, months; min, minutes; yr, year; wks, weeks. ^b High-intensity interval training (HIIT) or moderate-intensity continuous training (MICT); Resistance Exercise (RE).

In agreement, Rivas et al. identified several miRNAs that are differentially expressed in young men, after an acute session of resistance exercise (6 sets of 10 reps @ 80% 1RM), whereas they did not show differences in older adults [135]. In vitro analysis demonstrated miR-126-3p, belonging to the differentially expressed miRNA, regulates the expression of Akt/forkhead box protein O1 (Foxo1), MyoD, Myf5 and factors of the IGF-1 signaling, suggesting its role in the control of muscle protein synthesis pathways related to aging. miRNA that regulates several members of the Akt-mTOR signaling, such as miR-99a-5p, miR-99b-5p, miR-100-5p, miR-149-3p, miR-196b-5p, and miR-199a have also been demonstrated to be differentially expressed in older men compared to the young, in response to acute resistance exercise (3 sets of 14 reps @ 60% 1RM); this confirmed the relevance of the Akt-mTOR signaling in aging-related muscle plasticity [136]. Since weakened Akt-mTOR signaling activation is associated with the progression of muscle wasting during aging, altered miRNA expression profile following acute anabolic stimulus may contribute to the progressive weakening of skeletal muscle in the elderly, contributing to the onset of sarcopenia. In a study that analyzed the effects of 5 months of resistance training (3 days/week, 3 sets of 10 reps @ 70% 1RM) on older adults, the expression levels of the myomiR miR-133b was decreased in muscle tissue [142].

From a study analyzing the hypertrophic response of young individuals that performed 12 weeks of intense resistance exercise training (RT), recruited subjects have been recognized and classified as “low responders” or “high responders” to the training [143]. Following the resistance exercise training, miR-451 levels resulted increased, whereas miR-26a, miR-29a and miR-378 expression were decreased only in the “low responders”. The reduced expression of miR-26a, miR-29a and miR-378 correlate to IGF-1 mRNA and increased only in the “high responders” group. The IGF-1 mRNA levels remained unchanged in the low-responder group post-training, suggesting that changing in the miRNA profile may be a compensatory mechanism for the lack of key target genes providing mRNA substrate to protein synthesis machinery. Thus, it has to be taken into account that exercise training always has an influence, but the level of intensity dictates the response and, consequently, the expression of the miRNAs.

6.2. Exercise Modulates Circulating miRNAs Expression

Although miRNAs are mainly detected in the intracellular environment, a great number of miRNAs, known as circulating miRNAs, have also been found in various biological fluids, such as blood, urine, and saliva, and are transported as signaling molecules to mediate cell-cell communications [144]. Determining the circulating miRNAs levels may be useful for the estimation of muscle function, recognizing them as non-invasive candidate biomarkers of sarcopenia or other skeletal muscles-associated disorders.

Differential expression of circulating miRNAs may represent a marker of response to gene expression regulation derived by environmental adaptation, including exercise. In plasma or serum, miRNAs are detectable in a remarkably stable form, encapsulated into the extracellular vesicles such as microvesicles, exosomes, apoptotic bodies or bound to RNA-binding proteins or high-density lipoproteins, making them resistant to RNase digestion. Circulating miRNA have been suggested to be mediators of gene expression, allowing cell-to-cell communication. Moreover, they have been suggested as potential non-invasive biomarkers to reveal muscle function and adaptation to exercise in the elderly [145–147]. In the frailty geriatric syndrome in addition to sarcopenia, mitochondrial dysfunction, oxidative stress, aging-related loss of anabolic hormones, decreased peripheral perfusion and chronic inflammation (inflammaging) are reported that could be associated with altered presence of circulating miRNAs [148–151].

A recent study observed that miR-21 levels were increased in frailty condition, whereas miR-146a were downregulated [152]. A decrease of miR-146a expression in frailty has been shown to induce NF- κ B-dependent inflammation. Moreover, an increase in miR-483 level, which regulates the synthesis of the anti-aging hormone, melatonin, has been reported in frail patients [152].

The altered miRNA profile has also been demonstrated by comparing the expression of exosome-derived miRNA isolated from the plasma of young adults, robust, and frail elderly people [153]. The expression of a group of eight miRNAs (miR-10a-3p, miR-92a-3p, miR-185-3p, miR-194-5p, miR-326, miR-532-5p, miR-576-5p, and miR-760) was found altered with higher expression in frail older individuals. These miRNAs are predicted to be implicated in aging pathways such as the insulin signaling pathway, the AMPK signaling pathway, and the FoxO signaling pathway.

Altered expression of circulating miRNAs have been demonstrated in response to acute and chronic exercise, and have been extensively described in a recent review [154].

The lack of anabolic response to resistance exercise in the elderly can be found in the altered expression of circulating miRNA profile [140]. Nine circulating miRNAs (miR-19b-3p, miR-195-5p, miR-19a-3p, miR-106-5p, miR-20a-5p, miR-17-5p, miR-143-3p, miR-26b-5p, miR-93-5p) show a greater expression in younger compared to older subjects after exercise. Bioinformatics analyses of the potential targets of these miRNAs, showed the absence of factors involved in anabolic signaling, IGF-1, and mTOR signaling in older subjects, suggesting that a downregulation of these circulating miRNAs is indicative of “anabolic resistance” in elderly [155]. In addition to exercise, energy restriction influences the expression of circulating miRNAs that are inversely associated with whole-body protein synthesis [156]. Circulating miRNAs modulated by the exercise in the elderly are listed in Table 2.

A recent study has demonstrated that comparing two groups, one of older adults with at least 5 consecutive years of endurance-trained and one of sedentary males (≤ 1 day/weeks exercise), regular exercise significantly increased the expression of three miRs present in the exosomes, named exomiRS (miR-486-5p, miR-215-5p, miR-941) and decreased the expression of one exomiR (miR-151b) [160]. Acute exercise altered circulating exomiR expression in both trained groups. Pathway analysis prediction and validation experiments reported that the majority of exercises regulated exomiRs target transcripts of genes that are related to IGF-1 signaling [160].

Modified expression of circulating miRNAs has also been shown to correlate with exercise and diet weight loss intervention. Circulating miRNA-221 and -223 were found to be modulated following exercise and diet [159]. Studies on male marathon runners have demonstrated that prolonged aerobic exercises may change the expression of circulating miRNAs, such as miR-126 and miR-133, which may be potentially used as biomarkers of acute responses to physiological stress [157,158].

Further studies that will analyze the expression of circulating miRNAs in aging and in the adaptation to a healthy lifestyle, such as dietary choices and exercise may provide knowledge on the molecular mechanisms that sustain skeletal muscle structure and functionality.

Table 2. Circulating miRNAs differentially expressed in elderly compared to healthy young after exercise.

Subjects	Type of Exercise	Duration ^a	c-miRNAs ^b	Reference	
Male marathon runners (51.6–62 yr old)	Endurance acute exercise bout	30 min/4 hrs	Immediately post-exercise: ↑miR-126, miR-133	[157]	
Male marathon runners (50.4–53.2 yr old)	Endurance acute exercise bout	Immediately post/up to 24 hrs	Immediately post exercise: ↑miR-1, miR-126, miR-133a, miR-134, miR-146a, miR-208a, miR-499-5p	[158]	
Healthy, inactive, young (21–23 yr) and old (72–76 yr)	Resistance acute exercise bout	6 hrs	Young ↑miR-19b-3p, miR-195-5p, miR-19a-3p, miR-106-5p, miR-20a-5p, miR-17-5p, miR-143-3p, miR-26b-5p, miR-93-5p	[155]	
Low (40.6–52 yr) and high (42–54.4 yr) responding men and women to a weight loss intervention	Resistance exercise training and diet intervention	16 wks	Both groups: ↑221-3p, 223-3p Only Low responder: ↑miR-140	[159]	
Older trained and older sedentary men (>65 yr old)	Endurance acute exercise bout	40 min	Trained group	[160]	
			Immediately post exercise ↑miR-383-5p, miR-339-5p, miR-874-3p ↓miR-206, miR-486-5p, miR-148a-3p, let-7b-5p		3 hrs post exercise ↑miR-34b-3p, miR-129-2-3p, miR-138-1-3p, miR-671-3p, miR-885-5p ↓miR-486-5p, miR-629-5p, miR-16-2-3p
			Sedentary group		
			Immediately post exercise ↑ miR-505-3p, miR-29b-3p, miR-203a-3p, miR-384, miR-451a, miR-223-3p, miR-218-5p, miR-495-3p	3 hrs post exercise ↓miR-4433b-3p, miR-378c, miR-151b, miR-151a-5p, hsa-miR-151b	

^a hrs, hours; mos, months; min, minutes; yr, year; wks, weeks. ^b c-miRNAs, circulating miRNA.

7. Conclusions

Sarcopenia-related muscle dysfunction significantly affects life quality of elderly people. Skeletal muscle development, homeostasis, and metabolism during aging undergo changes in terms of gene expression regulation in which miRNAs have been demonstrated to play a crucial role. With aging, the altered expression profile of miRNAs that regulate the central processes of muscle cell biology contributes to the loss of muscle mass. Further studies on the molecular mechanisms of regulation of miRNAs during the multiple steps of skeletal myogenesis, as well as in sarcopenic/atrophy conditions will shed light to our knowledge on the functionality of skeletal muscle and on the identification of potential targets for therapies. Detection of circulating miRNAs in serum and plasma that can mirror skeletal muscle status is a potential opportunity to identify non-invasive biomarkers to improve clinical diagnosis and prognosis of sarcopenia.

Author Contributions: Conceptualization, S.F., G.G. and M.G.R.; writing—original draft preparation, S.F., G.G., T.D.S., M.G.R.; writing—review and editing, G.G., T.D.S., S.T., M.G.-L. and M.G.R.; supervision, M.V. and M.G.R.; project administration, M.V., L.D.P., F.S. and M.G.R.; funding acquisition, L.D.P., F.S. and M.G.R. All authors have read and agreed to the published version of the manuscript.

Funding: The study was partially supported by the Italian Ministry of Research and University (MIUR) 5-year special funding to strengthen and enhance excellence in research and teaching (<https://www.miur.gov.it/dipartimenti-di-eccellenza>).

Conflicts of Interest: The authors declare no conflict of interest.

References

1. Wilkinson, D.J.; Piasecki, M.; Atherton, P.J. The Age-Related Loss of Skeletal Muscle Mass and Function: Measurement and Physiology of Muscle Fibre Atrophy and Muscle Fibre Loss in Humans. *Ageing Res. Rev.* **2018**, *47*, 123–132. [[CrossRef](#)] [[PubMed](#)]
2. Sannicandro, A.J.; Soriano-Arroquia, A.; Goljanek-Whysall, K. Micro(RNA)-Managing Muscle Wasting. *J. Appl. Physiol.* **2019**, *127*, 619–632. [[CrossRef](#)] [[PubMed](#)]
3. Schmidt, M.; Schüler, S.C.; Hüttner, S.S.; von Eyss, B.; von Maltzahn, J. Adult Stem Cells at Work: Regenerating Skeletal Muscle. *Cell Mol. Life Sci.* **2019**, *76*, 2559–2570. [[CrossRef](#)]
4. Horak, M.; Novak, J.; Bienertova-Vasku, J. Muscle-Specific MicroRNAs in Skeletal Muscle Development. *Dev. Biol.* **2016**, *410*, 1–13. [[CrossRef](#)]
5. Bartel, D.P. MicroRNAs: Genomics, biogenesis, mechanism, and function. *Cell* **2004**, *116*, 281–297. [[CrossRef](#)]
6. Güller, I.; Russell, A.P. MicroRNAs in Skeletal Muscle: Their Role and Regulation in Development, Disease and Function. *J. Physiol.* **2010**, *588*, 4075–4087. [[CrossRef](#)]
7. Moresi, V.; Marroncelli, N.; Coletti, D.; Adamo, S. Regulation of Skeletal Muscle Development and Homeostasis by Gene Imprinting, Histone Acetylation and MicroRNA. *Biochim. Biophys. Acta* **2015**, *1849*, 309–316. [[CrossRef](#)] [[PubMed](#)]
8. Nie, M.; Deng, Z.-L.; Liu, J.; Wang, D.-Z. Noncoding RNAs, Emerging Regulators of Skeletal Muscle Development and Diseases. *Biomed Res. Int.* **2015**, *2015*, 676575. [[CrossRef](#)] [[PubMed](#)]
9. Zhao, Y.; Chen, M.; Lian, D.; Li, Y.; Li, Y.; Wang, J.; Deng, S.; Yu, K.; Lian, Z. Non-Coding RNA Regulates the Myogenesis of Skeletal Muscle Satellite Cells, Injury Repair and Diseases. *Cells* **2019**, *8*, 988. [[CrossRef](#)]
10. Jung, H.J.; Lee, K.-P.; Milholland, B.; Shin, Y.J.; Kang, J.S.; Kwon, K.-S.; Suh, Y. Comprehensive MiRNA Profiling of Skeletal Muscle and Serum in Induced and Normal Mouse Muscle Atrophy During Aging. *J. Gerontol. A Biol. Sci. Med. Sci.* **2017**, *72*, 1483–1491. [[CrossRef](#)]
11. Zheng, Y.; Kong, J.; Li, Q.; Wang, Y.; Li, J. Role of MiRNAs in Skeletal Muscle Aging. *Clin. Interv. Aging* **2018**, *13*, 2407–2419. [[CrossRef](#)] [[PubMed](#)]
12. Kosek, D.J.; Kim, J.S.; Petrella, J.K.; Cross, J.M.; Bamman, M.M. Efficacy of 3 days/wk resistance training on myofiber hypertrophy and myogenic mechanisms in young vs. older adults. *J. Appl. Physiol.* **2006**, *101*, 531–544. [[CrossRef](#)] [[PubMed](#)]
13. Nilwik, R.; Snijders, T.; Leenders, M.; Groen, B.B.; van Kranenburg, J.; Verdijk, L.B.; van Loon, L.J. The decline in skeletal muscle mass with aging is mainly attributed to a reduction in type II muscle fiber size. *Exp. Gerontol.* **2013**, *48*, 492–498. [[CrossRef](#)] [[PubMed](#)]

14. Lexell, J.; Downham, D.; Sjöström, M. Distribution of different fibre types in human skeletal muscles. Fibre type arrangement in m. vastuslateralis from three groups of healthy men between 15 and 83 years. *J. Neurol. Sci.* **1986**, *72*, 211–222. [[CrossRef](#)]
15. Cavedon, V.; Milanese, C.; Laginestra, F.G.; Giuriato, G.; Pedrinolla, A.; Ruzzante, F.; Schena, F.; Venturelli, M. Bone and skeletal muscle changes in oldest-old women: The role of physical inactivity. *Aging Clin. Exp. Res.* **2020**, *32*, 207–214. [[CrossRef](#)]
16. Naro, F.; Venturelli, M.; Monaco, L.; Toniolo, L.; Muti, E.; Milanese, C.; Zhao, J.; Richardson, R.S.; Schena, F.; Reggiani, C. Skeletal Muscle Fiber Size and Gene Expression in the Oldest-Old With Differing Degrees of Mobility. *Front. Physiol.* **2019**, *10*, 313. [[CrossRef](#)]
17. Venturelli, M.; Saggin, P.; Muti, E.; Naro, F.; Cancellara, L.; Toniolo, L.; Tarperi, C.; Calabria, E.; Richardson, R.S.; Reggiani, C.; et al. In vivo and in vitro evidence that intrinsic upper- and lower-limb skeletal muscle function is unaffected by ageing and disuse in oldest-old humans. *Acta Physiol.* **2015**, *215*, 58–71. [[CrossRef](#)]
18. Venturelli, M.; Reggiani, C.; Richardson, R.S.; Schena, F. Skeletal Muscle Function in the Oldest-Old: The Role of Intrinsic and Extrinsic Factors. *Exerc. Sport Sci. Rev.* **2018**, *46*, 188–194. [[CrossRef](#)]
19. Bogdanis, G.C. Effects of Physical Activity and Inactivity on Muscle Fatigue. *Front. Physiol.* **2012**, *3*, 142. [[CrossRef](#)]
20. Borst, S.E. Interventions for sarcopenia and muscle weakness in older people. *Age Ageing* **2004**, *33*, 548–555. [[CrossRef](#)]
21. Zacharewicz, E.; Lamon, S.; Russell, A.P. MicroRNAs in Skeletal Muscle and Their Regulation with Exercise, Ageing, and Disease. *Front. Physiol.* **2013**, *4*, 266. [[CrossRef](#)] [[PubMed](#)]
22. Domańska-Senderowska, D.; Laguette, M.-J.N.; Jegier, A.; Cieszczyk, P.; September, A.V.; Brzezińska-Lasota, E. MicroRNA Profile and Adaptive Response to Exercise Training: A Review. *Int. J. Sports Med.* **2019**, *40*, 227–235. [[CrossRef](#)] [[PubMed](#)]
23. Da Silva, F.C.; da Rosa Iop, R.; Andrade, A.; Costa, V.P.; Filho, P.J.B.G.; da Silva, R. Effects of Physical Exercise on the Expression of MicroRNAs: A Systematic Review. *J. Strength. Cond. Res.* **2020**, *34*, 270–280. [[CrossRef](#)] [[PubMed](#)]
24. Zhou, Q.; Shi, C.; Lv, Y.; Zhao, C.; Jiao, Z.; Wang, T. Circulating MicroRNAs in Response to Exercise Training in Healthy Adults. *Front. Genet.* **2020**, *11*, 256. [[CrossRef](#)] [[PubMed](#)]
25. Alles, J.; Fehlmann, T.; Fischer, U.; Backes, C.; Galata, V.; Minet, M.; Hart, M.; Abu-Halima, M.; Grässer, F.A.; Lenhof, H.P.; et al. An estimate of the total number of true human miRNAs. *Nucleic. Acids Res.* **2019**, *47*, 3353–3364. [[CrossRef](#)]
26. O'Brien, J.; Hayder, H.; Zayed, Y.; Peng, C. Overview of MicroRNA Biogenesis, Mechanisms of Actions, and Circulation. *Front. Endocrinol. (Lausanne)* **2018**, *9*, 402. [[CrossRef](#)]
27. Rodriguez, A.; Griffiths-Jones, S.; Ashurst, J.L.; Bradley, A. Identification of mammalian microRNA host genes and transcription units. *Genome Res.* **2004**, *14*, 1902–1910. [[CrossRef](#)]
28. Ha, M.; Kim, V.N. Regulation of microRNA biogenesis. *Nat. Rev. Mol. Cell Biol.* **2014**, *15*, 509–524. [[CrossRef](#)]
29. Broughton, J.P.; Lovci, M.T.; Huang, J.L.; Yeo, G.W.; Pasquinelli, A.E. Pairing beyond the Seed Supports MicroRNA Targeting Specificity. *Cell* **2016**, *64*, 320–333. [[CrossRef](#)]
30. Slack, F.J.; Chinnaiyan, A.M. The Role of Non-coding RNAs in Oncology. *Cell* **2019**, *179*, 1033–1055. [[CrossRef](#)]
31. Juźwik, C.A.; Drake, S.; Zhang, Y.; Paradis-Isler, N.; Sylvester, A.; Amar-Zifkin, A.; Douglas, C.; Morquette, B.; Moore, C.S.; Fournier, A.E. microRNA dysregulation in neurodegenerative diseases: A systematic review. *Prog. Neurobiol.* **2019**, *182*, 101664. [[CrossRef](#)]
32. Fochi, S.; Ciminale, V.; Trabetti, E.; Bertazzoni, U.; D'Agostino, D.M.; Zipeto, D.; Romanelli, M.G. NF-κB and MicroRNA Deregulation Mediated by HTLV-1 Tax and HBZ. *Pathogens* **2019**, *8*, 290. [[CrossRef](#)] [[PubMed](#)]
33. Calderon-Dominguez, M.; Belmonte, T.; Quezada-Feijoo, M.; Ramos-Sánchez, M.; Fernández-Armenta, J.; Pérez-Navarro, A.; Cesar, S.; Peña-Peña, L.; Veá, À.; Llorente-Cortés, V.; et al. Emerging role of microRNAs in dilated cardiomyopathy: Evidence regarding etiology. *Transl. Res.* **2020**, *215*, 86–101. [[CrossRef](#)]
34. Asfour, H.A.; Mohammed, Z.A.; Raed, S.S. Myogenic Regulatory Factors: The Orchestrators of Myogenesis after 30 Years of Discovery. *Exp. Biol. Med. (Maywood)* **2018**, *243*, 118–128. [[CrossRef](#)] [[PubMed](#)]
35. Musarò, A.; Cusella De Angelis, M.G.; Germani, A.; Ciccarelli, C.; Molinaro, M.; Zani, B.M. Enhanced expression of myogenic regulatory genes in aging skeletal muscle. *Exp. Cell Res.* **1995**, *221*, 241–248. [[CrossRef](#)] [[PubMed](#)]

36. Sousa-Victor, P.; Gutarra, S.; García-Prat, L.; Rodríguez-Ubreva, J.; Ortet, L.; Ruiz-Bonilla, V.; Jardí, M.; Ballestar, E.; González, S.; Serrano, A.L.; et al. Geriatric Muscle Stem Cells Switch Reversible Quiescence into Senescence. *Nature* **2014**, *506*, 316–321. [[CrossRef](#)] [[PubMed](#)]
37. Larsson, L.; Degens, H.; Li, M.; Salviati, L.; Lee, Y.I.; Thompson, W.; Kirkland, J.L.; Sandri, M. Sarcopenia: Aging-Related Loss of Muscle Mass and Function. *Physiol. Rev.* **2019**, *99*, 427–511. [[CrossRef](#)]
38. Joseph, A.-M.; Adhietty, P.J.; Buford, T.W.; Wohlgemuth, S.E.; Lees, H.A.; Nguyen, L.M.-D.; Aranda, J.M.; Sandesara, B.D.; Pahor, M.; Manini, T.M.; et al. The impact of aging on mitochondrial function and biogenesis pathways in skeletal muscle of sedentary high- and low-functioning elderly individuals. *Aging Cell* **2012**, *11*, 801–809. [[CrossRef](#)] [[PubMed](#)]
39. Gilles, G.; Sgarioni, N.; Kapchinsky, S.; Purves-Smith, F.; Norris, B.; Pion, C.H.; Barbat-Artigas, S.; Lemieux, F.; Taivassalo, T.; Morais, J.A.; et al. Increased sensitivity to mitochondrial permeability transition and myonuclear translocation of endonuclease G in atrophied muscle of physically active older humans. *FASEB J.* **2014**, *28*, 1621–1633. [[CrossRef](#)]
40. Sousa-Victor, P.; Muñoz-Cánoves, P. Regenerative Decline of Stem Cells in Sarcopenia. *Mol. Aspects Med.* **2016**, *50*, 109–117. [[CrossRef](#)]
41. Li, C.-W.; Yu, K.; Shyh-Chang, N.; Li, G.-X.; Jiang, L.-J.; Yu, S.-L.; Xu, L.-Y.; Liu, R.-J.; Guo, Z.-J.; Xie, H.-Y.; et al. Circulating factors associated with sarcopenia during ageing and after intensive lifestyle intervention. *J. Cachexia Sarcopenia Muscle* **2019**, *10*, 586–600. [[CrossRef](#)]
42. Forcina, L.; Miano, C.; Pelosi, L.; Musarò, A. An Overview About the Biology of Skeletal Muscle Satellite Cells. *Curr. Genom.* **2019**, *20*, 24–37. [[CrossRef](#)]
43. Fry, C.S.; Lee, J.D.; Mula, J.; Kirby, T.J.; Jackson, J.R.; Liu, F.; Yang, L.; Mendias, C.L.; Dupont-Versteegden, E.E.; McCarthy, J.J.; et al. Inducible Depletion of Satellite Cells in Adult, Sedentary Mice Impairs Muscle Regenerative Capacity without Affecting Sarcopenia. *Nat. Med.* **2015**, *21*, 76–80. [[CrossRef](#)]
44. Keefe, A.C.; Lawson, J.A.; Flygare, S.D.; Fox, Z.D.; Colasanto, M.P.; Mathew, S.J.; Yandell, M.; Kardon, G. Muscle stem cells contribute to myofibres in sedentary adult mice. *Nat. Commun.* **2015**, *6*, 7087. [[CrossRef](#)]
45. Englund, D.A.; Murach, K.A.; Dungan, C.M.; Figueiredo, V.C.; Vechetti, I.J.; Dupont-Versteegden, E.E., Jr.; McCarthy, J.J.; Peterson, C.A. Depletion of resident muscle stem cells negatively impacts running volume, physical function, and muscle fiber hypertrophy in response to lifelong physical activity. *Am. J. Physiol. Cell Physiol.* **2020**, *318*, C1178–C1188. [[CrossRef](#)]
46. Karlsen, A.; Soendenbroe, C.; Malmgaard-Clausen, N.M.; Wagener, F.; Moeller, C.E.; Senhaji, Z.; Damberg, K.; Andersen, J.L.; Schjerling, P.; Kjaer, M.; et al. Preserved capacity for satellite cell proliferation, regeneration, and hypertrophy in the skeletal muscle of healthy elderly men. *FASEB J.* **2020**, *34*, 6418–6436. [[CrossRef](#)]
47. Merritt, E.K.; Stec, M.J.; Thalacker-Mercer, A.; Windham, S.T.; Cross, J.M.; Shelley, D.P.; Craig Tuggle, S.; Kosek, D.J.; Kim, J.S.; Bamman, M.M. Heightened muscle inflammation susceptibility may impair regenerative capacity in aging humans. *J. Appl. Physiol.* **2013**, *115*, 937–948. [[CrossRef](#)]
48. Fan, J.; Kou, X.; Yang, Y.; Chen, N. MicroRNA-Regulated Proinflammatory Cytokines in Sarcopenia. *Mediat. Inflamm.* **2016**, *2016*, 1438686. [[CrossRef](#)]
49. Pedrinolla, A.; Colosio, A.L.; Magliozzi, R.; Danese, E.; Kirmizi, E.; Rossi, S.; Pogliaghi, S.; Calabrese, M.; Gelati, M.; Muti, E.; et al. The Vascular Side of Chronic Bed Rest: When a Therapeutic Approach Becomes Deleterious. *J. Clin. Med.* **2020**, *9*, 918. [[CrossRef](#)]
50. Yin, J.; Qian, Z.; Chen, Y.; Li, Y.; Zhou, X. MicroRNA regulatory networks in the pathogenesis of sarcopenia. *J. Cell Mol. Med.* **2020**, *24*, 4900–4912. [[CrossRef](#)] [[PubMed](#)]
51. Calvani, R.; Joseph, A.M.; Adhietty, P.J.; Miccheli, A.; Bossola, M.; Leeuwenburgh, C.; Bernabei, R.; Marzetti, E. Mitochondrial pathways in sarcopenia of aging and disuse muscle atrophy. *Biol. Chem.* **2013**, *394*, 393–414. [[CrossRef](#)] [[PubMed](#)]
52. Dungan, C.M.; Peck, B.D.; Walton, R.G.; Huang, Z.; Bamman, M.M.; Kern, P.A.; Peterson, C.A. In vivo analysis of γ H2AX+ cells in skeletal muscle from aged and obese humans. *FASEB J.* **2020**, *34*, 7018–7035. [[CrossRef](#)] [[PubMed](#)]
53. Van Rooij, E.; Quiat, D.; Johnson, B.A.; Sutherland, L.B.; Qi, X.; Richardson, J.A.; Kelm, R.J.; Olson, E.N., Jr. A family of microRNAs encoded by myosin genes governs myosin expression and muscle performance. *Dev. Cell* **2009**, *17*, 662–673. [[CrossRef](#)]

54. O'Rourke, J.R.; Georges, S.A.; Seay, H.R.; Tapscott, S.J.; McManus, M.T.; Goldhamer, D.J.; Swanson, M.S.; Harfe, B.D. Essential Role for Dicer during Skeletal Muscle Development. *Dev. Biol.* **2007**, *311*, 359–368. [[CrossRef](#)] [[PubMed](#)]
55. Vechetti, I.J.; Wen, Y., Jr.; Chaillou, T.; Murach, K.A.; Alimov, A.P.; Figueiredo, V.C.; Dal-Pai-Silva, M.; McCarthy, J.J. Life-long reduction in myomiR expression does not adversely affect skeletal muscle morphology. *Sci. Rep.* **2019**, *9*, 5483. [[CrossRef](#)]
56. Oikawa, S.; Lee, M.; Akimoto, T. Conditional Deletion of Dicer in Adult Mice Impairs Skeletal Muscle Regeneration. *Int. J. Mol. Sci.* **2019**, *20*, 5686. [[CrossRef](#)]
57. Kirby, T.J.; Chaillou, T.; McCarthy, J.J. The Role of MicroRNAs in Skeletal Muscle Health and Disease. *Front. Biosci.* **2015**, *20*, 37–77. [[CrossRef](#)]
58. Xu, M.; Chen, X.; Chen, D.; Yu, B.; Li, M.; He, J.; Huang, Z. Regulation of Skeletal Myogenesis by MicroRNAs. *J. Cell Physiol.* **2020**, *235*, 87–104. [[CrossRef](#)]
59. Cheung, T.H.; Quach, N.L.; Charville, G.W.; Liu, L.; Park, L.; Edalati, A.; Yoo, B.; Hoang, P.; Rando, T.A. Maintenance of Muscle Stem-Cell Quiescence by MicroRNA-489. *Nature* **2012**, *482*, 524–528. [[CrossRef](#)]
60. Fry, C.S.; Kirby, T.J.; Kosmac, K.; McCarthy, J.J.; Peterson, C.A. Myogenic Progenitor Cells Control Extracellular Matrix Production by Fibroblasts during Skeletal Muscle Hypertrophy. *Cell Stem Cell* **2017**, *20*, 56–69. [[CrossRef](#)]
61. Crist, C.G.; Montarras, D.; Buckingham, M. Muscle Satellite Cells Are Primed for Myogenesis but Maintain Quiescence with Sequestration of Myf5 mRNA Targeted by MicroRNA-31 in MRNP Granules. *Cell Stem Cell* **2012**, *11*, 118–126. [[CrossRef](#)]
62. Sato, T.; Yamamoto, T.; Sehara-Fujisawa, A. MiR-195/497 Induce Postnatal Quiescence of Skeletal Muscle Stem Cells. *Nat. Commun.* **2014**, *5*, 4597. [[CrossRef](#)] [[PubMed](#)]
63. Baghdadi, M.B.; Firmino, J.; Soni, K.; Evano, B.; Di Girolamo, D.; Mourikis, P.; Castel, D.; Tajbakhsh, S. Notch-Induced MiR-708 Antagonizes Satellite Cell Migration and Maintains Quiescence. *Cell Stem Cell* **2018**, *23*, 859–868.e5. [[CrossRef](#)] [[PubMed](#)]
64. Crist, C.G.; Montarras, D.; Pallafacchina, G.; Rocancourt, D.; Cumanò, A.; Conway, S.J.; Buckingham, M. Muscle Stem Cell Behavior Is Modified by MicroRNA-27 Regulation of Pax3 Expression. *Proc. Natl. Acad. Sci. USA* **2009**, *106*, 13383–13387. [[CrossRef](#)] [[PubMed](#)]
65. Chen, J.F.; Tao, Y.; Li, J.; Deng, Z.; Yan, Z.; Xiao, X.; Wang, D.Z. MicroRNA-1 and MicroRNA-206 Regulate Skeletal Muscle Satellite Cell Proliferation and Differentiation by Repressing Pax7. *J. Cell Biol.* **2010**, *190*, 867–879. [[CrossRef](#)]
66. Hirai, H.; Verma, M.; Watanabe, S.; Tastad, C.; Asakura, Y.; Asakura, A. MyoD Regulates Apoptosis of Myoblasts through MicroRNA-Mediated down-Regulation of Pax3. *J. Cell Biol.* **2010**, *191*, 347–365. [[CrossRef](#)]
67. Dey, B.K.; Gagan, J.; Dutta, A. MiR-206 and -486 Induce Myoblast Differentiation by Downregulating Pax7. *Mol. Cell Biol.* **2011**, *31*, 203–214. [[CrossRef](#)]
68. Goljanek-Whysall, K.; Sweetman, D.; Abu-Elmagd, M.; Chapnik, E.; Dalmay, T.; Hornstein, E.; Münsterberg, A. MicroRNA Regulation of the Paired-Box Transcription Factor Pax3 Confers Robustness to Developmental Timing of Myogenesis. *Proc. Natl. Acad. Sci. USA* **2011**, *108*, 11936–11941. [[CrossRef](#)]
69. Cui, S.; Li, L.; Mubarakah, S.N.; Meech, R. Wnt/ β -Catenin Signaling Induces the MyomiRs MiR-133b and MiR-206 to Suppress Pax7 and Induce the Myogenic Differentiation Program. *J. Cell Biochem.* **2019**, *120*, 12740–12751. [[CrossRef](#)]
70. Jiang, A.; Dong, C.; Li, B.; Zhang, Z.; Chen, Y.; Ning, C.; Wu, W.; Liu, H. MicroRNA-206 Regulates Cell Proliferation by Targeting G6PD in Skeletal Muscle. *FASEB J.* **2019**, *33*, 14083–14094. [[CrossRef](#)]
71. Chen, J.F.; Mandel, E.M.; Thomson, J.M.; Wu, Q.; Callis, T.E.; Hammond, S.M.; Conlon, F.L.; Wang, D.Z. The Role of MicroRNA-1 and MicroRNA-133 in Skeletal Muscle Proliferation and Differentiation. *Nat. Genet.* **2006**, *38*, 228–233. [[CrossRef](#)] [[PubMed](#)]
72. Zhang, D.; Li, X.; Chen, C.; Li, Y.; Zhao, L.; Jing, Y.; Liu, W.; Wang, X.; Zhang, Y.; Xia, H.; et al. Attenuation of P38-Mediated MiR-1/133 Expression Facilitates Myoblast Proliferation during the Early Stage of Muscle Regeneration. *PLoS ONE* **2012**, *7*, e41478. [[CrossRef](#)] [[PubMed](#)]
73. Feng, Y.; Niu, L.L.; Wei, W.; Zhang, W.Y.; Li, X.Y.; Cao, J.H.; Zhao, S.H. A Feedback Circuit between MiR-133 and the ERK1/2 Pathway Involving an Exquisite Mechanism for Regulating Myoblast Proliferation and Differentiation. *Cell Death Dis.* **2013**, *4*, e934. [[CrossRef](#)] [[PubMed](#)]

74. Wong, C.F.; Tellam, R.L. MicroRNA-26a Targets the Histone Methyltransferase Enhancer of Zeste Homolog 2 during Myogenesis. *J. Biol. Chem.* **2008**, *283*, 9836–9843. [[CrossRef](#)] [[PubMed](#)]
75. Juan, A.H.; Kumar, R.M.; Marx, J.G.; Young, R.A.; Sartorelli, V. Mir-214-Dependent Regulation of the Polycomb Protein Ezh2 in Skeletal Muscle and Embryonic Stem Cells. *Mol. Cell* **2009**, *36*, 61–74. [[CrossRef](#)]
76. Dey, B.K.; Gagan, J.; Yan, Z.; Dutta, A. MiR-26a Is Required for Skeletal Muscle Differentiation and Regeneration in Mice. *Genes. Dev.* **2012**, *26*, 2180–2191. [[CrossRef](#)]
77. Dey, B.K.; Pfeifer, K.; Dutta, A. The H19 Long Noncoding RNA Gives Rise to MicroRNAs MiR-675-3p and MiR-675-5p to Promote Skeletal Muscle Differentiation and Regeneration. *Genes. Dev.* **2014**, *28*, 491–501. [[CrossRef](#)]
78. Wang, H.; Garzon, R.; Sun, H.; Ladner, K.J.; Singh, R.; Dahlman, J.; Cheng, A.; Hall, B.M.; Qualman, S.J.; Chandler, D.S.; et al. NF-KB-YY1-MiR-29 Regulatory Circuitry in Skeletal Myogenesis and Rhabdomyosarcoma. *Cancer Cell* **2008**, *14*, 369–381. [[CrossRef](#)] [[PubMed](#)]
79. Zhou, L.; Wang, L.; Lu, L.; Jiang, P.; Sun, H.; Wang, H. A Novel Target of MicroRNA-29, Ring1 and YY1-Binding Protein (Rybp), Negatively Regulates Skeletal Myogenesis. *J. Biol. Chem.* **2012**, *287*, 25255–25265. [[CrossRef](#)] [[PubMed](#)]
80. Sarkar, S.; Dey, B.K.; Dutta, A. MiR-322/424 and -503 Are Induced during Muscle Differentiation and Promote Cell Cycle Quiescence and Differentiation by down-Regulation of Cdc25A. *Mol. Biol. Cell* **2010**, *21*, 2138–2149. [[CrossRef](#)]
81. Kong, D.; He, M.; Yang, L.; Zhou, R.; Yan, Y.Q.; Liang, Y.; Teng, C.B. MiR-17 and MiR-19 Cooperatively Promote Skeletal Muscle Cell Differentiation. *Cell Mol. Life Sci.* **2019**, *76*, 5041–5054. [[CrossRef](#)]
82. Hou, L.; Xu, J.; Jiao, Y.; Li, H.; Pan, Z.; Duan, J.; Gu, T.; Hu, C.; Wang, C. MiR-27b Promotes Muscle Development by Inhibiting MDFI Expression. *Cell Physiol. Biochem.* **2018**, *46*, 2271–2283. [[CrossRef](#)] [[PubMed](#)]
83. Hou, L.; Zhu, L.; Li, H.; Jiang, F.; Cao, L.; Hu, C.Y.; Wang, C. MiR-501-3p Forms a Feedback Loop with FOS, MDFI, and MyoD to Regulate C2C12 Myogenesis. *Cells* **2019**, *8*, 573. [[CrossRef](#)] [[PubMed](#)]
84. Qadir, A.S.; Woo, K.M.; Ryoo, H.M.; Yi, T.; Song, S.U.; Baek, J.H. MiR-124 Inhibits Myogenic Differentiation of Mesenchymal Stem Cells via Targeting Dlx5. *J. Cell Biochem.* **2014**, *115*, 1572–1581. [[CrossRef](#)] [[PubMed](#)]
85. Tan, S.B.; Li, J.; Chen, X.; Zhang, W.; Zhang, D.; Zhang, C.; Li, D.; Zhang, Y. Small Molecule Inhibitor of Myogenic MicroRNAs Leads to a Discovery of MiR-221/222-MyoD-MyomiRs Regulatory Pathway. *Chem. Biol.* **2014**, *21*, 1265–1270. [[CrossRef](#)] [[PubMed](#)]
86. Seok, H.Y.; Tatsuguchi, M.; Callis, T.E.; He, A.; Pu, W.T.; Wang, D.Z. MiR-155 Inhibits Expression of the MEF2A Protein to Repress Skeletal Muscle Differentiation. *J. Biol. Chem.* **2011**, *286*, 35339–35346. [[CrossRef](#)] [[PubMed](#)]
87. Wu, J.; Yue, B.; Lan, X.; Wang, Y.; Fang, X.; Ma, Y.; Bai, Y.; Qi, X.; Zhang, C.; Chen, H. MiR-499 Regulates Myoblast Proliferation and Differentiation by Targeting Transforming Growth Factor β Receptor 1. *J. Cell Physiol.* **2019**, *234*, 2523–2536. [[CrossRef](#)] [[PubMed](#)]
88. Yang, Z.; Song, C.; Jiang, R.; Huang, Y.; Lan, X.; Lei, C.; Chen, H. Micro-Ribonucleic Acid-216a Regulates Bovine Primary Muscle Cells Proliferation and Differentiation via Targeting SMAD Nuclear Interacting Protein-1 and Smad7. *Front. Genet.* **2019**, *10*, 1112. [[CrossRef](#)] [[PubMed](#)]
89. Du, J.; Zhang, Y.; Shen, L.; Luo, J.; Lei, H.; Zhang, P.; Pu, Q.; Liu, Y.; Shuai, S.; Li, Q.; et al. Effect of MIR-143-3p on C2C12 Myoblast Differentiation. *Biosci. Biotechnol. Biochem.* **2016**, *80*, 706–711. [[CrossRef](#)]
90. Cai, R.; Qimuge, N.; Ma, M.; Wang, Y.; Tang, G.; Zhang, Q.; Sun, Y.; Chen, X.; Yu, T.; Dong, W.; et al. MicroRNA-664-5p Promotes Myoblast Proliferation and Inhibits Myoblast Differentiation by Targeting Serum Response Factor and Wnt1. *J. Biol. Chem.* **2018**, *293*, 19177–19190. [[CrossRef](#)]
91. Choi, J.S.; Yoon, H.I.; Lee, K.S.; Choi, Y.C.; Yang, S.H.; Kim, I.S.; Cho, Y.W. Exosomes from differentiating human skeletal muscle cells trigger myogenesis of stem cells and provide biochemical cues for skeletal musculer regeneration. *J. Control Release* **2016**, *222*, 107–115. [[CrossRef](#)] [[PubMed](#)]
92. Bittel, D.C.; Jaiswal, J.K. Contribution of Extracellular Vesicles in Rebuilding Injured Muscles. *Front. Physiol.* **2019**, *10*, 828. [[CrossRef](#)] [[PubMed](#)]
93. Murach, K.A.; Vechetti, I.J.; Van Pelt, D.W., Jr.; Crow, S.E.; Dungan, C.M.; Figueiredo, V.C.; Kosmac, K.; Fu, X.; Richards, C.I.; Fry, C.S.; et al. Fusion-Independent Satellite Cell Communication to Muscle Fibers During Load-Induced Hypertrophy. *Function* **2020**, *1*, zqaa009. [[CrossRef](#)] [[PubMed](#)]

94. Drummond, M.J.; McCarthy, J.J.; Fry, C.S.; Esser, K.A.; Rasmussen, B.B. Aging Differentially Affects Human Skeletal Muscle MicroRNA Expression at Rest and after an Anabolic Stimulus of Resistance Exercise and Essential Amino Acids. *Am. J. Physiol. Endocrinol. Metab.* **2008**, *295*, E1333–E1340. [[CrossRef](#)]
95. Hamrick, M.W.; Herberg, S.; Arounleut, P.; He, H.Z.; Shiver, A.; Qi, R.Q.; Zhou, L.; Isales, C.M.; Mi, Q.S. The Adipokine Leptin Increases Skeletal Muscle Mass and Significantly Alters Skeletal Muscle MiRNA Expression Profile in Aged Mice. *Biochem. Biophys. Res. Commun.* **2010**, *400*, 379–383. [[CrossRef](#)]
96. Mercken, E.M.; Majounie, E.; Ding, J.; Guo, R.; Kim, J.; Bernier, M.; Mattison, J.; Cookson, M.R.; Gorospe, M.; de Cabo, R.; et al. Age-Associated MiRNA Alterations in Skeletal Muscle from Rhesus Monkeys Reversed by Caloric Restriction. *Aging* **2013**, *5*, 692–703. [[CrossRef](#)]
97. Drummond, M.J.; McCarthy, J.J.; Sinha, M.; Spratt, H.M.; Volpi, E.; Esser, K.A.; Rasmussen, B.B. Aging and MicroRNA Expression in Human Skeletal Muscle: A Microarray and Bioinformatics Analysis. *Physiol. Genom.* **2011**, *43*, 595–603. [[CrossRef](#)]
98. Naguibneva, I.; Ameyar-Zazoua, M.; Polesskaya, A.; Ait-Si-Ali, S.; Groisman, R.; Souidi, M.; Cuvellier, S.; Harel-Bellan, A. The MicroRNA MiR-181 Targets the Homeobox Protein Hox-A11 during Mammalian Myoblast Differentiation. *Nat. Cell Biol.* **2006**, *8*, 278–284. [[CrossRef](#)]
99. Xie, W.; Li, M.; Xu, N.; Lv, Q.; Huang, N.; He, J.; Zhang, Y. MiR-181a Regulates Inflammation Responses in Monocytes and Macrophages. *PLoS ONE* **2013**, *8*, e58639. [[CrossRef](#)]
100. Soriano-Arroquia, A.; House, L.; Tregilgas, L.; Canty-Laird, E.; Goljanek-Whysall, K. The Functional Consequences of Age-Related Changes in MicroRNA Expression in Skeletal Muscle. *Biogerontology* **2016**, *17*, 641–654. [[CrossRef](#)]
101. Lee, S.H.; Lee, J.H.; Lee, H.Y.; Min, K.J. Sirtuin Signaling in Cellular Senescence and Aging. *BMB Rep.* **2019**, *52*, 24–34. [[CrossRef](#)] [[PubMed](#)]
102. Lapiere, L.R.; Kumsta, C.; Sandri, M.; Ballabio, A.; Hansen, M. Transcriptional and epigenetic regulation of autophagy in aging. *Autophagy* **2015**, *11*, 867–880. [[CrossRef](#)] [[PubMed](#)]
103. Carnio, S.; LoVerso, F.; Baraibar, M.A.; Longa, E.; Khan, M.M.; Maffei, M.; Reischl, M.; Canepari, M.; Loeffler, S.; Kern, H.; et al. Autophagy impairment in muscle induces neuromuscular junction degeneration and precocious aging. *Cell Rep.* **2014**, *8*, 1509–1521. [[CrossRef](#)]
104. García-Prat, L.; Martínez-Vicente, M.; Perdiguero, E.; Ortet, L.; Rodríguez-Ubreva, J.; Rebollo, E.; Ruiz-Bonilla, V.; Gutarra, S.; Ballestar, E.; Serrano, A.L.; et al. Autophagy maintains stemness by preventing senescence. *Nature* **2016**, *529*, 37–42. [[CrossRef](#)] [[PubMed](#)]
105. Masiero, E.; Sandri, M. Autophagy inhibition induces atrophy and myopathy in adult skeletal muscles. *Autophagy* **2010**, *6*, 307–309. [[CrossRef](#)] [[PubMed](#)]
106. Kondo, H.; Kim, H.W.; Wang, L.; Okada, M.; Paul, C.; Millard, R.W.; Wang, Y. Blockade of Senescence-Associated MicroRNA-195 in Aged Skeletal Muscle Cells Facilitates Reprogramming to Produce Induced Pluripotent Stem Cells. *Aging Cell* **2016**, *15*, 56–66. [[CrossRef](#)]
107. Hu, Z.; Klein, J.D.; Mitch, W.E.; Zhang, L.; Martinez, I.; Wang, X.H. MicroRNA-29 Induces Cellular Senescence in Aging Muscle through Multiple Signaling Pathways. *Aging* **2014**, *6*, 160–175. [[CrossRef](#)]
108. Soriano-Arroquia, A.; McCormick, R.; Molloy, A.P.; McArdle, A.; Goljanek-Whysall, K. Age-Related Changes in MiR-143-3p: Igfbp5 Interactions Affect Muscle Regeneration. *Aging Cell* **2016**, *15*, 361–369. [[CrossRef](#)]
109. Onodera, Y.; Teramura, T.; Takehara, T.; Itokazu, M.; Mori, T.; Fukuda, K. Inflammation-Associated MIR-155 Activates Differentiation of Muscular Satellite Cells. *PLoS ONE* **2018**, *13*, e020486. [[CrossRef](#)]
110. Lee, K.P.; Shin, Y.J.; Kwon, K.S. MicroRNA for Determining the Age-Related Myogenic Capabilities of Skeletal Muscle. *BMB Rep.* **2015**, *48*, 595–596. [[CrossRef](#)]
111. Pardo, P.S.; Hajira, A.; Boriek, A.M.; Mohamed, J.S. MicroRNA-434-3p Regulates Age-Related Apoptosis through EIF5A1 in the Skeletal Muscle. *Aging* **2017**, *9*, 1012–1029. [[CrossRef](#)] [[PubMed](#)]
112. Connolly, M.; Paul, R.; Farre-Garros, R.; Natanek, S.A.; Bloch, S.; Lee, J.; Lorenzo, J.P.; Patel, H.; Cooper, C.; Sayer, A.A.; et al. MiR-424-5p Reduces Ribosomal RNA and Protein Synthesis in Muscle Wasting. *J. Cachexia Sarcopenia Muscle* **2018**, *9*, 400–416. [[CrossRef](#)]
113. Yanai, K.; Kaneko, S.; Ishii, H.; Aomatsu, A.; Ito, K.; Hirai, K.; Ookawara, S.; Ishibashi, K.; Morishita, Y. MicroRNAs in Sarcopenia: A Systematic Review. *Front. Med.* **2020**, *7*, 180. [[CrossRef](#)] [[PubMed](#)]
114. Guillet, C.; Prod'homme, M.; Balage, M.; Gachon, P.; Giraudet, C.; Morin, L.; Grizard, J.; Boirie, Y. Impaired Anabolic Response of Muscle Protein Synthesis Is Associated with S6K1 Dysregulation in Elderly Humans. *FASEB J.* **2004**, *18*, 1586–1587. [[CrossRef](#)]

115. Venturelli, M.; Morgan, G.R.; Donato, A.J.; Reese, V.; Bottura, R.; Tarperi, C.; Milanese, C.; Schena, F.; Reggiani, C.; Naro, F.; et al. Cellular aging of skeletal muscle: Telomeric and free radical evidence that physical inactivity is responsible and not age. *Clin. Sci.* **2014**, *127*, 415–421. [[CrossRef](#)]
116. Kumar, V.; Selby, A.; Rankin, D.; Patel, R.; Atherton, P.; Hildebrandt, W.; Williams, J.; Smith, K.; Seynnes, O.; Hiscock, N.; et al. Age-Related Differences in the Dose-Response Relationship of Muscle Protein Synthesis to Resistance Exercise in Young and Old Men. *J. Physiol.* **2009**, *587*, 211–217. [[CrossRef](#)] [[PubMed](#)]
117. Iannuzzi-Sucich, M.; Prestwood, K.M.; Kenny, A.M. Prevalence of sarcopenia and predictors of skeletal muscle mass in healthy, older men and women. *J. Gerontol. A Biol. Sci. Med. Sci.* **2002**, *57*, M772–M777. [[CrossRef](#)]
118. Marzetti, E.; Calvani, R.; Cesari, M.; Buford, T.W.; Lorenzi, M.; Behnke, B.J.; Leeuwenburgh, C. Mitochondrial dysfunction and sarcopenia of aging: From signaling pathways to clinical trials. *Int. J. Biochem. Cell Biol.* **2013**, *45*, 2288–2301. [[CrossRef](#)]
119. Prior, S.J.; Ryan, A.S.; Blumenthal, J.B.; Watson, J.M.; Katznel, L.I.; Goldberg, A.P. Sarcopenia Is Associated With Lower Skeletal Muscle Capillarization and Exercise Capacity in Older Adults. *J. Gerontol. A Biol. Sci. Med. Sci.* **2016**, *71*, 1096–1101. [[CrossRef](#)]
120. Beyer, I.; Mets, T.; Ivan Bautmans, I. Chronic low-grade inflammation and age-related sarcopenia. *Curr. Opin. Clin. Nutr. Metab. Care* **2012**, *5*, 12–22. [[CrossRef](#)]
121. Layec, G.; Trinity, J.D.; Hart, C.R.; Le Fur, Y.; Zhao, J.; Reese, V.; Jeong, E.K.; Richardson, R.S. Impaired Muscle Efficiency but Preserved Peripheral Hemodynamics and Mitochondrial Function With Advancing Age: Evidence From Exercise in the Young, Old, and Oldest-Old. *J. Gerontol. A Biol. Sci. Med. Sci.* **2018**, *73*, 1303–1312. [[CrossRef](#)] [[PubMed](#)]
122. Gopinath, B.; Kifley, A.; Flood, V.M.; Mitchell, P. Physical Activity as a Determinant of Successful Aging over Ten Years. *Sci. Rep.* **2018**, *8*, 10522. [[CrossRef](#)] [[PubMed](#)]
123. Bickel, C.S.; Cross, J.M.; Bamman, M.M. Exercise dosing to retain resistance training adaptations in young and older adults. *Med. Sci. Sports Exerc.* **2011**, *43*, 1177–1187. [[CrossRef](#)] [[PubMed](#)]
124. Stec, M.J.; Thalacker-Mercer, A.; Mayhew, D.L.; Kelly, N.A.; Tuggle, S.C.; Merritt, E.K.; Brown, C.J.; Windham, S.T.; Dell'Italia, L.J.; Bickel, C.S.; et al. Randomized, four-arm, dose-response clinical trial to optimize resistance exercise training for older adults with age-related muscle atrophy. *Exp. Gerontol.* **2017**, *99*, 98–109. [[CrossRef](#)]
125. Groennebaek, T.; Vissing, K. Impact of Resistance Training on Skeletal Muscle Mitochondrial Biogenesis, Content, and Function. *Front. Physiol.* **2017**, *8*, 713. [[CrossRef](#)]
126. Adelnia, F.; Cameron, D.; Bergeron, C.M.; Fishbein, K.W.; Spencer, R.G.; Reiter, D.A.; Ferrucci, L. The Role of Muscle Perfusion in the Age-Associated Decline of Mitochondrial Function in Healthy Individuals. *Front. Physiol.* **2019**, *10*, 427. [[CrossRef](#)]
127. Petriz, B.A.; Gomes, C.P.; Almeida, J.A.; de Oliveira, G.P.; Ribeiro, F.M., Jr.; Pereira, R.W.; Franco, O.L. The Effects of Acute and Chronic Exercise on Skeletal Muscle Proteome. *J. Cell Physiol.* **2017**, *232*, 257–269. [[CrossRef](#)]
128. Danese, E.; Benati, M.; Sanchis-Gomar, F.; Tarperi, C.; Salvagno, G.L.; Paviati, E.; Montagnana, M.; Schena, F.; Lippi, G. Influence of Middle-Distance Running on Muscular Micro RNAs. *Scand. J. Clin. Lab. Investig.* **2018**, *78*, 165–170. [[CrossRef](#)]
129. Ultimo, S.; Zauli, G.; Martelli, A.M.; Vitale, M.; McCubrey, J.A.; Capitani, S.; Neri, L.M. Influence of Physical Exercise on MicroRNAs in Skeletal Muscle Regeneration, Aging and Diseases. *Oncotarget* **2018**, *9*, 17220–17237. [[CrossRef](#)]
130. Montero, D.; Lundby, C. Refuting the myth of non-response to exercise training: ‘non-responders’ do respond to higher dose of training. *J. Physiol.* **2017**, *595*, 3377–3387. [[CrossRef](#)]
131. Keller, P.; Vollaard, N.B.; Gustafsson, T.; Gallagher, I.J.; Sundberg, C.J.; Rankinen, T.; Britton, S.L.; Bouchard, C.; Koch, L.G.; Timmons, J.A. A transcriptional map of the impact of endurance exercise training on skeletal muscle phenotype. *J. Appl. Physiol.* **2011**, *110*, 46–59. [[CrossRef](#)]
132. Nielsen, S.; Scheele, C.; Yfanti, C.; Akerström, T.; Nielsen, A.R.; Pedersen, B.K.; Laye, M.J. Muscle specific microRNAs are regulated by endurance exercise in human skeletal muscle. *J. Physiol.* **2010**, *588*, 4029–4037. [[CrossRef](#)]

133. Russell, A.P.; Lamon, S.; Boon, H.; Wada, S.; Güller, I.; Brown, E.L.; Chibalin, A.V.; Zierath, J.R.; Snow, R.J.; Stepto, N.; et al. Regulation of miRNAs in human skeletal muscle following acute endurance exercise and short-term endurance training. *J. Physiol.* **2013**, *591*, 4637–4653. [[CrossRef](#)]
134. Margolis, L.M.; McClung, H.L.; Murphy, N.E.; Carrigan, C.T.; Pasiakos, S.M. Skeletal Muscle myomiR Are Differentially Expressed by Endurance Exercise Mode and Combined Essential Amino Acid and Carbohydrate Supplementation. *Front. Physiol.* **2017**, *8*, 182. [[CrossRef](#)] [[PubMed](#)]
135. Rivas, D.A.; Lessard, S.J.; Rice, N.P.; Lustgarten, M.S.; So, K.; Goodyear, L.J.; Parnell, L.D.; Fielding, R.A. Diminished Skeletal Muscle MicroRNA Expression with Aging Is Associated with Attenuated Muscle Plasticity and Inhibition of IGF-1 Signaling. *FASEB J.* **2014**, *28*, 4133–4147. [[CrossRef](#)] [[PubMed](#)]
136. Zacharewicz, E.; Della Gatta, P.; Reynolds, J.; Garnham, A.; Crowley, T.; Russell, A.P.; Lamon, S. Identification of MicroRNAs Linked to Regulators of Muscle Protein Synthesis and Regeneration in Young and Old Skeletal Muscle. *PLoS ONE* **2014**, *9*, e114009. [[CrossRef](#)] [[PubMed](#)]
137. Elia, L.; Contu, R.; Quintavalle, M.; Varrone, F.; Chimenti, C.; Russo, M.A.; Cimino, V.; De Marinis, L.; Frustaci, A.; Catalucci, D.; et al. Reciprocal Regulation of MicroRNA-1 and Insulin-like Growth Factor-1 Signal Transduction Cascade in Cardiac and Skeletal Muscle in Physiological and Pathological Conditions. *Circulation* **2009**, *120*, 2377–2385. [[CrossRef](#)]
138. McLean, C.S.; Mielke, C.; Cordova, J.M.; Langlais, P.R.; Bowen, B.; Miranda, D.; Coletta, D.K.; Mandarino, L.J. Gene and MicroRNA Expression Responses to Exercise; Relationship with Insulin Sensitivity. *PLoS ONE* **2015**, *10*, e0127089. [[CrossRef](#)]
139. Lin, J.; Wu, P.H.; Tarr, P.T.; Lindenberg, K.S.; St-Pierre, J.; Zhang, C.Y.; Mootha, V.K.; Jäger, S.; Vianna, C.R.; Reznick, R.M.; et al. Defects in Adaptive Energy Metabolism with CNS-Linked Hyperactivity in PGC-1alpha Null Mice. *Cell* **2004**, *119*, 121–135. [[CrossRef](#)]
140. Carrer, M.; Liu, N.; Grueter, C.E.; Williams, A.H.; Frisard, M.I.; Hulver, M.W.; Bassel-Duby, R.; Olson, E.N. Control of Mitochondrial Metabolism and Systemic Energy Homeostasis by MicroRNAs 378 and 378. *Proc. Natl. Acad. Sci. USA* **2012**, *109*, 15330–15335. [[CrossRef](#)] [[PubMed](#)]
141. Fyfe, J.J.; Bishop, D.J.; Zacharewicz, E.; Russell, A.P.; Stepto, N.K. Concurrent Exercise Incorporating High-Intensity Interval or Continuous Training Modulates mTORC1 Signaling and MicroRNA Expression in Human Skeletal Muscle. *Am. J. Physiol. Regul. Integr. Comp. Physiol.* **2016**, *310*, R1297–R1311. [[CrossRef](#)] [[PubMed](#)]
142. Zhang, T.; Birbrair, A.; Wang, Z.M.; Messi, M.L.; Marsh, A.P.; Leng, I.; Nicklas, B.J.; Delbono, O. Improved Knee Extensor Strength with Resistance Training Associates with Muscle Specific miRNAs in Older Adults. *Exp. Gerontol.* **2015**, *62*, 7–13. [[CrossRef](#)] [[PubMed](#)]
143. Davidsen, P.K.; Gallagher, I.J.; Hartman, J.W.; Tarnopolsky, M.A.; Dela, F.; Helge, J.W.; Timmons, J.A.; Phillips, S.M. High responders to resistance exercise training demonstrate differential regulation of skeletal muscle microRNA expression. *J. Appl. Physiol.* **2011**, *110*, 309–317. [[CrossRef](#)] [[PubMed](#)]
144. Weber, J.A.; Baxter, D.H.; Zhang, S.; Huang, D.Y.; Huang, K.H.; Lee, M.J.; Galas, D.J.; Wang, K. The MicroRNA Spectrum in 12 Body Fluids. *Clin. Chem.* **2010**, *56*, 1733–1741. [[CrossRef](#)] [[PubMed](#)]
145. Bär, C.; Thum, T.; de Gonzalo-Calvo, D. Circulating miRNAs as Mediators in Cell-to-Cell Communication. *Epigenomics* **2019**, *11*, 111–113. [[CrossRef](#)]
146. Li, J.; Jiang, X.; Wang, K. Exosomal miRNA: An alternative mediator of cell-to-cell communication. *ExRNA* **2019**, *1*, 1–6. [[CrossRef](#)]
147. Margolis, L.M.; Rivas, D.A. Potential Role of MicroRNA in the Anabolic Capacity of Skeletal Muscle with Aging. *Exerc. Sport Sci. Rev.* **2018**, *46*, 86–91. [[CrossRef](#)]
148. Calvani, R.; Marini, F.; Cesari, M.; Tosato, M.; Anker, S.D.; von Haehling, S.; Miller, R.R.; Bernabei, R.; Landi, F.; Marzetti, E. SPRINTT consortium. Biomarkers for Physical Frailty and Sarcopenia: State of the Science and Future Developments. *J. Cachexia Sarcopenia Muscle* **2015**, *6*, 278–286. [[CrossRef](#)]
149. Landi, F.; Calvani, R.; Cesari, M.; Tosato, M.; Martone, A.M.; Bernabei, R.; Onder, G.; Marzetti, E. Sarcopenia as the Biological Substrate of Physical Frailty. *Clin. Geriatr. Med.* **2015**, *31*, 367–374. [[CrossRef](#)]
150. Rusanova, I.; Fernández-Martínez, J.; Fernández-Ortiz, M.; Aranda-Martínez, P.; Escames, G.; García-García, F.J.; Mañas, L.; Acuña-Castroviejo, D. Involvement of Plasma miRNAs, Muscle miRNAs and Mitochondrial miRNAs in the Pathophysiology of Frailty. *Exp. Gerontol.* **2019**, *124*, 110637. [[CrossRef](#)]
151. Mantovani, E.; Zucchella, C.; Schena, F.; Romanelli, M.G.; Venturelli, M.; Tamburin, S. Towards a Redefinition of Cognitive Frailty. *J. Alzheimers Dis.* **2020**. [[CrossRef](#)] [[PubMed](#)]

152. Rusanova, I.; Diaz-Casado, M.E.; Fernández-Ortiz, M.; Aranda-Martínez, P.; Guerra-Librero, A.; García-García, F.J.; Escames, G.; Mañas, L.; Acuña-Castroviejo, D. Analysis of Plasma MicroRNAs as Predictors and Biomarkers of Aging and Frailty in Humans. *Oxid. Med. Cell Longev.* **2018**, *2018*, 7671850. [[CrossRef](#)] [[PubMed](#)]
153. Ipson, B.R.; Fletcher, M.B.; Espinoza, S.E.; Fisher, A.L. Identifying Exosome-Derived MicroRNAs as Candidate Biomarkers of Frailty. *J. Frailty Aging* **2018**, *7*, 100–103. [[CrossRef](#)]
154. Sapp, R.M.; Shill, D.D.; Roth, S.M.; Hagberg, J.M. Circulating MicroRNAs in Acute and Chronic Exercise: More than Mere Biomarkers. *J. Appl. Physiol.* **2017**, *122*, 702–717. [[CrossRef](#)] [[PubMed](#)]
155. Margolis, L.M.; Lessard, S.J.; Ezzyat, Y.; Fielding, R.A.; Rivas, D.A. Circulating MicroRNA Are Predictive of Aging and Acute Adaptive Response to Resistance Exercise in Men. *J. Gerontol. A Biol. Sci. Med. Sci.* **2017**, *72*, 1319–1326. [[CrossRef](#)] [[PubMed](#)]
156. Margolis, L.M.; Rivas, D.A.; Pasiakos, S.M.; McClung, J.P.; Ceglia, L.; Fielding, R.A. Upregulation of Circulating MyomiR Following Short-Term Energy Restriction Is Inversely Associated with Whole Body Protein Synthesis. *Am. J. Physiol. Regul. Integr. Comp. Physiol.* **2017**, *313*, R298–R304. [[CrossRef](#)]
157. Baggish, A.L.; Park, J.; Min, P.K.; Isaacs, S.; Parker, B.A.; Thompson, P.D.; Troyanos, C.; D’Hemecourt, P.; Dyer, S.; Thiel, M.; et al. Rapid Upregulation and Clearance of Distinct Circulating MicroRNAs after Prolonged Aerobic Exercise. *J. Appl. Physiol.* **2014**, *116*, 522–531. [[CrossRef](#)] [[PubMed](#)]
158. Uhlemann, M.; Möbius-Winkler, S.; Fikenzer, S.; Adam, J.; Redlich, M.; Möhlenkamp, S.; Hilberg, T.; Schuler, G.C.; Adams, V. Circulating MicroRNA-126 Increases after Different Forms of Endurance Exercise in Healthy Adults. *Eur. J. Prev. Cardiol.* **2014**, *21*, 484–491. [[CrossRef](#)] [[PubMed](#)]
159. Parr, E.B.; Camera, D.M.; Burke, L.M.; Phillips, S.M.; Coffey, V.G.; Hawley, J.A. Circulating MicroRNA Responses between ‘High’ and ‘Low’ Responders to a 16-Wk Diet and Exercise Weight Loss Intervention. *PLoS ONE* **2016**, *11*, e0152545. [[CrossRef](#)] [[PubMed](#)]
160. Nair, V.D.; Ge, Y.; Li, S.; Pincas, H.; Jain, N.; Seenarine, N.; Amper, M.; Goodpaster, B.H.; Walsh, M.J.; Coen, P.M.; et al. Sedentary and Trained Older Men Have Distinct Circulating Exosomal MicroRNA Profiles at Baseline and in Response to Acute Exercise. *Front. Physiol.* **2020**, *11*, 605. [[CrossRef](#)]




© 2020 by the authors. Licensee MDPI, Basel, Switzerland. This article is an open access article distributed under the terms and conditions of the Creative Commons Attribution (CC BY) license (<http://creativecommons.org/licenses/by/4.0/>).

RESEARCH

Open Access



Effects of a 4400 km ultra-cycling non-competitive race and related training on body composition and circulating progenitors differentiation

Maria Teresa Valenti², Michele Braggio¹, Arianna Minoia¹, Gianluigi Dorelli¹, Jessica Bertacco¹, Francesco Bertoldo¹, Mattia Cominacini¹, Tonia De Simone², Maria Grazia Romanelli², Lekhana Bhandary³, Monica Mottes² and Luca Dalle Carbonare^{1*} 

Abstract

Background: NorthCape4000 (NC4000) is the most participated ultra-endurance cycling race. Eight healthy male Caucasian amateur cyclists were evaluated: (a) before starting the preparation period; (b) in the week preceding NC4000 (after the training period); (c) after NC4000 race, with the aim to identify the effects of ultra-cycling on body composition, aerobic capacity and biochemical parameters as well as on the differentiation of progenitor cells.

Methods: Bioelectrical impedance analysis (BIA) and dual energy x-ray absorptiometry (DEXA) assessed body composition; cardiopulmonary exercise test (CPET) evaluated aerobic capacity. Differentiation of circulating progenitor cells was evaluated by analyzing the modulation in the expression of relevant transcription factors. In addition, in vitro experiments were performed to investigate the effects of sera of NC4000 participants on adipogenesis and myogenesis. The effects of NC4000 sera on Sestrins and Sirtuin modulation and the promotion of brown adipogenesis in progenitor cells was investigated as well. Two-tailed Student's paired-test was used to perform statistical analyses.

Results: We observed fat mass decrease after training as well as after NC4000 performance; we also recorded that vitamin D and lipid profiles were affected by ultra-cycling. In addition, our findings demonstrated that post-NC4000 participant's pooled sera exerted a positive effect in stimulating myogenesis and in inducing brown adipogenesis in progenitor cells.

Conclusions: The training program and Ultra-cycling lead to beneficial effects on body composition and biochemical lipid parameters, as well as changes in differentiation of progenitor cells, with significant increases in brown adipogenesis and in MYOD levels.

Keywords: Ultra-cycling, Training, Progenitor cells, Transcription factors, Body composition, Fat mass, Aerobic capacity, Biochemical parameters

Background

In recent years, a trend towards greater participation and better performance times in ultra-endurance cycling has been recorded, despite the increasing average age of participants [1, 2].

*Correspondence: luca.dallecarbonare@univr.it

¹ Department of Medicine, Section of Internal Medicine, University of Verona, Piazzale Scuro, 10, Policlinico G.B. Rossi, 37134 Verona, Italy
Full list of author information is available at the end of the article



© The Author(s) 2022. **Open Access** This article is licensed under a Creative Commons Attribution 4.0 International License, which permits use, sharing, adaptation, distribution and reproduction in any medium or format, as long as you give appropriate credit to the original author(s) and the source, provide a link to the Creative Commons licence, and indicate if changes were made. The images or other third party material in this article are included in the article's Creative Commons licence, unless indicated otherwise in a credit line to the material. If material is not included in the article's Creative Commons licence and your intended use is not permitted by statutory regulation or exceeds the permitted use, you will need to obtain permission directly from the copyright holder. To view a copy of this licence, visit <http://creativecommons.org/licenses/by/4.0/>. The Creative Commons Public Domain Dedication waiver (<http://creativecommons.org/publicdomain/zero/1.0/>) applies to the data made available in this article, unless otherwise stated in a credit line to the data.

Ultra-cycling performances lead to important energy deficit, especially in master athletes, due to the physiological impossibility of maintaining a positive balance with caloric replenishment [3]. In fact, a prolonged energy deficit is the main mechanism involved in fat mass (FM) loss [4].

Discrepancies regarding weight loss and possible lean mass alterations in ultra-endurance emerge in the literature. FM and fat-free mass (FFM) were analyzed before the Swiss-cycling Marathon with the aim to characterize competitive ultra-cyclers [5]. Variations in these parameters were evaluated in races like XX Alps 2004, with decrease in both FM and FFM using skin-folds method [6]. The same results were observed using Dual-Energy X-ray Absorptiometry (DEXA) after an 8,835 km mountain bike race [7]. However, others highlighted an increase in lean mass after an 883 km 6-days cycling stage race [8]. Bioelectrical Impedance analysis (BIA) showed a reduction in FM and an increase in body mass and FFM after 1000 km laboratory-based nonstop cycling, probably due to liquid retention [9]. Total body water also increased after a 600 km ultra-cycling race, which lead to a reduction in FM but no decrease in skeletal muscle mass (MM) measured with skin-folds method [9].

Little is known whether FM and lean mass modifications persist after a short period of recovery and if these modifications are related to aerobic capacity (e.g. $VO_2\max$): in fact, some authors reported a $VO_2\max$ decrease [7] while others reported no significant changes [10].

Ultra-endurance might also lead to blood biochemical parameters alterations, including liver enzymes, creatinine, and lipid profile; anyhow in general, only case reports on ultra-cycling [7] and data on a small number of elite athletes [11] are available. On the other hand, few studies have reported that low vitamin D levels may be associated with musculoskeletal injuries, and that supplementation could improve performance [12], but to the best of our knowledge, nobody has evaluated possible vitamin D alterations in ultra-endurance cycling performance.

Despite the growing interest in amateur sports, few studies have been conducted in this field aiming at the evaluation of ultra-endurance exercise effects on health. In particular, changes in FM and LM and their possible association with markers of muscle and adipose cells metabolism following ultra-endurance races are not deeply understood. A comprehensive analysis on training parameters and aerobic capacity may help to clarify these modifications. Therefore, the aim of this study was to evaluate the effects of both preparation and competition of a 4400 km ultra-cycling adventure on body composition, aerobic capacity and biochemical parameters,

and their possible association with circulating progenitors commitment in order to evaluate the impact of such physical exercise in the prevention of degenerative diseases.

Awareness of the impact of such physical efforts may set amateur sportsmen towards a more mindful and personalized training.

Methods

The race

NorthCape4000 (NC4000) is the most participated ultra-endurance unsupported cycling adventure.

The 4th edition began July, 24th, 2021. It covered 4,400 km and an elevation gain of 40,000 m and consisted of an unsupported, non-drifting race, where participants arrived to North-Kapp (NRW), starting from Rovereto (ITA), passing through 4 mandatory checkpoints (Lake Balaton, Krakow, Riga, Rovaniemi). Organizers set a completion time limit of 22 days.

Monitored temperature fluctuations were between 32° and 7 °C.

Participants

Eight healthy male amateur Caucasian cyclists (47.5 ± 13.5 years) who attended the NC4000 4th edition were contacted via social media and underwent clinical evaluation, bioelectrical impedance analysis (BIA), cardiopulmonary exercise testing (CPET) and venipuncture for blood samples collection, before the preparation period (BPP), from 21st Dec 2020 to 2nd Mar 2021), the week before NC4000 (BN) and up to 10 days after NC4000 (AN). Dual energy x-ray absorptiometry (DEXA) was taken BN and AN. All data reported during NC4000 were assessed at the visit AN.

The study was approved by the ethical committee of Azienda Ospedaliera Universitaria Integrata of Verona, Italy (number 1538; Dec. 3, 2012; local ethical committee of Azienda Ospedaliera Integrata di Verona). The study design and methods comply with the Declaration of Helsinki.

Cyclists gave their voluntary written consent before the procedures.

Clinical evaluation and questionnaires

All subjects underwent clinical evaluation to exclude any condition that might have altered performance or laboratory tests results.

BPP and BN training was reported as the mean of number of sessions per week, total kilometers per week and hours per week in the previous 3 months.

Sleeping hours per night, coffee and alcohol intake (measured as standard drinks) were also reported.

Body composition measures

Total body dual-energy X-ray absorptiometry (DEXA) was taken BN and AN to measure total (FM) and segmental fat (truncal FM), visceral adipose tissue (VAT) and lean mass (LM) (QDR Discovery Acclaim; Hologic, Waltham, MA, USA). DEXA's body composition analysis were the same as previously described [13].

Tetra-polar dual frequency BIA (InBody 120; Cerritos, USA) was used BPP, BN and AN to measure weight and to estimate FM, FFM, and MM. Impedance measurements were performed after voiding, in the morning after at least 24 h of rest, with the athlete barefoot, standing in an upright position, in light cycling wear. Two measures were taken each time for each subject and the mean value was reported. Body height was measured to the nearest 0.5 cm while subjects stood barefoot.

Blood samples collection

Blood samples were collected in the morning BPP, BN, AN. Biochemical parameters considered in this study were: ALT, AST, creatinine, 25-hydroxy vitamin D (Liaison[®] Assay, DiaSorin, Italy), total cholesterol, HDL, LDL, triglycerides concentrations.

Circulating progenitor cells (CPCs)

We isolated CPCs from heparinized blood, as previously reported [14]. After the collection of peripheral blood mononuclear cells (PBMCs) by a gradient centrifugation ($800 \times g$ for 30 min at 20 °C), we removed the unwanted hematopoietic cells by using a RosetteSep antibody cocktail (Stemcell Technologies Inc., Vancouver, Canada), according to manufacturer's instructions. Collected cells were washed in phosphate-buffered saline (PBS) and phenotype analyses were performed as previously described [14].

In Vitro Myogenic Differentiation.

Human Skeletal muscle cells (SKMC) were obtained from PromoCells (C-12580; PromoCell, GMBH Heidelberg, Germany). SKMCs were cultured with Skeletal Muscle Cell Growth medium (Low serum) (C-23060PromoCell, GMBH Heidelberg, Germany) and differentiated by using Skeletal Muscle Differentiation Medium Supplements (C-23061; PromoCell, GMBH Heidelberg, Germany), as we previously reported [15]. Differentiating SKMCs were cultured with or without pooled sera of participants at 5% final concentration. The medium was changed every 3 days after initial plating.

RNAs extraction and reverse transcription

146b and 34a miRNAs were extracted from PBMCs by using miRNeasy kit (Qiagen, Hilden, Germany),

accordingly to manufacturer's instruction. Total RNA from CPCs or differentiating cells was extracted with the "RNeasy[®] protect mini kit" (Qiagen, Hilden, Germany), following the manufacturer's protocol and quantified by a Qubit[™] 3 fluorometer using a "Qubit[™] RNA HS assay kit (Invitrogen, Carlsbad, USA). Two micrograms of the extracted RNAs were reverse transcribed by using the TaqMan microRNA Reverse Transcription kit (ThermoFisher Corporation, Waltham, MA, USA) or the First Strand cDNA Synthesis kit (GE Healthcare, Little Chalfont, UK), as previously reported [15]. RNA and cDNA samples were stored at -80 °C.

Real time RT-PCR

For miRNA or RNAs expression analysis we used Real-time PCR using TaqMan Universal PCR Master Mix (ThermoFisher Corporation, Waltham, MA, USA) and TaqMan pre-designed probes for each gene (RUNX2, hs00231692_m1; sestrin1, hs00902782_m1; miR-146b-5, PN4440886; miR-34a, PN4427975; U6 snRNA, 001,973; MYOD, Hs00159528_m1; PPARG2, hs01115513_m1; ACTB, Hs99999903_m1). Ct values for each reaction were calculated by using TaqMan SDS analysis software (Applied Biosystems; Foster City, California, USA) and the relative gene expression levels between different samples, was analyzed by using the $2^{-\Delta\Delta CT}$ method, as previously reported [14].

Western blotting

Ripa buffer (Thermo Fisher Scientific, Waltham, MA, USA) was used to extract the protein and concentrations were calculated with BCA assay (Thermo Scientific, Waltham, MA, USA) as previously reported [14]. Protein samples were diluted in Laemmli's sample buffer (Biorad, CA, US) and heated for 5 min at 95 °C, and then separated by sodium dodecyl sulfate–polyacrylamide gel electrophoresis (SDS PAGE). Proteins were transferred onto polyvinylidene difluoride (PVDF) membranes (Thermo Fisher Scientific, Waltham, MA, USA). PVDF membranes were probed with the primary (antiMyoD (MA1-41,017; Thermo Scientific, Waltham, MA, USA); β ACTIN (BA3R; Thermo Scientific, Waltham, MA, USA); sirtuin (PA5-23,063; Invitrogen, Waltham, MA, USA); SESN1 (PA5-98,142; Invitrogen, Waltham, MA, USA); SESN2 (ab-178518; Abcam, Cambridge, MA); p53 (2524; Cell Signaling Technology, Danvers, Massachusetts, USA); p21 (M7202; Dako, Denmark A/S); UCP1 (ab-10983; Abcam, Cambridge, MA)) and secondary antibodies Anti-mouse (7076; Cell Signaling Technology) and Anti-rabbit (7074, Cell Signaling Technology). Signals were detected with a chemiluminescence reagent (ECL, Millipore, Burlington, MA, USA) and images were recorded using a LAS4000 Digital Image Scanning

System (GE Healthcare, Little Chalfont, UK). Densitometric analysis was performed as we previously reported [16].

Cardiopulmonary exercise test (CPET)

CPET was carried out on a cycle ergometer with clip-on pedals (Monark®, LC6 Novo; Vansbro, Sweden), using a gas analyzer (COSMED® Quark PFT; Milan, Italy). Ventilation per minute (VE), oxygen uptake (VO₂), carbon dioxide production (VCO₂), first (VT1) and second (VT2) ventilatory thresholds and maximal oxygen uptake (VO₂max) were assessed. VT1 was determined by V-slope method and VT2 by ventilatory equivalent method. Subjects performed a ramp test protocol with increments of 15, 20 or 25 W per minute until volitional exhaustion. The protocol was chosen based on age and training, as to reach at least 8 min of incremental phase [17] and a 6–20 modified Borg scale was used [18]. Cadence ranged between 70 and 100 rpm, as chosen by each subject. Each subject performed the same CPET protocol BPP, BN, AN. Heart rate (HR) and electrocardiogram (ECG) were constantly monitored. CPET was considered maximal when the following criteria were achieved: (a) a plateau > 20 s in the oxygen consumption (VO₂) versus exercise intensity relationship (b) respiratory exchange ratio (RER > 1.10), (c) HR [\geq 85% of (220-age)], (d) a rating of perceived exhaustion (RPE) of 19–20 on the Borg modified scale. After the test, all respiratory data were averaged at 10-s intervals to determine VO₂max, taken as the highest average value.

The above-mentioned measurements were made in the following order during the same day, in the morning: blood samples, body composition measures (BIA and DEXA), CPET.

Subjects avoided heavy physical effort at least 24 h before the tests, slept at least 6–8 h the night before and had a light meal at least 2 h before the tests. Sera were stored at – 80 °C until use.

Statistical analysis

Results were expressed as mean \pm SD. Statistical analysis was assessed by two-tailed Student's paired-test. Differences were considered significant with $p < 0.05$. For in vitro data, analyses were applied to experiments carried out at least three times. We used SPSS for Windows, version 22.0 (SPSS Inc., Chicago, IL, USA) to analyze the data.

Results

Anthropometric characteristics of cyclists are reported in Table 1. 6 out of 8 participants completed NC4000 within 22 days: finishing time was 21.24 ± 8.41 days, which consisted of 229.85 ± 68.76 km per day. Bike plus

Table 1 - Characteristics of the cyclists and training for NC4000

	BPP	BN	p
Age (years)	47.5 \pm 13.5	–	
Height (cm)	178.8 \pm 5.1	–	
Weight (kg)	79.25 \pm 8.98	77.68 \pm 8.16	0.042*
BMI (kg/m ²)	24.79 \pm 2.50	24.31 \pm 2.34	0.040*
Training sessions	3.13 \pm 0.84	3.50 \pm 1.20	0.80
Time per week (hours)	11.25 \pm 3.54	11.25 \pm 2.44	0.999
Distance per week (km)	241.25 \pm 148.75	259.38 \pm 113.34	0.448
Sleeping hours	7.13 \pm 1.00	6.81 \pm 1.13	0.279

BMI body mass index; BPP before preparation period; BN before NC4000 performance (post training period); AN after NC4000 performance

* $p < 0.05$

Table 2 Pre- and post-training body composition variables (BIA)

	BPP	BN	p
FM _{BIA} (kg)	13.81 \pm 6.41	11.18 \pm 5.05	0.014*
FFM _{BIA} (kg)	65.44 \pm 4.37	66.50 \pm 4.99	0.055
FFM _{BIA} (%)	83.05 \pm 6.07	85.94 \pm 85.94	0.007*
MM _{BIA} (kg)	37.06 \pm 2.39	37.73 \pm 2.80	0.060

BIA Bioelectrical impedance analysis; BPP before preparation period; BN before North-Cape4000; FM fat mass; FFM fat free mass; MM muscular mass

* $p < 0.05$

bags weight at start was 20.44 ± 4.30 kg. None of the cyclists had experienced a multi-day ultra-cycling race before. None of them followed a professional training or a specific diet, there were no significant differences in dietary habits of participants. None of them were vegetarian or had food allergies or intolerances.

Reported individual training program did not change significantly between BPP and BN.

Effects of the training program before ultracycling performance

Weight and FM_{BIA} were significantly reduced after the training for NC4000 (Table 2). Coffee intake and sleeping hours were the same BPP and BN. A total of 6 cyclists used supplements between BPP and BN evaluation, and in particular saline solutions (5 out of 8), branched-chain amino acids (BCAAs, 3 out of 8), maltodextrins (2 out of 8), Vitamin B complex (1 out of 8), Vitamin C (1 out of 8) and Omega3 (1 out of 8).

Total cholesterol and LDL decreased significantly between BPP and BN, while HDL and triglycerides, liver enzymes and creatinine did not change after training. Vitamin D levels rose significantly between BPP and BN (Table 3).

Table 3 - Pre- and post-training biochemical parameters

	BPP	BN	p
Vitamin D (ng/mL)	20.35 ± 7.19	32.38 ± 8.18	< 0.001*
Creatinine (mg/dL)	0.94 ± 0.11	0.91 ± 0.07	0.500
AST (IU/L)	25.13 ± 8.08	23.75 ± 4.30	0.500
ALT (IU/L)	23.38 ± 6.57	21.25 ± 5.75	0.190
Total cholesterol (mg/dL)	224.13 ± 34.48	204.88 ± 25.73	0.013*
LDL (mg/dL)	134.88 ± 28.62	117.75 ± 23.96	0.010*
HDL (mg/dL)	66.5 ± 14.60	63.63 ± 11.46	0.280
Triglycerides (mg/dL)	107.38 ± 48.25	117.50 ± 40.14	0.450

ALT alanine amino transferase; AST aspartate amino transferase; HDL high density lipoproteins; LDL low density lipoproteins

*p < 0.05

Table 4 VO₂max and ventilatory thresholds pre- and post-training

	BPP	BN	p
VO ₂ max (L/min)	3871.50 ± 649.36	3792.25 ± 365.42	0.492
VO ₂ max (mL/min*kg ⁻¹)	49.61 ± 10.51	49.43 ± 7.64	0.884
VT1 (mL/min*kg ⁻¹)	35.85 ± 7.73	35.06 ± 6.23	0.738
VT2 (mL/min*kg ⁻¹)	45.94 ± 10.57	45.49 ± 6.43	0.803

VO₂max maximal oxygen uptake; VT1 first ventilatory threshold; VT2 second ventilatory threshold

Absolute and relative VO₂max, as well as ventilatory thresholds didn't increase after training for NC4000 (Table 4).

Effects of NC4000 on body composition, ventilator parameters and biochemical markers

Subjects were evaluated AN 5.8 ± 2.2 days of recovery.

Reported water intake during NC4000 was 6.13 ± 2.37 L per day. Sleeping hours decreased significantly during NC4000 (6.81 ± 1.13 vs 5.25 ± 1.60; p = 0.027), while coffee intake did not change (2.75 ± 1.49 vs 3.50 ± 1.39; p = 0.307), as well as alcoholic intake (0.69 ± 0.59 vs 0.63 ± 0.79; p = 0.844).

All the subjects took supplements while ultra-cycling: the most used were saline solutions (7 of 8) and branched-chain amino acids (BCAAs, 6 of 8), followed by Vitamin B complex (5 of 8), Vitamin C (4 of 8), maltodextrins (2 of 8) and carnitine and Omega3 (1 of 8). Six cyclists used nonsteroidal anti-inflammatory drugs (NSAIDs) due to musculoskeletal injuries, none of them related to direct trauma. Illness or other significant health complaints were not reported.

Weight (77.68 ± 8.16 kg) and BMI (24.31 ± 2.34 kg/m²) did not decrease after NC4000, compared to BN. However, FM decreased, measured both with DEXA and BIA. DEXA also revealed a significant decrease in segmental

Table 5 - Body composition Before NC4000—After NC4000

	BN	AN	p
FM _{DEXA}	18.24 ± 5.58	15.97 ± 4.54	0.002*
VAT (g)	474 ± 267	378 ± 184	0.019*
TF (kg)	8.63 ± 3.87	7.09 ± 3.06	0.003*
LM (kg)	55.65 ± 3.05	56.44 ± 3.17	0.122
LM (%)	72.94 ± 4.71	75.31 ± 4.18	< 0.001*
LAM (kg)	8.25 ± 0.34	8.34 ± 0.48	0.283
FM _{BIA} (kg)	11.18 ± 5.05	9.21 ± 3.75	0.019*
FFM _{BIA} (kg)	66.50 ± 4.99	66.95 ± 5.24	0.450
MM _{BIA} (kg)	37.73 ± 2.80	37.88 ± 2.97	0.676
FFM _{BIA} (%)	85.94 ± 5.06	88.05 ± 4.23	0.013*

AN after NC4000; BIA bioelectrical impedance analysis; BN before NC4000; DEXA dual energy x-ray absorptiometry; FM fat mass; LAM lean appendicular mass; TF truncal fat; VAT visceral adipose tissue

*p < 0.05

Table 6 Pre- and post-race biochemical parameters

	BN	AN	p
Vitamin D (ng/mL)	32.38 ± 8.18	29.00 ± 5.81	0.042*
Creatinine (mg/dL)	0.91 ± 0.07	0.85 ± 0.10	0.021*
AST (IU/L)	23.75 ± 4.30	49.00 ± 46.23	0.162
ALT (IU/L)	21.25 ± 5.75	57.00 ± 65.48	0.153
Total cholesterol (mg/dL)	204.88 ± 25.73	201.63 ± 21.33	0.652
LDL (mg/dL)	117.75 ± 23.96	99.75 ± 17.12	0.047*
HDL (mg/dL)	63.63 ± 11.46	66.00 ± 9.89	0.462
Triglycerides (mg/dL)	117.50 ± 40.14	175.25 ± 64.16	0.004*

ALT alanine amino transferase; AST aspartate amino transferase; HDL high density lipoproteins; LDL low density lipoproteins

*p < 0.05

fat, and an increase in relative LM. BIA highlighted an increase in FFM% but not in MM or absolute FFM (Table 5).

Serum 25-hydroxy Vitamin D decreased significantly after the race. Lipid profile showed an increase in triglycerides and a reduction in LDL concentration, whereas there was no variation in total cholesterol and HDL levels. Creatinine decreased significantly after NC4000. Liver enzymes concentrations did not change after ultra-cycling (Table 6).

After NC4000, there was a slight tendency in reduction of maximal oxygen uptake as well as oxygen uptake at first and second ventilatory threshold, but it was not statistically significant (Table 7).

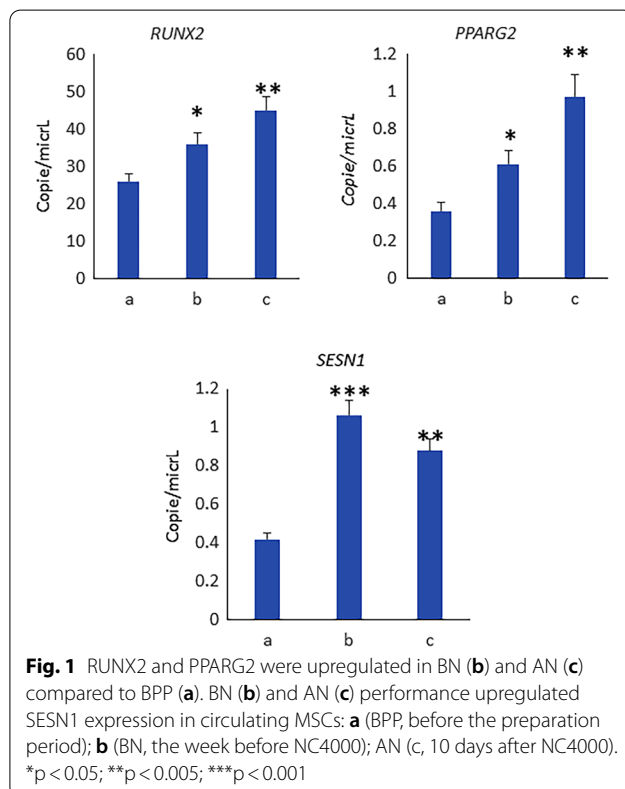
Effects of training and NC4000 on mesenchymal stem cells commitment

In order to identify the effects of training and NC4000 on Mesenchymal Stem Cells (MSCs) commitment, we

Table 7 VO₂max and ventilatory thresholds pre- and post-NC4000

	BN	AN	p
VO ₂ max (L/min)	3792.25 ± 365.42	3690.25 ± 331.89	0.178
VO ₂ max (mL/min*kg ⁻¹)	49.43 ± 7.64	48.74 ± 5.58	0.587
VT1 (mL/min*kg ⁻¹)	35.06 ± 6.23	34.20 ± 5.15	0.564
VT2 (mL/min*kg ⁻¹)	45.49 ± 6.43	45.23 ± 4.28	0.816

VO₂max maximal oxygen uptake; VT1 first ventilatory threshold; VT2 second ventilatory threshold



analyzed circulating MSCs for the expression of the transcription factors RUNX2 and PPARG2, involved in osteogenesis and adipogenesis, respectively. As shown in Fig. 1, the osteogenic and adipogenic transcription factors, RUNX2 and PPARG2 were upregulated BN and AN. The training as well as ultra-cycling, upregulated Sestrin 1 (SESN1) expression in circulating MSCs.

Training increases sestrins and sirtuin levels in SK muscle cells

Since Sestrins regulate muscle stem cell homeostasis [19], we analyzed the SESN1 and SESN2 levels in SK muscle cells cultured in the presence of sera collected BPP, BN and AN. As shown in Fig. 2, both sestrins increased after

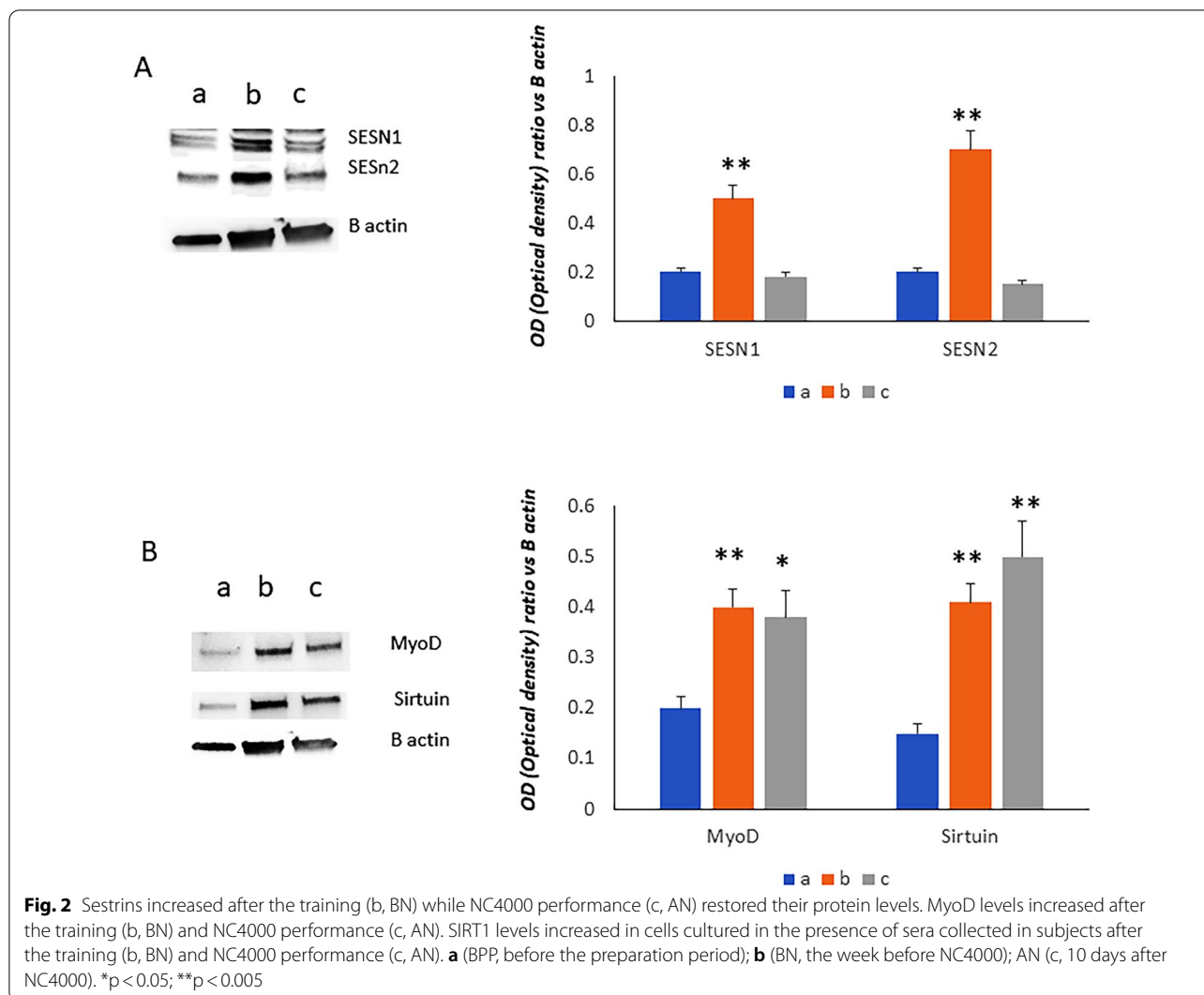
the training while ultra-cycling restored their protein levels. Accordingly, MyoD levels were increased after the training and NC4000 (Fig. 2). Considering that sirtuin 1 (SIRT1), in the presence of MyoD, is involved in the regulation of cellular metabolism, we analyzed the protein levels of SIRT1 in SK muscle cells cultured in the presence of sera collected before, after the training and following ultra-cycling. As shown in Fig. 2B, SIRT1 levels increased in cells cultured in the presence of sera collected BN and AN.

Training and ultra-cycling counteract adipogenesis aging and increases brown adipogenesis

In order to evaluate the effects of training and ultra-cycling on adipogenesis, we cultured MSCs during adipogenesis in the presence of sera collected BPP, BN and AN. We observed increased levels of sirtuin in adipogenic differentiating cells after training and NC4000 (Fig. 3). In addition, we observed increased levels of p53 and reduced levels of p21, a target gene of p53 associated to senescence (Fig. 3). The observed reduction of p21 suggests a reduced transcriptional function of p53. Interestingly, it has been reported that p21 deficiency caused a suppression of adipocyte differentiation [20]. To explain the increased levels of sirtuin, we investigated the expression of its targeting microRNA, miR146b as shown in Fig. 3B, miR 146b was downregulated in MSCs in presence of sera collected in subjects after the training and NC4000 performance. As it has been reported that sirtuin plays an important role in the induction of brown adipose tissue (BAT) associated genes [21], we evaluated the levels of the uncoupling protein (UCP1) in differentiating cells. As shown in Fig. 4, UCP1 levels increased after the training as well as after ultra-cycling.

Discussion

Ultra-Endurance cycling is a very challenging performance, typically defined as a race that is over 100 miles. This experience can take place on almost any surface and with any sort of bike, but its duration is the main characteristic. Ultra-cycling is associated with a multitude of physiological consequences. Although in recent years an increased interest in ultra-endurance sports has arisen, few studies have evaluated the impact of this physical effort in the modulation of biochemical parameters and in the commitment of progenitor cells. This is a relevant aspect as progenitor cell homeostasis is a pivotal factor in the pathogenesis of degenerative diseases and all factors influencing and maintaining this homeostasis are potential target in disease prevention. In addition, another original aspect is that the present study has been performed on amateur competitive cyclists subjected to lower training volumes than professional cyclists [22].



Therefore, in our study, we highlighted the possible connection between changes in body composition, adipogenesis and myogenesis.

Fat mass decrease could be explained by the well-known high-energy deficit caused by ultra-endurance events, especially in amateur cyclists [3, 23]. In this study, for the first time we evaluated the possible driver genes and transcriptional factors involved in this mechanism. In fact, physical training promotes the differentiation of Mesenchymal Stem Cells [24]. As previously reported [14], we observed increased expression of RUNX2 in cMSCs after the training, suggesting their osteogenic commitment. The increased RUNX2 expression in cMSCs was maintained AN. We also observed increased levels of PPARG2 after the training as well after NC4000. These findings could suggest an increase of adipogenic commitment too. However, the increased PPARG2 expression is in agreement with

its role in regulating insulin sensitivity and the utilization of glucose to maintain energy homeostasis [25]. Accordingly, we also observed in cMSCs the expression of SESN1 gene, coding for a small stress-inducible protein which has been demonstrated to be able to improve insulin sensitivity [26]. Interestingly, for the first time, we investigated the expression of Sestrin in circulating progenitor cells. The increased expression of SESN1 in progenitors highlights the effective role of physical exercise in degenerative diseases considering the protective role of sestrin [27]. Therefore, given the role of sestrins in the modulation of muscle metabolism following exercise, we investigated SESN1 and SESN2 protein levels in skeletal muscle cells treated with serum collected before and after training as well after NC4000. Interestingly, we observed increased levels of SESN1 and SESN2 in SK muscle cells treated with sera collected after the training while both SESN1 and

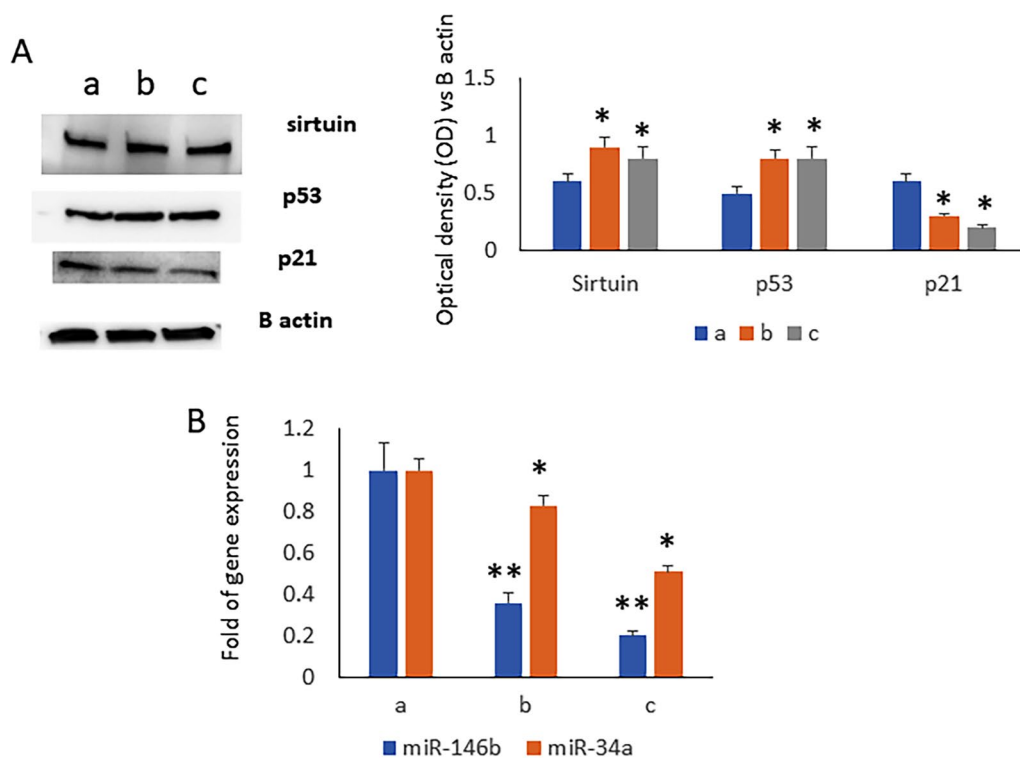


Fig. 3 Increased levels of Sirtuins and p53 and reduced levels of p21 as well of miR-146b expression were observed in MSCs in presence of sera collected in subjects after the training (b, BN) and NC4000 performance (c, AN). **a** (BPP, before the preparation period); **b** (BN, the week before NC4000); AN (c, 10 days after NC4000). * $p < 0.05$; ** $p < 0.005$

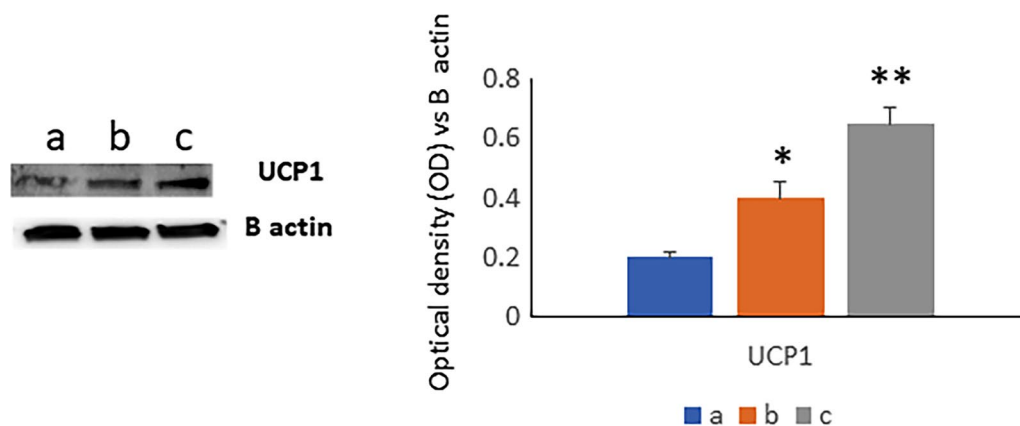


Fig. 4 The levels of UCP1, associated to the brown adipose tissue (BAT) differentiation increased after the training as well as after ultra-cycling. **a** (BPP, before the preparation period); **b** (BN, the week before NC4000); AN (c, 10 days after NC4000). * $p < 0.05$; ** $p < 0.005$

SESN2 levels returned to baseline in cells treated with serum after NC4000 performance. Considering that sestrins have protective activity against diseases affecting the musculoskeletal system [27], it can be considered that training is useful to counteract sarcopenia, muscle atrophy, osteopenia and arthritic pathologies.

Despite some studies reported a decrease in free fat mass (FFM) and fat mass (FM) after ultra-cycling [6, 7], we observed a decrease in FM and maintenance of muscular and lean mass: this was consistent also with training to ultra-cycling. Previous different results may be explained by the hydration status of the subjects studied

and the scheduled evaluation in the immediate post-competition time, which causes localized edema in the main muscle groups analyzed, an effect that can alter DEXA results [28].

Furthermore, we did not observe alterations in ALT and AST concentrations, which are implicated in muscular and subsequent liver damage following strenuous exercise. We can speculate that these parameters were higher immediately after NC4000 [29] and reparation of muscle fibers was ongoing. These findings were not altered by modifications in coffee and alcohol intake during NC4000. Super-compensation in storage of skeletal muscle glycogen and fluids could have affected the lean mass measurements AN, considering that cyclists were evaluated about one week after recovery from the NC4000 and that serum creatinine levels were significantly reduced. Additional evidence comes from Knechtle et al., who stated that ultra-cycling does not alter skeletal muscle mass [30].

Therefore, we investigated the role of training and ultra-cycling on skeletal muscle cells. It has been reported that the expression of SESN1 is induced during myotube differentiation [26]. Accordingly, we observed increased levels of sestrins as well of MYOD in SK muscle cells treated with sera collected after the training. The increased levels of MYOD have been maintained also after NC4000 performance, despite their tendency to decrease. Sirtuin1, is a histone/protein deacetylase which regulates the caloric restriction-mediated longevity [31]. It has been demonstrated that in the presence of MyoD, SIRT1 is able to induce positive self-regulation of the expression of the peroxisome proliferator activated receptor- γ co-activator-1 α (PGC-1 α), a master regulator of genes involved in the regulation of metabolism [32]. In skeletal muscle, exercise induces PGC-1 α expression probably in response to decreased ATP levels [33]. Therefore, the increased levels of MYOD and Sirtuin 1 observed in SK muscle cells treated with sera collected after training suggest the role of physical exercise in driving muscle-specific gene expression and metabolism.

We also evaluated whether aerobic capacity, in terms of VO₂max and ventilatory thresholds were affected by individual training and ultra-cycling. Interestingly, VO₂max, VT1 and VT2 were not modified. Our explanation for these results is that our subjects already had good aerobic capacity and that their training habits did not change before NC4000. No changes were highlighted after ultra-cycling, despite other studies having reported a general increase in aerobic capacity [10]. With regard to this aspect, our subjects were better trained and during ultra-cycling pedaled an average of more than 220 km per day, which is much more than what has been previously reported. Even if aerobic

capacity was not affected by training and NC4000, skeletal muscle metabolism was positively stimulated.

Sirtuin 1 levels also increased in MSCs during adipogenic differentiation in the presence of sera collected after the training and ultra-cycling. The increased levels of Sirtuin 1 reduced the transcriptional activity of p53. We observed reduced levels of p21, a downstream target gene of p53, even if p53 levels increase after training and NC4000. Moreover, it has been demonstrated that SIRT1 can prevent the transcriptional activity of p53 by deacetylation process [34]. Importantly, it has been demonstrated that SIRT1 activation during adipogenesis promotes the transcription of brown adipose tissue specific genes [35]. In addition, SIRT1 is also involved in the downregulation of WAT gene expression [36].

Thus, we observed increased levels of the uncoupling protein1 (UCP1), uniquely expressed in BAT cells, in MSCs during adipogenesis in the presence of sera collected after training. Importantly, the increase of UCP1 was more pronounced in the presence of sera collected AN. These results highlighted the relationship between BAT and the substantial reduction in truncal and visceral adipose tissue (VAT) as a marker of negative energy balance observed after NC4000.

VAT has important implications on whole cardiovascular risk and sequestration of vitamin D: thus, we evaluated lipid profile and Vitamin D levels. We observed a significant decrease of total cholesterol and LDL during the preparation period. LDL decreased also after NC4000, which may be related to a higher demand of fatty acids for beta-oxidation. On the other hand, HDL remained at high levels during the study, without substantial modifications also after NC4000. These results are consistent with the increase UCP1 expressed in activated BAT, that is confirmed as a lipid profile modulator [37]. This result is in contrast with ultramarathon running and underlines the differences in these sports [38]. Vitamin D levels and lipid profile were not altered by supplements, because only one cyclist reported the use of carnitine and another one omega 3.

We found a clear increase in triglycerides concentration after NC4000: others had explained this aspect by a catecholaminergic stimulus induced by exercise; this result seems to be in contrast with what we found about other lipid profile parameters, but this may be due to increased hepatic VLDL-triglyceride production or to increased circulating non-esterified fatty acids (NEFAs) after the competition [10] which mask the plasma triglyceride lowering.

Serum 25-hydroxy Vitamin D increased significantly between BPP and BN: this could be explained by a better sun exposition during spring and summer months [12].

However, Vitamin D concentrations slightly decreased after NC4000, and this outcome may be justified by the consumption of adipose deposits in a short period or by the delay in determining vitamin D levels after the end of the competition, confirming the complex relationship between ultra-endurance and vitamin D metabolism [39].

By considering that the activation of BAT, as well as the body composition modulation, had been suggested to reduce obesity related diseases, the aim to further investigate the role of strenuous physical exercise in relation to cardiovascular and degenerative diseases appears particularly interesting. In order to identify epigenetic factors involved in the increase of sirtuin1, we analyzed the expression of miR targeting sirtuin1. Accordingly, we observed reduced miR146b and miR34a in cells treated with sera collected after BN and AN. Interestingly, MiR-146b has been suggested as a regulator of human visceral adipogenesis and its expression is altered in human obesity (40), confirming the importance of the modulation of this metabolic pathway in preventing cardiovascular and degenerative diseases.

Therefore, our study, for the first time, evaluates the functional biochemical parameters with the modulation of changes in the progenitor cells and analyzes, as in the case of sestrins, the impact of physical exercise on molecules involved in the the pathogenesis of degenerative diseases. The results of our study, conducted on healthy subjects, can therefore be useful to better understand the impact of physical performance related to ultra-endurance activity in the commitment of progenitor cells and therefore in a possible prevention of degenerative diseases.

Conclusions

The training program leads to beneficial effects on body composition and biochemical lipid parameters, as well as a switch in brown adipogenesis and substantial modification in cellular processes related to SESN1 and SESN2 expression, even when oxygen uptake and ventilatory thresholds are unaltered in trained amateur cyclists.

Ultra-cycling does not alter body weight or aerobic capacity but produces an acute and prolonged energy imbalance that induces a reduction in fat mass, changes in commitment of MSCs, with significant increase in brown adipogenesis and UCP1 and a maintenance of MYOD levels in skeletal muscle cells. Finally, due to the increasing number of participants in ultra-endurance events, future research should focus on non-elite ultra-cyclers, particularly on preparation and training for ultra-endurance performance. Research is also needed exploring the long-term effects of ultra-cycling and on the persistence of post-acute metabolic modifications..

Acknowledgements

We thank the "Centro Piattaforme Tecnologiche (CPT-UNIVR)" of the University of Verona for technical support.

Author contributions

LB, MM and MGR, interpretation of data, data curation; MB, FB, AM, JB, GD, MC and TDS generation, collection, and assembly of data; interpretation of data; MTV, MB and LDC, conception and design, interpretation of data, critical revision of the manuscript, study supervision. The authors read and approved the final version of the manuscript.

Funding

This study was supported by FUR-Dep of Medicine, University of Verona (LDC).

Availability of data and materials

The datasets used and/or analyzed during the current study are available from the corresponding author upon a reasonable request.

Declarations

Ethical approval and consent to participate

The procedures were approved by the ethical committee of Azienda Ospedaliera Universitaria Integrata of Verona, Italy (number 1538; 3 December 2012; local ethical committee of Azienda Ospedaliera Integrata di Verona). The donors of peripheral blood provided informed consent. Informed consent was obtained from all subjects involved in the study.

Consent for publication

Not applicable.

Competing interests

The authors have no disclosures to report and declare no competing financial interests.

Author details

¹Department of Medicine, Section of Internal Medicine, University of Verona, Piazzale Scuro, 10, Policlinico G.B. Rossi, 37134 Verona, Italy. ²Department of Neurosciences, Biomedicine and Movement Sciences, University of Verona, 37100 Verona, Italy. ³Flaskworks, LLC, 38 Wareham St, Boston, MA 02118, USA.

Received: 23 June 2022 Accepted: 14 August 2022

Published online: 04 September 2022

References

- Rüst CA, Rosemann T, Lepers R, Knechtle B. Gender difference in cycling speed and age of winning performers in ultra-cycling—the 508-mile "Furnace Creek" from 1983 to 2012. *J Sports Sci.* 2015;33(2):198–210.
- Scheer V. Participation trends of ultra endurance events. *Sports Med Arthrosc Rev.* 2019;27(1):3–7.
- Rosenkilde M, Morville T, Andersen PR, Kjær K, Rasmussen H, Holst JJ, et al. Inability to match energy intake with energy expenditure at sustained near-maximal rates of energy expenditure in older men during a 14-d cycling expedition. *Am J Clin Nutr.* 2015;102(6):1398–405.
- Knechtle B. Nutrition and ultra-endurance: an overview. In: Bagchi D, Nair S, Sen CK, editors. *Nutrition and enhanced sports performance.* Cambridge: Elsevier; 2013. p. 161–70.
- Knechtle B, Wirth A, Knechtle P, Rüst CA, Rosemann T. A comparison of ultra-endurance cyclists in a qualifying ultra-cycling race for paris-brest-paris and race across America—Swiss cycling marathon. *Percept Mot Skills.* 2012;114(1):96–110.
- Bircher S, Enggist A, Jehle T, Knechtle B. Effects of an extreme endurance race on energy balance and body composition—a case study. *J Sports Sci Med.* 2006;5(1):154.
- Jagim A, Levers K, Galvan E, Joubert D, Rasmussen C, Greenwood M, et al. Effects of an ultra-endurance event on body composition, exercise performance and markers of clinical health: a case study. *Bioenergetics.* 2014;3(119):2.

8. Rehrer N, Hellemans I, Rolleston A, Rush E, Miller B. Energy intake and expenditure during a 6-day cycling stage race. *Scand J Med Sci Sports*. 2010;20(4):609–18.
9. Knechtle B, Knechtle P, Kohler G. The effect of 1000 km nonstop cycling on fat mass and skeletal muscle mass. *Res Sports Med*. 2011;19(3):170–85.
10. Clemente-Suarez VJ. Changes in biochemical, strength, flexibility, and aerobic capacity parameters after a 1700 km ultraendurance cycling race. *BioMed Res Int*. 2014;2014:8.
11. Sánchez-Muñoz C, Zabala M, Muros J. Nutritional intake and anthropometric changes of professional road cyclists during a 4-day competition. *Scand J Med Sci Sports*. 2016;26(7):802–8.
12. de la Puente Yague M, Collado Yurrita L, Ciudad Cabanas MJ, Cuadrado Cenxual MA. Role of vitamin D in athletes and their performance: current concepts and new trends. *Nutrients*. 2020;12(2):579.
13. Kelly T, Berger N, Richardson TL. DXA body composition: theory and practice. *Appl Radiat Isot*. 1998;49:511–3.
14. Dalle Carbonare L, Mottes M, Cheri S, Deiana M, Zamboni F, Gabbiani D, et al. Increased gene expression of RUNX2 and SOX9 in mesenchymal circulating progenitors is associated with autophagy during physical activity. *Oxid Med Cell Longev*. 2019;2019:1.
15. Dalle Carbonare L, Dorelli G, Li Vigni V, Minoia A, Bertacco J, Cheri S, et al. Physical activity modulates miRNAs levels and enhances MYOD expression in myoblasts. *Stem Cell Rev Rep*. 2022. <https://doi.org/10.1007/s12015-022-10361-9>.
16. Deiana M, Dalle Carbonare L, Serena M, Cheri S, Parolini F, Gandini A, et al. New insights into the runt domain of RUNX2 in melanoma cell proliferation and migration. *Cells*. 2018;7(11):220.
17. Wasserman K, Hansen JE, Sue DY, Whipp BJ, Froelicher VF. Principles of exercise testing and interpretation. *J Cardiopulm Rehabil Prev*. 1987;7(4):189.
18. Borg G. Borg's perceived exertion and pain scales: human kinetics. Washington: American Psychological Association; 1998.
19. Yang BA, Castor-Macias J, Fraczek P, Cornett A, Brown LA, Kim M, et al. Sestrins regulate muscle stem cell metabolic homeostasis. *Stem Cell Rep*. 2021;16(9):2078–88.
20. Inoue N, Yahagi N, Yamamoto T, Ishikawa M, Watanabe K, Matsuzaka T, et al. Cyclin-dependent kinase inhibitor, p21WAF1/CIP1, is involved in adipocyte differentiation and hypertrophy, linking to obesity, and insulin resistance. *J Biol Chem*. 2008;283(30):21220–9.
21. Kurylowicz A. Role of sirtuins in adipose tissue development and metabolism. In: Szablewski L, editor. *Adipose tissue-an update*. London: IntechOpen; 2019.
22. Jeukendrup AE, Craig NP, Hawley JA. The bioenergetics of world class cycling. *J Sci Med Sport*. 2000;3(4):414–33.
23. Armstrong LE, Casa DJ, Emmanuel H, Ganio MS, Klau JF, Lee EC, et al. Nutritional, physiological, and perceptual responses during a summer ultraendurance cycling event. *J Strength Cond Res*. 2012;26(2):307–18.
24. Valenti MT, Deiana M, Cheri S, Dotta M, Zamboni F, Gabbiani D, et al. Physical exercise modulates miR-21-5p, miR-129-5p, miR-378-5p, and miR-188-5p expression in progenitor cells promoting osteogenesis. *Cells*. 2019;8(7):742.
25. Leonardini A, Laviola L, Perrini S, Natalicchio A, Giorgino F. Cross-talk between PPAR and insulin signaling and modulation of insulin sensitivity. *PPAR Res*. 2009;2009:12.
26. Kim M, Sujkowski A, Namkoong S, Gu B, Cobb T, Kim B, et al. Sestrins are evolutionarily conserved mediators of exercise benefits. *Nat Commun*. 2020;11(1):1–14.
27. Chen Y, Huang T, Yu Z, Yu Q, Wang Y, Ja Hu, et al. The functions and roles of sestrins in regulating human diseases. *Cell Mol Biol Lett*. 2022;27(1):1–24.
28. Toomey CM, McCormack WG, Jakeman P. The effect of hydration status on the measurement of lean tissue mass by dual-energy X-ray absorptiometry. *Eur J Appl Physiol*. 2017;117(3):567–74.
29. Lippi G, Schena F, Salvagno GL, Aloe R, Banfi G, Guidi GC. Foot-strike haemolysis after a 60-km ultramarathon. *Blood Transfus*. 2012;10(3):377.
30. Knechtle B, Wirth A, Knechtle P, Rosemann T. An ultra-cycling race leads to no decrease in skeletal muscle mass. *Int J Sports Med*. 2009;30(03):163–7.
31. McBurney MW, Yang X, Jardine K, Hixon M, Boekelheide K, Webb JR, et al. The mammalian SIR2a protein has a role in embryogenesis and gametogenesis. *Mol Cell Biol*. 2003;23(1):38–54.
32. Amat R, Planavila A, Chen SL, Iglesias R, Giralto M, Villarroya F. SIRT1 controls the transcription of the peroxisome proliferator-activated receptor- γ co-activator-1 α (PGC-1 α) gene in skeletal muscle through the PGC-1 α autoregulatory loop and interaction with MyoD. *J Biol Chem*. 2009;284(33):21872–80.
33. Russell AP, Hesselink MK, Lo SK, Schrauwen P. Regulation of metabolic transcriptional co-activators and transcription factors with acute exercise. *FASEB J*. 2005;19(8):986–8.
34. Furukawa A, Tada-Oikawa S, Kawanishi S, Oikawa S. H2O2 accelerates cellular senescence by accumulation of acetylated p53 via decrease in the function of SIRT1 by NAD⁺ depletion. *Cell Physiol Biochem*. 2007;20(1–4):045–54.
35. Lo KA, Sun L. Turning WAT into BAT: a review on regulators controlling the browning of white adipocytes. 2013. *Biosci Rep*. <https://doi.org/10.1042/BSR20130046>.
36. Favero G, Krajčiková K, Bonomini F, Rodella LF, Tomečková V, Rezzani R. Browning of adipose tissue and sirtuin involvement. In: Szablewski L, editor. *adipose tissue*. London: IntechOpen; 2018.
37. Hoeke G, Kooijman S, Boon MR, Rensen PC, Berbée JF. Role of brown fat in lipoprotein metabolism and atherosclerosis. *Circ Res*. 2016;118(1):173–82.
38. Wu H-J, Chen K-T, Shee B-W, Chang H-C, Huang Y-J, Yang R-S. Effects of 24 h ultra-marathon on biochemical and hematological parameters. *World J Gastroenterol*. 2004;10(18):2711.
39. Mieszkowski J, Stankiewicz B, Kochanowicz A, Niespodziński B, Kowalik T, Zmijewski MA, et al. Ultra-marathon-induced increase in serum levels of vitamin d metabolites: a double-blind randomized controlled trial. *Nutrients*. 2020;12(12):3629.
40. Chen L, Dai Y-M, Ji C-B, Yang L, Shi C-M, Xu G-F, et al. MiR-146b is a regulator of human visceral preadipocyte proliferation and differentiation and its expression is altered in human obesity. *Mol Cell Endocrinol*. 2014;393(1–2):65–74.

Publisher's Note

Springer Nature remains neutral with regard to jurisdictional claims in published maps and institutional affiliations.

Ready to submit your research? Choose BMC and benefit from:

- fast, convenient online submission
- thorough peer review by experienced researchers in your field
- rapid publication on acceptance
- support for research data, including large and complex data types
- gold Open Access which fosters wider collaboration and increased citations
- maximum visibility for your research: over 100M website views per year

At BMC, research is always in progress.

Learn more biomedcentral.com/submissions

